GEORGIA DOT RESEARCH PROJECT 13-26

FINAL REPORT

Evaluation of Vehicle Detection Technologies for Applications in Georgia

OFFICE OF RESEARCH
15 KENNEDY DRIVE
FOREST PARK, GA 30297

1.Report No.: FHWA-GA-10-1326	2. Government Accession No.:	3. Recipient's Catalog No.:
4. Title and Subtitle: Evaluation of Vehicle Detection Technologies for Applications in Georgia	5. Report Date: October 2015	
	6. Performing Organization Code:	
7. Author(s): Jidong (James) Yang, Sung-Hee Kim and Bashan Zuo Kennesaw State University	8. Performing Organ. Report No.: 13-26	
9. Performing Organization Name and Address: Kennesaw State University, Georgia Pavement and Traffic Research Center, 1100 South Marietta Parkway, Marietta, GA, 30060	10. Work Unit No.:	
	11. Contract or Grant No.: RP 13-26	
12. Sponsoring Agency Name and Address: Georgia Department of Transportation Office of Materials & Research 15 Kennedy Drive Forest Park, GA 30297-2534	13. Type of Report and Period Covered: Final Report, January 2014 – October 2015	
	14. Sponsoring Agency Code:	
15. Supplementary Notes: Prepared in cooperation with the U.S. Department of Transportation, Federal Highway Administration.		

16. Abstract:

Vehicle detection technologies have been rapidly evolved over the past decade due to the advancement of sensors and wireless communication technologies and the increasing deployment of traffic-responsive and adaptive traffic control systems, which heavily rely on robust vehicle detection. Given a variety of vehicle detection technologies available, each has its advantages and disadvantages and may or may not be appropriate for specific situations or contexts. This research study is conducted to identify the contexts appropriate for different detection technologies. High-resolution data were collected in the field from three test sites selected in Georgia. Data mining techniques were employed to identify potential factors underlying variation in detection errors of different technologies and quantify their respective effects. The quantified effects were then used to construct technical performance measures in terms of accuracy and reliability, referred to as technical performance criteria. An agency survey was also conducted in Georgia to assess nontechnical performance criteria, such as life cycle cost and ease of installation and maintenance. Both technical and nontechnical performance criteria were considered in evaluating vehicle detection technologies through a multicriteria framework. Finally, practical constraints frequently encountered in Georgia were considered as part of respective application contexts. Based on the results and findings, specific guidelines were developed to promote consistency in application of various detection technologies and to enhance efficiency and safety in traffic signal operations in Georgia.

17. Key Words: Erroneous calls, detection errors, accuracy, reliability, efficiency, safety.		18. Distribution Statement:	
19. Security Classification (of this report): Unclassified	20. Security Classification (of this page): Unclassified	21. Number of Pages: 148	22. Price:

Form DOT 1700.7 (8-69)

GDOT Research Project No. 13-26

Final Report

EVALUATION OF VEHICLE DETECTION TECHNOLOGIES FOR APPLICATIONS IN GEORGIA

Prepared by

Jidong (James) Yang, Ph.D., P.E.

Assistant Professor
Georgia Pavement and Traffic Research Center
Kennesaw State University
1100 South Marietta Parkway
Marietta, GA 30060

Sung-Hee Kim, Ph.D., P.E.

Associate Professor
Georgia Pavement and Traffic Research Center
Kennesaw State University
1100 South Marietta Parkway
Marietta, GA 30060

Bashan Zuo
Research Assistant
Kennesaw State University

Contract with

Georgia Department of Transportation

In cooperation with

U.S. Department of Transportation
Federal Highway Administration

October 2015

DISCLAIMER

The contents of this report reflect the views of the authors, who are solely responsible for the facts and accuracy of the data, the opinions, and the conclusions presented herein. The contents do not necessarily reflect the official view or policies of the Georgia Department of Transportation (GDOT), Federal Highway Administration (FHWA), and the Georgia University System. This report does not constitute a standard, specification, or regulation, and its contents are not intended for construction, bidding, or permit purposes. The use of names or specific products or manufacturers listed herein does not imply endorsement of those products or manufacturers.

ACKNOWLEDGMENTS

This project was conducted in cooperation with the Georgia Department of Transportation (GDOT) and the Federal Highway Administration. The authors would like to gratefully acknowledge the contributions of many individuals to the successful completion of this research project. This especially includes Ms. Gretel Sims, project manager at the GDOT and Mr. Alan Davis, state signal engineer at the GDOT, who have provided administrative support and technical guidance through the course of this project. Mr. Challa Bonja, Mr. Duane Farist, and Mr. Tim Cox at the City of Marietta were extremely helpful with the selection of test sites and mounting of test devices in the field. Finally, the authors would like to thank the following individuals who have provided tremendous technical supports and assistance with field installation and configuration of test devices.

Winter Horbal, Temple, Inc.
Bobby McGraw, Control Technologies
Jan Seigler, Wavetronix
Mark Zinn, Southern Lighting & Traffic Systems

EXECUTIVE SUMMARY

This study was primarily focused on evaluating the stop bar vehicle detection for actuated traffic signal operations. Six vehicle detection devices were evaluated for stop bar presence detection, including three video imaging cameras (Autoscope AIS-IV, RZ4 Advance WDR, and Vantage SmartSpan) and one thermal imaging camera (FC-334T), wireless magnetometers, and SmartSensor Matrix. Besides stop bar presence detection, two radar-based devices (SmartSensor Advance and Vantage Vector Hybrid) were also evaluated for indecision zone detection. High-resolution data based on a 100-millisecond sampling interval were collected at three test sites located in City of Marietta, Georgia. The data set covers approximately 32 days in November 2014 through March 2015 with a wide range of weather and environmental conditions. Two technical criteria, accuracy and reliability, were specifically defined and used to evaluate the technical performance of stop bar detection devices. The accuracy is defined by a "mean" error under the "ideal" or "desirable" conditions. Reliability is defined by collective adverse marginal effects of applicable factors when deviating from the "ideal" conditions.

Based on the study, the most accurate device is the RZ4 Advance WDR camera (error = 0.117 seconds), followed by the wireless magnetometer (0.360 seconds), the Autoscope AIS-IV camera (0.572 seconds), the FC-334T thermal imaging camera (0.658 seconds), the SmartSensor Matrix (0.699 seconds), and the Vantage SmartSpan camera (1.416 seconds). It should be noted that the RZ4 Advance WDR camera was mounted higher than the other devices at test site 2, which likely contributes to the smaller error.

The most reliable device is the wireless magnetometers, which appears to be robust to the weather and environmental conditions experienced. It is followed by the SmartSensor Matrix (collective adverse marginal effect = 0.297 seconds), the RZ4 Advance WDR camera (0.396 seconds), the Autoscope AIS-IV camera (0.672 seconds), the FC-334T thermal imaging camera (0.727 seconds), and the Vantage SmartSpan camera (4.901 seconds).

Besides the technical performance criteria, i.e., accuracy and reliability, other nontechnical performance criteria, such as life cycle cost and ease of installation and maintenance, were also considered through a multicriteria evaluation framework. A composite score was computed for each device by considering both technical and nontechnical performance criteria. The composite score was computed on a 0-100 point scale, where a higher score indicates a better overall performance. The computation was carried out for each device with respect to two commonly used detection schemes together with eight typical intersection geometries.

Among the three mast arm mounted cameras, the RZ4 Advance WDR camera scored the highest (in the range of 74.88-80.22), followed by the FC-334T thermal imaging camera

(73.00-78.34) and Autoscope AIS-IV camera (72.75-78.42). In most cases, the SmartSensor Matrix scored the highest (79.58-85.68) among all six stop bar detection devices. The wireless magnetometer has the second highest score (74.64-84.65) in most cases where the detection is less intensive (detection scheme 1). However, the score decreases (65.12-81.48) as more intensive detection is required (detection scheme 2). Among the six devices, the Vantage SmartSpan camera scored the lowest (36.03-42.32), which is mainly due to its much lower reliability rating compared to other devices.

For the indecision zone detection, two radar devices, SmartSensor Advance and Vantage Vector Hybrid, were compared to each other by referencing the existing setback loop. A count of consistency is retained if both radar devices either detect or not detect a vehicle conditional upon the same vehicle had been detected by the setback loop located at the upstream entry point to the indecision zone such defined. The field data indicates an 87 percent consistency between the two devices. Note that both radar-based devices provide continuous detection of vehicles traversing the indecision zone. To evaluate the duration of detection over the indecision zone, the setback loop, a point detector, cannot be used as a benchmark. Instead, the detection durations rendered by the two radar devices were compared to each other. Hypothesis tests (paired t and Wilcoxon signed-rank) were performed, indicating the detection durations by the two radar devices are significantly different.

TABLE OF CONTENTS

List of Tables

List of Figures

1. INTRODUCTION

Vehicle detection technologies have been rapidly evolved over the past decade due to the advancement of sensors and wireless communication technologies and increasing deployment of traffic-responsive and adaptive traffic control systems, which heavily rely on robust vehicle detection. Each vehicle detection technology has its advantages and disadvantages and may or may not be appropriate for specific situations or contexts. The traditional inductive-loop detector was introduced in the early 1960s and since then has become the most widely used vehicle sensor in modern traffic signal control systems. With a long history of deployment, inductive-loop detectors have exposed many practical issues. They are relatively inexpensive and effective for installation on new pavements, but are labor intensive for maintenance over time and cause traffic disruption for repair. Additionally, resurfacing of roadways or utility repairs may require reinstallation of these types of sensors. Because of those concerns, less intrusive or non-intrusive vehicle detection technologies have emerged to replace inductive loops. Among those, wireless magnetometers have been extensively used because they can be quickly installed, cause less damage to the pavement, and are less vulnerable to pavement distresses. Video imaging detection is another popular alternative and has been used by many agencies in the U.S. Traditional video detection requires mast arm installation and detection accuracy is largely influenced by visibility and lighting conditions. Comparing to traditional video detection cameras, thermal imaging cameras aim to resolve the issues associated with lighting conditions by producing images of "heat" radiation based on temperature differences between objects. However, they may not be reliable during heavy rains or when temperature difference between vehicles and the pavement is small. More recently, special types of cameras have been developed to allow for mounting on span wires. Besides video detection cameras, radar-based detection technologies have also been deployed for vehicle detection. Radar detectors are robust to various lighting and weather conditions, but may require special installation accommodations, such as mounting locations. Given the more or less limitation of different technologies, there is no single technology that prevails in all possible field situations. As such, decisions on selecting detection technologies should be context-sensitive.

Some state departments of transportation (DOTs) have their own guideline for using detection technologies depending on their experience. In Georgia, the preferred method of detecting vehicles at traffic signals is the inductive loop detector [GDOT signal design guideline, 2014]. However, consideration has been given to other types of nonintrusive detectors where loops are not feasible, such as on bridge decks, or are impractical where pavement surface conditions are poor. In those circumstances, a possible alternate

technology is Intersection Video Detection System (IVDS) as specified in Special Provision Section 937 of the GDOT Standard Specifications – Construction of Transportation Systems.

Besides IVDS, other detection technologies, such as wireless magnetometers, SmartSensor, and thermal imaging cameras, have seen increasing deployment in Georgia and in other states as well. Given the availability of a wide range of technologies for vehicle detection, and their mixed advantages and disadvantages under various conditions or situations, there is an increasing need for identifying application contexts appropriate for different detection technologies or devices.

1.1 Background

Many research studies have been undertaken to evaluate vehicle detection technologies for freeway or arterial applications. For freeway applications, the sensors have typically been used to gather traffic flow (e.g., counts), speed, occupancy, and vehicle classification data. Those data are primarily used for planning and engineering studies, or as live feeds to Advanced Traveler Information Systems (ATIS).

On the other hand, arterial applications have been focused on vehicle detection at signalized intersections, which provides inputs to local traffic controllers for actuated traffic signal control and/or relayed to a traffic management center (TMC) for region-wide traffic management. Vehicle detection for actuated signal operations is a real-time application and requires a higher level of accuracy and reliability. There are two typical applications of vehicle detection for actuated signal control: (1) stop bar detection, and (2) advance detection. Stop bar detection often uses presence mode for the detector with non-locking mode for the controller to detect the presence of a vehicle(s) at the stop bar. The accuracy and reliability of stop bar detection is directly related to the efficiency of traffic signal operations. Those detectors are used to call (initiate) and/or extend a phase subject to other timing parameters, such as passage time, minimum and maximum greens, for improved signal operations. The errors associated with vehicle detection usually lead to a reduction in operational efficiency. For example, if a vehicle waiting at the stop bar is not detected, the corresponding phase could be skipped, resulting in extended waiting time for the vehicle and those arriving afterward. On the other hand, if the detector places an erroneous call in absence of a vehicle at the stop bar, the phase will be initiated without legitimate demand, resulting in extended waiting time for other vehicles in conflicting phases. The former is referred to as a "missed" call and the latter is referred to as a "false" call. Once a vehicle is detected upon its arrival at the stop bar and a call (non-locking) is placed to the controller, two other types of errors could occur afterward. If the call is erroneously dropped before the departure of the vehicle, it is referred to as a "dropped" call. Conversely, if the call continues to be held after the departure of the vehicle, it is referred to as a "stuck-on' call. All four types of erroneous calls could reduce the efficiency

of traffic signal operations. Detailed discussions about the four types of erroneous calls are provided in Section 2.

Different from the stop bar detection, advance detectors are normally used for two types of applications: volume density and indecision zone. For the volume-density application, small-size zones, such as 6ft × 6ft inductive loops, are often installed in the through lanes in advance of the stop bar. These advance loop detectors serve as a counter to estimate the required time to add to the initial green during the red and respond to the density of upstream traffic flow during the green by gradually reducing the passage time to a predetermined minimum value so to effect smoother operations. Typically, stop bar detectors are not used for through lanes if volume-density detectors have been installed. Any detection errors from volume-density detectors may undermine the efficiency of traffic signal operations and pose safety concerns as well. Inductive loops, more recently wireless magnetometers, have been predominantly used for the volume-density application.

In contrast, the indecision zone application aims to properly terminate green for high-speed approaches so to minimize drivers' exposure to indecision zones. In this case, safety is of main concern. For example, if an approaching high-speed vehicle was not detected in the indecision zone, the green phase could be ill-timely terminated and result in potential collisions of left turn, angle, or rear-end types. Similar to the volume-density application, inductive loops or wireless magnetometers have been commonly used for the indecision zone application. Many nonintrusive detection technologies have also been experimented, but have not been widely adopted for the indecision zone application. Middleton et al. (2008) showed some evidences of unacceptable performance of video camera detectors for indecision zone detection. More recently, radar-based detectors have been developed for the indecision zone application, which permit continuous tracking of vehicles in the indecision zone.

1.2 Objective and Scope

The main objective of this research study is to evaluate vehicle detection technologies for actuated traffic signal control and to identify contexts appropriate for their applications. The focus of the study is on the stop bar presence detection. However, potential use of emerging nonintrusive detection technologies, such as radar-based detectors, for indecision zone detection will also be examined. Based on discussion with GDOT staff, eight vehicle detection devices (six for stop bar detection and two for advance detection) were selected for evaluation and are presented in Table 1.1. For practicality, the detection technologies selected for this study are either currently used or under consideration for deployment in Georgia.

Table 1.1 Vehicle Detection Devices for Evaluation

Stop Bar Detection Application		Advance Detection Application	
Device	**Technology**	**Device**	**Technology**
Wireless Magnetometer (Sensys)	• 3-axis magnetic field sensing (128 Hz sampling rate) • Frequency Band: 2400 to 2483.5 MHz (ISM unlicensed band)	SmartSensor Advance (Wavetronix)	Radar 10.5–10.55 GHz (X-band)
SmartSensor Matrix (Wavetronix)	Radar 24.0–24.25 GHz (K-band)	Vantage Vector Hybrid (Iteris)	Radar 24GHz (K-band)
FC-334T Thermal Imaging Camera (Flir)	Thermal Imaging		
RZ4 Advanced WDR Camera (Iteris)	Video Imaging		
Autoscope AIS-IV Camera (Econolite)	Video Imaging		
Vantage SmartSpan Camera (Iteris)	Video Imaging		

1.3 Organization of the Report

The research approach is first discussed in Section 2, followed by a review of literature and technologies in Section 3. An agency survey on the vehicle detection technologies has been conducted in Georgia and is presented in Section 4. Section 5 describes the selection of test sites and the setup of test devices. Data acquisition, including data logging and retrieval, is presented in Section 6. Section 7 discusses how the data acquired in the field were compiled, coded, and merged for analysis purposes. Section 8 presents data analysis in three levels of increasing complexity. Following the data analysis, a multicriteria evaluation was conducted and the results are presented in Section 9. Based on the analysis results in Sections 8 and 9, specific application contexts were identified, general guidelines were developed for different detection technologies and are presented in Section 10.

2. RESEARCH APPROACH

This section discusses the research approach. First, literature and practices pertaining to the scope of this study are reviewed. To learn what vehicle detection devices are currently used in Georgia, an agency survey is conducted. For the sake of practicality, this study is focused on the technologies or devices currently used in Georgia. Emerging technologies currently being tested (e.g., span wire mounted cameras) are also considered.

2.1 Study Approach - Experimental versus Observational

Experimental studies typically require a well-controlled environment, such as in a laboratory, and randomly assigned groups by targeted factors, which are impractical and generally not supported by highway agencies due to financial accountability. In other words, any changes or improvements to the existing highway systems should not be "experimental", but made to the public interest and/or benefits. As such, an observational study approach was used.

1. Selection of test sites

   All test sites selected in this study are existing signalized intersections with inductive loop detectors. The test devices are mounted and connected to the existing cabinet for tracking purposes, but are not connected to the controller, meaning that the controller still takes inputs from the existing loop detectors and maintains existing signal operations. This is to ensure no interruption with the existing signal operations during testing periods.

2. Installation and configuration of test devices at test sites

   All test devices are installed at test sites by professional technicians to meet specific site conditions. Detection cameras will be mounted at typical heights (e.g., 21 feet -26 feet) with a reasonable view for the purpose of stop bar detection. They are not intended for counting vehicles or measuring speeds, which otherwise would require a higher mounting location.

3. Field data acquisition

   After the installation of test devices, the data acquisition equipment is connected to the cabinet for monitoring and logging the outputs of all detectors (including both inductive loops and test devices), together with traffic signal indications (i.e., green, yellow, and red) in real time. A digital video recorder (DVR) is used to record videos from detection cameras. Detailed field setups for data acquisition are presented in Section 5.

2.2 Performance Criteria

Regardless of practical drawbacks, inductive loops have been recognized as the most accurate and reliable vehicle detector if working properly and thus used as the benchmark or ground truth for evaluating other detection technologies selected for this study. To ensure proper functioning of the inductive loops, they are crosschecked with the videos recorded during the field test.

2.2.1 Definition of Detection Errors

To measure the performance of test devices, four error types in terms of erroneous calls are defined in Table 2.1 in reference to the status of the corresponding loop detector immediately before and after a discrepancy.

Table 2.1 Definition of Detector Errors (Erroneous Calls)

Status Change	Type of Erroneous Calls							
	Associated with initiation of a call (0 to 1)				Associated with termination of a call (1 to 0)			
	Missed Call		False Call		Stuck-on Call		Dropped Call	
	Loop	Device	Loop	Device	Loop	Device	Loop	Device
Before (t -)	0	0	0	0	1	1	1	1
After (t +)	1	0	0	1	0	1	1	0

Notes:
Detector status "0" – off, indicating absence of vehicle(s) or no call.
Detector status "1" – on, indicating presence of vehicle(s) or a registered call.

Assuming the correct detection of the inductive loop detector, a missed call is defined as the loop detector registered a call (status =1) while the test device did not (status =0). A dropped call is defined as a previously registered call was released by the test device but still held by the loop detector (status = 1). A false call is defined as the test device registered a call but the loop detector did not. A stuck-on call is defined as the loop detector released a previously registered call while the test device still held the call. These four types of detection errors or erroneous calls are graphically illustrated in Figure 4.1 for stop bar presence detection.

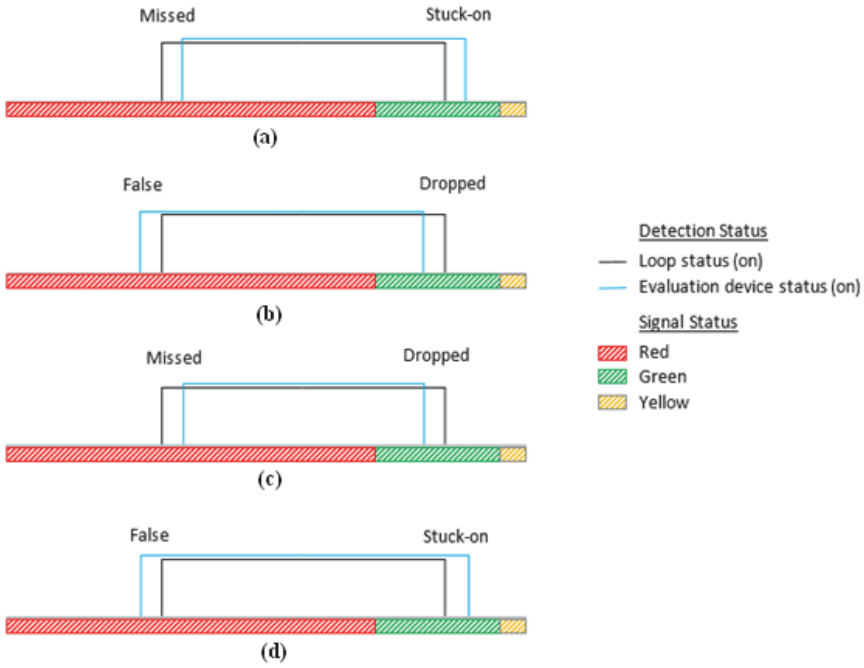

Figure 2.1 Illustration of the types of detection errors or erroneous calls

As seen in Figure 2.1, the black rectangle indicates the duration that the loop detector was occupied by a vehicle(s); the light blue rectangle indicates the duration of same vehicle(s) being detected by the test device. The coincidence or overlapping of the two rectangles indicates no error. A discrepancy between the two rectangles could result in four types of errors or erroneous calls depending on where it has occurred. By referencing the beginning (left-side edge) of the black rectangle, the lagging blue rectangle indicates a missed call (Figure 2.1, (a) and (c)), the leading blue rectangle indicates a false call (Figure 2.1, (b) and (d)). By referencing the end (right-side edge) of the black rectangle, the early ending of the blue rectangle indicates a dropped call (Figure 2.1, (b) and (c)) and the late ending of the blue rectangle indicates a stuck-on call (Figure 2.1, (a) and (d)). Based on this definition, it becomes apparent that the occurrence and magnitude of the four error types largely depend on the configuration of detection zones in the field. Although not shown in Figure 2.1, an isolated single rectangle (i.e., no overlapping) indicates either a complete missed call (an isolated black rectangle) or a complete false call (an isolated blue rectangle).

2.3 Performance Evaluation

Depending on detection technologies, the occurrence and magnitude of erroneous calls may vary. For example, the erroneous calls for a video camera is largely governed by the mounting location (such as aspect ratio, offset, etc.), the size and location of detection zones, and may also be influenced by many other factors, such as vehicle mix (color and size) in the traffic flow, uneven shade or shadow, occlusion, visibility, lighting conditions (day, night, and street light), glare and reflections, wind direction and speed, and various weather events (e.g., rain, fog, snow, etc.). This implies that a detection error is practically

inevitable for video imaging cameras. Similarly, other nonintrusive detection technologies may be susceptible to varying weather and environmental conditions because of greater separation between the detectors and the target objects (i.e., vehicles). As such, it is practically important to identify influential factors and proper contexts for application of nonintrusive detection technologies. Besides the technical performance in terms of detection errors, agencies are also interested in some other nontechnical performances, such as life cycle cost and ease of installation and maintenance. Those aspects are also evaluated through a multicriteria framework. Once field data are collected, the following steps are undertaken.

1. Data Coding and Compilation

   The raw data sampled at the 100-millisecond interval are aggregated by signal cycle and the average detection error is computed by type and compiled with concurrent weather and environmental variables.

2. Data Analysis

   The data analysis is focused on the technical performance in terms of detection errors. Three levels of analysis are conducted in an order of increasing complexity. For level 1 analysis, simple descriptive statistics are generated and temporal errors are plotted along with corresponding weather and environmental conditions. For level 2 analysis, conditional inference trees are used to partition errors. For level 3 analysis, regression models are developed to quantify the marginal effects of specific factors.

3. Multicriteria evaluation

   Based on the regression models, marginal effects of pertaining factors are estimated and used to evaluate the technical performance of deferent detection devices. The technical performance criteria, together with nontechnical performance criteria (e.g., life cycle cost and ease of installation and maintenance), are considered through a multicriteria framework.

4. Identification of application contexts

   Based on the analysis results, specific contexts appropriate for different vehicle detection technologies are identified.

3. REVIEW OF LITERATURE AND VEHICLE DETECTION TECHNOLOGIES

3.1 Literature Review

Many research studies have been conducted to evaluate various vehicle detection technologies. Majority of the previous studies had been focused on single or a limited number of technologies. Simple statistical methods (e.g., hypothesis tests) have been typically used. A comprehensive literature review has been conducted and the most recent studies pertaining to the scope of this research are discussed below. An expanded list of literature reviewed is presented in Table 3.1.

Medina et al. (2012) conducted a study to evaluate smart sensor vehicle detectors at intersections under normal weather conditions. Two products, Wavetronix and Intersector, were evaluated. Results were presented in terms four types of errors (false, missed, stuck-on, and dropped calls). At the stop bar, at least 94% of detections for Wavetronix and 96% for Intersector were correct. At stop bar zones, the overall occurrence of false calls for Wavetronix ranged from 0.56% to 1.62%. Missed calls vary depending on the zones. Also, stuck-on calls and dropped calls were only observed in certain zone. For Intersector, false calls ranged from 1.4% to 3.56% and missed calls ranged between 0.05% and 0.27%. Stuck-on calls ranged from 0.92% for 2.83% and dropped calls were very low (0% and 0.19%). At the advance zones, at least 91% of detections for Wavetronix and 99% for Intersector were correct. For the advance zone, a direct comparison of the two systems was not performed because Wavetronix covered all three lanes combined, but Intersector had one zone covering only the center lane. Wavetronix did not have any stuck-on or dropped calls, missed calls were 1.07%, and false calls were 8.29% for the summer and fall datasets combined. Intersector had no dropped calls, 0.04% stuck-on calls (only one call), 0.8% missed calls, and 0.7% false calls.

Medina et al. (2011) evaluated the Sensys wireless vehicle detection system under adverse and normal weather conditions. A comparison of the results from the datasets collected in adverse weather conditions and the datasets collected in the fall season with no rain/snow and dry pavement (modified setup) showed no significant effect in the functioning of the sensors. However, the change in the driving patterns due to snow and rain may result in an increase in the incidence of false calls, particularly those due to vehicles in the adjacent lane (as vehicles may be off-centered in the marked traveled lanes). This increase in the false calls has been observed to be up to 8% for a particular zone at the stop bar (in snow conditions), but it was also as low as 2% for a different zone.

Day et al. (2010) conducted a field study to evaluate wireless magnetometers for each of two left-turn pockets at an actuated, coordinated signalized intersection, discrepancies between the detection and non-detection states were quantified with high resolution log data of traffic events. Wireless magnetometers were found to perform similarly to loops in

relation to missed calls and had a slightly higher tendency to generate false detection calls. Detection state changes in the wireless magnetometers had typical (85th percentile) reporting latencies of 0.2 s or less for activation and 0.5 s or less for state termination. The paper concluded by recommending 8-ft spacing of the sensors adjacent to the stop bar to minimize missed calls.

Middleton et al. (2010) proposed a video image vehicle detection systems (VIVDS) test concept and a set of performance measures that can be incorporated in future purchasing decisions and used to uniformly evaluate VIVDS products. The test concept acknowledged the stochastic detection characteristics of VIVDS rather than the more precise detection characteristics of point detectors. It aimed to define an improved framework for Texas Department of Transportation (TxDOT) and other agencies to use for procurement and testing. In a different study, Middleton et al. (2008) showed some evidence of unacceptable video detector performance for dilemma zone protection. Based on the preliminary findings from data collected at one test site, the detection discrepancies between video imaging vehicle detection systems and in-pavement sensors are significantly different. It was stated that these discrepancies are not always critical to safety but would increase intersection delay.

Rhodes et al. (2005) evaluated the accuracy of stop bar video vehicle detection at signalized intersections. A test intersection in Indiana was used. Different locations of cameras were studied. A small incremental increase in performance was observed when the camera was mounted farther from the pole as cross-lane occlusion events are minimized because the view will be of a head-on perspective rather than a side view. However, it was stated that this marginal improvement likely does not justify the additional expense of mast arm, pole, and pole foundation associated with this camera location.

Bonneson and Abbas (2002) developed a manual to assist engineers with the planning, design, and operation of a VIVDS. The manual includes specific guidelines on the camera location (offset and height) and detection zone layout.

To gather high-resolution real time data, Abdel-Rahim and Johnson (2008) presented a data logging device that can be used in real-time traffic monitoring at signalized intersections. The data logging device can be connected to traffic cabinets using different connection modes. The data logging device logs the status of all input and output communication channels and updates their status continuously. The device was used to generate continuous time-occupancy and signal indication graphs for different movements. It was also used to estimate average delay and speed values for signalized intersection approaches using detector occupancy and signal indication data. A similar data acquisition approach was adopted in our study to acquire high-resolution and real-time data, which is discussed in Section 6.

Table 3.1 Summary of Recent Literature

Author(s)	Title	Year	Devices Evaluated	Application	Criteria	Factors Considered
Dan Middleton, Mark Shafer, Debbie Jasek	Initial Evaluation of the Existing Technologies for Vehicle Detection	1997	Video image detection system, passive infrared, active infrared, passive magnetic, radar, Doppler microwave, passive acoustic, loop	Stop Bar, Advance	Functional quality, reliability, cost	Weather, lighting
Raghuram Dharmaraju, David A. Noyce, Joshua D. Lehman	An Evaluation of Technologies for Automated Detection and Classification of Pedestrians and Bicycles	2001	Microwave, Ultrasonic and Acoustic, Passive Infrared, Active Infrared, Video Image Sensing, Piezoelectric	Stop Bar, Advance	Evaluating and promoting new bicycle- and pedestrian-counting technologies by synthesizing the results of current pilot-testing efforts	Different types of object
Dan Middleton, Ricky Parker	Vehicle Detector Evaluation	2002	Peek ADR-6000, Autoscope Solo Pro, Iteris Vantage, RTMS Doppler Radar, SAS-1, 3M microloop	Stop Bar, Advance	Classification accurary, speed accurary, presence, occupancy, count accuracy	Peak hour, avg speed, different lane
Karl Zimmerman, James A. Bonneson, Dan Middleton, and Montasir M. Abbas	Improved Detection and Control System for Isolated High-Speed Signalized Intersections	2003	D-CS(multiple advance detector system)	Advance	A dynamic dilemma zone allocation system with a control algorithm	Cycle length, control delay, percentage of vehicles stopping, percentage of vehicles running the red light, percentage of vehicles in the dilemma zone at yellow onset
Peter T. Martin, Yuqi Feng, Xiaodong Wang	Detector Technology Evaluation	2003	Loop, magnetic, pneumatic road tube, active infrared, passive infrared, microwave radar, ultrasonic, passive acoustic, and	Stop Bar, Advance	Data type, data accuracy, cost, and ease of installation and maintenance	Traffic volume, penetration, wind, temperature, light
Dr. Peter T. Martin, Gayathri Dharmavaram, Aleksandar Stevanovic	Evaluation of Udot's Video Detection Systems---System's Perfoemance in Various Test Conditions	2004	Loop, Traficon NV, Autoscope, VideoTrak, Vantage	Stop Bar	Percentage of correct detection(as detected by loop), percentage of discrepant call, percentage of important discrepant calls	Weather, lighting, firmware, processor's algorithms, camera location, camera height, adjusting the focus,different phase(red green yellow)
Jialin Tian, Mark R. Virkler, and Carlos Sun	Field Testing for Automated Identification of Turning Movements at Signalized Intersections	2004	Camera	Stop Bar	Turning-movement counts	Camera location, camera angle, intersection geometrics, sensitivity of the video detection system, occlusion, traffic conditions, shadows, pedestrians, bicylists
Avery Rhodes, Darcy M. Bullock, James Sturdevant, Zachary Clark, and David G. Candey, Jr.	Evaluation of The Accuracy of Stop Bar Video Vehicle Detection at Signalized Intersections	2005	Camera(Econolite Solo Pro video detection unit)	Stop Bar	Camera error (missed and false) and loop error	Distance from strain pole, weather, traffic, lighting conditions
JD Margulici, Samuel Yang, Chin-Woo Tan, Pulkit Grover, and Andre Markarian	Evaluation of Wireless Traffic Sensors by Sensys Networks, Inc.	2006	Sensys wireless detection system	On Road	Installation procedures, wireless communications performance, data quality; i.e., completeness and validity, accuracy	Volume , speed, and occupancy
Zong Tian, Thomas Urbanik	Green Extension and Traffic Detection Schemes at Signalized Intersections	2006	Akcelik(softwear)	Advance	Average green extensions	Maximum allowable headway, lane volume distribution, arrival patterns, number of lanes, vehicle types
Dan Middleton, Ricky Parker, and Ryan Longmire	Investigation of Vehicle Detector Performance and ATMS Interface	2007	Autoscope camrea, Iteris Vantage camera, Peek ADR-6000 loop, SAS-1 Acoustic, Sensys Magnetometer, SmartSensor Radar, Traficon camera	Stop Bar, Advance	Cost, accuracy, and ease of setup	Different time (peek, off-peak)
Juan C. Medina, Madhav Chitturi, Rahim F. Benekohal	Illumination and Wind Effects on Video Detection Performance at Signalized Intersections	2007	Autoscope camrea, Peek camrea, Iteris camrea	Stop Bar	Number of four types error calls(false missed stuck-on dropped)	Day/night, shadows, windy
Dan Middleton, Eun Sug Park, Hassan Charara, and Ryan Longmire	Evidence of Unacceptable Video Detector Performance for Dilemma Zone Protection	2008	Loop, Sensys Networks Magnetometers, Iteris, Autoscope, Traficon	Advance	Time discrepanicies between vivdss and in-pavement sensor	Lighting, vehicle volume, camera location
Ahmed Abdel-Rahim, Brian k. Johnson	An Intersection Traffic Data Collection Device Utilizing Logging Capabilities of Traffic Controllers and Current Traffic Sensors	2008	Data Logging Device, VISSIM simulation network	Stop Bar (Pulse & Presence)	Time-occupancy, delay, speed	Different flow rate, stopped and non-stopping vehicles in cycle, volume

Table 3.2 Summary of Recent Literature (Continued)

Author(s)	Title	Year	Devices Evaluated	Application	Criteria	Factors Considered
Dan Middleton, Hassan Charara, and Ryan Longmire	Alternative Vehicle Detection Technologies for Traffic Signal Systems: Technical Report	2009	VIVDS camera, loop, Wavetronix Advance, Sensys Networks Magnetometers, GTT Magnetometers	Stop Bar, Advance	Detection accuracy, equipment reliability, initial costs, user-friendliness	Field site, traffic volumes, approach speeds
Christopher M. Day, Hiromal Premachandra, Thomas M. Brennan, James R. Sturdevant, Darcy M. Bullock	Operational Evaluation of Wireless Magnetometer Vehicle Detectors at a Signalized Intersection	2009	Loop, Sensys Networks Magnetometers	Stop Bar, Advance	Duration of discrepancy, activation and termination latency	Dection thresholds, different phase(red green yellow), sensys position
Dan Middleton, Ryan Longmire, Darcy M. Bullock, and James R. Sturdevant	Proposed Concept for Specifying Vehicle Detection Performance	2009	Video image detection system	Advance	Stochastic variation in sensor performance	Lighting, differdent camera vendor
Dan Middleton, Ryan Longmire, Hassan Charara	Video Library for Video Imaging Detection at Intersection Stop Lines	2010, April	VIVDS camera	Stop Bar	Accuracy	Traffic/hightway conditions, camera position, weather and lighting
Dan Middleton, Ryan Longmire, Hassan Charara, Darcy Bullock	Video Library for Video Imaging Detection at Intersection Stop Lines	2010, August	VIVDS camera, loop	Stop Bar	Reaction speed (how quickly vivds detect vehicles)	Horizontal camera angle, vehicle heights and shapes, different phase(red green yellow)
Christopher M. Day, Hiromal Premachandra, Thomas M. Brennan, Jr., James R. Sturdevant, and Darcy M. Bullock	Operational Evaluation of Wireless Magnetometer Vehicle Detectors at Signalized Intersection	2010	Sensys Networks Magnetometers	Stop Bar, Advance	Duration of discrepancy	Different phase(red green yellow),
Edward J. Smaglik, Zachary Davis, R. Christopher Steele,William Nau, and Craig A. Roberts	Supplementing Signalized Intersection Infrastructure To Provide Automated Performance Measures With Existing Video Detection Equipment	2010	Traficon camera	Stop Bar	Volume-to-capacity (v/c) ratio and cumulative counts	Cost, different time, difference phase
Erik Minge, Jerry Kotzenmacher, Scott Peterson	Evaluation of Non-Intrusive Technologies for Traffic Detection	2010	Radar, Magnetic, Active Infrarer(Laser)	Road Side	Classification accurary, speed accurary	Different lane, weather, and vehicle type.
Jonathan Corey, Yunteng Lao, Yao-Jan Wu, and Yinhai Wang	Detection and Correction of Inductive Loop Detector Sensitivity Errors by Using Gaussian Mixture Models	2011	Inductive loop	Stop Bar, Advance	Accuracy	Sensitivity settings
Juan C. Medina, Rahim F. Benekohal, and Ali Hajbabaie	Evaluation of Sensys Wireless Vehicle Detection System: Results from Adverse Weather Conditions	2011	Sensys wireless vehicle detection system, loop	Stop Bar, Advance	Frequency of four types of error calls	Weather, different lane, different position, railroad factor
Karl Zimmerman, Devendra Tolani, Roger Xu, Tao Qian, and Peter Huang	Detection, Control, and Warning System for Mitigating Dilemma Zone Problem	2012	Loop	Advance	The number of vehicles in the dilemma zone, the number and percentage of vehicles requiring warning, and the number of warning events per hour	Vehicle types, vehicle volume, single loop, multiple loops
Juan C. Medina, Rahim F. Benekohal, and Hani Ramezani	Field Evaluation of Smart Sensor Vehicle Detectors at Intersections –Volume 1: Normal Weather Conditions	2012	Wavetronix Matrix, Wavetronix Advance, Intersector, loop	Stop Bar, Advance	Frequency of four types of error calls	Different vehicle tpye, vehicle volume in different time, different lane, length of the advance detection zone
J. Grossman, A. Hainen, S. Remias, D. M. Bullock	Evaluation of Thermal Image Video Sensors for Stop Bar Detection at Signalized Intersections	2012	Thermal Image Video Sensors	Stop Bar	Activation and termination errors	Day and night
Woeber W., Kefer M., Kubinger W., and Szuegyi D.	Evaluation of Daylight and Thermal Infra-red Based Detection for Platooning Vehicles	2012	Thermal Infra-red Based Detection	Detect platooning vehicles	Matching rate and error rate	Different classifers and scenarios
Iwasaki Y., Misumi M., and Nakamiya T.	Robust Vehicle Detection under Various Environmental Conditions Using an Infrared Thermal Camera and Its Application to Road Traffic Flow Monitoring	2013	Thermal Infra-red Based Detection	Detect vehicle position and movement	Correct and false detection	Various environmental conditions

3.2 Characteristics of Vehicle Detection Technologies

Inductive loops have long been used as the "standard" vehicle detector. They are relatively inexpensive. If properly installed and maintained, they are generally reliable and robust to high and low traffic volumes and various weather and light conditions. However, the long history of its use has exposed some practical drawbacks. Inductive loops are intrusive in nature. They weaken the pavement structure if installation or repair requires saw cut; cause disruption to traffic during installation and maintenance; cannot be reused if the pavement is to be milled for resurfacing. Often, cracking of pavements can easily break the wires of loops. In contrast, nonintrusive detectors are almost always safer to install at intersections than inductive loops because of the greater separation between passing motorists and the field crews installing the detectors (Middleton et al. 2008). In combating those drawbacks of inductive loops, four major technologies have emerged as practical alternatives to inductive loops and are discussed below.

3.2.1 Video Imaging Cameras

The use of video cameras or video imaging vehicle detection systems (VIVDSs) has increased dramatically due to their practical advantages over inductive loops. First, they are easier and safer to install and maintain; cause no damage to the pavement; and detection zones can be easily adjusted as needed when travel lanes are realigned or reassigned due to widening or re-marking of the pavement. One camera, if set up properly, can detect up to four or five lanes for a single approach, making it economically attractive. However, if continuous update and calibration is required for cameras to work properly, it may not provide the economic advantage over inductive loops. In addition, the video images of traffic stream can be transmitted to and viewed from a traffic management center if communication exists.

Regardless of the practical advantages, regular video cameras are susceptible to varying lighting, weather, and environmental conditions. A previous study conducted at the Jet Proportion Laboratory (JPL Pub. D-15779, 1998) indicated much higher error rates during dusk and night conditions. The study also noted that low sensitivity and resolution, improper focal length of lens, non-ideal mounting height, inadequate video signal, and lack of sun shade contributed to degraded performance of detection cameras.

3.2.2 Thermal Imaging Cameras

Thermal imaging cameras recently find their applications in the field of vehicle detection. Use of the thermal imaging technologies for vehicle detection has been evaluated by several studies (Grossman et al., 2012; Iwasaki et al., 2013; and Woeber et al., 2012). Since regular imaging cameras rely on the reflected light to generate quality images, they cannot accurately detect vehicles if there is not enough visible light, such as during the night where there is inadequate street lighting. Different from regular imaging cameras, thermal imaging cameras produce images based on difference in thermal energy emitted by objects, not visible light. Thus, they are considered to be more robust to low-light conditions.

3.2.3 Wireless Magnetometers

Wireless magnetometers have been widely deployed throughout the U.S. With no need for cabling from the cabinet to the in-pavement sensors, it is much easier to install and maintain, and cause less disruption to traffic for installation and repair as compared to inductive loops. Unlike inductive loops, wireless magnetometers can be retrieved and reused if the pavement is to be resurfaced. In addition, the directional sensors can reduce the false calls from vehicles traveling in different directions. However, because of wireless communication (unlicensed frequency band of 2400 to 2483.5 MHz) between the in-pavement sensors and an access point or a repeater, interference might occur. Also, latency might be an issue depending on field conditions. Day et al. (2009) have reported latencies of 0.2 seconds or less for activation and 0.5 seconds or less for state termination.

3.2.4 Radar-Based Detectors

Compared to detection cameras, the radar sensors are robust to different lighting conditions, and more resilient to adverse weather and environmental conditions. Some radar-based detection devices have been developed for indecision zone application that allow for continuous tracking of individual vehicles while they are traversing indecision zones based on their actual speed and the estimated time of arrival at the stop bar. An example of such an application is presented in Figure 3.1.

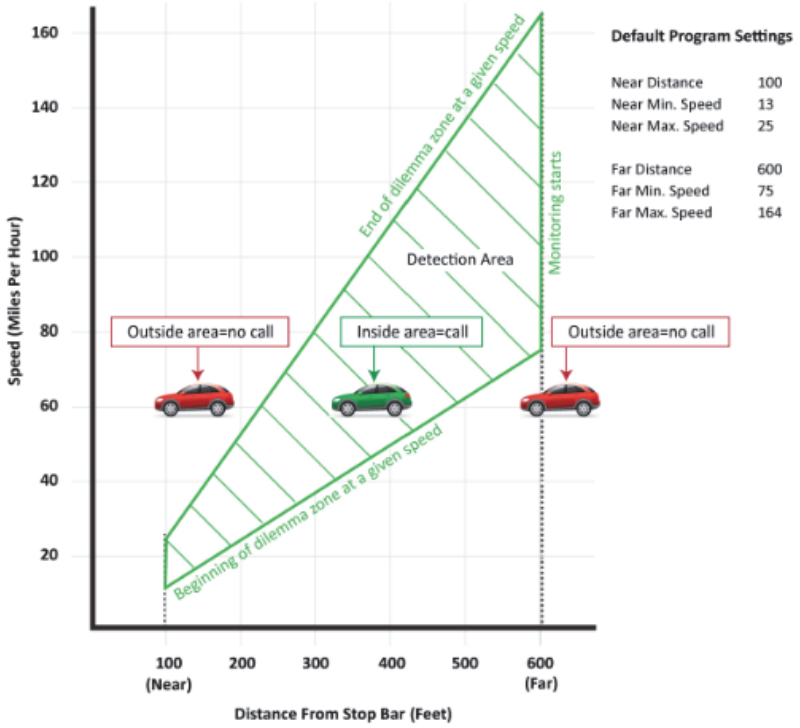

Figure 3.1 Vantage Vector's virtual dilemma zone

[Source: White Paper: The Iteris Vantage Vector® Solution Eliminates the Dilemma Zone, 2013]

The advantages and disadvantages of various detection technologies are summarized in Table 3.3.

Table 3.3 Comparison of Vehicle Detection Technologies

Detection Technologies	Advantages	Disadvantages	Typical Applications
Inductive Loop	• Highest level of accuracy • Relatively low cost of installation	• Intrusive • Extended exposure of crew to the traffic during installation/repair • Susceptible to pavement distresses • Pavement cut/traffic disruption • Maintenance issues • Unsuitable for bad pavement	Stop bar & Advance
Video Camera	• Nonintrusive • Ease of installation and maintenance • Lower installation and maintenance cost	• Specific requirements for mounting locations • Susceptible to adverse weather and environmental conditions • Occlusion issues	Stop bar
Thermal Imaging Camera	• Nonintrusive • Ease of installation and maintenance • Lower installation and maintenance cost • Robust to low light conditions.	• Specific requirements for mounting locations • Occlusion issues • May not work well during heavy rains.	Stop bar
Wireless Magnetometer	• Less intrusive (compared to inductive loops) • Ease of installation and maintenance (compared to inductive loops) • Magnetometers could be reused.	• Intrusive • Functioning of in-pavement sensors relies on an embedded battery. Heavy traffic tends to drain the battery faster. • Use unlicensed frequency band and require reliable wireless communication	Stop bar & Advance
Radar-based Sensor	• Nonintrusive • Ease of installation and maintenance • Robust to low visibility and adverse weather and environmental conditions	• Specific requirements for mounting locations • Possible signal interruption (e.g., heavy trucks) • Relatively expensive for detection applications at smaller intersections	Stop bar & Advance

4. A SURVEY OF VEHICLE DETECTION TECHNOLOGIES IN GEORGIA

An online survey was conducted through the Institute of Transportation Engineers (ITE) Georgia Section website. The survey form is included in Appendix D. Ten responses from various agencies in Georgia were received. Based on the survey, a list of vehicle detection devices currently used for stop bar and advance detection applications are summarized in Table 4.1.

Table 4.1 Vehicle Detection Devices Currently Used by Agencies in Georgia

STOP Bar Detection	Advance Detection (Dilemma Zone or Volume-Density)
Inductive loop	Inductive Loop
Econolite Autoscope Duo	Sensys wireless magnetometers
Econolite Autoscope AIS IV	MS SEDCO, Model # TC26-B
Econolite Autoscope AIS V	Wavetronix SmartSensor Advance
Econolite Autoscope AIS Color	Iteris Vantage Vector Hybrid
Econolite Autoscope Rack Vision Terra & Encore	Econolite Autoscope Rack Vision Terra & Encore
Iteris VerisCam	Iteris RZ4 Advanced WDR
Iteris RZ-4 Advanced WDR	Trafficware Valence PODS
Iteris Vantage Vector Hybrid	
Flir thermal imaging camera	
Wavetronix SmartSensor Matrix	
Sensys wireless magnetometers	
GridSmart fisheye camera	
Peek IVDS	

The survey also included questionnaire on the importance of criteria related to the performance of detection devices, such as price, ease of installation and maintenance, reliability, and accuracy. A summary of survey results are presented in Figure 4.1. Among the four criteria targeted in this survey, reliability appears to be the most important one to the agencies, followed by accuracy, ease of installation and maintenance, and price. The least important factor is price, which is not a surprise because the price can be easily offset by improved performance in terms of other criteria throughout the life cycle of the devices.

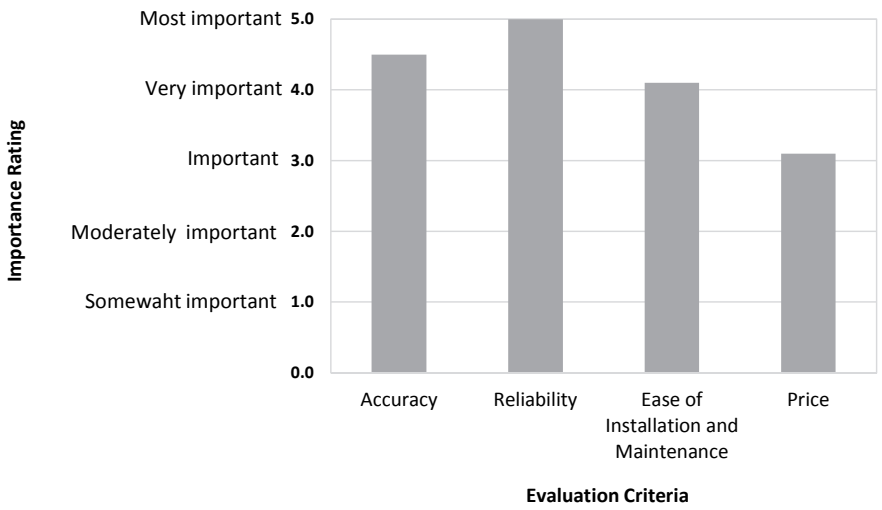

Figure 4.1 Importance of criteria for vehicle detection technologies

Given the practical experience gained through the use of three popular technologies (i.e., detection cameras, SmartSensor, and Wireless Magnetometer) in Georgia, agencies were also asked a specific question on how easy for them to install and maintain those types of devices as compared to inductive loops. The responses are presented in Figure 4.2. A 1-5 point scale was used for the survey and a score of 3 indicates same level of ease for installation and maintenance as compared to inductive loops. As shown in Figure 4.2, all three technologies exceed inductive loops in terms of this particular criterion. The SmartSensor appears to be somewhat easier to install and maintain as compared to the video cameras and wireless magnetometers.

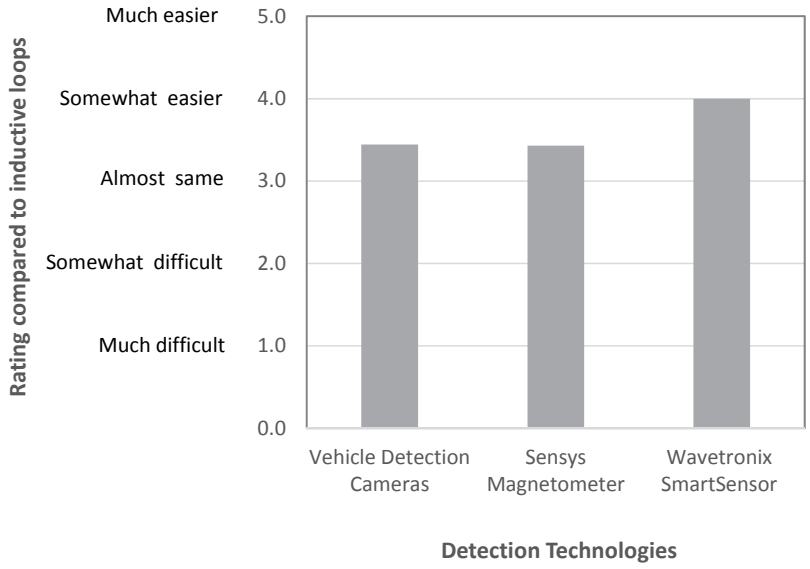

Figure 4.2 Ease of installation and maintenance as compared to inductive loops

5. SELECTION OF TEST SITES AND FIELD SETUP

5.1 Selection of Test Sites

As previously described in Section 2 (Research Approach), an observational study approach was used. For observational studies, selection of proper sites is critical to reveal potential effects of prevailing factors of concern. A range of factors common in Georgia has been considered subject to some practical constraints.

The specific factors considered as part of the site selection process include:

- Potential glare issue
- Uneven shadows by trees (presence of trees at the corners of intersections)
- Approach grade (upgrade/downgrade)
- Approach curvature (straight/curved)
- Potential mounting locations of test devices (distance to the stop bar, height, and offset)
- Traffic mix (truck volume)
- Street lighting

Besides the site-related factors, practical constraints were recognized as well, including:

- Vicinity of sites
- Availability of cabinet space for test devices and data collection equipment
- Availability of conduit space for pulling all wires required
- Existing inductive loops and/or wireless magnetometers
- Signal support (mast arm or span wire) as desired

As a result, three sites were selected within the City of Marietta in the vicinity of the Marietta campus of the Kennesaw State University. The general location of the test sites is indicated in Figure 5.1. A closer view of the sites are shown in Figure 5.2.

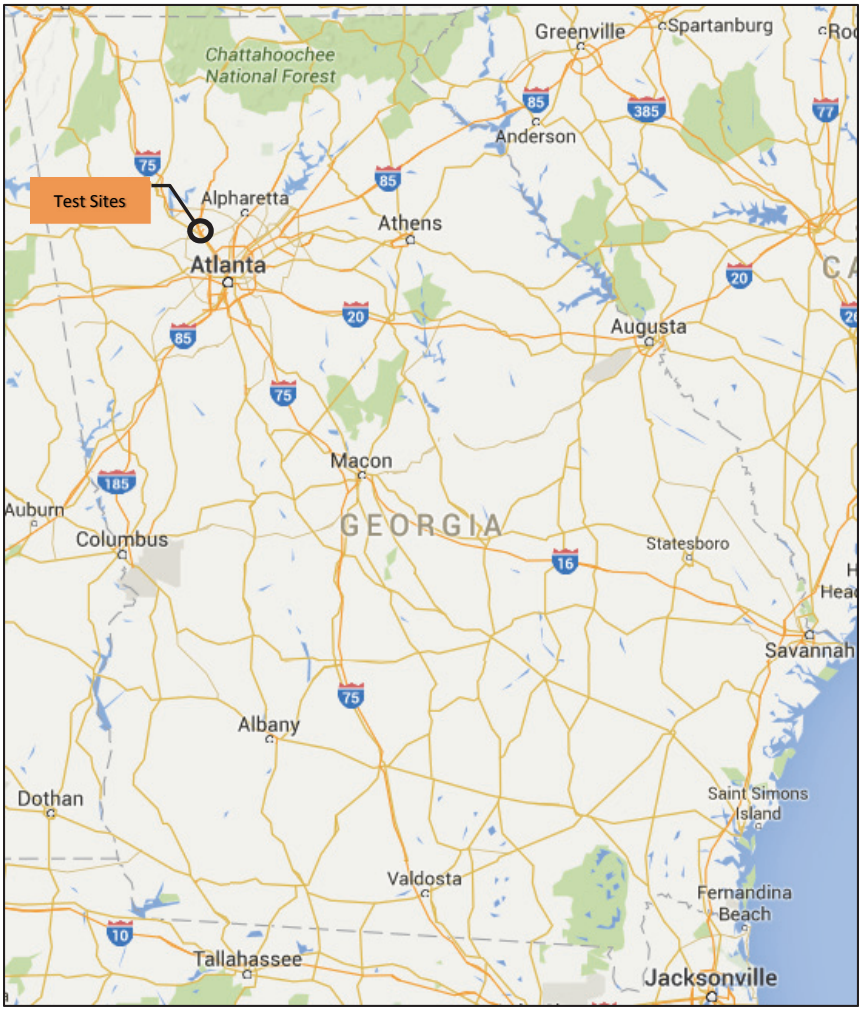

Figure 5.1 General location of the test sites (Source: Google Map data 2015)

Figure 5.2 Locations of the test sites

As seen in Figure 5.2, site 1 is located in a residential and service area, where frequent heavy trucks are expected. Site 2 is located in a residential area with little truck traffic. Site 3 is located in a commercial and service area with heavy truck traffic. Detailed characteristics of those sites are discussed subsequently.

5.2 Field Setup of Detection Devices

For the purpose of this study, specific test devices were installed at specific test sites. The characteristics of the test sites and corresponding test devices are presented in Table 5.1.

Table 5.1 Characteristics of Test Sites and Device Setups

Test Site	Site 1 N. Marietta Pkwy (Major Street) & Fairground St (Minor Street)	Site 2 Allgood Rd (Major/Minor Street) & Scufflegrit Rd (Major Street)	Site 3 S. Marietta Pkwy (Major Street) & Technology Pkwy SE (Minor Street)
Size	Large, four-leg intersection	Small, three-leg intersection	Large, four-leg intersection
Support	Mast Arm	Mast Arm	Span Wire
Devices tested	Stop bar: A, F, R, SM	Stop bar: A, F, R, SM Advance: SA, VV	Stop bar: WM, VS
Approach / Movement / Characteristics	Left turn from Major Street, westbound approach (tested device: A, F, and R) • Slight upgrade • Straight • Far side • Larger offset Left turn from Major Street, eastbound approach (tested device: SM) • Slight upgrade • Straight • Near side Note: Wavetronix SmartSensor Matrix was installed for the eastbound approach (near side) due to technical requirements and site constraints.	Left turn from Minor St., westbound approach (tested device A, F, R, SM) • Slight downgrade • Curve Through Movement, southwestbound approach (tested devices: SA, VV) • Level • Straight	• Left turn from Minor Street, northbound approach (tested device: WM) • Left turn from Major Street, westbound approach (tested device: VS)
Posted Speed	40 mph	30 mph	40 mph
Traffic Volume	High truck volume	Low truck volume (predominately passenger cars)	Northbound approach: low truck volume Westbound approach: high truck volume
Street Lighting	Ambient street lighting	Absence of street lighting	Street lighting
Other Effects	• Possible glare (sunny days in the morning) • More susceptible to wind	• Uneven shadow casted by the trees (sunny day in the afternoon) • Possible glare (sunny day in the morning) • Less susceptible to wind	• Possible glare (westbound approach, sunny days in the morning) • More susceptible to wind

Practical Constraints / Opportunities	Given the limited space of existing conduits at this site, the cameras were installed one at a time at the same location and height.	Ample space and extra conduits are available at this site, which allows all cameras to be installed at the same time. Vendors/distributors were present at the same time to install and configure their devices in such a way they deemed as appropriate.	At the time of the field test, the City of Marietta was in the process of replacing all existing loops with wireless magnetometers at this site. This technology transition allows the research team to install wireless magnetometers in the northbound left turn lane within the confine of the existing loop. Note: the inductive loops for the northbound through lane had already been replaced with wireless magnetometers.
Site Setup and Adjustment Made During the Test	Cameras were installed one at a time at the same location on the mast arm. The FC-334T thermal imaging camera was initially mounted on a longer riser and adjusted later to reflect the same height of other cameras. The RZ4 Advanced WDR camera was adjusted during the test by reducing sensitivity and adding pedestrian screening. <u>Height of Mount:</u> • Autoscope AIS-IV: 21'11" • FC-334T: 21'11" & 26' • RZ4 Advanced WDR: 21'11" • Smart Sensor Matrix 18"	After noticing some relatively large false calls, the size of the detection zone for the Autoscope AIS-IV camera was adjusted (reduced). <u>Height of Mount:</u> • FC-334T: 22' • Autoscope AIS-IV: 22' • RZ4 Advanced WDR: 26' • SmartSensor Matrix: 18'1" • SmartSensor Advance: 21'2" • Vantage Vector Hybrid: 21'2"	After observing some large stuck-on calls, a repeater was added to the pole (mounting height: 24' 8") at the southwest corner of the intersection.

Letter code for test devices:

A – Autoscope AIS-IV Camera
F – FC-334T Thermal Imaging Camera
R – RZ4 Advanced WDR Camera
VV –Vantage Vector Hybrid
SM – SmartSensor Matrix
SA – SmartSensor Advance
WM – Wireless Magnetometer
VS – Vantage SmartSpan Camera

The technical personnel representing each test device were informed of the purpose of this research study, and participated in and assisted with the field installation and configuration of their respective devices to meet the specific site conditions for proper operations of the devices.

5.2.1 Test Site 1 – North Marietta Parkway and Fairground Street

The intersection of North Marietta Parkway and Fairground Street was the first test site. Figure 5.3 shows a picture taken in the field. At this site, three test cameras were mounted one at a time at the same location on the mast arm as indicated in the picture. For the FC-334T camera, it was first mounted on a longer riser (mounting height = 26'), and then lowered to the same mounting height (21'11") of the other two cameras.

Figure 5.3 Field setup at site 1

The SmartSensor Matrix detector was installed on the same mast arm, but at different location as indicated in Figure 5.3. This setup was recommended by the professional technicians representing the device. It should be noted that all three cameras were mounted to detect the same westbound left turn movement (far side). But, the SmartSensor Matrix detector was mounted to detect the eastbound left turn movement (near side) considering the technical requirements of the device and site constraints. A three-dimension aerial view of the field setup is illustrated in Figure 5.4 and a plan view is shown in Figure 5.5.

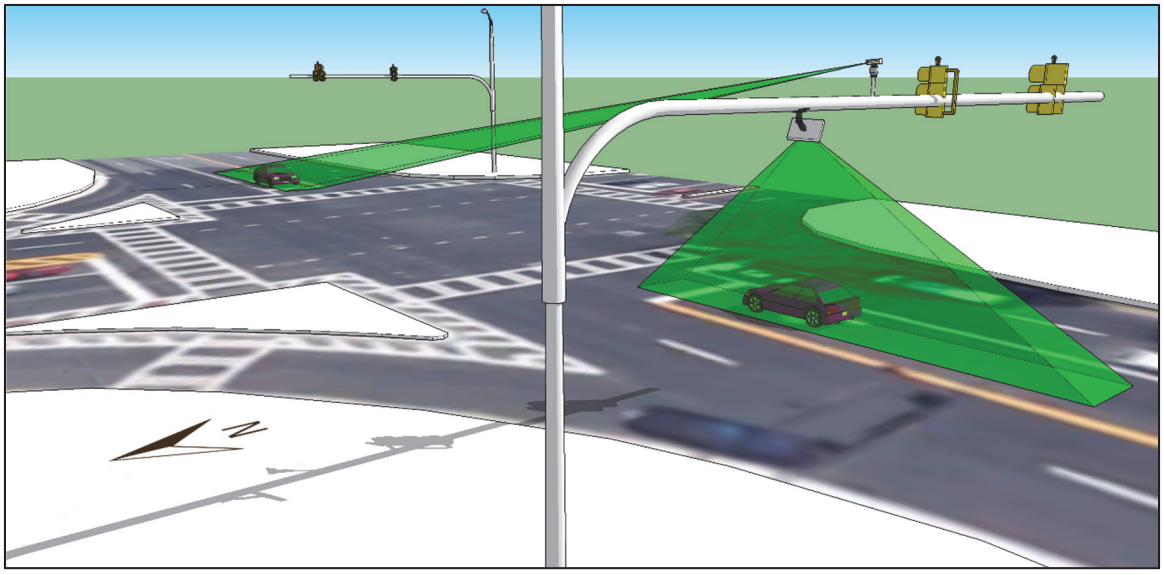

Figure 5.4 Three-dimension illustration - field setup of stop bar detection devices at site 1

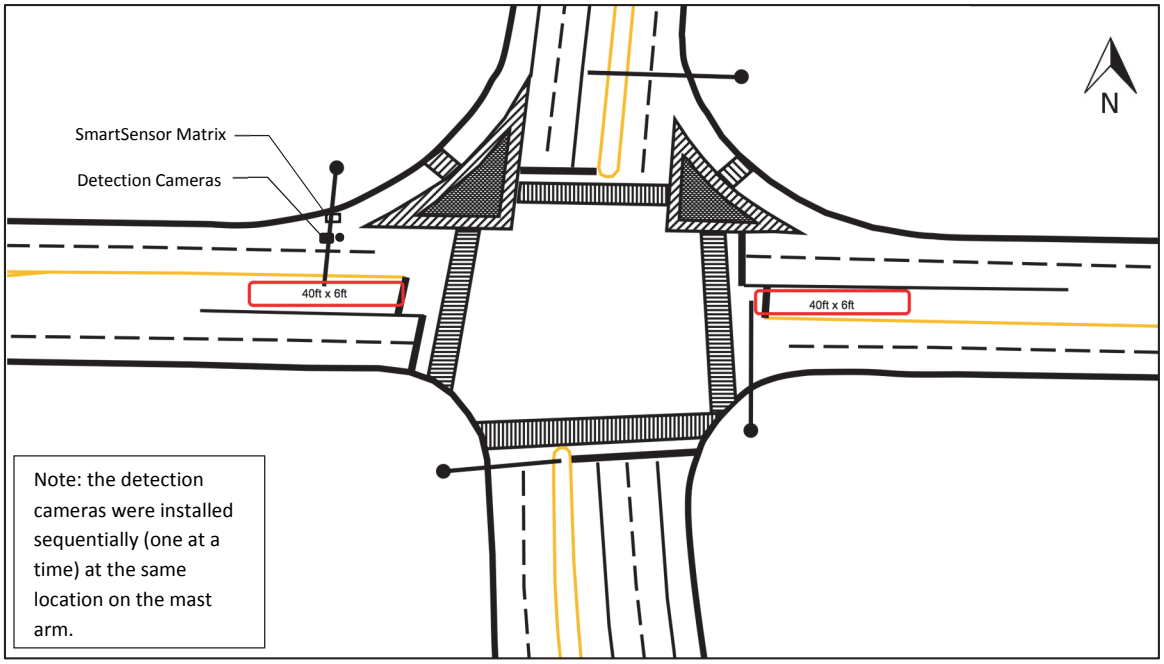

Figure 5.5 Plan view of detection zones at site 1

5.2.2 Test Site 2 – Allgood Road and Scufflegrit Road

Both stop bar and advance detection devices were tested at this site. The stop bar detection devices were installed on the mast arm facing the westbound approach (Allgood Road). The mounting locations are shown in Figure 5.6 (a picture taken in the field after installation).

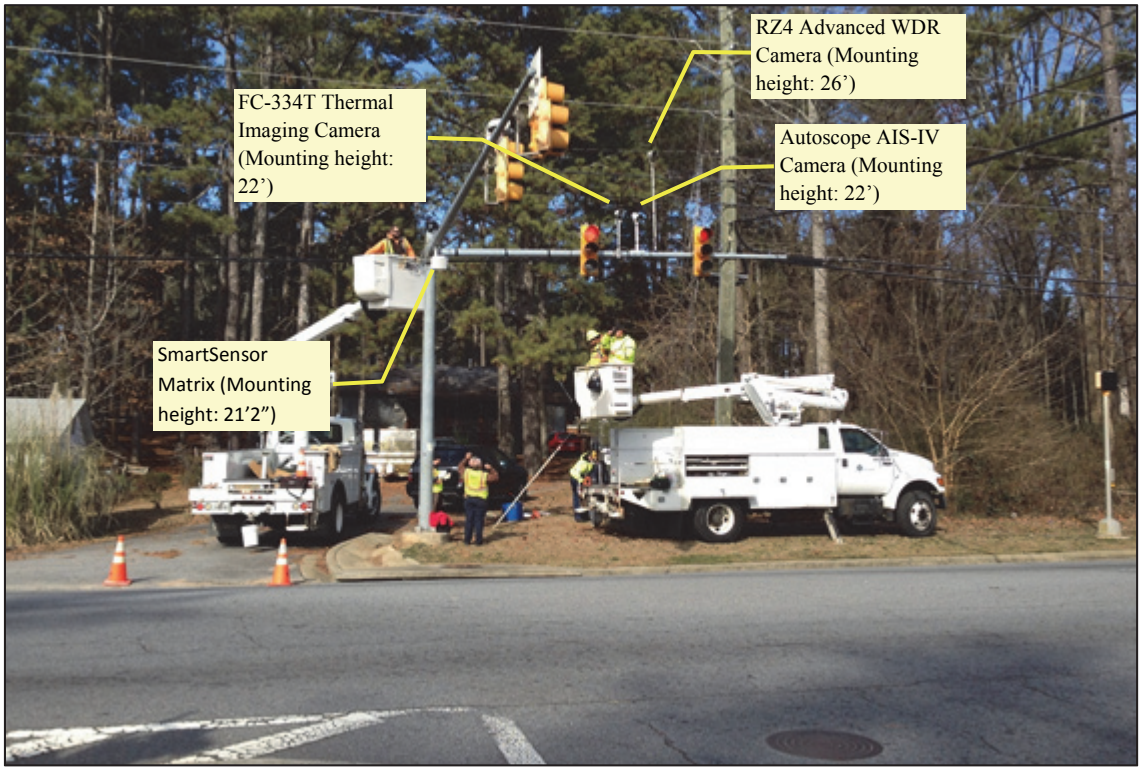

Figure 5.6 Field setup of the stop bar detection devices at site 2

Figure 5.7 shows a picture taken during the field installation. At this site, a potential glare issue is evident for the westbound approach in the morning. Two three-dimension aerial views of the field setup for the stop bar detection are illustrated in Figure 5.8

Figure 5.7 Potential glare issue in the morning of a sunny and clear day (site 2)

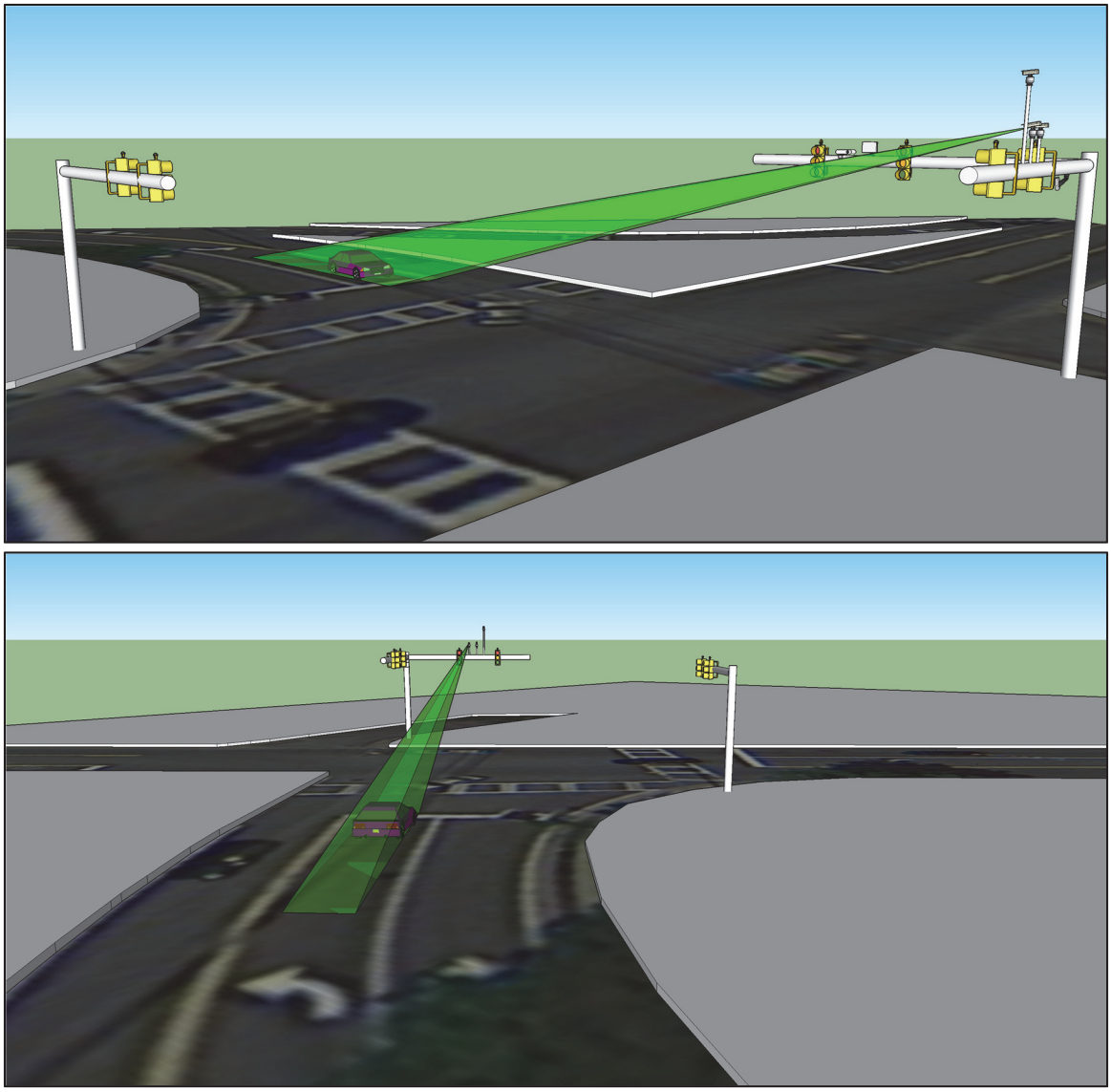

Figure 5.8 Three-dimension aerial view - field setup of stop bar detection devices at site 2

In addition to the test devices for stop bar detection, two advance detection devices (SmartSensor Advance and Vantage Vector Hybrid) were also installed and tested at this site. Both test devices were set up to detect the through movement on the southwest approach (Scufflegrit Road) of the intersection. A picture of the field setup is shown in Figure 5.9. Two three-dimension aerial views of the setup are shown in Figure 5.10.

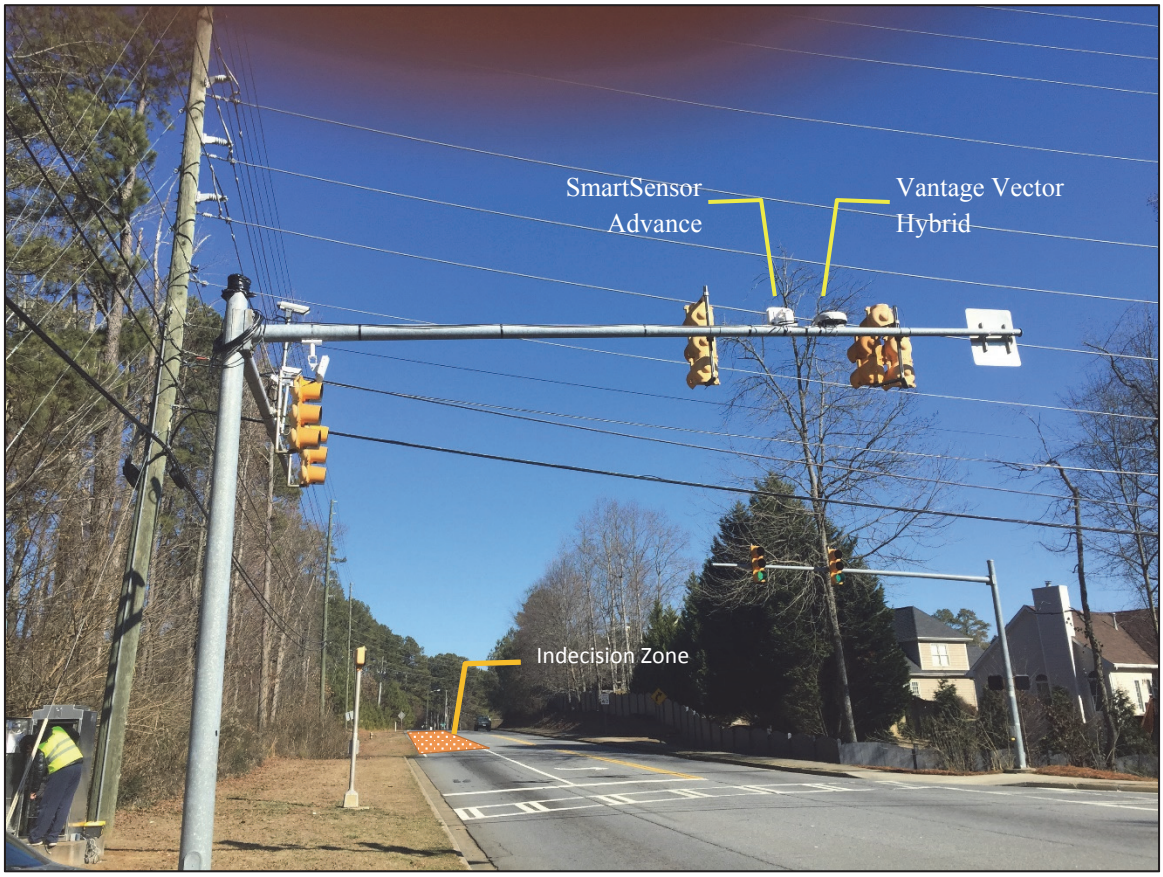

Figure 5.9 Field installation of the advance detection devices for indecision zone detection at site 2

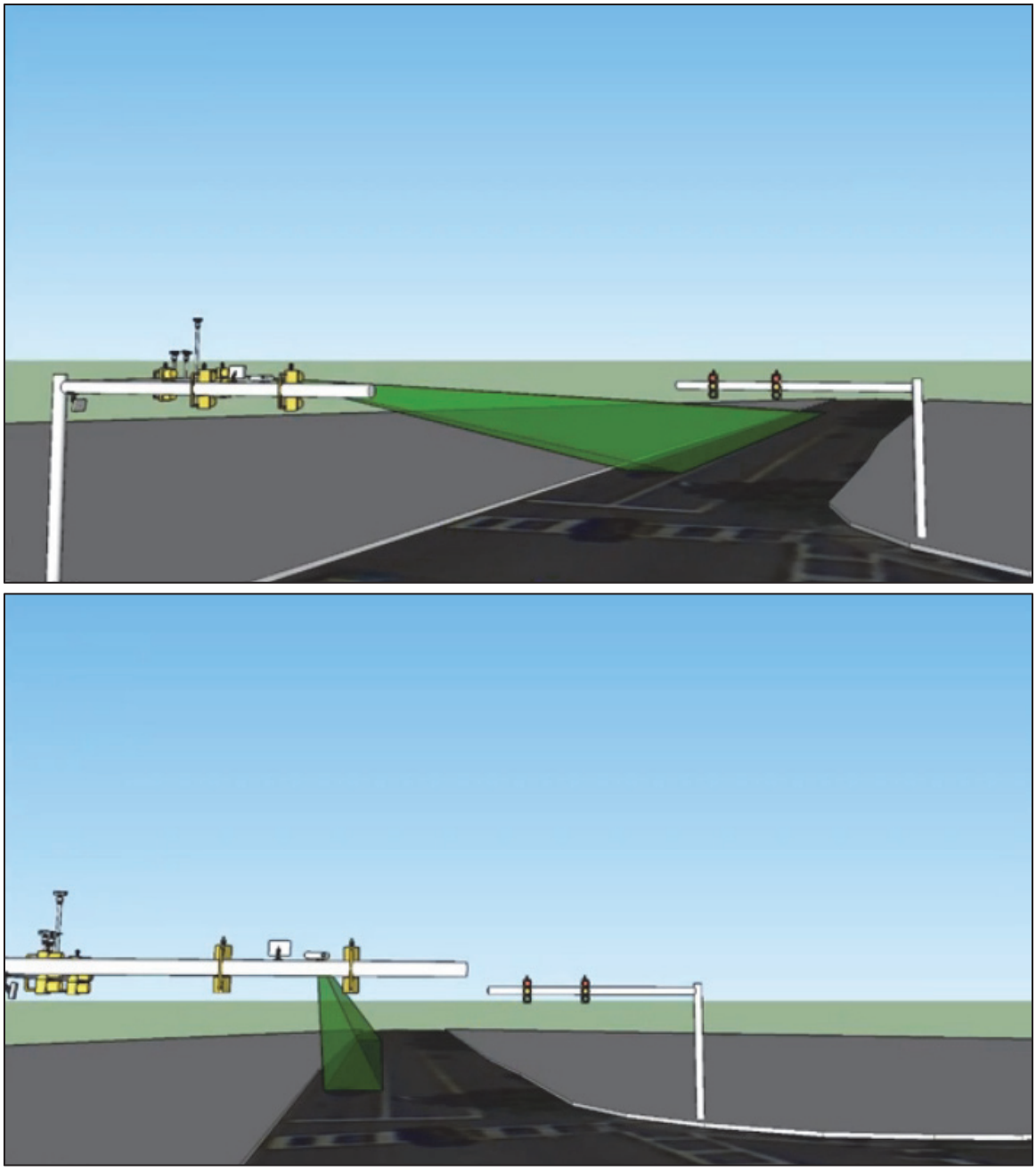

Figure 5.10 Three-dimension aerial view – indecision zone detection at site 2

A plan view of site 2 detection zone layout for both stop bar and indecision zone is shown in Figure 5.11.

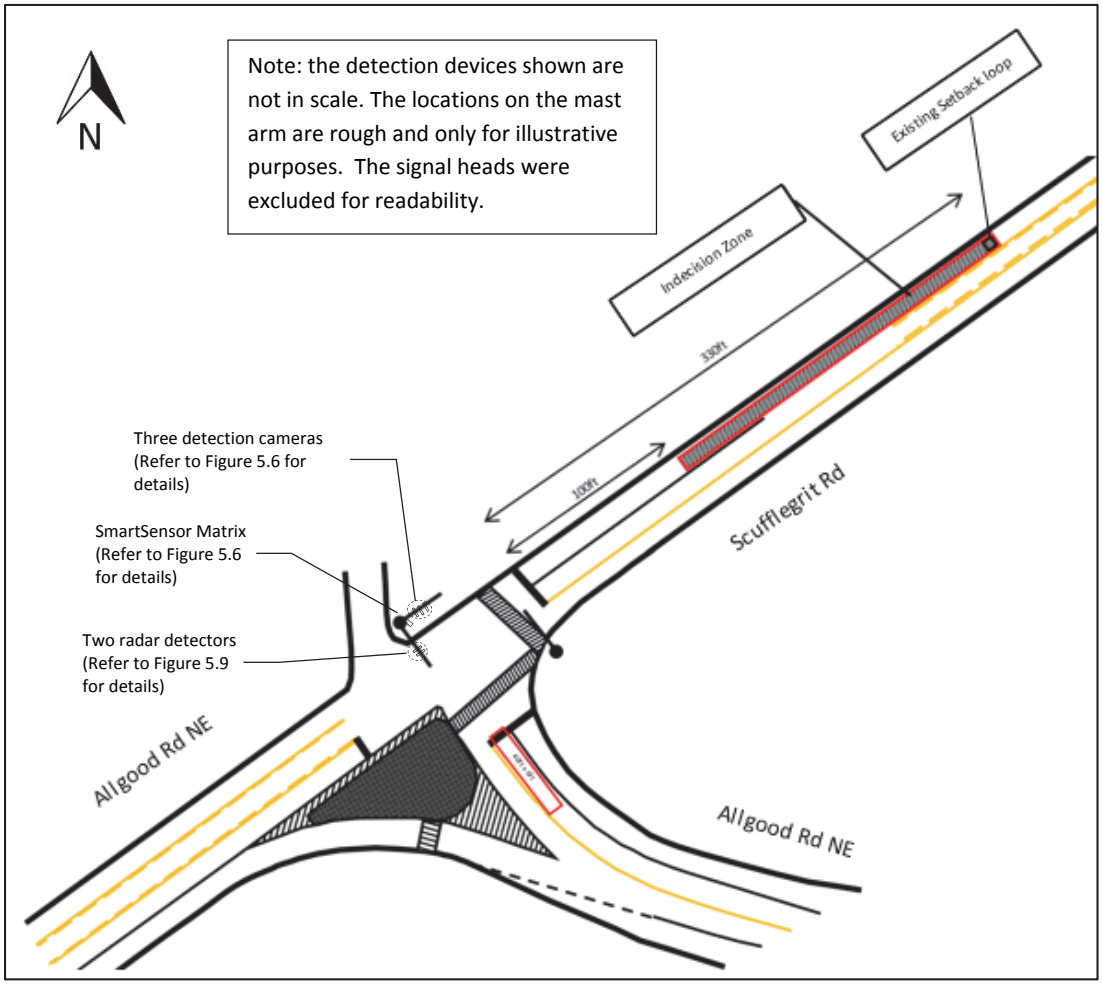

Figure 5.11 Plan view of detection zone layout at site 2

5.2.3 Test Site 3 – South Marietta Parkway and Technology Parkway SE

This site has a span wire support for traffic signals. Two stop bar detection devices, wireless magnetometers and Vantage SmartSpan camera, were evaluated at this site. The wireless magnetometers do not require mast arms for installation. Vantage SmartSpan camera is designed for mounting on a span wire. At the time of installation, the City of Marietta was in the process of replacing all inductive loops with wireless magnetometers at this site. This transition in detection technology allows the research team to install three wireless magnetometers in the northbound left turn lane within the confine of the existing loop as shown in Figure 5.12. In this setting, the inductive loop was used as a benchmark to evaluate the wireless magnetometers.

Figure 5.12 Field installation of wireless magnetometers in the northbound left turn lane (site 3)

For the Vantage SmartSpan camera, it would be preferred to install the camera to target the same northbound left turn lane for comparison purposes. However, the northbound approach is susceptible to view blocking due to the frequent passing of heavy trucks on South Marietta Parkway. This can be seen in Figure 5.13.

Figure 5.13 Northbound approach – view blocking due to frequent passing of heavy trucks on South Marietta Parkway.

Because of the issue of view blocking, the Vantage SmartSpan camera was installed to detect the westbound left turn movement (dual left turn lanes). The field setup of the wireless magnetometers and the Vantage SmartSpan camera is illustrated in Figure 5.14 and Figure 5.15.

Besides the view blocking, it should be noted that heavy trucks often move slowly and sometimes stalled in the middle of the intersection due to extended queues at the intersection downstream (South Marietta Parkway & Cobb Parkway) during the peak periods of traffic. This likely interrupts the communication between the Sensys wireless magnetometers and the antenna located on the strain pole at the northeast corner of the intersection. In fact, some large stuck-on calls were captured in the field. Because of this, a repeater was later added to the strain pole at the southwest corner to improve communication.

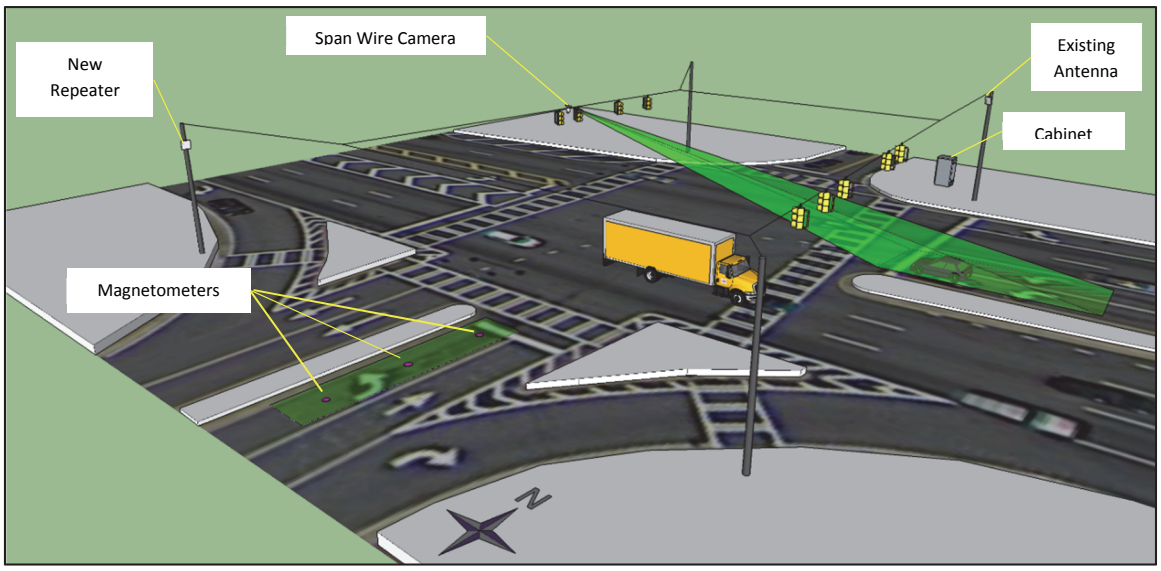

Figure 5.14 Three-dimension aerial view – field setup of wireless magnetometer and Vantage SmartSpan camera.

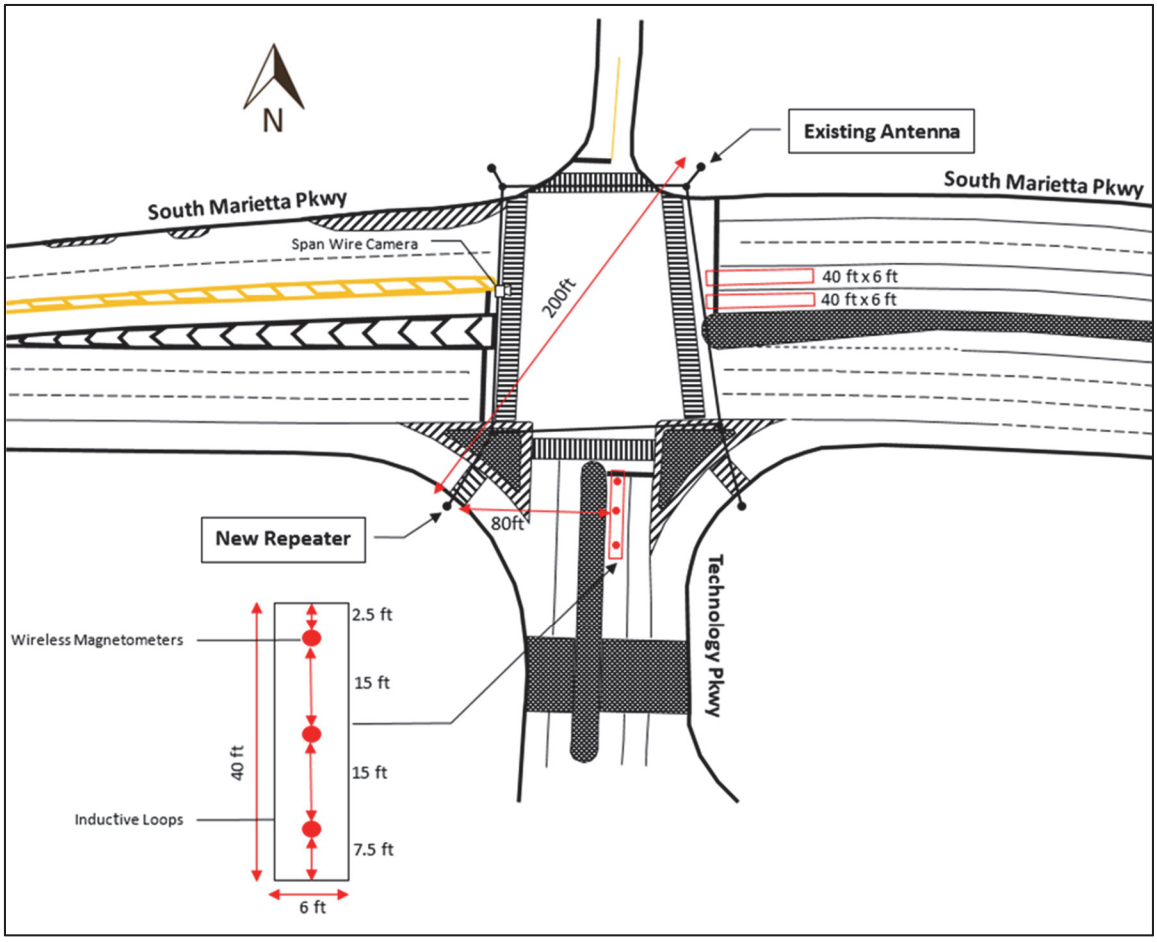

Figure 5.15 Plan view of detection zone layout for wireless magnetometers and Vantage SmartSpan camera.

6. DATA ACQUISITION

6.1 Data Logging

All three test sites selected have a 332A cabinet, which is the primary cabinet type in Georgia. The data acquisition device was connected to the back panel of the cabinets to obtain actual detector status data in real time. The signal display status, i.e., green, yellow, and red, was also monitored and recorded simultaneously. The data acquisition device was directly connected to a laptop computer for data logging. A digital video recorder (DVR) was used to record the videos from all detection cameras. The cabinet connection for data acquisition is illustrated in Figure 6.1.

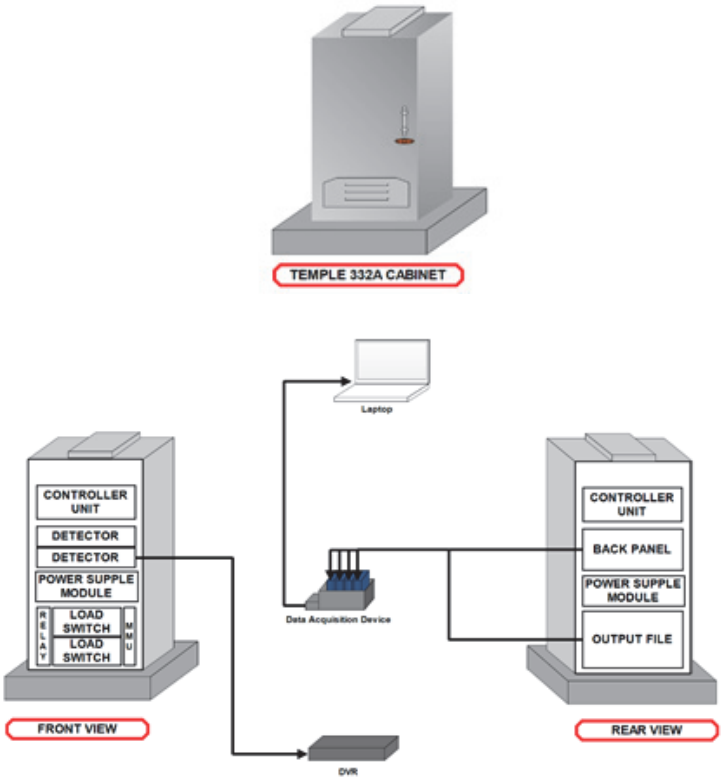

Figure 6.1 Illustration of field setup for data acquisition

For inductive loops, the pulse operating mode generates a short pulse signal between 100 and 150 milliseconds each time a vehicle enters the loop. To be able to distinguish this short pulse, a sampling interval of 100 milliseconds or 0.1 seconds is considered to be suitable for the purpose of this study and thus chosen for data sampling in the field.

For each sampling interval, the detector status takes on one of two values: 0 (off) and 1 (on) depending on the voltage output of the detector. "0" indicates absence of vehicle(s) in the detection zone and "1" indicates presence of vehicle(s) in the detection zone.

6.2 Data Retrieval

The data were gathered by the data acquisition device and automatically exported to Excel files. An excerpt of the raw data for the stop bar detection is shown in Figure 6.2

	A	C	D	E	F	G	I	J
1	Time	Voltage_2	Voltage_3	Voltage_5	Voltage_7	Voltage_14	Voltage_12	Voltage_13
7681	1/9/2015 16:26:35.963	0	0	0	0	0	1	0
7682	1/9/2015 16:26:36.063	0	0	0	0	0	1	0
7683	1/9/2015 16:26:36.163	0	0	0	0	0	1	0
7684	1/9/2015 16:26:36.263	0	0	0	0	0	1	0
7685	1/9/2015 16:26:36.363	0	0	0	0	0	1	0
7686	1/9/2015 16:26:36.463	0	0	0	0	0	1	0
7687	1/9/2015 16:26:36.563	0	0	0	0	1	1	0
7688	1/9/2015 16:26:36.663	0	0	0	0	1	1	0
7689	1/9/2015 16:26:36.763	0	0	0	0	1	1	0
7690	1/9/2015 16:26:36.863	0	0	0	0	1	1	0
7691	1/9/2015 16:26:36.963	0	0	0	0	1	1	0
7692	1/9/2015 16:26:37.063	0	0	0	0	1	1	0
7693	1/9/2015 16:26:37.163	0	0	0	0	1	1	0
7694	1/9/2015 16:26:37.263	0	1	0	0	1	1	0
7695	1/9/2015 16:26:37.363	1	1	1	0	1	1	0
7696	1/9/2015 16:26:37.463	1	1	1	0	1	1	0
7697	1/9/2015 16:26:37.563	1	1	1	0	1	1	0
7698	1/9/2015 16:26:37.663	1	1	1	0	1	1	0
7699	1/9/2015 16:26:37.763	1	1	1	0	1	1	0
7700	1/9/2015 16:26:37.863	1	1	1	1	1	1	0
7701	1/9/2015 16:26:37.963	1	1	1	1	1	1	0
7702	1/9/2015 16:26:38.063	1	1	1	1	1	1	0
7703	1/9/2015 16:26:38.163	1	1	1	1	1	1	0
7704	1/9/2015 16:26:38.263	1	1	1	1	1	1	0
7705	1/9/2015 16:26:38.363	1	1	1	1	1	1	0
7706	1/9/2015 16:26:38.463	1	1	1	1	1	1	0
7707	1/9/2015 16:26:38.563	1	1	1	1	1	1	0
7708	1/9/2015 16:26:38.663	1	1	1	1	1	1	0
7709	1/9/2015 16:26:38.763	1	1	1	1	1	1	0
7710	1/9/2015 16:26:38.863	1	1	1	1	1	1	0

Figure 6.2 Illustration of field setup for data acquisition

To understand the raw data in Figure 6.2, annotation and color schemes were added as shown in Figure 6.3. The orange areas indicate when the vehicles were detected. The red areas indicate when the traffic signal was red. As seen, the starting points of the detection window for different devices were not perfectly aligned. This difference is largely due to variability in field setup and detection zone configuration.

	A													
1	Time	Vol	_2	Volt	_3	Volt	_5	Vol	_7	Volt	_14	Volt	_12	Vol	_13
7680	1/9/2015 16:26:35.863	0		0		0		0		0		1		0	
7681	1/9/2015 16:26:35.963	0		0		0		0		0		1		0	
7682	1/9/2015 16:26:36.063	0		0		0		0		0		1		0	
7683	1/9/2015 16:26:36.163	0		0		0		0		0		1		0	
7684	1/9/2015 16:26:36.263	0		0		0		0		0		1		0	
7685	1/9/2015 16:26:36.363	0		0		0		0		0		1		0	
7686	1/9/2015 16:26:36.463	0		0		0		0		0		1		0	
7687	1/9/2015 16:26:36.563	0		0		0		0		1		1		0	
7688	1/9/2015 16:26:36.663	0		0		0		0		1		1		0	
7689	1/9/2015 16:26:36.763	0		0		0		0		1		1		0	
7690	1/9/2015 16:26:36.863	0		0		0		0		1		1		0	
7691	1/9/2015 16:26:36.963	0		0		0		0		1		1		0	
7692	1/9/2015 16:26:37.063	0		0		0		0		1		1		0	
7693	1/9/2015 16:26:37.163	0		0		0		0		1		1		0	
7694	1/9/2015 16:26:37.263	0		1		0		0		1		1		0	
7695	1/9/2015 16:26:37.363	1		1		1		0		1		1		0	
7696	1/9/2015 16:26:37.463	1		1		1		0		1		1		0	
7697	1/9/2015 16:26:37.563	1		1		1		0		1		1		0	
7698	1/9/2015 16:26:37.663	1		1		1		0		1		1		0	
7699	1/9/2015 16:26:37.763	1		1		1		0		1		1		0	
7700	1/9/2015 16:26:37.863	1		1		1		1		1		1		0	
7701	1/9/2015 16:26:37.963	1		1		1		1		1		1		0	
7702	1/9/2015 16:26:38.063	1		1		1		1		1		1		0	
7703	1/9/2015 16:26:38.163	1		1		1		1		1		1		0	
7704	1/9/2015 16:26:38.263	1		1		1		1		1		1		0	
7705	1/9/2015 16:26:38.363	1		1		1		1		1		1		0	
7706	1/9/2015 16:26:38.463	1		1		1		1		1		1		0	
7707	1/9/2015 16:26:38.563	1		1		1		1		1		1		0	
7708	1/9/2015 16:26:38.663	1		1		1		1		1		1		0	
7709	1/9/2015 16:26:38.763	1		1		1		1		1		1		0	
7710	1/9/2015 16:26:38.863	1		1		1		1		1		1		0	
7711	1/9/2015 16:26:38.963	1		1		1		1		1		1		0	
7712	1/9/2015 16:26:39.063	1		1		1		1		1		1		0	
7713	1/9/2015 16:26:39.163	1		1		1		1		1		1		0	
7714	1/9/2015 16:26:39.263	1		1		1		1		1		1		0	
7715	1/9/2015 16:26:39.363	1		1		1		1		1		1		0	
7716	1/9/2015 16:26:39.463	1		1		1		1		1		1		0	
7717	1/9/2015 16:26:39.563	1		1		1		1		1		1		0	
7718	1/9/2015 16:26:39.663	1		1		1		1		1		1		0	
7719	1/9/2015 16:26:39.763	1		1		1		1		1		1		0	
7720	1/9/2015 16:26:39.863	1		1		1		1		1		1		0	
7721	1/9/2015 16:26:39.963	1		1		1		1		1		1		0	
7722	1/9/2015 16:26:40.063	1		1		1		1		1		1		0	
7723	1/9/2015 16:26:40.163	1		1		1		1		1		1		0	
7724	1/9/2015 16:26:40.263	1		1		1		1		1		1		0	
7725	1/9/2015 16:26:40.363	1		1		1		1		1		1		0	
7726	1/9/2015 16:26:40.463	1		1		1		1		1		1		0	
7727	1/9/2015 16:26:40.563	1		1		1		1		1		1		0	
7728	1/9/2015 16:26:40.663	1		1		1		1		1		1		0	

Figure 6.3 Data sample of stop bar detection

Similar raw data were logged for the indecision zone detection as well and are shown in Figure 6.4. The orange areas indicate when vehicles were detected. As seen, the loop and two radar devices detected vehicles nearly at the same time. But, the detection signal of the loop was captured by two sample intervals (200 milliseconds) because of the pulse mode. As seen, both the SmartSensor Advance and the Vantage Vector Hybrid were able to continuously track the vehicles traversing the indecision zone depending on their speed and estimated arrival times at the stop bar. As indicated in Figure 6.4, the detection durations rendered by the two radar devices appear to be different.

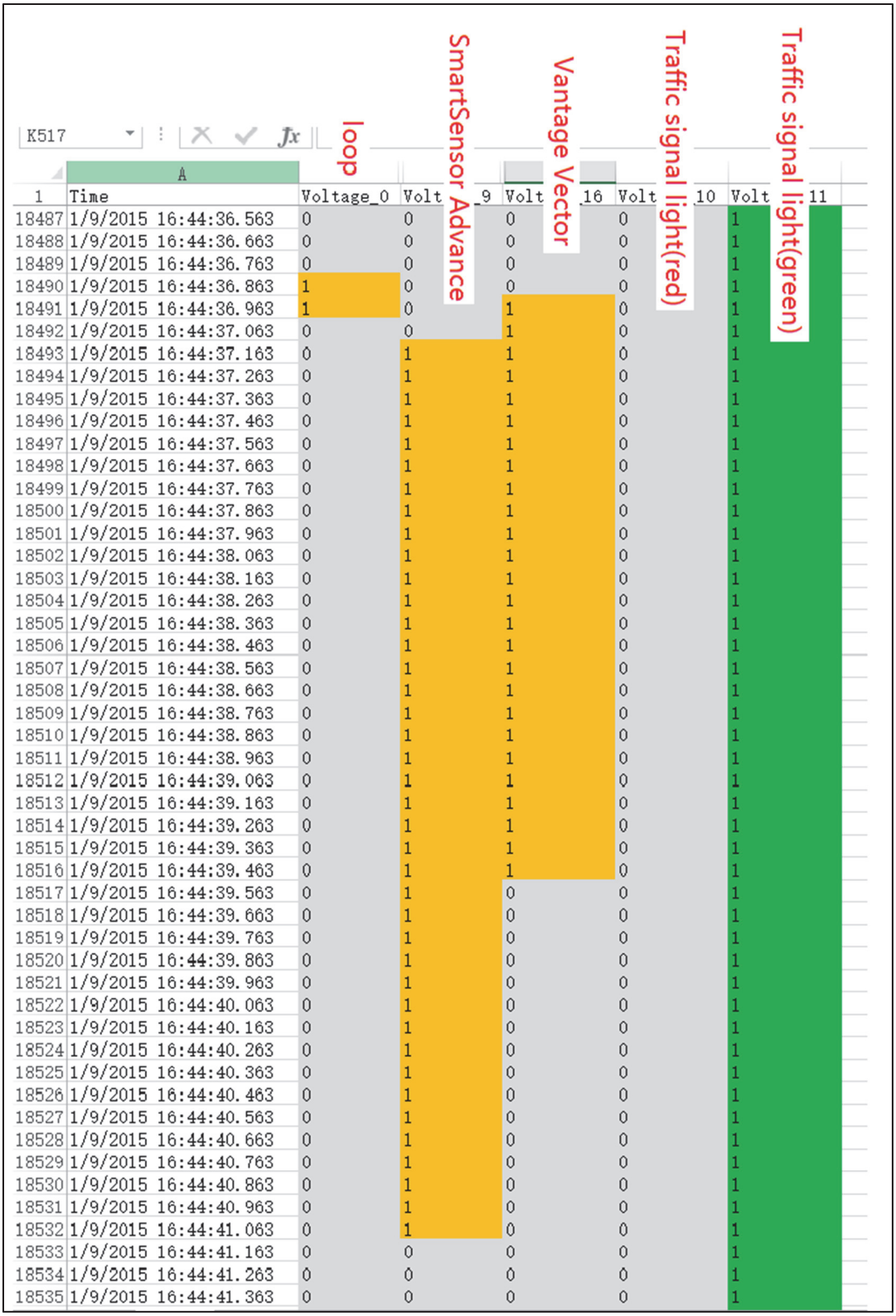

	A									
1	Time	Voltage_0	Volt	_9	Volt	_16	Volt	_10	Volt	_11
18487	1/9/2015 16:44:36.563	0	0		0		0		1	
18488	1/9/2015 16:44:36.663	0	0		0		0		1	
18489	1/9/2015 16:44:36.763	0	0		0		0		1	
18490	1/9/2015 16:44:36.863	1	0		0		0		1	
18491	1/9/2015 16:44:36.963	1	0		1		0		1	
18492	1/9/2015 16:44:37.063	0	0		1		0		1	
18493	1/9/2015 16:44:37.163	0	1		1		0		1	
18494	1/9/2015 16:44:37.263	0	1		1		0		1	
18495	1/9/2015 16:44:37.363	0	1		1		0		1	
18496	1/9/2015 16:44:37.463	0	1		1		0		1	
18497	1/9/2015 16:44:37.563	0	1		1		0		1	
18498	1/9/2015 16:44:37.663	0	1		1		0		1	
18499	1/9/2015 16:44:37.763	0	1		1		0		1	
18500	1/9/2015 16:44:37.863	0	1		1		0		1	
18501	1/9/2015 16:44:37.963	0	1		1		0		1	
18502	1/9/2015 16:44:38.063	0	1		1		0		1	
18503	1/9/2015 16:44:38.163	0	1		1		0		1	
18504	1/9/2015 16:44:38.263	0	1		1		0		1	
18505	1/9/2015 16:44:38.363	0	1		1		0		1	
18506	1/9/2015 16:44:38.463	0	1		1		0		1	
18507	1/9/2015 16:44:38.563	0	1		1		0		1	
18508	1/9/2015 16:44:38.663	0	1		1		0		1	
18509	1/9/2015 16:44:38.763	0	1		1		0		1	
18510	1/9/2015 16:44:38.863	0	1		1		0		1	
18511	1/9/2015 16:44:38.963	0	1		1		0		1	
18512	1/9/2015 16:44:39.063	0	1		1		0		1	
18513	1/9/2015 16:44:39.163	0	1		1		0		1	
18514	1/9/2015 16:44:39.263	0	1		1		0		1	
18515	1/9/2015 16:44:39.363	0	1		1		0		1	
18516	1/9/2015 16:44:39.463	0	1		1		0		1	
18517	1/9/2015 16:44:39.563	0	1		0		0		1	
18518	1/9/2015 16:44:39.663	0	1		0		0		1	
18519	1/9/2015 16:44:39.763	0	1		0		0		1	
18520	1/9/2015 16:44:39.863	0	1		0		0		1	
18521	1/9/2015 16:44:39.963	0	1		0		0		1	
18522	1/9/2015 16:44:40.063	0	1		0		0		1	
18523	1/9/2015 16:44:40.163	0	1		0		0		1	
18524	1/9/2015 16:44:40.263	0	1		0		0		1	
18525	1/9/2015 16:44:40.363	0	1		0		0		1	
18526	1/9/2015 16:44:40.463	0	1		0		0		1	
18527	1/9/2015 16:44:40.563	0	1		0		0		1	
18528	1/9/2015 16:44:40.663	0	1		0		0		1	
18529	1/9/2015 16:44:40.763	0	1		0		0		1	
18530	1/9/2015 16:44:40.863	0	1		0		0		1	
18531	1/9/2015 16:44:40.963	0	1		0		0		1	
18532	1/9/2015 16:44:41.063	0	1		0		0		1	
18533	1/9/2015 16:44:41.163	0	0		0		0		1	
18534	1/9/2015 16:44:41.263	0	0		0		0		1	
18535	1/9/2015 16:44:41.363	0	0		0		0		1	

Figure 6.4 Data sample of indecision zone detection

6.2.1 Stop Bar Detection

Figure 6.5 shows the temporal change in the detection status of the stop bar detection devices. The rectangular signals indicate the "on" status of detectors. To be able to distinguish the status change of different devices, the rectangles varied by height. The lower green, red, and yellow rectangles at the bottom indicate traffic signal status in same color. By inspecting Figure 6.5, all devices are relatively consistent in registering and releasing calls. A typical pattern is that the calls were registered (the starting points of rectangles) in red and released (the ending points of rectangles) in green.

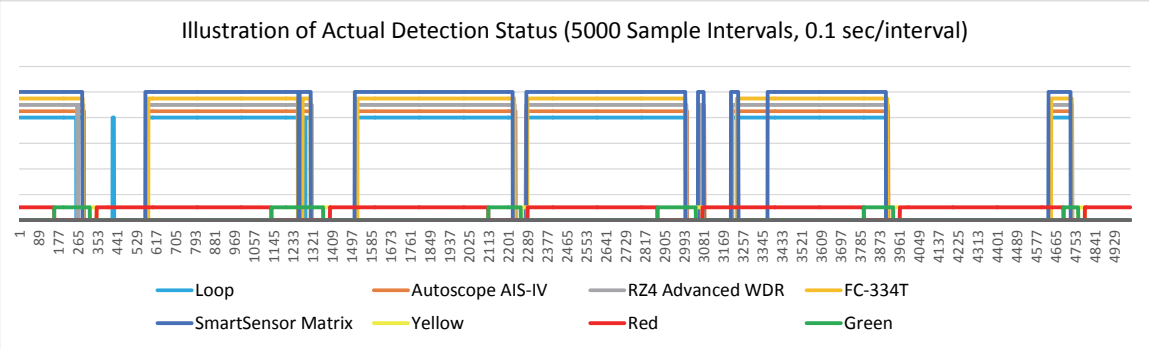

Figure 6.5 An example of actual detection status over time (stop bar detection at site 2)

6.2.2 Indecision Zone Detection

Traditional loop-based indecision zone protection systems were designed for specific speeds, which are only effective if all vehicles travel at targeted speeds. The radar-based detection systems are capable of continuously tracking the speed of individual vehicles and estimating their times of arrival at the stop bar, thus provide dynamic real-time indecision zone protection. Figure 6.6 shows an example of the detection status change over time for the indecision zone detection. As seen, the inductive loop is a point detector with short pulse signals (in blue). The two radar detectors provide continuous detection, shown as wider rectangles (in orange and grey). As seen, the detection signals of the two radar detectors match relatively well, but with an apparent difference in duration.

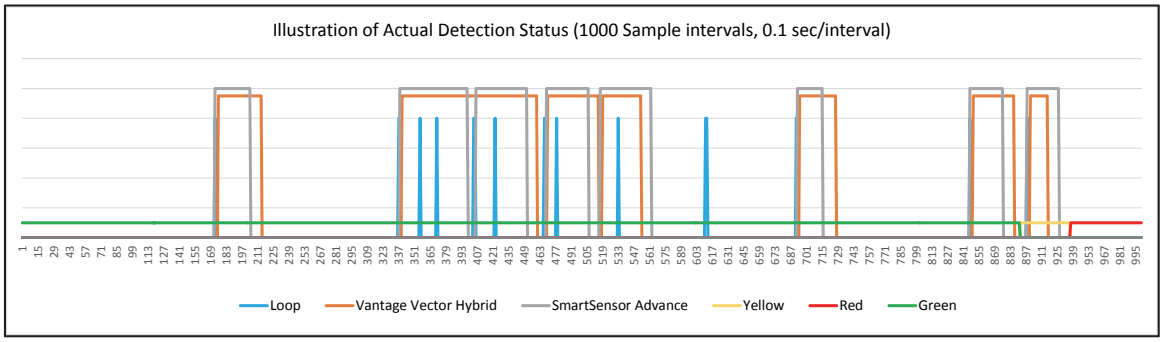

Figure 6.6 An example of actual detection status over time (indecision zone detection at site 2)

7. DATA COMPILATION, CODING, AND ANALYSIS

7.1 Data Compilation

The main purpose of vehicle detection is to facilitate efficient allocation of right-of-way among conflicting movements, resulting in cycling of phase sequence. Each cycle typically involves two basic detection events: calling a phase during the red and extending a phase during the green. This cyclic patterns are clearly shown in Figure 6.5 and Figure 6.6. From the perspective of traffic signal operations, the performance of test devices was evaluated on a per-cycle base. The raw data collected at the 100-millisecond (0.1 seconds) sampling interval were aggregated and normalized to obtain average detection errors per cycle.

7.2 Weather Information and Coding

Many erroneous calls for nonintrusive detection devices are a result of adverse weather events and/or environmental conditions. Detection devices are more or less influenced by certain weather and/or environmental conditions. Concurrent weather information during the test periods were extracted from the closest weather station through the weather underground website (wunderground.com), including wind speed, humidity, dew point, temperature, weather events (e.g., clear, cloudy, rain, mist, fog, snow, etc.) , and visibility. For analysis purposes, weather events were grouped by similarity. Weather events experienced at the test sites during the test periods and corresponding coding are presented in Table 7.1. For example, weather events of rain, light thunderstorm and thunderstorm were assigned a code of 4 and those weather events were only experienced at site 1 by the Autoscope AIS-IV Camera and the SmartSensor Matrix. As seen, the coding for weather events is ordinal and was used for level 2 analysis - conditional reference trees in Section 8. To account for specific effects of different weather events, which are likely to be nonlinear, dummy variables were created for each weather category and used for level 3 analysis - regression models in Section 8. Four dummy variables were created by referencing the "clear" weather condition as the reference base.

C1 = 1 if weather code = 1, C1 = 0 otherwise
C2 = 1 if weather code = 2, C2 = 0 otherwise
C3 = 1 if weather code = 3, C3 = 0 otherwise
C4 = 1 if weather code = 4, C4 = 0 otherwise

To capture the site effect, data sets for site 1 and site 2 were combined and a "Site" dummy variable was added by referencing site 2 as the base (i.e., Site = 0 if site 2; Site = 1 if site 1).

Table 7.1 Test Periods and Coding of Weather Events

Test Site		Site 1 N. Marietta Pkwy & Fairground St					Site 2 Allgood Rd & Scufflegrit Rd								Site 3 S. Marietta Pkwy & Technology Pkwy SE		
Test Device		A	F	R	SM		A	F	R	SM	A	F	R/ VV	SM/ SA	WM	WM (RP)	VS
Period of Field Study	From	11/21/14 1:55:59 PM	12/19/14 1:22:59 PM	12/17/14 9:06:08 AM	11/21/14 1:55:59 PM	12/17/2014 9:06:08 AM	1/9/15 3:14:04 PM				1/16/2015 4:00:56 PM				2/13/15 10:10:28 AM	3/11/15 1:19:43 PM	3/11/15 1:19:58 PM
	To	11/24/14 12:48:06 PM	12/23/14 10:06:53 AM	12/19/14 10:46:42 AM	11/24/2014 12:43:39 PM	12/23/14 10:04:28 AM	1/14/2015 9:03:37 AM				1/20/15 11:05:14 AM				2/20/15 1:31:08 PM	3/20/15 1:15:05 PM	3/20/15 1:15:18 PM
Weather Event	Clear	0	0	0	0	0	0				0				0	0	0
	Partly Cloudy	1	1	1	1	1	1				1				1	1	1
	Scattered Clouds	1	1	1	1	1	1				1				1	1	1
	Mostly Cloudy	1	1	1	1	1	1				1				1	1	1
	Overcast	1	1	1	1	1	1				1				1	1	1
	Light Rain	2	2	2	2	2	2				-				2	2	2
	Light Drizzle	2	2	2	2	2	2				-				2	2	2
	Mist	-	-	-	-	-	3				-				-	3	3
	Fog	-	-	-	-	-	3				-				-	3	3
	Fog, Light Drizzle	-	-	-	-	-	3				-				-	3	3
	Haze	-	-	-	-	-	-				-				-	3	3
	Rain	4	-	-	4	-	-				-				-	-	-
	Light Thunderstorms and Rain	4	-	-	4	-	-				-				-	-	-
	Thunderstorms and Rain	4	-	-	4	-	-				-				-	-	-
	Light Snow	-	-	-	-	-	-				-				5	-	-

Letter Code of Test Device:
A, Autoscope AIS-IV Camera
F, FC-334T Thermal Imaging Camera
R, RZ4 Advanced WDR Camera
VV, Vantage Vector Hybrid
SM, SmartSensor Matrix
SA, SmartSensor Advance
WM, Wireless Magnetometer
VS, Vantage SmartSpan Camera
RP, Addition of the new repeater

Weather Code:
0 = Clear
1 = Partly scattered, mostly cloudy, or overcast
2 = Light rain or drizzle
3 = Mist, fog, or haze
4 = Rain or thunderstorm
5 = Light snow
"-" = Not applicable

7.3 Data Merging

The cycle-based detection errors were linked to the weather and environmental conditions by referencing the time they actually occurred. Site specific features and device adjustments made during the test periods were coded and added to the data set. This allows to study the effects of site specific features and device adjustments on detection errors. The definition and coding of variables for stop bar detection are presented in Table 7.2.

Table 7.2 Definition and Coding of Variables (Stop Bar Detection)

Factor	Variable	Description	Unit/Value	Applicable Site(s)	Applicable Device(s)*
Detection Error	Amiss	Average duration of missed calls per cycle	0.1 sec.	All	All
	Afalse	Average duration of false calls per cycle	0.1 sec.	All	All
	Astuck	Average duration of stuck-on calls per cycle	0.1 sec.	All	All
	Adrop	Average duration of dropped calls per cycle	0.1 sec.	All	All
Wind Speed	Wspeed	Actual wind speed	mph	All	
Weather Event	C0	Clear	Reference base	All	All
	C1	Partly, scattered, mostly cloudy, or overcast	No = 0 Yes = 1	All	All
	C2	Light rain or drizzle	No = 0 Yes = 1	All	All
	C3	Mist, fog, or haze	No = 0 Yes = 1	Sites 2 & 3	All
	C4	Rain or thunderstorms	No = 0 Yes = 1	Site 1	A, SM
	C5	Light snow	No = 0 Yes = 1	Site 3	WM
Lighting	Night	Day or Night	Day = 0 Night = 1	All	All
Visibility Level	Visibility	Distance	Mile	All	All
Uneven shade	Shade	Shadow cast from the trees, occurred during afternoon of a clear, partly or scattered cloudy day.	No = 0 Yes = 1	Site 2	A, F, R, SM
Potential Glare	Glare	Defined as sunny and clear weather condition from 9:00 am to 12:00 pm	No = 0 Yes = 1	All	A, F, R, VS

Occupancy percent per cycle	OP	Percent of time occupied by vehicles per cycle	percent	All	All
Percent of occupancy during Green	POG	Percent of occupancy occurred during Green	percent	All	All
Peak period of traffic	PH	7:00 am-10:00 am or 4:00 pm-7:00 pm	Off peak = 0 Peak = 1	All	All
Installation Height	LH	The installation height was reduced to match other test devices.	Before (higher) = 0 After (lower) = 1	Site 1	F
Detection zone adjustment	ZA	The detection zone was reduced due to excessive false calls during the study period.	Before (larger) = 0 After (smaller) = 1	Site 2	A
Adjustment	AD	Sensitivity adjusted from 10 to 1; added pedestrian screening.	Before = 0 After = 1	Site 1	R
Repeater	RP	A repeater was added.	Before (without the repeater) = 0 After (with the repeater = 1	Site 3	WM
Test Site	Site	Site 1: larger aspect ratio and offset; heavy truck volume Site 2: smaller aspect ratio and offset; mainly passenger vehicles	Site 2 = 0 Site 1 = 1	Sites 1 & 2	A, F, R,SM

*Notes:

A, Autoscope AIS-IV Camera
F, FC-334T Thermal Imaging Camera
R, RZ4 Advanced WDR Camera
SM, SmartSensor Matrix & Advance
WM, Wireless Magnetometer
VS, Vantage SmartSpan Camera

An excerpt of the compiled data set is shown in Table 7.3.

Table 7.3 An Example of Condensed Data Set

Cycle Start Time	Cycle End Time	Loop Occupancy during (Red)	Loop Non-occupancy (Red)	Loop Occupany (Green)	Loop Non-occupancy (Green)	Loop Occupany (Yellow)	Loop Non-occupancy (Yellow)	Avg. missed call (ms)	Avg. false calls (ms)	Avg. stuck-on calls (ms)	Avg. dropped calls (ms)	Humidity (%)	Wind Speed (mph)	Visibility (mile)	Weather Event	C1	C2	C3	Night	PH	Glare	Shade
1	2	3	4	5	6	7	8	9	10	11	12	13	14	15	16	17	18	19	20	21	22	23
1/9/2015 15:14	1/9/2015 15:15	566	221	122	38	0	30	3	0	4	0	38	11.5	10	1	1	0	0	0	0	0	0
1/9/2015 15:15	1/9/2015 15:17	595	118	168	65	0	30	1	1	3	0	38	11.5	10	1	1	0	0	0	0	0	0
1/9/2015 15:17	1/9/2015 15:18	585	0	115	31	7	23	2	0	4	0	38	11.5	10	1	1	0	0	0	0	0	0
1/9/2015 15:18	1/9/2015 15:20	592	134	128	44	13	17	5	0	6	0	38	11.5	10	1	1	0	0	0	0	0	0
1/9/2015 15:20	1/9/2015 15:21	61	676	101	31	0	30	0	0	7	0	38	11.5	10	1	1	0	0	0	0	0	0
1/9/2015 15:21	1/9/2015 15:23	557	451	35	31	0	30	0	0	4	0	38	11.5	10	1	1	0	0	0	0	0	0
1/9/2015 15:23	1/9/2015 15:25	585	252	142	31	0	30	7	0	4	0	38	11.5	10	1	1	0	0	0	0	0	0
1/9/2015 15:25	1/9/2015 15:26	562	182	58	43	0	30	2	0	5	0	38	11.5	10	1	1	0	0	0	0	0	0
1/9/2015 15:26	1/9/2015 15:28	569	544	53	39	0	30	3	0	6	0	38	11.5	10	1	1	0	0	0	0	0	0
1/9/2015 15:28	1/9/2015 15:30	544	165	66	54	0	30	5	0	10	0	38	11.5	10	1	1	0	0	0	0	0	0
1/9/2015 15:30	1/9/2015 15:31	678	68	125	35	0	30	1	0	7	0	38	11.5	10	1	1	0	0	0	0	0	0
1/9/2015 15:31	1/9/2015 15:32	4	497	98	43	0	30	4	0	8	0	38	11.5	10	1	1	0	0	0	0	0	0
1/9/2015 15:32	1/9/2015 15:34	558	301	1	59	0	30	1	0	0	0	38	11.5	10	1	1	0	0	0	0	0	0
1/9/2015 15:34	1/9/2015 15:36	570	525	82	56	0	30	6	0	5	0	38	11.5	10	1	1	0	0	0	0	0	0
1/9/2015 15:36	1/9/2015 15:37	15	485	78	64	0	30	8	0	5	0	38	11.5	10	1	1	0	0	0	0	0	0
1/9/2015 15:37	1/9/2015 15:39	557	196	1	59	0	30	0	0	0	0	38	11.5	10	1	1	0	0	0	0	0	0
1/9/2015 15:39	1/9/2015 15:40	559	130	54	31	0	30	2	0	7	0	38	11.5	10	1	1	0	0	0	0	0	0
1/9/2015 15:40	1/9/2015 15:41	724	33	106	30	0	30	1	0	5	0	38	11.5	10	1	1	0	0	0	0	0	0
1/9/2015 15:41	1/9/2015 15:43	572	353	103	31	0	30	9	0	5	0	38	11.5	10	1	1	0	0	0	0	0	0
1/9/2015 15:43	1/9/2015 15:44	558	72	56	30	0	30	3	0	2	0	38	11.5	10	1	1	0	0	0	0	0	0
1/9/2015 15:44	1/9/2015 15:45	63	297	99	34	0	30	1	0	4	0	38	11.5	10	1	1	0	0	0	0	0	0
1/9/2015 15:45	1/9/2015 15:47	558	81	34	34	0	30	1	0	4	0	38	11.5	10	1	1	0	0	0	0	0	0
1/9/2015 15:47	1/9/2015 15:48	676	87	35	32	0	30	4	0	8	0	38	11.5	10	1	1	0	0	0	0	0	0
1/9/2015 15:48	1/9/2015 15:50	553	179	78	48	0	30	11	0	8	0	38	11.5	10	1	1	0	0	0	0	0	0
1/9/2015 15:50	1/9/2015 15:51	470	395	95	30	0	30	2	0	5	0	38	11.5	10	1	1	0	0	0	0	0	0
1/9/2015 15:51	1/9/2015 15:53	527	201	70	37	0	30	5	0	10	0	38	11.5	10	1	1	0	0	0	0	0	0
1/9/2015 15:53	1/9/2015 15:54	701	0	96	34	2	28	1	0	6	0	38	11.5	10	1	1	0	0	0	0	0	0
1/9/2015 15:54	1/9/2015 15:57	569	1069	147	53	16	14	5	1	5	0	38	11.5	10	1	1	0	0	0	0	0	0

For reference purposes, a column number is indicated in the second row of the table. As shown in Table 7.3, each data row indicates a signal cycle. The first two columns indicate the starting and ending time of each cycle. Columns 3 and 4 are the occupancy and non-occupancy times during red. Columns 5 and 6 are the occupancy and non-occupancy time during green. Columns 7 and 8 are the occupancy and non-occupancy time during yellow. Columns 9-12 show the average detection error per cycle by type. The rest of columns indicate weather and environmental conditions. The coding of those conditions was described in Table 7.2.

8. DATA ANALYSIS

As described previously, errors are practically inevitable for nonintrusive detection devices. For a specific device, the occurrence, type and magnitude of detection errors are largely dependent on field setup and configuration. Note the requirement for field setup and configuration generally varies across technologies. This variation makes direct comparison of different detection devices rather difficult if not impossible. Additional variance can easily be introduced by technicians who have varying levels of skills and subjective judgment. As such, the purpose of this study is not to directly compare different detection devices to identify the winner of all, rather to discern the factors or conditions underlying the variation in detection errors such that proper contexts can be recognized for application of different detection technologies or devices. For this purpose, data mining techniques and econometric methods were employed.

8.1 Stop Bar Detection

It is quite challenging to relate detection errors to potentially influential factors. After aggregating detection errors by cycle, average detection errors per cycle were computed and used as a basic performance indicator. Three levels of analysis with increasing complexity were conducted to understand the data and identify any associations or causality between the detection errors and potential factors. The lower level (I and II) analyses are exploratory in nature and used to inform the higher level (III) analysis. For level 1 analysis, statistics and error distributions were generated first, followed by a plotting of temporal error variation along with potential factors to help discern any pattern associations. Further, the recorded videos were reviewed for the time points when large errors occurred. For level 2 analysis, conditional inference trees were used to explore potential associations between detection errors and corresponding weather and environmental conditions. Finally, level 3 analysis draws on regression models to quantify the marginal effects of influential factors on detection errors.

8.1.1 Level 1 Analysis

8.1.1.1 Statistics and Error Distributions

The summaries of statistics for the variables considered are presented in Tables 8.1-8.4 for sites 1 and 2, and in Tables 8.5 and 8.6 for site 3. Note that the same four devices (Autoscope AIS-IV camera, FC-334T Thermal Imaging Camera, RZ4 Advanced WDR Camera, and SmartSensor Matrix) were tested at both site 1 and site 2 and the data from the two sites were pooled together for analysis purposes. A dummy variable was added to the pooled data set to indicate which site the data came from.

Table 8.1 Summary of Descriptive Statistics (Autoscope AIS-IV, Sites 1 and 2)

Variable	Unit	Freq	Mean	SD	Median	Min	Max
Amiss	0.1 sec.	5,730	6.6	35.6	0.0	0.0	662.0
Afalse	0.1 sec.	5,730	12.1	51.0	3.0	0.0	1267.0
Astuck	0.1 sec.	5,730	42.7	115.7	7.0	0.0	2567.0
Adrop	0.1 sec.	5,730	7.6	41.3	0.0	0.0	557.0
Wspeed	mph	5,730	6.0	3.9	5.8	0.0	16.1
Visibility	mile	5,730	7.7	3.8	10.0	0.2	10.0
OP	percent	5,730	47.8	28.4	51.2	0.0	100.0
POG	percent	5,730	20.9	24.8	12.4	0.0	100.0
C0	Y	821					
C1	Y	3,813					
C2	Y	528					
C3	Y	525					
C4	Y	43					
Night	N	3,795					
	Y	1,935					
PH	N	4,554					
	Y	1,176					
Shade	N	5,506					
	Y	224					
Glare	N	5,284					
	Y	446					
Site	N (Site 2)	5,094					
	Y (Site 1)	636					
ZA	N (Larger)	3,344					
	Y (Smaller)	2,386					

For the statistics of Autoscope AIS-IV camera in Table 8.1, "Freq" indicates frequency or the number of observations or cycles that were applicable to the variables indicated. For example, the "Freq" of 821 for C0 (the code for clear weather) indicates that 821 cycles occurred during the clear weather condition. The "Freq" of 1935 for Night (Y) indicates that 1935 cycles occurred at night. The mean value of 6.6 for "Amiss" indicates that the average missed call error is 0.66 seconds (6.6 milliseconds). The standard deviation (SD) of the missed calls is 3.56 seconds (35.6 milliseconds). "Median" indicate the median value of the variable as applicable. "Min" and "Max" are the minimum and maximum value of the variable. Similar summaries of descriptive statistics are presented in Tables 8.2-8.6 for other detection devices.

Table 8.2 Summary of Descriptive Statistics (FC-334T Thermal, Sites: 1 and 2)

Variable	Unit	Freq	Mean	SD	Median	Min	Max
Amiss	0.1 sec.	5,687	9.4	35.0	6.0	0.0	608.0
Afalse	0.1 sec.	5,687	1.3	19.3	0.0	0.0	796.0
Astuck	0.1 sec.	5,687	6.9	28.7	3.0	0.0	1134.0
Adrop	0.1 sec.	5,687	2.2	24.2	0.0	0.0	835.0
Wspeed	mph	5,687	5.7	3.7	5.8	0.0	16.1
Visibility	mile	5,687	7.6	3.8	10.0	0.2	10.0
OP	percent	5,687	48.0	28.3	51.4	0.0	100.0
POG	percent	5,687	21.0	24.9	12.5	0.0	100.0
C0	Y	688					
C1	Y	3,959					
C2	Y	489					
C3	Y	551					
Night	N	3,750					
	Y	1,937					
PH	N	4,507					
	Y	1,180					
Shade	N	5,463					
	Y	224					
Glare	N	5,347					
	Y	340					
Site	N (Site 2)	5,094					
	Y (Site 1)	593					
LH	N (High)	549					
	Y (Low)	5,138					

Table 8.3 Summary of Descriptive Statistics (RZ4 Advanced WDR, Sites 1 and 2)

Variable	Unit	Freq	Mean	SD	Median	Min	Max
Amiss	0.1 sec.	5,608	3.1	7.6	2.0	0.0	493.0
Afalse	0.1 sec.	5,608	3.8	15.9	0.0	0.0	560.0
Astuck	0.1 sec.	5,608	5.6	14.3	4.0	0.0	792.0
Adrop	0.1 sec.	5,608	2.9	23.5	0.0	0.0	827.0
Wspeed	mph	5,608	5.8	3.8	5.8	0.0	16.1
Visibility	mile	5,608	7.9	3.7	10.0	0.2	10.0
OP	percent	5,608	49.0	28.1	52.8	0.0	100.0
POG	percent	5,608	21.0	25.0	12.3	0.0	100.0
C0	Y	759					
C1	Y	3,889					
C2	Y	435					
C3	Y	525					
Night	N	3,661					
	Y	1,947					
PH	N	4,502					
	Y	1,106					
Shade	N	5,384					
	Y	224					
Glare	N	5,268					
	Y	340					
Site	N (Site 2)	5,094					
	Y (Site 1)	514					
AD	N	268					
	Y	5,340					

Table 8.4 Summary of Descriptive Statistics (SmartSensor Matrix, Sites 1 and 2)

Variable	Unit	Freq	Mean	SD	Median	Min	Max
Amiss	0.1 sec.	7,124	2.3	7.5	0.0	0.0	270.0
Afalse	0.1 sec.	7,124	7.8	23.6	6.0	0.0	977.0
Astuck	0.1 sec.	7,124	6.1	23.6	3.0	0.0	884.0
Adrop	0.1 sec.	7,124	14.9	58.9	0.0	0.0	641.0
Wspeed	mph	7,124	6.2	3.8	5.8	0.0	17.3
Visibility	mile	7,124	7.6	3.7	10.0	0.2	10.0
OP	percent	7,124	44.5	27.7	43.9	0.0	100.0
POG	percent	7,124	19.4	23.0	11.9	0.0	100.0
C0	Y	904					
C1	Y	4,874					
C2	Y	754					
C3	Y	557					
C4	Y	35					
Night	N	4,682					
	Y	2,442					
PH	N	5,459					
	Y	1,665					
Shade	N	6,900					
	Y	224					
Glare	N	6,708					
	Y	416					
Site	N (Site 2)	5,094					
	Y (Site 1)	2,030					

Table 8.5 Summary of Descriptive Statistics (Wireless Magnetometers, Site 3)

Variable	Unit	Freq	Mean	SD	Median	Min	Max
Amiss	0.1 sec.	5,229	4.0	10.0	4.0	0.0	457.0
Afalse	0.1 sec.	5,229	0.4	8.0	0.0	0.0	278.0
Astuck	0.1 sec.	5,229	22.6	72.3	2.0	0.0	686.0
Adrop	0.1 sec.	5,229	5.0	46.6	0.0	0.0	1194.0
Wspeed	mph	5,229	9.3	4.8	8.1	0.0	23.0
Visibility	mile	5,229	8.6	2.8	10.0	0.5	10.0
OP	percent	5,229	26.9	29.0	14.7	0.0	100.0
POG	percent	5,229	26.1	37.8	6.3	0.0	100.0
C0	Y	637					
C1	Y	3,927					
C2	Y	615					
C3	Y	15					
C5	Y	35					
Night	N	3,493					
	Y	1,736					
PH	N	3,627					
	Y	1,602					
RP	N	2,182					
	Y	3,047					

Table 8.6 Summary of Descriptive Statistics (Vantage SmartSpan, Site 3)

Variable	Unit	Freq	Mean	SD	Median	Min	Max
Amiss	0.1 sec.	3,908	2.3	8.0	0.0	0.0	97.0
Afalse	0.1 sec.	3,908	39.1	125.7	6.0	0.0	2816.0
Astuck	0.1 sec.	3,908	141.0	314.2	18.0	0.0	6052.0
Adrop	0.1 sec.	3,908	2.3	10.0	0.0	0.0	298.0
Wspeed	mph	3,908	7.6	3.7	8.1	0.0	18.4
Visibility	mile	3,908	7.9	3.3	10.0	0.5	10.0
OP	percent	3,908	55.7	30.2	57.1	0.2	98.2
POG	percent	3,908	11.4	10.3	7.9	0.1	90.0
C0	Y	191					
C1	Y	3,149					
C2	Y	539					
C3	Y	29					
Night	N	2,384					
	Y	1,524					
PH	N	2,627					
	Y	1,236					
Glare	N	3,825					
	Y	83					

By compiling the error statistics from Tables 8.1-8.6, the error statistics across devices are summarized in Table 8.7. As shown, the largest mean error (which is the stuck-on call error) is 14.1 seconds (141.0 milliseconds), experienced by the Vantage SmartSpan camera. The smallest mean error (which is the false call error) is 0.13 seconds (1.3 milliseconds), experienced by the FC-334T thermal imaging camera. Even though the results in Table 8.7 shed a light on the levels of accuracy and reliability of each device, but it should not be used directly to compare the performance of the devices because different groups of devices were tested at different sites under different weather and environmental conditions (Tables 7.1 and 7.2) and adjustments were made to specific devices during the test period (Table 7.2). For appropriate comparison, those differences should be accounted for or controlled through proper statistical techniques, which is discussed subsequently.

A clear observation in Table 8.7 is that the standard deviations are much larger than the means for all devices and error types, indicating a tendency of over-dispersion of the errors.

Table 8.7 Comparison of Detection Errors across Test Devices

Device	Error Type	Sample Size	Mean	SD	Median	Min	Max
Autoscope AIS-IV Camera	Missed call	5,730	6.6	35.6	0.0	0.0	662.0
	False call	5,730	12.1	51.0	3.0	0.0	1267.0
	Stuck-on call	5,730	42.7	115.7	7.0	0.0	2567.0
	Dropped call	5,730	7.6	41.3	0.0	0.0	557.0
FC-334T Thermal Imaging Camera	Missed call	5,687	9.4	35.0	6.0	0.0	608.0
	False call	5,687	1.3	19.3	0.0	0.0	796.0
	Stuck-on call	5,687	6.9	28.7	3.0	0.0	1134.0
	Dropped call	5,687	2.2	24.2	0.0	0.0	835.0
RZ4 Advanced WDR Camera	Missed call	5,608	3.1	7.6	2.0	0.0	493.0
	False call	5,608	3.8	15.9	0.0	0.0	560.0
	Stuck-on call	5,608	5.6	14.3	4.0	0.0	792.0
	Dropped call	5,608	2.9	23.5	0.0	0.0	827.0
SmartSensor Matrix	Missed call	7,124	2.3	7.5	0.0	0.0	270.0
	False call	7,124	7.8	23.6	6.0	0.0	977.0
	Stuck-on call	7,124	6.1	23.6	3.0	0.0	884.0
	Dropped call	7,124	14.9	58.9	0.0	0.0	641.0
Wireless Magnetometer	Missed call	5,229	4.0	10.0	4.0	0.0	457.0
	False call	5,229	0.4	8.0	0.0	0.0	278.0
	Stuck-on call	5,229	22.6	72.3	2.0	0.0	686.0
	Dropped call	5,229	5.0	46.6	0.0	0.0	1194.0
Vantage SmartSpan Camera	Missed call	3,908	2.3	8.0	0.0	0.0	97.0
	False call	3,908	39.1	125.7	6.0	0.0	2816.0
	Stuck-on call	3,908	141.0	314.2	18.0	0.0	6052.0
	Dropped call	3,908	2.3	10.0	0.0	0.0	298.0

Note: errors were measured in 100 milliseconds or 0.1 seconds.

Besides descriptive statistics, error distributions are also plotted in Figure 8.1, where excessive zeros are evident.

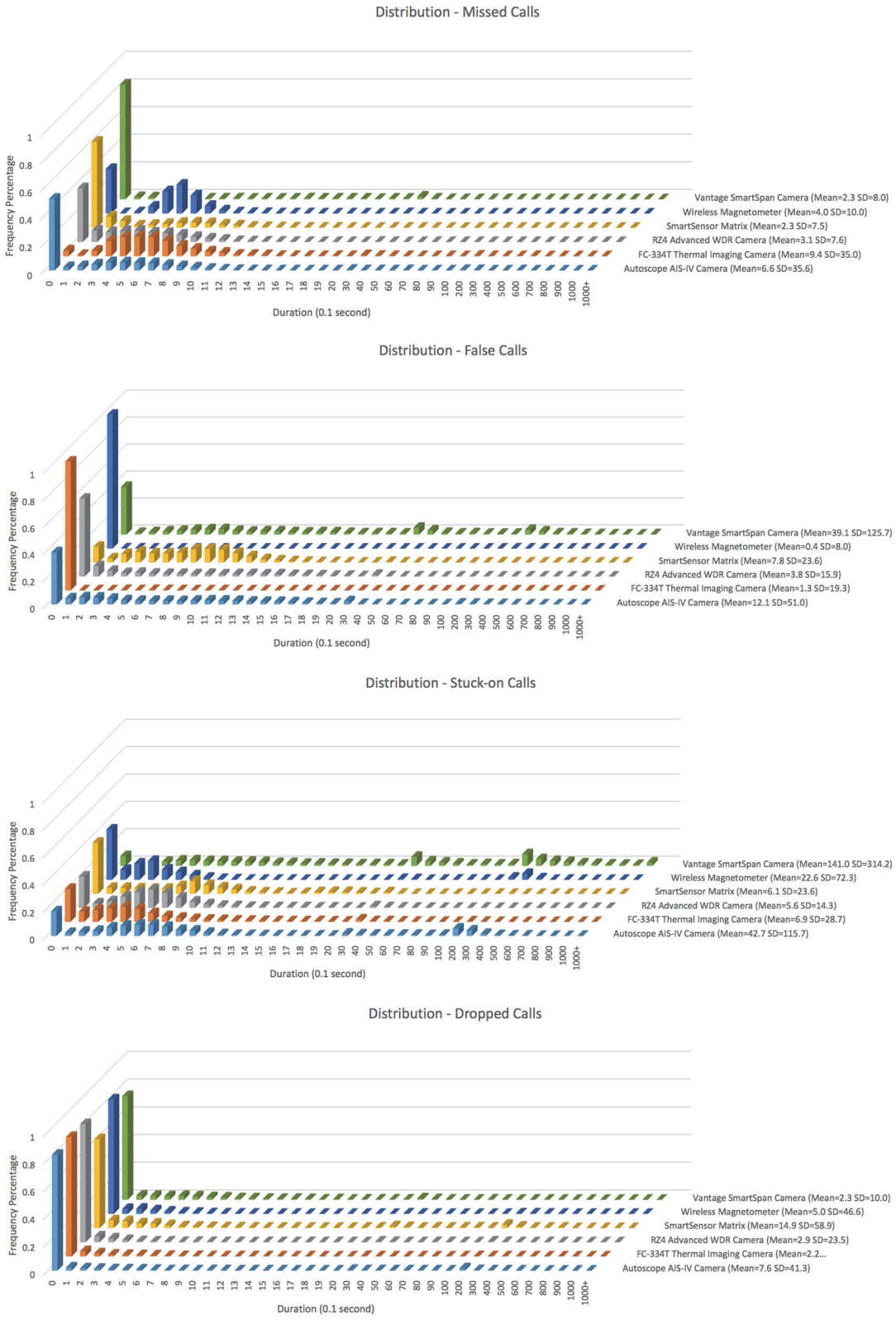

Figure 8.1 Distribution of call errors.

8.1.1.2 Temporal Error Plots and Video Review

To identify any associations between errors and weather and environmental conditions, temporal variation of errors and concurrent weather and environmental conditions were plotted side by side. This permits a visual check on potential associations of any error patterns with the weather and environmental conditions. To better observe data trends or patterns, moving average techniques were applied. The plots of all six test devices for stop bar detection are included in Appendices A, B, and C. By inspecting the plots, it is rather difficult to identify any associations between the errors and the corresponding weather and environmental conditions. However, a sudden reduction of false and stuck-on call errors is clearly noted for the Wireless Magnetometers following the installation of the new repeater (Figures 8.2 and 8.3).

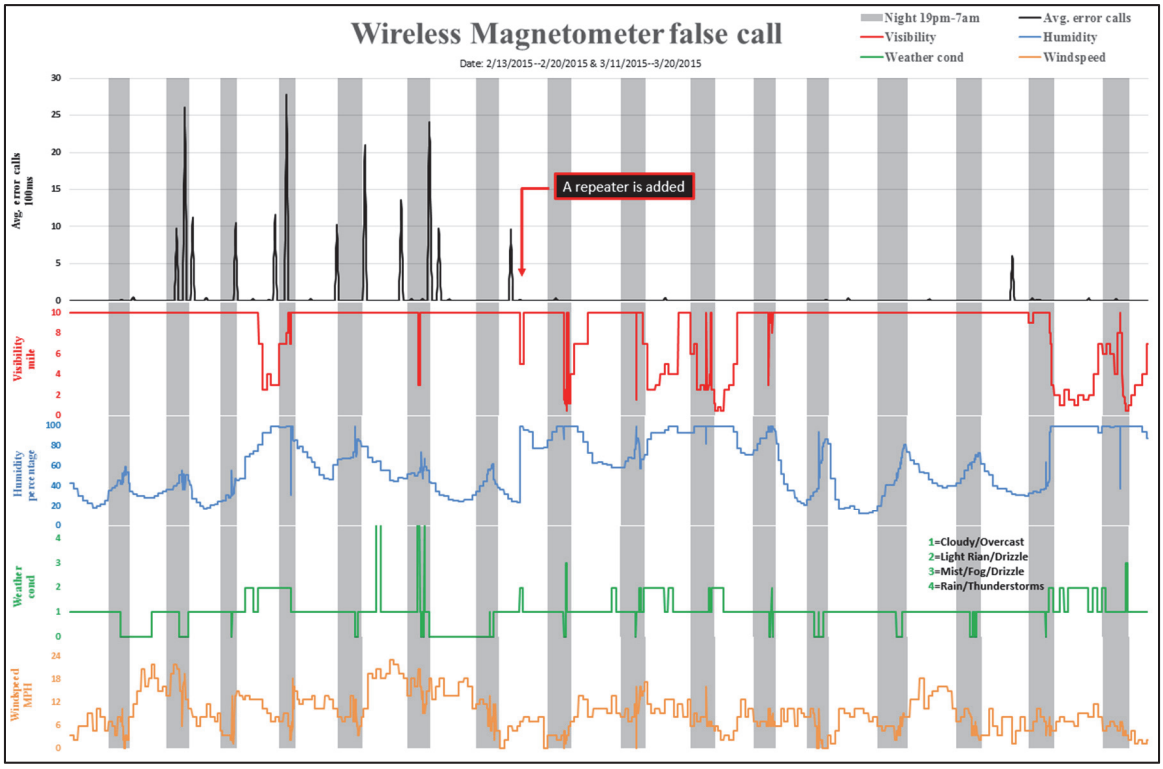

Figure 8.2 Evident reduction of detection errors (false calls) for wireless magnetometers after installation of the new repeater.

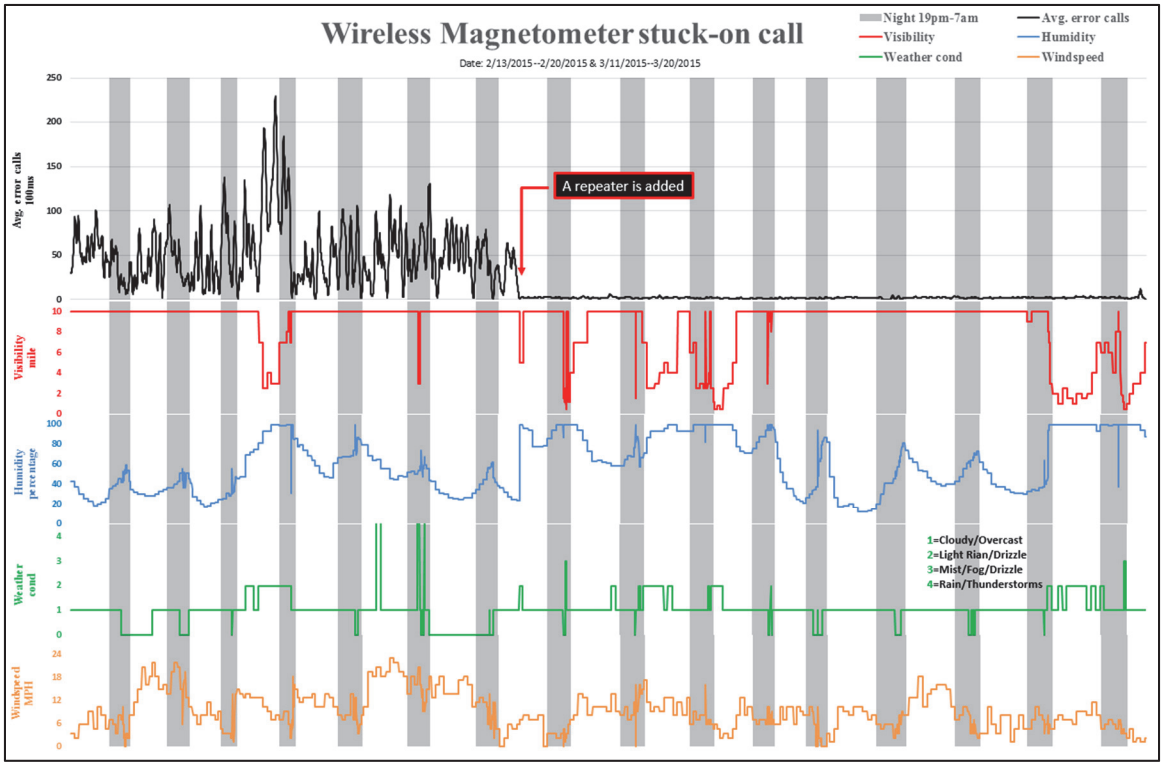

Figure 8.3 Evident reduction of detection errors (stuck-on calls) for wireless magnetometers after installation of the new repeater.

Besides the temporal plots, videos recorded through the detection cameras were reviewed for the time points when the large errors occurred. This permits the research team to verify the large errors and likely causes. Some images were extracted from the videos and are presented in Figures 8.4-8.7. Figures 8.4 and 8.5 show correct detection during normal day and night conditions. Figure 8.6 captures a false call by the Autoscope AIS-IV camera due to the tree shadow at site 2.

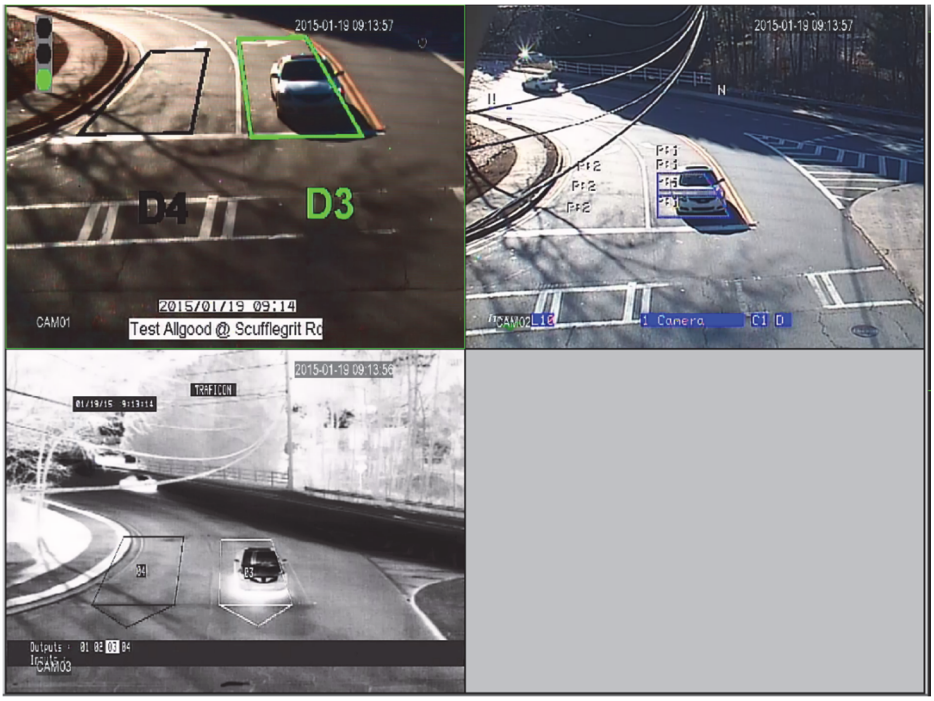

Figure 8.4 Normal conditions – daytime (site 2; upper left: Autoscope AIS-IV; upper right: RZ4 Advanced WDR; lower left: FC-334T Thermal)

Figure 8.5 Nornal conditions – nighttime (site 2; upper left: Autoscope AIS-IV; upper right: RZ4 Advanced WDR; lower left: FC-334T Thermal)

Figure 8.6 Potential false call due to uneven shade (site 2; upper left: Autoscope AIS-IV; upper right: RZ4 Advanced WDR; lower left: FC-334T Thermal)

Figure 8.7 captures the detection of the Vantage SmartSpan camera under different weather and environmental conditions. As seen by the relative locations of zones and vehicles, the Vantage SmartSpan camera is generally affected by wind, headlight at night, and reflection due to wet pavement.

Figure 8.7 Detection under different conditions (site 3; Vantage SmartSpan Camera)

8.1.2 Level 2 Analysis - Partition of Detection Errors using Conditional Inference Trees

Recursive partitioning is a fundamental tool in data mining. It helps explore the structure of data, while developing easy-to-visualize decision rules for predicting a categorical (classification tree) or continuous (regression tree) outcome. Conditional inference trees (ctree implemented in the R party package) is a non-parametric class of regression trees embedding tree-structured regression models into a well-defined theory of conditional inference procedures, where the conditional distribution of statistics measuring the association between responses and covariates is the basis for unbiased selection among covariates measured at different scales (Hothorn et al. 2006). In this study, ctree is used as an exploratory tool to identify any associations of detection errors with weather and environmental conditions.

Details on ctree procedures were described by Hothorn et al. (2006). Specifically, a generic algorithm that recursively partition a sample is formulated using non-negative integer valued case weights. Each node of a tree is represented by a vector of case weights, which have non-zero elements when the corresponding observations are elements of the node and are zero otherwise. The algorithm involves two steps: (1) variable selection, and (2) splitting. In step 1, the covariate of strongest association with the response is selected for splitting. In step 2, a permutation test framework (Strasser and Weber, 1999) is used to find the optimal binary split for the selected covariate in step 1. The goodness of a split is evaluated by a two-sample linear statistic that measures the discrepancy between the samples. The two steps are repeated recursively until the global null hypothesis of independence between the response and any of the covariates cannot be rejected at a pre-specified level, say 0.05. The Bonferroni-adjusted p-value was used in this case.

8.1.2.1 Mast Arm Installation (Site 1 and Site 2)

Four detection devices, (1) Autoscope AIS IV camera, (2) FC-334T Thermal Imaging camera, (3) RZ4 Advanced WDR camera, and (4) SmartSensor Matrix, were installed and tested at site1 and site 2, where mast arms are used for traffic signals support. As discussed previously, data collected at the two sites were pooled together and a dummy variable (to indicate test sites) was created to account for potential site effect.

For each test device, conditional inference trees were estimated separately for each error type as applicable and are presented in Figures 8.8-8.22.

1) Conditional Inference Trees for the Autoscope AIS-IV Camera

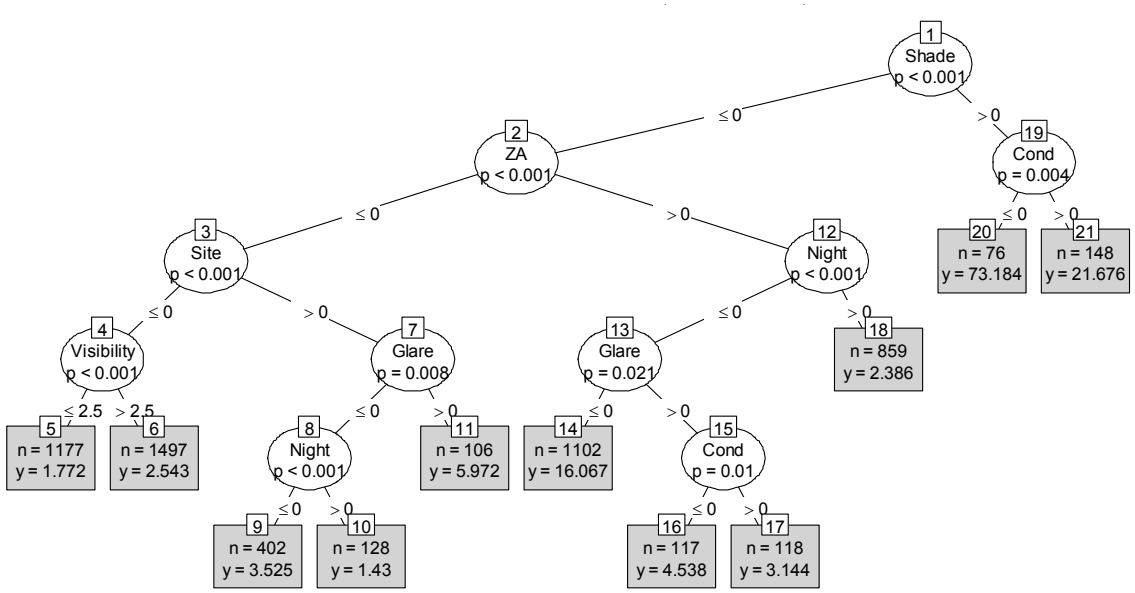

Figure 8.8 Autoscope AIS-IV camera (missed calls)

As shown in Figure 8.8, uneven shade has strongest association with the missed call error of the Autoscope AIS-IV camera. The largest mean error (approximately 7.3 seconds, i.e., 73.184*0.1) was computed when uneven shade (Shade > 0) is present during the clear weather condition (Cond = 0). The second largest mean error (2.2 seconds) was computed for the cloudy condition (Cond =1) under which the uneven shade become less stark. The third largest mean error (1.6 seconds) was computed in the combined context of no uneven shade (Shade < 0), reduced detection zone (ZA>0), daytime (Night <0), and no potential glare (Glare < 0). Given the relatively favorable environmental conditions, this relatively large mean error is likely due to the reduced detection zone (ZA>0) because the smaller the detection zone is, the more likely a vehicle would be missed.

At site 1 (Site>0), a larger mean missed call error (0.6 seconds) was observed when the potential glare condition is present. Under the condition of reduced detection zone (ZA > 0), the potential glare condition is associated with a smaller mean error, which is due to the fact that the data for this condition are from site 2, where the potential glare issue was practically avoided because of the smaller aspect ratio (horizontal / vertical) at this site.

The smaller mean error associated with the night condition (Night >0) is likely a result of light traffic, which “generates” excessive “zero” errors.

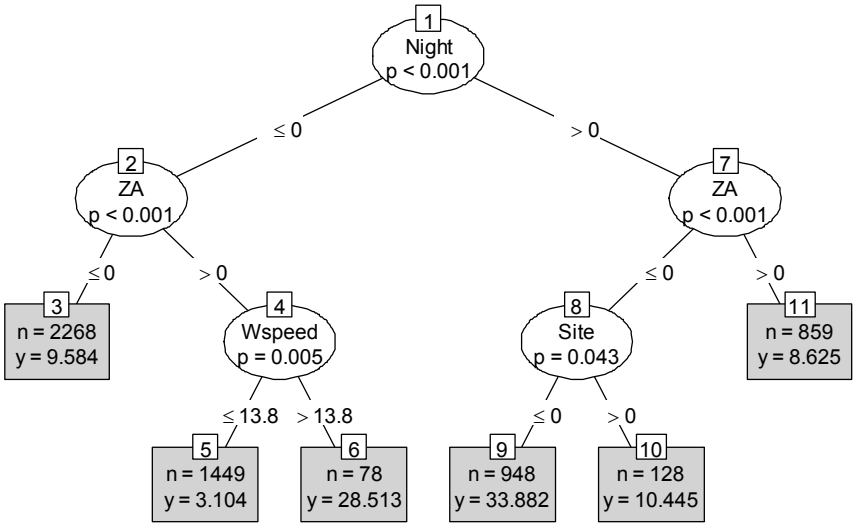

Figure 8.9 Autoscope AIS-IV camera (false calls)

As shown in Figure 8.9, the night condition (Night > 0) has strongest association with the false call error of the Autoscope AIS-IV camera. The largest mean error (3.4 seconds, i.e., 33.882*0.1) was computed in the combined context of night condition, larger detection zone (ZA ≤ 0), and site 2 (Site ≤ 0). The second largest mean error (2.9 seconds, i.e., 28.513*0.1) was computed in the combined context of daytime (Night ≤ 0), reduced detection zone (ZA > 0), and higher wind speed (Wspeed >13.8 mph). As seen, a higher wind speed was associated with a larger mean false call error when the detection zone is smaller. This appears to be intuitive as a smaller detection zone makes the detection more sensitive to wind.

Additionally, site 1 has a much smaller mean false call error compared to site 2 at night before the detection zone was adjusted (reduced). This is likely due to the existence of ambient street lighting at site 1, but not at site 2.

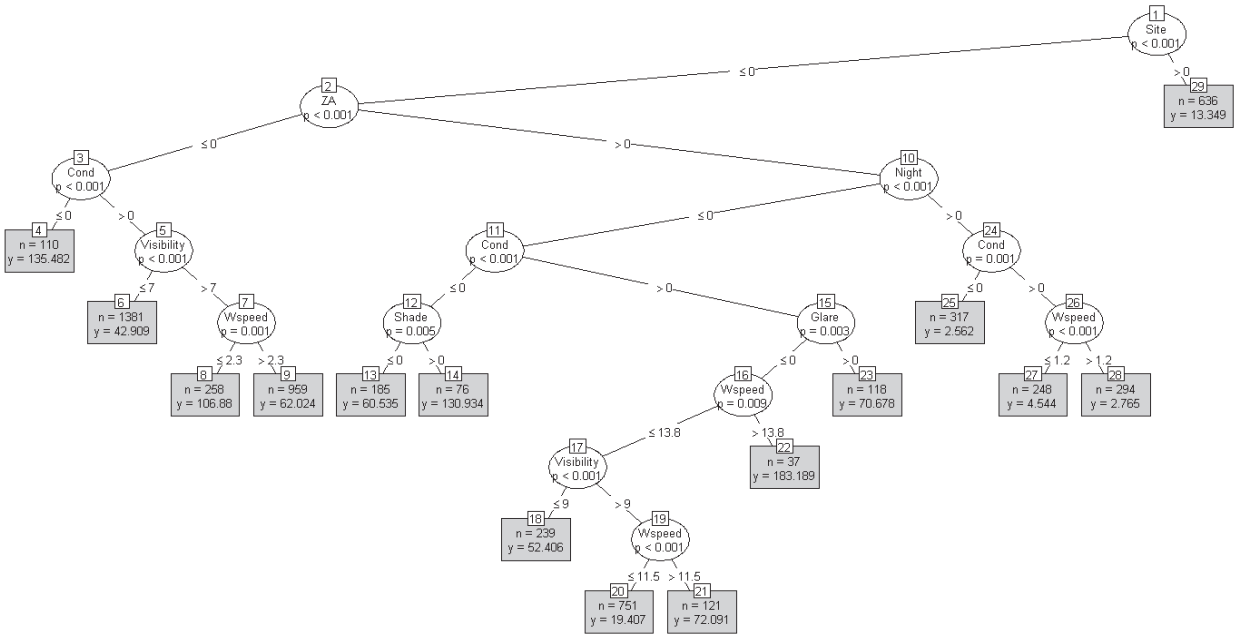

Figure 8.10 Autoscope AIS-IV camera (stuck-on calls)

As shown in Figure 8.10, the stuck-on call error of the Autoscope AIS-IV camera was associated with many factors in a rather complex way. The stuck-on call error has the strongest association with site 2 (Site ≤ 0). The largest mean error (18.3 seconds, i.e., 183.189*0.1) was computed in the combined context of site 2, reduced detection zone (ZA>0), daytime (Night ≤ 0), adverse weather conditions (Cond > 0), no glare (Glare ≤ 0), and higher wind speed (Wspeed > 13.8 mph). Wind speed may increase or decrease the stuck-on call error depending on other factors, such as weather conditions, visibility level, and whether it is during the day or night. Overall, a smaller detection zone (ZA >0) appears to reduce the stuck-on call error.

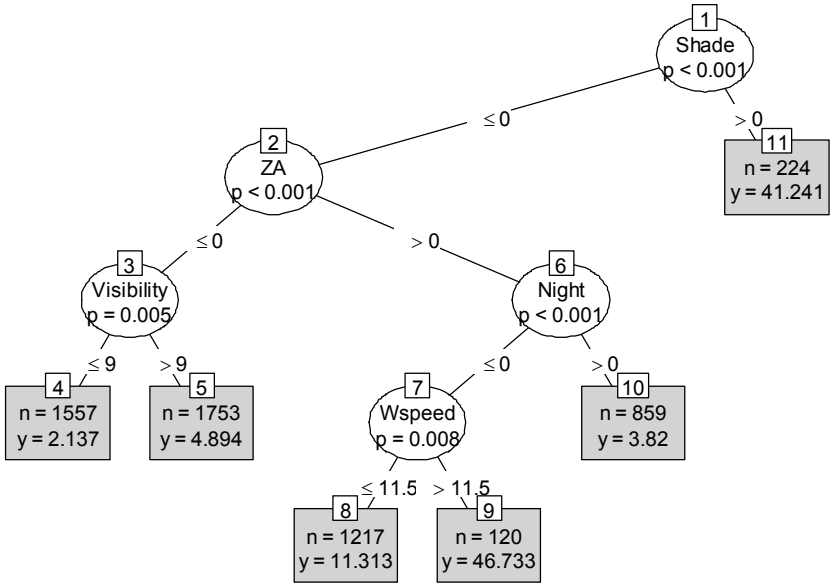

Figure 8.11 Autoscope AIS-IV camera (dropped calls)

As seen in Figure 8.11, uneven shade has the strongest association with the dropped call error. The largest mean error (4.7 seconds, i.e., 46.733*0.1) was computed in the combined context of no uneven shade (Shade ≤ 0), reduced detection zone (ZA>0), daytime (Night ≤ 0), and higher wind speed (Wspeed > 11.5 mph). This indicates that a smaller detection zone and a higher wind speed likely result in a larger dropped call error, which is intuitive. The second largest mean error (4.1 seconds) was computed for the uneven shade condition (Shade > 0). Improved visibility (Visibility > 9 miles) was associated with a larger mean dropped call error. The smaller mean error associated with the night condition is likely due to light traffic.

2) Conditional Inference Trees for the FC-334T Thermal Imaging Camera

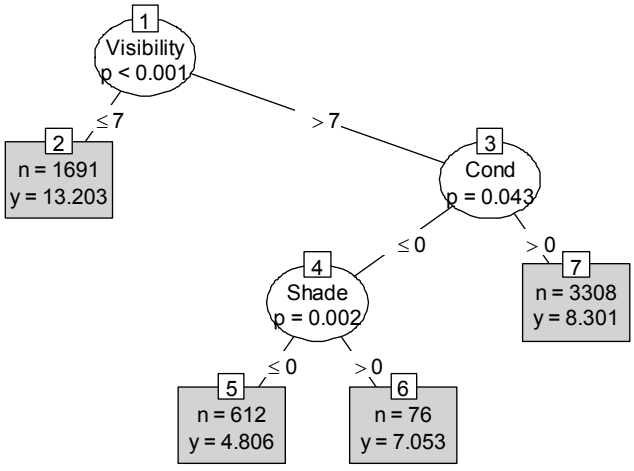

Figure 8.12 FC-334T thermal imaging camera (missed calls)

As shown in Figure 8.12, visibility has the strongest association with the missed call error for the FC-334T thermal imaging camera. The largest mean error (1.3 seconds, i.e., 13.203*0.1) was computed under a relatively lower visibility condition (Visibility ≤ 7 miles). The second largest mean error (0.8 seconds) was computed in the joint context of higher visibility (Visibility > 7 miles) and adverse weather conditions (Cond > 0). Under the clear weather condition (Cond = 0), uneven shade (Shade >0) was associated with a larger missed call error.

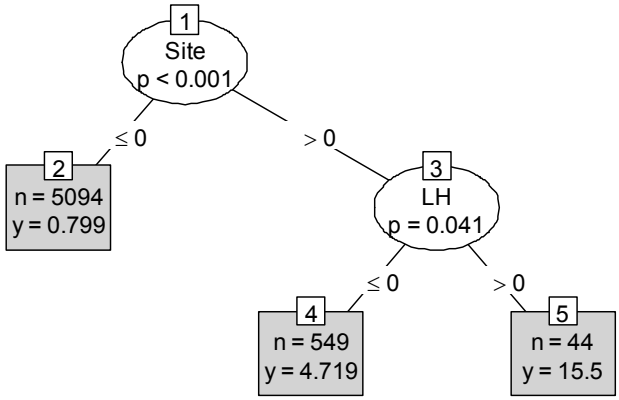

Figure 8.13 FC-334T thermal imaging camera (false calls)

As shown in Figure 8.13, site 1 (Site > 0) has the strongest association with the false call error. The largest mean error (1.6 seconds, i.e., 15.5*0.1) was computed in the joint context of site 1 and lower mounting height (LH > 0).

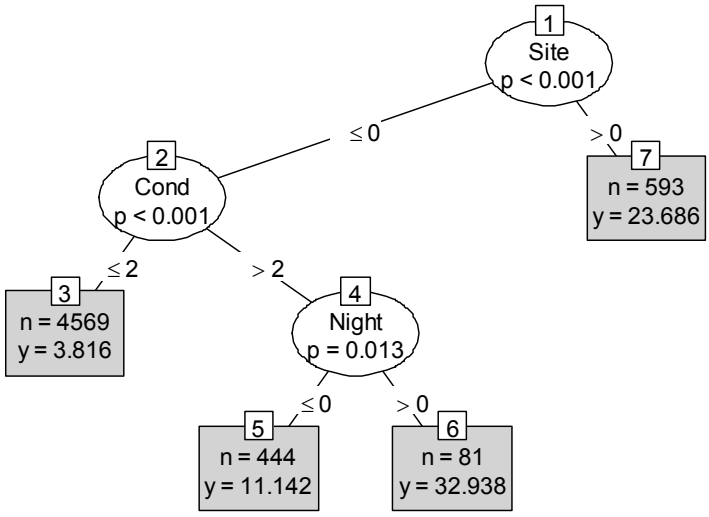

Figure 8.14 FC-334T thermal imaging camera (stuck-on calls)

As shown in Figure 8.14, site 1 (Site >0) has the strongest association with the stuck-on call error. However, the largest mean error (3.3 seconds, i.e., 32.938*0.1) was computed

in the combined context of site 2 (Site ≤ 0), adverse weather (Cond >2), and night condition (Night >0). The second largest mean error (2.4 seconds) was computed for site 1.

Note that a conditional inference tree for the dropped call error was not estimated for the FC-334T thermal imaging camera.

3) Conditional Inference Trees for the RZ4 Advanced WDR Camera

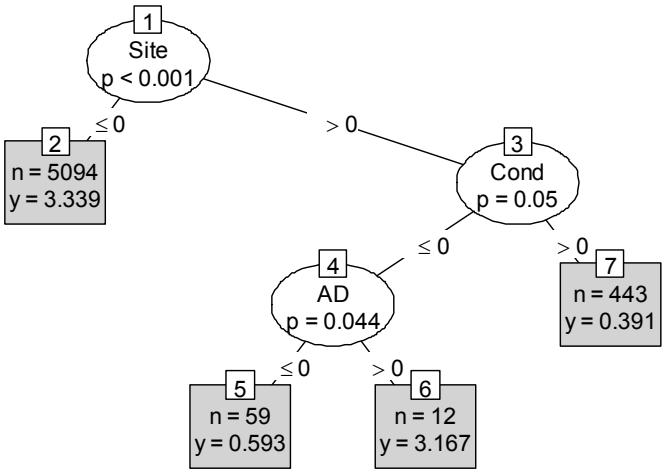

Figure 8.15 RZ4 advance WDR camera (missed calls)

As shown in Figure 8.15, site 2 (Site ≤ 0) has the strongest association with the missed call error for the RZ4 advance WDR camera. The largest mean error (0.3 seconds, i.e., 3.339*0.1) was computed for site 2. The second largest mean error was computed at site 1 after the adjustment (AD > 0) was made. The adjustment includes reduced sensitivity and screening of pedestrian crossings.

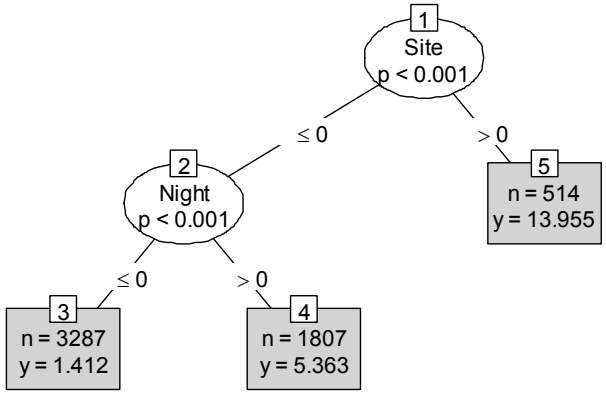

Figure 8.16 RZ4 advance WDR camera (false calls)

As shown in Figure 8.16, site 1 (Site >0) has the strongest association with the false call error. The largest mean error (1.4 seconds, i.e., 13.955*0.1) was computed for site 1. This

is likely due to the farther distance of the camera from the detection zone (a larger aspect ratio) at site 1 as compared to site 2. At site 2, a larger mean false error was computed at night (Night >0).

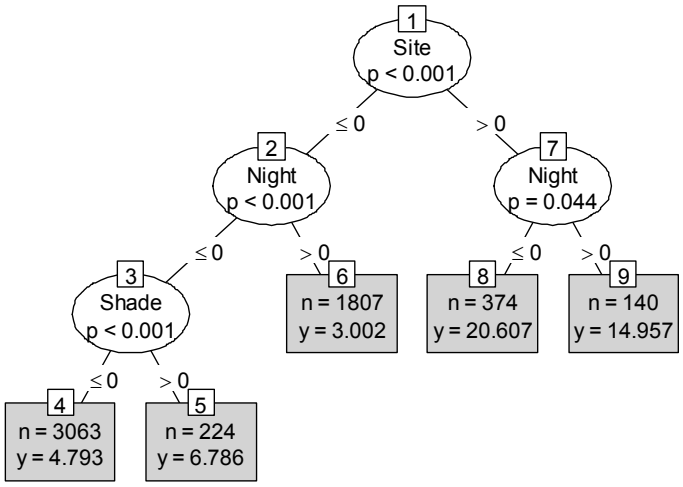

Figure 8.17 RZ4 advance WDR camera (stuck-on calls)

As shown in Figure 8.17, site 1 (Site >0) has the strongest association with the stuck-on call error. The largest mean error (2.1 seconds, i.e., 20.607*0.1) was computed in the joint context of site 1 and night. Night condition was associated with relatively smaller stuck-on call errors. A slightly larger mean stuck-on error was computed under the uneven shade condition (Shade > 0).

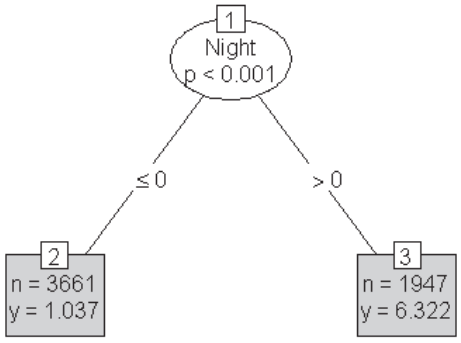

Figure 8.18 RZ4 advance WDR camera (dropped calls)

For the dropped call error, the night condition (Night) appears to be the only factor. As indicated in Figure 8.18, a larger mean dropped call error was computed at night.

4) Conditional Inference Trees for the SmartSensor Matrix

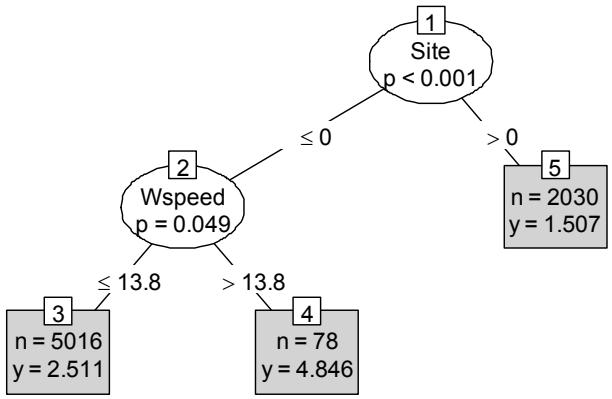

Figure 8.19 SmartSensor Matrix (missed calls)

As shown in Figure 8.19, site 2 has the strongest association with the missed call error. A smaller mean error was computed at site 1 (Site > 0). This is likely due to the fact that the SmartSensor Matrix sensor was mounted to detect the eastbound left turn movement, which is on the near side approach, at site 1. Note that the three detection cameras tested at site 1 were mounted on the same mast arm, but targeted at the far side approach, i.e., the westbound left turn movement. A larger mean missed call error was computed when the wind speed is higher (Wspeed > 13.8 mph).

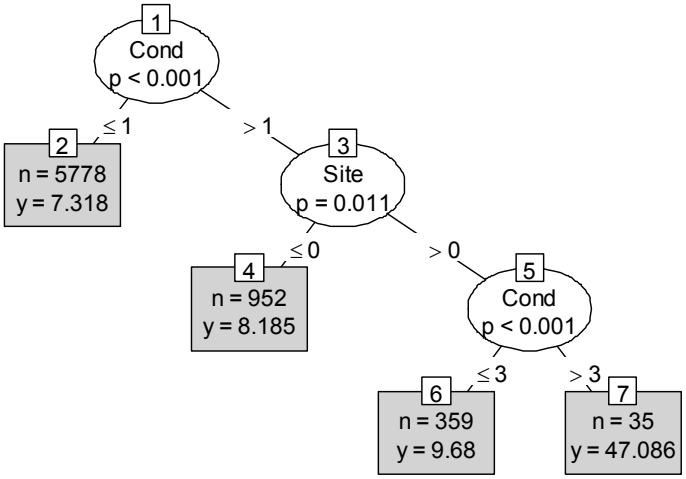

Figure 8.20 SmartSensor Matrix (false calls)

As shown in Figure 8.20, the largest mean false call error (4.7 seconds, i.e., 47.086*0.1) was computed in the joint context of site 1 (Site >0) and the severe weather condition (Cond > 3, i.e., Cond = 4, which indicates rain/thunderstorm).

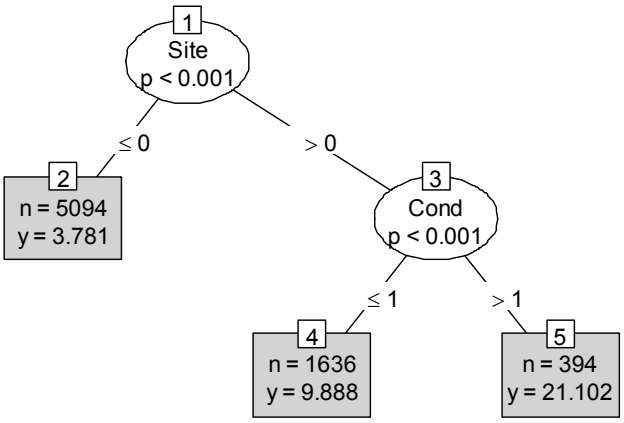

Figure 8.21 SmartSensor Matrix (stuck-on calls)

As shown in Figure 8.21, site 1 has much larger stuck-on call errors than site 2. The largest mean error (2.1 seconds, i.e., 21.102*0.1) was computed at site 1 (Site >0) when adverse weather conditions (Cond > 1) were present.

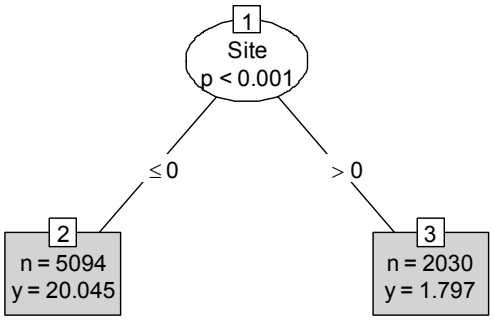

Figure 8.22 SmartSensor Matrix (dropped calls)

As shown in Figure 8.22, Site appears to be the only factor for the dropped call error. A much larger mean dropped call error (2.0 seconds, i.e., 20.045*0.1) was computed for site 2 (approximately 0.2 seconds, i.e., 1.797*0.1). Given that fact that the SmartSensor Matrix was mounted at nearly same height (approximately 18 feet from the pavement) at both sites, the much larger mean error at site 2 is likely due to the farther horizontal distance of the camera from the detection zone and the curved approach. Note that the SmartSensor was mounted for the near-side detection at site 1 while it was mounted for the far-side detection at site 2.

Based on the conditional inference tree results discussed above, the direction of error association with different factors was identified and is presented in Table 8.8, where the "+" sign indicates a positive association and the "-" sign indicates a negative association. The "+/-" sign indicates a mixed association depending on other factors. For example, a higher visibility was associated with larger missed and dropped call errors for the

Autoscope AIS-IV camera. Note each row in Table 8.8 represents a factor, more cells filled with signs (colored) indicate increasing sensitivity (in terms of the increasing number of associated factors) of the corresponding device.

Table 8.8 Summary of Conditional Inference Tree Analysis (Sites 1 and 2)

Factor	Detection Errors (Erroneous Calls)															
	Missed				False				Stuck-on				Dropped			
	A	R	F	SM	A	R	F	SM	A	R	F	SM	A	R	F	SM
Site	+	-		-	-	+	+	+	-	+	+	+				-
Night	-				+	+			-	-	+		-	+		
Weather	-	-	+					+	+/-		+					
Visibility	+		-						+/-				+			
ZA	+				-				-				+			
AD		+														
Wind speed				+	+				+/-			+	+			
Shade	+		+						+	+			-			
Glare	+								+							
LH							+									

Notes:
+, positive association
-, negative association
+/-, mixed, i.e., the association changes depending on some other factors.
Letter code for test devices:
A – Autoscope AIS-IV Camera
R – RZ4 Advanced WDR Camera
F – FC-334T Thermal Imaging Camera
SM- SmartSensor Matrix

8.1.2.2 Span Wire Installation (Site 3)

Similarly, conditional inference trees were also estimated for the Wireless Magnetometers and the Vantage SmartSpan camera, which were tested at site 3. The results are shown in Figures 8.23-8.28. For the Wireless Magnetometers, conditional inference trees were estimated only for false call and stuck-on call errors.

a) Conditional Inference Trees for the Wireless Magnetometers

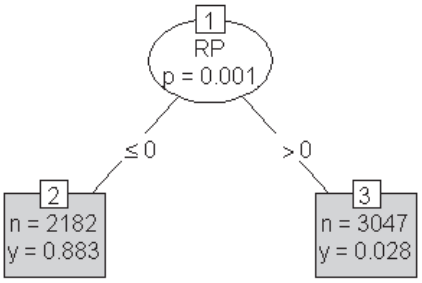

Figure 8.23 Sensys wireless magnetometers (false calls)

As seen in Figure 8.23, the addition of the new repeater results in a smaller mean false call error.

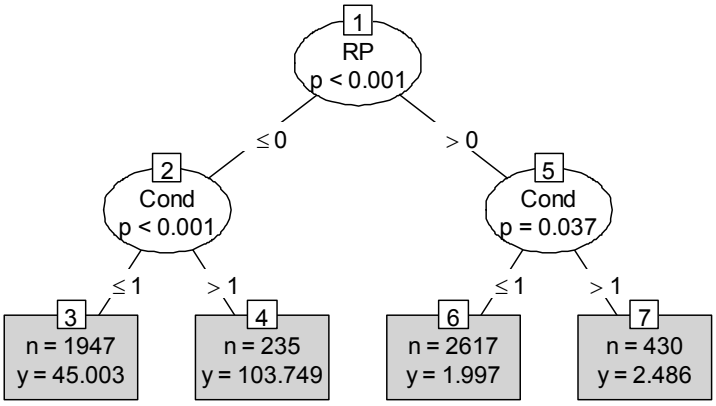

Figure 8.24 Sensys wireless magnetometers (stuck-on calls)

Similar to the false call error, Figure 8.24 indicates that the addition of the repeater results in a much smaller mean stuck-on call error. The significantly reduced error difference across the two weather groups (Cond ≤ 1 vs. Cond >1) reveals much improved robustness of the wireless magnetometers against more adverse weather conditions due to the addition of the repeater.

b) Conditional Inference Trees for the Vantage SmartSpan Camera

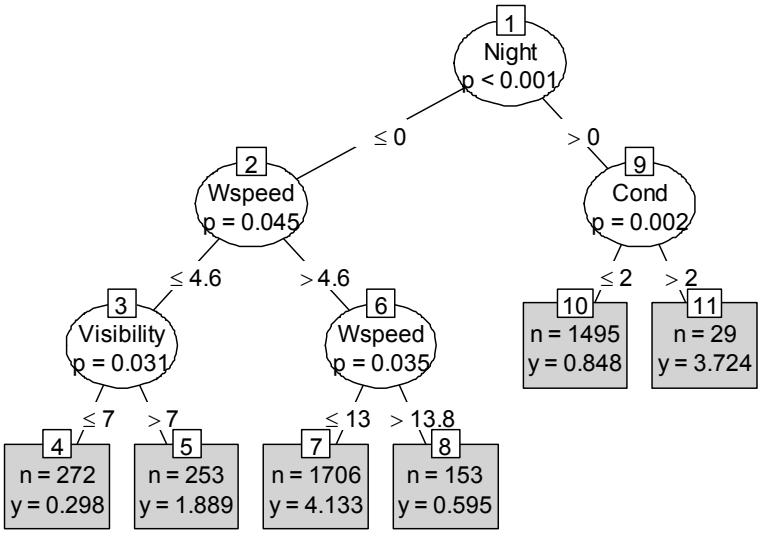

Figure 8.25 Vantage SmartSpan camera (missed calls)

As shown in Figure 8.25, the night condition (Night >0) has the strongest association with the missed call error for the Vantage SmartSpan camera. A larger mean missed call error was computed under more adverse weather conditions (Cond > 2) at night. Moderate wind (4.6 mph < Wspeed ≤ 13.8 mph) was associated with larger missed call errors. But, a smaller mean missed call error was computed for stronger wind (Wspeed > 13.8 mph). A smaller mean missed call error was computed at a higher level of visibility (Visibility > 7 miles).

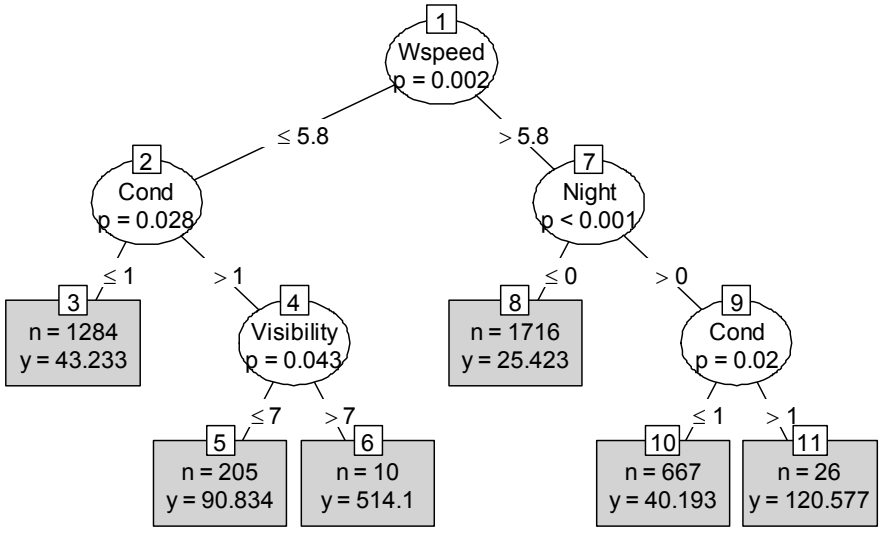

Figure 8.26 Vantage SmartSpan camera (false calls)

As indicated in Figure 8.26, wind speed exhibits the strongest association with the false call error for the Vantage SmartSpan camera. As expected, a larger mean false call error was computed under adverse weather conditions (Cond > 1). The largest mean false call error (51.4 seconds, i.e., 514.1*0.1) was computed in the combined context of lower wind speed (Wspeed ≤ 5.8 mph), adverse weather conditions (Cond > 1), and higher visibility (Visibility > 7 miles). The second largest mean false call error (12.1 seconds, i.e., 120.577*0.1) was computed in the combined context of higher wind speed (Wspeed > 5.8 mph), night (Night >0), and adverse weather conditions (Cond > 1).

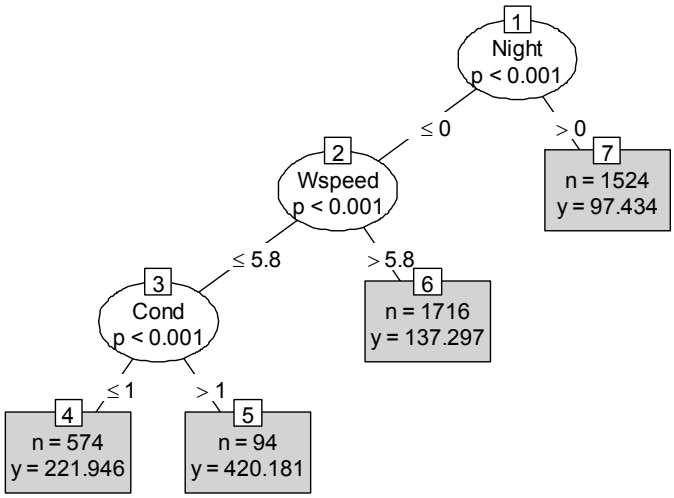

Figure 8.27 Vantage SmartSpan camera (stuck-on calls)

As shown in Figure 8.27, for the Vantage SmartSpan camera, the largest mean stuck-on call error (42.0 seconds, i.e., 420.181*0.1) was computed in the combined context of daytime, lower wind speed (Wspeed ≤ 5.8 mph), and adverse weather conditions (Cond > 1).

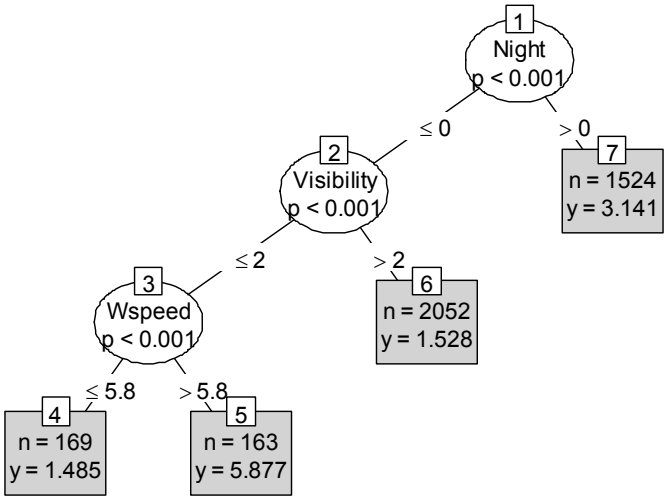

Figure 8.28 Vantage SmartSpan camera (dropped calls)

As shown in Figure 8.28, the night condition has the strongest association with the dropped call error. The largest mean error (0.6 seconds, i.e., 5.877*0.1) was computed in the combined context of daytime, lower visibility (Visibility ≤ 2), and higher wind speed (Wspeed > 5.8 mph). The second largest mean error (0.3 seconds, i.e., 3.141*0.1) was computed under the night condition (Night >0).

Based on the conditional inference tree results at site 3, the direction of error association with different factors was identified and is presented in Table 8.9.

Table 8.9 Summary of Conditional Inference Tree Analysis (Site 3)

Factor	Wireless Magnetometer				Vantage SmartSpan Camera			
	Missed	False	Stuck-on	Dropped	Missed	False	Stuck-on	Dropped
Night					-	+	-	+
Weather			+		+	+	+	
Visibility					+	+		-
Wind speed					+/-	-	-	+
Repeater		-	-					

Notes:
+, positive association
-, negative association
+/-, mixed, i.e., the association changes depending on some other factors.

As seen, more cells filled with both "+" and "-"signs for the SmartSpan camera indicate its higher sensitivity to weather and environmental conditions. For the Wireless Magnetometers, adverse weather appears to have a tendency to increase the stuck-on call error. The addition of the new repeater reduced both false and stuck-on call errors.

In summary, the conditional inference tree analysis is exploratory in nature and helpful to identify the associations between different call errors and potential factors. However, it should be pointed out that the associations identified may or may not reflect causation. For quantitative analysis, regression models were developed and are presented in the following section.

8.1.3 Level 3 Analysis - Regression Models

As described in the Section 6 - Data Acquisition, a sampling interval of 100 milliseconds or 0.1 seconds was deemed appropriate for the purpose of this study and thus used for data sampling in the field. For each sampling interval, the discrepancy status (0 or 1) of each test device were recorded with respect to the error type (i.e., missed, false, stuck-on, and dropped). The status of "1" indicates an error state (discrepancy) and "0" indicates an error-free state (no discrepancy).

For a certain error type, the count of consecutive status 1's (referred to as an error block) reveals the extent or magnitude of the error. Depending on vehicle arrival patterns, there could be multiple error blocks within a single cycle. In such cases, the average or mean of the error counts per cycle were computed. This averaging process aims to remove the possible effect of varying cycle lengths and different vehicle arrival patterns. The mean error count (or block length) per cycle can be treated as a random count variable. Typical distributions for count variables are Poisson and Negative Binomial (NB) depending on the dispersion of the data. If data indicate excess "zeros" (i.e., no errors), zero-inflated models (Lambert 1992) might be appropriate. An overview of various count models, including zero-inflated ones, can be found in Cameron and Trivedi (1998 and 2005).

Comparing to the regular or standard Poisson and NB models, zero-inflated models are mixture models that combine two components: a point mass at zero and a count distribution, where zeros arise from two sources, the point mass and the count component. For modeling the unobserved state (zero vs. count), a differentiable binary choice model form (i.e., logit) has been frequently used to determine which of the two processes the zero outcome is associated with. For modeling the count process, a Poisson or NB model can be used depending on dispersion of the count data. This results in either zero-inflated Poisson (ZIP) models or zero-inflated Negative Binomial (ZINB) models.

Throughout the rest of this section, it will be shown that the ZINB model generally fits the data better in most cases than its counterpart of the NB model. This was previously

informed by and consistent with the excessive zeros indicated in Figure 8.1 and the greater-than-mean variances shown in Table 8.7.

For Poisson distribution, the probability density function can be expressed as:

$$f(y,\mu) = \frac{\exp(-\mu)\cdot\mu^{y}}{y!} \quad (1)$$

For NB distribution, the probability density function takes the form of:

$$f(y,\mu,\theta) = \frac{\Gamma(y+\theta)}{y!\Gamma(\theta)} \cdot \frac{\mu^{y}\cdot\theta^{\theta}}{(\mu+\theta)^{y+\theta}} \quad (2)$$

Where,

μ = mean,
θ = shape parameter
Γ(·) = gamma function

As seen, Poisson distribution only have one parameter μ, which is the mean and also the variance since they are equal. NB distribution has two parameters μ and θ. It allows the variance $\left(\mu + \frac{\mu^2}{\theta}\right)$ to be greater than the mean (μ) through the shape parameter θ.

Denote the point mass at zero as $I_{\{0\}}(\mathrm{y})$ and the count distribution as $f_{count}(y; x, \beta)$. Further, let the probability of zero from the component of point mass at zero be $\pi = f_{zero}(0; z, \gamma)$, the combined zero-inflated distribution can be written as:

$$f_{zero-inflated}(y; x, z, \beta, \gamma) = f_{zero}(0; z, \gamma) \cdot I_{\{0\}}(y) + (1 - f_{zero}(0; z, \gamma)) \cdot f_{count}(y; x, \beta) \quad (3)$$

If using canonical log link, the mean for a particular observation i can be expressed as

$$\mu_i = \pi_i \cdot 0 + (1 - \pi_i) \cdot \mathrm{e}^{\mathrm{x}_i\beta} \quad (4)$$

where,

x = the vector of regressors in count model
β = the vector of parameters for regressors in count model
z = the vector of regressors in zero-inflation model
γ = the vector of parameters for regressors in zero-inflation model
θ = dispersion parameter for NB model

Note that Equation (4) is not restricted to the form of count models. Both ZIP and ZINB models can be estimated by the maximum likelihood method. For a NB model, the likelihood function can be written as:

$$L(\mu,\theta|y)=\prod_{i=1}^{n}\exp\left(y_i\ln\left(\frac{\mu_i}{\theta+\mu_i}\right)-\theta\ln\left(1+\frac{\mu_i}{\theta}\right)+ln\Gamma(y_i+\theta)-ln\Gamma(y_i+1)-ln\Gamma(\theta)\right) \quad (5)$$

To estimate parameter μ and θ, the log-likelihood function, which convert the multiplication to summation, is typically used and shown below.

$$LL(\mu,\theta|y)=\sum_{i=1}^{n}\left(y_i\ln\left(\frac{\mu_i}{\theta+\mu_i}\right)-\theta\ln\left(1+\frac{\mu_i}{\theta}\right)+ln\Gamma(y_i+\theta)-ln\Gamma(y_i+1)-ln\Gamma(\theta)\right) \quad (6)$$

For the ZINB model, the expression of the likelihood function depends on whether the observed value is a zero or not. If a logistic model is used, the probability (p) of $y_i>0$ versus $y_i=0$ can be expressed as:

$$p_i=\frac{1}{1+\exp(-z_i\gamma)} \quad (7)$$

Then, the log-likelihood function for the ZINB model becomes:

$$LL(\mu,\gamma,\theta|y,x,z)=\sum_{i=1}^{n}\begin{cases}\ln(p_i)+(1-p_i)\left(\frac{\theta}{\theta+\mu_i}\right)^{\theta}, & y_i=0\\ \ln(p_i)+y_i\ln\left(\frac{\mu_i}{\theta+\mu_i}\right)-\theta\ln\left(1+\frac{\mu_i}{\theta}\right)+ln\Gamma(y_i+\theta)-ln\Gamma(y_i+1)-ln\Gamma(\theta), & y_i>0\end{cases} \quad (8)$$

By replacing μ_i with $\exp(x_i\beta)$ and p_i with $1/(1+\exp(-z_i\gamma))$, Equation (9) is obtained.

$$LL(\mu,\gamma,\theta|y,x,z)=\sum_{i=1}^{n}\begin{cases}\ln\left(\frac{1}{1+\exp(-z_i\gamma)}\right)+\left(1-\frac{1}{1+\exp(-z_i\gamma)}\right)\left(\frac{\theta}{\theta+\exp(x_i\beta)}\right)^{\theta}, & y_i=0\\ \ln\left(\frac{1}{1+\exp(-z_i\gamma)}\right)+y_i\ln\left(\frac{\exp(x_i\beta)}{\theta+\exp(x_i\beta)}\right)-\theta\ln\left(1+\frac{\exp(x_i\beta)}{\theta}\right)+ln\Gamma(y_i+\theta)-ln\Gamma(y_i+1)-ln\Gamma(\theta), & y_i>0\end{cases} \quad (9)$$

Parameters β, γ, and θ can be estimated by maximizing the log-likelihood function. R software (R Core Team, 2014) was used for model estimation (Zeileis et al. 2008).

8.1.3.1 Test Devices with Mast Arm Installation (Sites 1 and 2)

The model estimation results for the four devices tested at both site 1 and site 2 are presented in Tables 8.9 – 8.12. Each table includes four models corresponding to the four error types. Either the standard count models (Poisson or NB) or the zero-inflated count models (ZIP or ZINB) were estimated as appropriate. The first section (top) of the tables present the estimation results of count models. The second section (middle) of the tables show the estimation results of zero-inflation models. The third section (bottom) of the table presents the results of Vuong tests for validity of zero-inflated count models versus standard count models.

Table 8.10 Model Estimation (Autoscope AIS-IV Camera)

Count Model

Variable	Missed Call (NB)				False Call (NB)				Stuck-on Call (NB)				Dropped Call (NB)			
	Estimate	z	p value		Estimate	z	p value		Estimate	z	p value		Estimate	z	p value	
Constant	0.845	5.098	0.000	***	2.802	33.798	0.000	***	5.943	38.800	0.000	***	2.903	9.405	0.000	***
Wspeed	0.119	7.032	0.000	***	0.069	9.804	0.000	***	0.022	4.137	0.000	***	0.006	0.362	0.718	
C1	0.730	5.001	0.000	***					-0.218	-3.169	0.002	**	-0.339	-1.735	0.083	.
C2	1.171	3.843	0.000	***	1.110	7.206	0.000	***	-0.448	-3.709	0.000	***	0.184	0.588	0.557	
C3	0.886	3.453	0.001	***	0.672	4.974	0.000	***	-0.587	-4.282	0.000	***	-1.757	-5.000	0.000	***
C4	0.666	0.523	0.601		5.860	4.758	0.000	***	0.107	0.406	0.685		-0.559	-0.768	0.442	
Visibility									0.030	2.848	0.004	**				
Glare	-0.776	-8.265	0.000	***	-0.421	-4.182	0.000	***	0.252	3.088	0.002	**	-0.556	-2.245	0.025	*
Shade	0.842	6.656	0.000	***	1.634	6.492	0.000	***	0.335	2.783	0.005	**	1.049	3.358	0.001	***
Night	-0.464	-5.360	0.000	***	0.826	16.188	0.000	***	-1.044	-17.689	0.000	***	-1.148	-6.429	0.000	***
ZA	1.235	17.764	0.000	***	-0.545	-9.902	0.000	***	-1.322	-21.653	0.000	***	0.565	3.554	0.000	***
Site	0.289	2.882	0.004	**					-2.372	-28.958	0.000	***				
PH	-0.402	-6.123	0.000	***					-0.856	-14.122	0.000	***	-1.068	-5.538	0.000	***
OP	-0.005	-3.823	0.000	***	-0.017	-16.754	0.000	***	-0.017	-15.102	0.000	***	0.013	4.897	0.000	***
POG									-0.014	-12.432	0.000	***	-0.034	-11.918	0.000	***
Wspeed:C1	-0.085	-4.754	0.000	***												
Wspeed:C2	-0.149	-3.742	0.000	***	-0.184	-8.866	0.000	***								
Wspeed:C3	-0.144	-2.799	0.005	**	-0.152	-5.379	0.000	***								
Wspeed:C4	-0.156	-1.463	0.143		-0.493	-4.756	0.000	***								
Log(theta)	-0.736	-13.983	0.000	***	-0.592	-20.769	0.000	***	-0.807	-45.032	0.000	***	-2.622	-37.076	0.000	***

Zero-Inflation Model (Binomial with Logit Link)

	Estimate	z	p value		Estimate	z	p value		Estimate	z	p value		Estimate	z	p value	
(Intercept)	-0.307	-2.273	0.023	*	-5.075	-15.438	0.000	***	3.075	12.508	0.000	***	1.252	4.489	0.000	***
Visibility	-0.139	-10.589	0.000	***	0.334	15.106	0.000	***					-0.128	-5.932	0.000	***
Night	1.514	13.379	0.000	***	-2.310	-16.298	0.000	***								
OP					0.012	4.058	0.000	***	-0.009	-2.012	0.044	*	0.022	6.303	0.000	***
POG					0.053	17.035	0.000	***	-1.317	-11.308	0.000	***	-0.142	-9.413	0.000	***

Vuong Non-Nested Hypothesis Test-Statistic

	z	p-value	z	p-value	z	p-value	z	p-value
Raw	5.561	0.000	13.804	0.000	21.726	0.000	6.745	0.000
AIC-corrected	5.561	0.000	13.804	0.000	21.726	0.000	6.745	0.000
BIC-corrected	4.989	0.000	13.318	0.000	21.428	0.000	5.522	0.000

Significance level: *** 0.001, ** 0.01, * 0.05, · 0.10.

As shown in Table 8.10, positive coefficient estimates for the count model (the top section of the table) indicate a tendency of increasing errors by the corresponding factors while negative coefficient estimates indicate a tendency of decreasing errors by the corresponding factors. On the other hand, positive coefficient estimates for the zero-inflation model (the middle section of the table) indicate a higher chance of "zero" or a lower chance of errors while negative coefficient estimates indicate a lower chance of "zero"

or a higher chance of errors. The column of asterisk or dot sign indicates the significance level as noted. Same interpretation applies to Tables 8.11 – 8.15.

For the Autoscope AIS-IV camera, the wind speed has a significant (at 0.001 significance level) effect on the missed, false and stuck-on call errors. A higher wind speed results in larger missed, false, and stuck-on call errors because of the positive coefficient estimates. All weather events (C1-C4) tend to increase the missed call error. Adverse weather events (C2-C4) results in larger false call errors. Weather events C1-C3 tend to reduce the stuck-on call error. Weather event C3 (fog, mist, or haze) tends to reduce the dropped call error.

The higher the visibility level, the larger the stuck-on call error. The potential glare situation tends to reduce the missed, false, and dropped call errors, but increase the stuck-on call error. This is likely due to the favorable weather condition (clear) associated with the potential glare situation, rather than the glare itself. Uneven shade tends to increase errors of all types. By inspecting the coefficient estimates of "Night" in the zero-inflated model, the chance of a missed call is lower while the chance of a false call is higher at night. By referencing the count model estimation, the error at night tends to be smaller for missed, stuck-on, and dropped calls, but larger for false calls.

Reducing the size of the detection zone (ZA =1) increases the missed call error but decreases the false call error. This is intuitive because the larger the detection zone is, the more likely a vehicle in the subject lane would be detected (reducing the missed call error) and likewise a vehicle in the adjacent lane is likely to be detected as well (increasing the false call error). Conversely, the smaller the detection zone is, the less likely a vehicle in the subject lane is detected (increasing the missed call error) and likewise the less likely a vehicle in the adjacent lane is detected (reducing the false call error). In light of this observation, the detection zone should be carefully drawn to optimize operations by considering both types of errors. The small p value of the Vuong test suggests that the ZINB model provides significant improvement over the standard NB model for all error types.

Table 8.11 Model Estimation (FC-334T Thermal Imaging Camera)

Count Model

Variable	Missed Call (NB)				False Call (NB)				Stuck-on Call (NB)				Dropped Call (NB)			
	Estimate	z	p value		Estimate	z	p value		Estimate	z	p value		Estimate	z	p value	
Constant	2.813	14.496	0.000	***	-6.849	-4.963	0.000	***	1.566	7.643	0.000	***				
Wspeed	0.031	3.398	0.001	***	0.284	7.944	0.000	***	0.020	4.104	0.000	***	0.037	1.783	0.075	.
C1	0.499	6.586	0.000	***	7.421	5.862	0.000	***	0.368	6.228	0.000	***	-0.168	-0.805	0.421	
C2	0.454	2.792	0.005	**	6.403	4.708	0.000	***	-0.136	-1.452	0.146		-1.724	-5.436	0.000	***
C3	0.347	2.875	0.004	**	8.779	6.304	0.000	***	1.193	11.877	0.000	***	-0.573	-1.905	0.057	.
Visibility	-0.075	-13.988	0.000	***	-0.117	-2.436	0.015	*	-0.058	-8.395	0.000	***	-0.163	-6.771	0.000	***
Glare	-0.519	-8.473	0.000	***					-0.129	-1.666	0.096	.	-1.277	-4.224	0.000	***
Shade	-0.361	-4.549	0.000	***					-0.155	-1.634	0.102					
Night									0.249	6.533	0.000	***	1.025	6.737	0.000	***
LH	-0.6227	-3.6660	0.0002	***					-0.3476	-1.8910	0.0586	.				
Site	-0.640	-3.855	0.000	***	1.470	3.805	0.000	***	1.389	7.841	0.000	***	1.361	3.675	0.000	***
OP	0.004	6.731	0.000	***	-0.048	-10.305	0.000	***					0.023	7.862	0.000	***
POG									0.007	9.411	0.000	***	0.019	5.396	0.000	***
Wspeed:C1	-0.018	-1.838	0.066	.												
Wspeed:C2	-0.091	-3.701	0.000	***												
Wspeed:C3	-0.099	-4.769	0.000	***												
Log(theta)	0.144	7.318	0.000	***					-0.242	-10.376	0.000	***	-3.107	-62.615	0.000	***
Theta					0.015	13.514	0.000	***								

Zero-Inflation Model (Binomial with Logit Link)

	Estimate	z	p value		Estimate	z	p value		Estimate	z	p value	
(Intercept)					2.982	5.299	0.000	***	2.661	4.069	0.000	***
OP	-0.339	-4.956	0.000	***	-1.110	-4.994	0.000	***	-0.072	-3.137	0.002	**
Night	-3.370	-3.249	0.001	**	-1.809	-3.976	0.000	***				
LH									-3.669	-4.935	0.000	***

Vuong Non-Nested Hypothesis Test-Statistic

	z	p-value	z	p-value	z	p-value
Raw	2.689	0.004	7.433	0.000	3.806	0.000
AIC-corrected	2.689	0.004	7.433	0.000	3.806	0.000
BIC-corrected	1.852	0.032	6.597	0.000	1.909	0.028

Significance level: *** 0.001, ** 0.01, * 0.05, · 0.10.

As shown in Table 8.11, for the FC-334T thermal imaging camera, the higher the wind speed is, the larger the errors tend to be. Adverse weather events (C1-C3) tend to increase the missed and false call errors. Weather events of C1 and C3 tend to increase the stuck-on call error. Weather event C2 (light rain/drizzle) has a tendency to reduce the dropped call error as indicated by the negative sign of coefficient estimate (at the 0.001 significance level).

Better visibility results in smaller errors. Site 1 has a smaller missed call error, but larger false, stuck-on, dropped call errors compared to site 2. Lower mount appears to increase the chance of dropped call errors, but reduce the magnitude of missed and stuck-on call errors if occurred. The small p value of the Vuong test suggests that the ZINB model provides significant improvement over the corresponding NB model for missed, stuck-on, and dropped call errors. For the false call error, the ZINB model did not fit the data better than the NB model.

Table 8.12 of Model Estimation (RZ4 Advanced WDR Camera)

Count Model

Variable	Missed Call (NB)				False Call (NB)				Stuck-on Call (NB)				Dropped Call (NB)			
	Estimate	z	p value		Estimate	z	p value		Estimate	z	p value		Estimate	z	p value	
Constant	0.496	2.615	0.009	**	0.691	5.310	0.000	***	1.440	21.221	0.000	***	-1.404	-4.956	0.000	***
Wspeed	0.027	3.177	0.001	**					-0.006	-1.681	0.093	.	-0.181	-9.633	0.000	***
C1	0.169	2.127	0.033	*					0.106	2.682	0.007	**	0.382	1.816	0.069	.
C2	0.771	5.021	0.000	***	0.251	1.981	0.048	*	0.596	8.678	0.000	***	0.514	1.699	0.089	.
C3	0.301	2.406	0.016	*	0.559	3.986	0.000	***	0.188	2.571	0.010	*	-0.999	-3.239	0.001	**
Visibility					-0.026	-2.159	0.031	*	0.012	2.169	0.030	*				
Glare													-2.537	-6.566	0.000	***
Shade					-0.851	-4.997	0.000	***	0.406	7.097	0.000	***	2.209	6.283	0.000	***
Night	0.270	7.886	0.000	***	1.316	19.711	0.000	***					3.192	20.684	0.000	***
AD	1.053	6.106	0.000	***												
Site	-1.405	-12.120	0.000	***	1.701	19.444	0.000	***	1.334	39.076	0.000	***	2.471	10.947	0.000	***
OP	-0.007	-13.003	0.000	***									0.023	9.053	0.000	***
POG					0.018	14.734	0.000	***								
Wspeed:C1	-0.029	-3.106	0.002	**												
Wspeed:C2	-0.055	-2.430	0.015	*												
Wspeed:C3	-0.038	-1.644	0.100													
Log(theta)	0.812	16.247	0.000	***	-0.330	-4.071	0.000	***	0.916	27.585	0.000	***				
Theta													0.048	24.342	0.000	***

Zero-Inflation Model (Binomial with Logit Link)

	Estimate	z	p value		Estimate	z	p value		Estimate	z	p value	
(Intercept)	-0.932	-6.651	0.000	***	0.749	5.737	0.000	***	-2.113	-15.110	<2e-16	***
Night	0.658	7.913	0.000	***	-0.495	-5.819	0.000	***	2.521	19.230	<2e-16	***
Visibility					-0.053	-4.508	0.000	***				
Wspeed	-0.059	-5.654	0.000	***								
OP	0.003	1.769	0.077	.	-0.011	-5.682	0.000	***	-0.018	-10.400	<2e-16	***
POG	-0.004	-2.022	0.043	*								

Vuong Non-Nested Hypothesis Test-Statistic

	z	p-value	z	p-value	z	p-value
Raw	4.561	0.000	3.339	0.000	8.999	0.000
AIC-corrected	4.561	0.000	3.339	0.000	8.999	0.000
BIC-corrected	4.237	0.000	2.714	0.003	8.848	0.000

Significance level: *** 0.001, ** 0.01, * 0.05, · 0.10.

By referring to the zero-inflation model in Table 8.12, the wind speed is significant for the missed call error. The negative coefficient estimate (-0.059) indicates that a higher wind speed increases the chance of a missed call error. This might be due to the fact that the RZ4 Advanced WDR camera was mounted higher than the other cameras (i.e., Autoscope AIS-IV camera and FC-334T Thermal Imaging camera) at site 2, making it more susceptible to wind. The negative coefficient estimate (-0.053) of visibility for the false call indicates that higher visibility tends to increase the chance of a false call error. This could be due to erroneous events (rather than the targeted vehicles) that trigger false calls. The night condition tends to reduce the chance of missed and stuck-on calls, which is likely due to light traffic at night, but increases the chance of a false call, which could be due to the headlight issue.

By referring to the count model, adverse weather events increase the missed, false, and stuck-on call errors. But, the weather event C3 (fog, mist, or haze) tends to reduce the

dropped call error. The uneven shade increases stuck-on and dropped call errors, but reduces the false call error.

The missed and false call errors, especially the dropped call error, if occurred, tend to be larger at night. The potential glare situation tends to "reduce" the dropped call error. Note the camera was set up to avoid the potential sun glare issue, the reduced dropped call error is likely due to the clear weather condition that coincides with the potential glare situation. The configuration adjustment (AD), i.e., reducing sensitivity and adding pedestrian screening, increases the missed call error. Site 1 has smaller missed call error, but larger false, stuck-on, and dropped call errors as compared to site 2. The Vuong test suggests that the ZINB models provide significant improvement over the corresponding NB models for missed, false, and stuck-on call errors. A NB model was estimated for the dropped call error.

Table 8.13 Model Estimation (SmartSensor Matrix)

Count Model

Variable	Missed Call (NB)				False Call (NB)				Stuck-on Call (Poisson)				Dropped Call (NB)			
	Estimate	z	p value		Estimate	z	p value		Estimate	z	p value		Estimate	z	p value	
Constant	1.684	28.883	0.000	***	2.404	57.166	0.000	***	1.594	57.650	0.000	***	4.302	28.929	0.000	***
Wspeed									0.033	21.711	0.000	***				
C1					0.083	2.487	0.013	*	0.111	6.631	0.000	***				
C2					0.249	5.616	0.000	***	0.625	33.021	0.000	***				
C3					0.118	2.424	0.015	*	0.217	8.125	0.000	***				
C4					1.751	12.878	0.000	***	0.892	22.867	0.000	***				
Night									0.437	40.481	0.000	***	-0.217	-2.404	0.016	*
Site	-0.961	-21.015	0.000	***	-0.325	-11.281	0.000	***	0.297	22.818	0.000	***	-2.370	-20.207	0.000	***
OP	0.004	4.759	0.000	***	-0.008	-17.290	0.000	***	-0.003	-12.163	0.000	***	-0.008	-4.752	0.000	***
POG	0.001	1.731	0.083	.	0.006	9.079	0.000	***	0.004	16.438	0.000	***	-0.035	-21.373	0.000	***
Log(theta)	0.120	2.093	0.036	*	0.545	26.719	0.000	***					-1.981	-56.925	0.000	***

Zero-Inflation Model (Binomial with Logit Link)

	Estimate	z	p value		Estimate	z	p value		Estimate	z	p value		Estimate	z	p value	
(Intercept)	-1.494	-15.408	0.000	***	-0.865	-6.513	0.000	***	-0.978	-17.290	0.000	***	3.404	13.587	0.000	***
OP	0.034	23.778	0.000	***	-0.232	-15.605	0.000	***	0.006	6.714	0.000	***	-0.066	-10.733	0.000	***
POG					0.054	21.281	0.000	***					-0.090	-7.880	0.000	***
Night	0.623	8.713	0.000	***					0.507	9.479	0.000	***	-1.956	-8.069	0.000	***

Vuong Non-Nested Hypothesis Test-Statistic

	z	p-value	z	p-value	z	p-value	z	p-value
Raw	5.447	0.000	10.704	0.000	22.742	0.000	10.310	0.000
AIC-corrected	5.447	0.000	10.704	0.000	22.742	0.000	10.310	0.000
BIC-corrected	5.320	0.000	10.589	0.000	22.708	0.000	9.562	0.000

Significance level: *** 0.001, ** 0.01, * 0.05, · 0.10.

For the SmartSensor Matrix, by referring to the zero-inflation model in Table 8.13, the positive coefficients (0.623 and 0.507) for "Night" indicates a lower chance of missed and stuck-on call errors at night, which is likely due to light traffic at night. The count model indicates a larger stuck-on call error and a smaller dropped call error, if occurred, at night. A higher wind speed tends to increase the stuck-on call error. All adverse weather events increase false and stuck-on call errors. The severe weather (C4 – rain and thunderstorm) has a much larger effect on the false calls (i.e., a larger coefficient estimate: 1.751). A

larger stuck-on call error but smaller missed, false, and dropped call errors are expected at site 1 compared to site 2. This is likely due to the fact that the SmartSensor Matrix was mounted on the near side mast arm at site 1, but on the far side mast arm at site 2. Finally, the small p value of the Vuong test suggests that the ZINB model provides significant improvement over the NB or Poisson model for all error types.

8.1.3.2 Devices with Span Wire Installation (Site 3)

Wireless magnetometers do not require mast arm installation. Vantage SmartSpan cameras are designed for span wire installation. Both devices were evaluated at site 3, which has a span wire. Similar to those devices evaluated at the mast arm sites (site 1 and site 2), regression models were estimated for both devices at site 3. The model estimation results are shown in Table 8.14 and Table 8.15 for the wireless magnetometers and the Vantage SmartSpan camera, respectively.

Table 8.14 Model Estimation (Wireless Magnetometers)

Count Model

Variable	Missed Call (NB)				False Call (NB)				Stuck-on Call (NB)				Dropped Call (NB)			
	Estimate	z	p value		Estimate	z	p value		Estimate	z	p value		Estimate	z	p value	
Constant	2.054	72.850	0.000	***					4.297	123.580	<2e-16	***	1.766	11.634	0.000	***
OP	-0.001	-2.261	0.024	*									0.014	4.663	0.000	***
POG	-0.021	-34.416	0.000	***	0.019	2.242	0.025	*					-0.027	-13.131	0.000	***
RP	-0.150	-6.397	0.000	***	-4.683	-8.896	0.000	***	-3.226	-68.500	<2e-16	***				
Log(theta)	1.216	31.391	0.000	***					-0.602	-27.060	<2e-16	***	-2.783	-42.444	0.000	***
Theta					0.002	5.670	0.000									

Zero-Inflation Model (Binomial with Logit Link)

	Estimate	z	p value						Estimate	z	p value		Estimate	z	p value	
(Intercept)	-1.535	-26.607	0.000	***					5.560	17.762	0.000	***	0.860	6.033	0.000	***
Night	0.266	2.976	0.003	**												
OP									-0.039	-7.696	0.000	***				
POG									-2.466	-15.054	0.000	***	-0.603	-2.991	0.003	**

Vuong Non-Nested Hypothesis Test-Statistic

	z	p-value			z	p-value			z	p-value		
Raw	2.743	0.003			39.099	0.000			7.360	0.000		
AIC-corrected	2.743	0.003			39.099	0.000			7.360	0.000		
BIC-corrected	2.678	0.004			38.819	0.000			6.697	0.000		

Significance level: *** 0.001, ** 0.01, * 0.05, · 0.10.

As shown in Table 8.14, the addition of the repeater significantly reduces the missed, false and stuck-on call errors, especially the false and stuck-on calls, as seen by the large negative coefficient estimates in the count model. Night conditions explain many zero missed calls because of light traffic. The small p value of the Vuong test suggests that the ZINB model provides significant improvement over the corresponding NB models for missed, stuck-on, and dropped call errors. A NB model was estimated for the false call error.

Table 8.15 Model Estimation (Vantage SmartSpan Camera)

Count Model

Variable	Missed Call (Poisson)				False Call (NB)				Stuck-on Call (NB)				Dropped Call (NB)			
	Estimate	z	p value		Estimate	z	p value		Estimate	z	p value		Estimate	z	p value	
Constant	1.831	12.333	0.000	***	4.468	38.006	0.000	***	4.052	24.707	0.000	***	1.613	5.263	0.000	***
Wspeed									-0.038	-5.172	0.000	***	-0.075	-4.979	0.000	***
C1	0.775	5.290	0.000	***	0.427	3.373	0.001	***	0.636	4.741	0.000	***	0.786	2.722	0.006	**
C2	0.579	3.883	0.000	***	0.834	5.719	0.000	***	1.348	8.660	0.000	***	0.851	2.722	0.006	**
C3	0.798	4.603	0.000	***	-0.680	-1.993	0.046	*	-1.525	-4.436	0.000	***	1.076	2.239	0.025	*
Glare	-0.950	-7.300	0.000	***	0.858	2.996	0.003	**								
Night	-0.494	-15.100	0.000	***					-0.453	-7.090	0.000	***	0.597	5.809	0.000	***
OP	0.002	5.426	0.000	***	-0.027	-21.737	0.000	***								
POG									0.010	3.700	0.000	***	-0.018	-3.411	0.001	***
PH					0.269	3.951	0.000	***	0.227	3.638	0.000	***				
Visibility									0.053	5.133	0.000	***				
Log(theta)					-0.910	-26.900	0.000	***	-0.975	-49.723	0.000	***	-0.765	-6.387	0.000	***

Zero-Inflation Model (Binomial with Logit Link)

	Estimate	z	p value		Estimate	z	p value		Estimate	z	p value		Estimate	z	p value	
(Intercept)	1.722	11.019	0.000	***	-2.874	-8.545	0.000	***	-139.613	-4.296	0.000	***	1.955	8.133	0.000	***
OP	-0.003	-1.801	0.072	.	0.048	12.196	0.000	***	1.413	4.237	0.000	***	-0.010	-4.983	0.000	***
POG													-0.012	-1.976	0.048	*
Night	0.710	6.463	0.000	***	-1.887	-9.056	0.000	***	4.373	6.894	0.000	***	-0.608	-5.475	0.000	***
Wspeed	-0.025	-2.108	0.035	*	-0.130	-7.310	0.000	***					-0.173	-8.457	0.000	***
Visibility													0.118	8.097	0.000	***

Vuong Non-Nested Hypothesis Test-Statistic

	z	p-value	z	p-value	z	p-value	z	p-value
Raw	20.239	0.000	12.443	0.000	4.750	0.000	7.607	0.000
AIC-corrected	20.239	0.000	12.443	0.000	4.750	0.000	7.607	0.000
BIC-corrected	20.213	0.000	11.728	0.000	3.928	0.000	6.104	0.000

Significance level: *** 0.001, ** 0.01, * 0.05, · 0.10.

As shown in Table 8.15, the Vantage SmartSpan camera appears to be sensitive to wind. A higher wind speed increases the chance of missed, false, and dropped call errors per the zero-inflation model, but reduces the stuck-on and dropped call errors per the count model.

As indicated by the zero-inflation model, there is a lower chance of missed and stuck-on call errors, but a higher chance of false and dropped call errors at night. Better visibility reduces the chance of the dropped call error per the zero-inflation model, but increase the stuck-on call error per the count model.

Adverse weather events have a tendency to increase most call errors except that less or smaller false call and stuck-on call errors are expected under the mist/foggy/haze (C3) condition. Potential glare tends to increase the false call error, but reduce the missed call error. Larger false and stuck-on call errors are expected during peak hours of traffic.

Based on the Vuong test, the ZINB and ZIP models provide significant improvement over the corresponding NB and Poisson models.

8.2 Indecision Zone Detection

An indecision zone is defined as an area on a high speed (greater than 35mph) approach to a signalized intersection. The concept of indecision zone is based on the rationale that drivers within a few seconds travel time of the intersection tend to be indecisive about their ability to stop upon the onset of the yellow indication. This indecisiveness results in a zone in advance of the stop bar wherein some drivers may choose to proceed and others may choose to stop. The location of this zone is depicted in Figure 8.29.

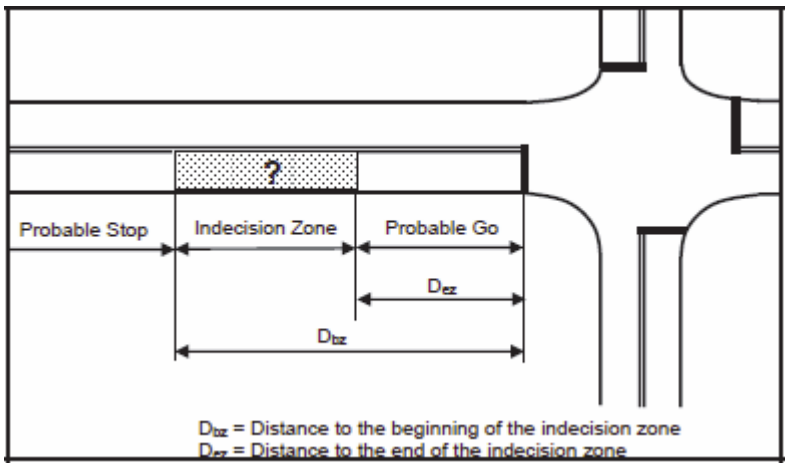

Figure 8.29 Indecision zone boundaries on a typical intersection approach (Koonce et al., 2008)

The indecision zone location has generally been defined in one of three ways based on (1) distances where 90 and 10 percent of drivers would stop upon the onset of a yellow indication, (2) travel time to the stop line (e.g. 2 and 5 seconds of travel time), and (3) stopping sight distance based on AASHTO (2011). Indecision zones based on the three definitions are illustrated in Figure 8.30.

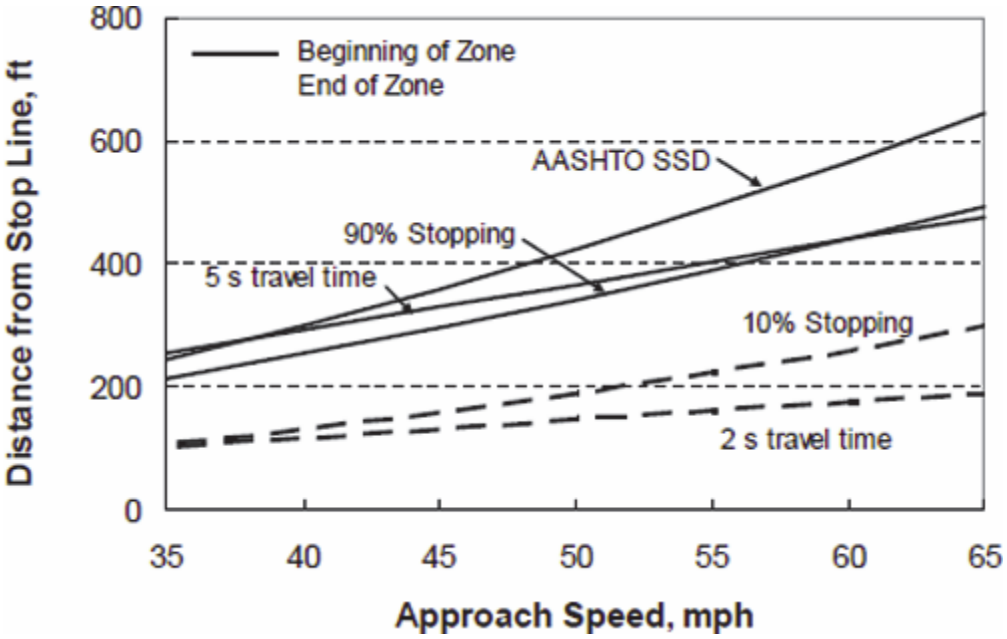

Figure 8.30 Distance to the beginning and end of the indecision zone (Koonce et al., 2008)

For indecision zone protection, multiple detectors have been used by some agencies. For the multiple-detector design, the furthest detector in advance of the stop bar is usually located at the beginning of the indecision zone of the approach design speed (85th-percentile approach speed). This is usually at a distance of 5 to 5.5 seconds of travel time. Subsequent detectors have a design speed of 10 mph lower than the upstream detector. Typically 3 to 4 detectors are used to enable safe termination of the high speed approach phase. The detectors are allowed to extend the phase by the passage time programmed in the controller or by the extension time on the detector itself (Koonce et al., 2008).

Two radar-based devices, SmartSensor Advance and Vantage Vector Hybrid, were evaluated for indecision zone detection at site 2. The two devices were mounted to target the southwestbound approach (Allgood Road). The posted speed of Allgood Road is 40 mph. The existing volume-density loop is located 330 feet in advance of the stop bar. This is equivalent to approximately 5.5-second travel time at the posted speed. To be able to verify the presence of a vehicle using the existing volume-density loop, the indecision zone was defined and configured to start at the existing volume-density loop (i.e., 330 feet from the stop bar) and end at 100 feet from the stop bar (Figure 5.11).

The two advance detection devices were mounted side by side on the mast arm as shown in Figure 5.9 and sequentially configured to target two speed traps: 35-100 mph and 40-100 mph.

8.2.1 Data Extraction

For the radar detectors to detect any vehicles in the indecision zone, vehicle speeds are required to be high enough (within the targeted speed traps) to trigger detection. For the actual field test, this will not likely happen if traffic is heavy, i.e., impeded flow, or when vehicles are arriving during the red because of the slowdown, or when vehicles start to move upon the onset of green because of startup delay, acceleration, and queue clearance. Given those practical considerations, only vehicles arriving during the late portion of green interval plus the yellow interval (when vehicle speeds are expected to exceed the lower limits of target speed traps) were tracked and used for comparing the two devices. The tracking window is defined and illustrated in Figure 8.31.

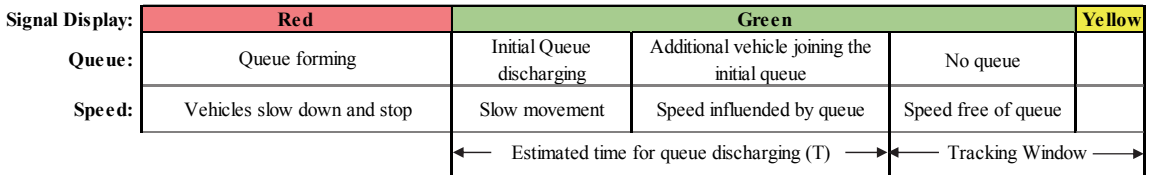

Figure 8.31 Illustration of tracking window for advance detection.

The starting point of the tracking window in Figure 8.31 is estimated based on a typical startup delay and time required for queue discharging. The number vehicles in the queue during the red interval plus those joining the queue during the initial portion of the subsequent green interval are counted by the upstream volume-density loop. Assuming a startup delay of 4 seconds for the queued vehicles and a queue discharge rate of 2 seconds per vehicle, the total time (T) required to discharge the counted vehicle is estimated. Note that T is not fixed and varies by cycle depending on the arrivals of vehicles. Once T defined above expires, the detection statuses of both test devices are tracked and logged through the rest of green plus the yellow interval. This process is repeated for all cycles throughout the test periods.

8.2.2 Detection Frequency

A frequency analysis was performed to check if both test devices either detect or not detected a vehicle registered by the volume-density loop. As described previously, the indecision zone was defined to start at the location of the existing volume-density loop (330 feet in advance of the stop bar). Using the tracking window defined in Figure 8.31, vehicles entering the indecision zone were tracked. The detection status of each test device was recorded when the volume-density loop registered a vehicle. As such, four scenarios are possible based on the detection statuses of the two test devices: (1) both devices detected a vehicle as the loop did, (2) both devices did not detect a vehicle as the loop did, (3) the SmartSensor Advance detected a vehicle as the loop did, but the Vantage Vector failed to detect the same vehicle, (4) the Vantage Vector detected a vehicle as the loop did, but the SmartSensor Advance failed to detect the same vehicle. Apparently, the first two

scenarios indicate a detection consistency of the two devices. Note it is possible for both test devices to correctly not detect a vehicle if the speed of the vehicle falls outside of the limits of the target speed traps. This is likely the case for low-speed vehicles given the high upper limit (100 mph) of the speed traps.

The frequencies corresponding to the four scenarios described above are presented in Table 8.16 for the two speed traps. As seen, the two devices shows approximately 87 percent consistency for both speed traps.

Table 8.16 Comparison of Detection Frequencies

Device			Consistency	Freqency				Percent			
IL	VVH	SA		ST 1		ST 2		ST 1		ST 2	
1	1	1	Yes	14,509	**15,468**	9,586	**11,504**	81.63%	**87.03%**	72.78%	**87.34%**
1	0	0	Yes	959		1,918		5.40%		14.56%	
1	1	0	No	1,422	**2,306**	828	**1,667**	8.00%	**12.97%**	6.29%	**12.66%**
1	0	1	No	884		839		4.97%		6.37%	
			Total	17,774		13,171		100%		100%	

Notes:
IL - Inductive Loop
VVH - Vantage Vector Hybrid
SA - SmartSensor Advance
ST 1 - Speed Trap of 35-100 mph
ST 2 - speed Trap of 40-100 mph

8.2.3 Detection Duration

Different from the stop bar detection evaluation, the 6ft × 6ft setback loop for volume-density detection cannot be used as a benchmark for verifying the continuous detection by the radar devices because it only provides point detection at the entry to the indecision zone as such defined. Given this constraint, the two radar devices, Vantage Vector Hybrid and SmartSensor Advance, were compared with each other in terms of duration of detecting vehicles within the indecision zone. A sample of detection durations for both test devices are shown in Figure 8.32.

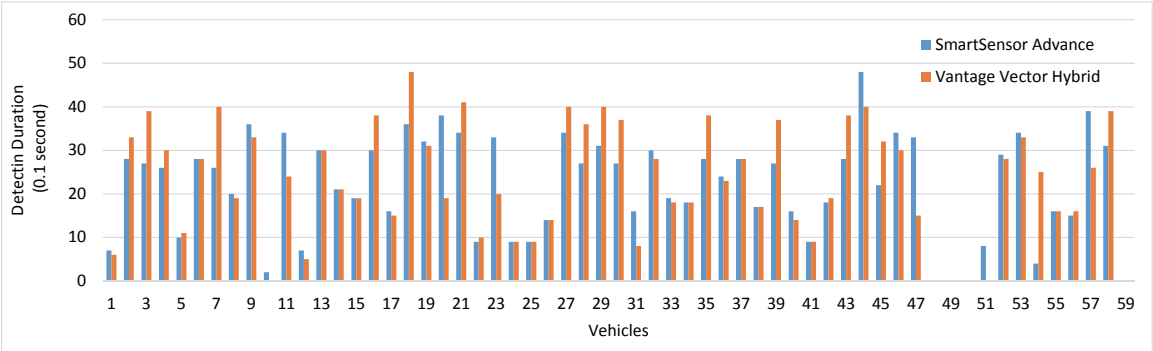

Figure 8.32 Detection Durations of SmartSensor Advance and Vantage Vector Hybrid.

By inspecting Figure 8.32, the difference in detection duration between the two test devices is apparent.

The statistics of the duration data are shown in Table 8.17. Two hypothesis tests, paired t test and Wilcoxon signed-rank test, were used to evaluate if the detection durations by the two devices are significantly different. Different than paired t test, Wilcoxon signed-rank test assesses whether the mean ranks differ without assuming normal distribution. The results are included in Table 8.17 as well. Both hypothesis tests consistently indicate a significant difference in detection duration between the two devices. This can be seen by the small p values in Table 8.17.

Table 8.17 Difference in Duration between the Two Test Devices

Detection	Speed Trap 1 (35 - 100 mph)			Speed Trap 2 (40 - 100 mph)		
Device	Mean	SD	CV	Mean	SD	CV
SmartSensor Advance	22.34	10.00	0.45	18.06	10.68	0.59
Vantage Vector Hybrid	26.56	13.08	0.49	22.44	14.00	0.62
Sample size (n)	17,253			12,356		
t statistic[1]	67.65			48.60		
p value	0.00			0.00		
v statistic[2]	21,618,807			13,125,098		
p value	0.00			0.00		

Notes:

1, based on paired t test between the two detection devices.

2, based on Wilcoxon signed-rank test.

SD - Standard Deviation

CV - Coefficient of Variation

9. MULTICRITERIA EVALUATION

A multicriteria evaluation was conducted to evaluate the six stop bar detection devices. Four criteria were considered, including (1) accuracy, (2) reliability, (3) ease of installation and maintenance, and (4) life cycle cost. The first two criteria are related to technical performance in terms of detection errors. They are directly related to users' or motorists' experience. The last two criteria are nontechnical in nature, but they are of main concern to the agencies that operate and maintain vehicle detection devices.

Accuracy and reliability are defined based on detection errors. To properly measure accuracy and reliability, only detection errors associated with the missed calls and false calls were used due to following reasons:

- Missed or false calls are associated with the initiation of an actual call. They are easier to observe and verify during the field setup.
- Missed or false calls are more reliable or less volatile to the variability in the field setup and configuration.
- Stuck-on and dropped call errors often occur concurrently with missed calls or false calls depending on the configuration of detection zones. For example, for a camera, a missed call is typically followed by a stuck-on call and a false call is typically followed by a dropped call if the detection zone was originally configured to match the inductive loop. As such, exclusion of stuck-on and dropped calls eliminates potentially double counting of detection errors.

9.1 Accuracy, Marginal Effects, and Reliability

Due to the mixed structure of the zero-inflated Poisson (ZIP) or zero-inflated negative binomial (ZINB) models, the coefficient estimates do not directly reveal the overall effect of factors that were included in both the count model and the zero-inflation model. To better interpret model results, the marginal effect of each factor on the two targeted detection errors (i.e., missed calls and false calls) were predicted by applying the estimated models. Specifically, the two errors (missed call and false call) under the "ideal-mean" condition were first predicted by applying the estimated models for each device. A weighted average of the two errors was then computed based on proportion of each error type per observation. This weighted average error is used as a measure of accuracy. By this definition, the smaller this weighted average error is under the ideal-mean condition, the higher the level of accuracy will be.

The ideal-mean condition represents the ideal weather condition (sunny and clear) with average wind speed and visibility level, and proper adjustments of respective devices. It should be noted that the weather event (C4), uneven shade, site effect, and the effect of the

new repeater were not considered for the multicriteria evaluation because those factors do not apply to all the devices (see Table 9.1).

Once the accuracy measure is computed under the ideal-mean condition, the detection errors were predicted by the models again by "unfavorably" deviating the value of each factor (one at a time) by one unit of measurement from the ideal-mean condition while holding other factors constant. The difference in predicted errors between the deviated condition and the ideal-mean condition (computed previously) indicates how reliable each detection device is with respect to each individual factor. Finally, the collective adverse effect (sum of adverse effects) of applicable factors common to all six devices is used as a measure of overall reliability. The reliability, as such defined, is risk-adverse, which reflects public and agencies' attitude toward risk. By this definition, the smaller the change in error when deviating from the ideal-mean condition, the higher the level of reliability.

The marginal effects and corresponding accuracy and reliability measures are summarized in Table 9.1.

Table 9.1 Marginal Effects based on the Regression Models

Site	Device	Detection Error		Ideal-Mean Condition*	Marginal Effect											Risk-Averse Reliability
					Wspeed	C1	C2	C3	C4	Visibility	Glare	Shade	Night	Site	RP	
Site 1 and 2, Mast Arm	**Autoscope AIS-IV Camera**	Missed	45%	3.05	0.38	0.75	0.98	0.08	-0.72	-0.09	-1.64	4.02	-1.13	1.02	n/a	0.89
		False	55%	7.93	0.57	0.00	0.04	-1.68	136.46	0.74	-2.72	32.71	10.18	0.00	n/a	11.52
		Total	**100%**	**5.72**	**0.48**	**0.34**	**0.46**	**-0.89**	**74.53**	**0.37**	**-2.24**	**19.76**	**5.07**	**0.46**	**n/a**	**6.72**
	FC-334T Thermal Imaging Camera	Missed	91%	7.28	0.42	6.52	-0.97	-2.76	n/a	1.05	-5.49	-4.11	0.00	-6.41	n/a	8.00
		False	9%	0.00	0.00	0.40	0.14	1.56	n/a	0.00	0.00	0.00	0.00	0.00	n/a	0.40
		Total	**100%**	**6.58**	**0.38**	**5.94**	**-0.86**	**-2.35**	**n/a**	**0.95**	**-4.97**	**-3.72**	**0.00**	**-5.80**	**n/a**	**7.27**
	RZ4 Advanced WDR Camera	Missed	48%	1.04	0.04	0.19	1.21	0.37	n/a	0.00	0.00	0.00	0.08	-0.79	n/a	1.89
		False	52%	1.29	0.00	0.00	0.37	0.97	n/a	0.00	0.00	-0.74	4.55	5.77	n/a	5.89
		Total	100%	**1.17**	**0.02**	**0.09**	**0.77**	**0.68**	**n/a**	**0.00**	**0.00**	**-0.38**	**2.39**	**2.61**	**n/a**	**3.96**
	SmartSensor Matrix	Missed	30%	3.36	0.00	0.00	0.00	0.00	0.00	0.00	0.00	0.00	-1.01	-2.07	n/a	0.00
		False	70%	8.53	0.00	0.74	2.41	1.07	40.58	0.00	0.00	0.00	0.00	-2.37	n/a	4.22
		Total	**100%**	**6.99**	**0.00**	**0.52**	**1.70**	**0.75**	**28.55**	**0.00**	**0.00**	**0.00**	**-0.30**	**-2.28**	**n/a**	**2.97**
Site 3, Span Wire	**Wireless Magnetometer**	Missed	99%	3.62	0.00	0.00	0.00	0.00	n/a	0.00	0.00	n/a	-0.19	n/a	-0.50	0.00
		False	1%	1.63	0.00	0.00	0.00	0.00	n/a	0.00	0.00	n/a	0.00	n/a	-1.61	0.00
		Total	**100%**	**3.60**	**0.00**	**0.00**	**0.00**	**0.00**	**n/a**	**0.00**	**0.00**	**n/a**	**-0.18**	**n/a**	**-0.51**	**0.00**
	Vantage SmartSpan Camera	Missed	3%	1.45	0.03	1.70	1.14	1.77	n/a	0.00	-0.89	n/a	-0.96	n/a	n/a	1.01
		False	97%	14.58	0.43	7.77	18.98	-7.19	n/a	0.00	19.80	n/a	3.63	n/a	n/a	50.61
		Total	**100%**	**14.16**	**0.42**	**7.58**	**18.40**	**-6.90**	**n/a**	**0.00**	**19.13**	**n/a**	**3.48**	**n/a**	**n/a**	**49.01**

Notes:
The numbers are in unit of 100 milliseconds or 0.1 seconds.
*Ideal-mean condition assumes following:
Clear weather
No glare
No uneven shade
Daytime
Site 2 (note: site 2 is more desirable compared to site 1)
Non-peak period
No repeater, this is only applicable to Sensys Magnetometer
Average visibility level
Average wind speed
Average percent of occupancy per cycle
Average percent of occupancy during green per cycle
Adjustment with improvements
"n/a" : not applicable

As shown in Table 9.1, the columns with shaded "n/a" cells indicate the factors that are not applicable to all six devices. Those factors were not considered in the multicriteria evaluation that aims to compare all six devices. The effects of those factors are discussed first, followed by the factors common to all six devices.

Effect of the severe weather event (C4, rain/thunderstorm)

As shown in Table 9.1, the severe weather event (C4, rain/thunderstorm) is only applicable to the Autoscope AIS IV camera and the SmartSensor Matrix at site 1. As seen, the rain/thunderstorm condition increases the false calls of both devices to a much larger degree, approximately 13.6 seconds (136.46 milliseconds) for the Autoscope AIS IV camera and 4.1 seconds (40.58 milliseconds) for the SmartSensor Matrix.

Effect of uneven shade

The effects of uneven shade are only applicable to four devices at site 2 (i.e., Autoscope AIS IV camera, FC-334T Thermal Imaging camera, RZ4 Advance WDR camera, and SmartSensor Matrix) because the uneven shade condition is only present at site 2. For visual comparison, the effects of uneven shade for the four devices in Table 9.1 are plotted in Figure 9.1.

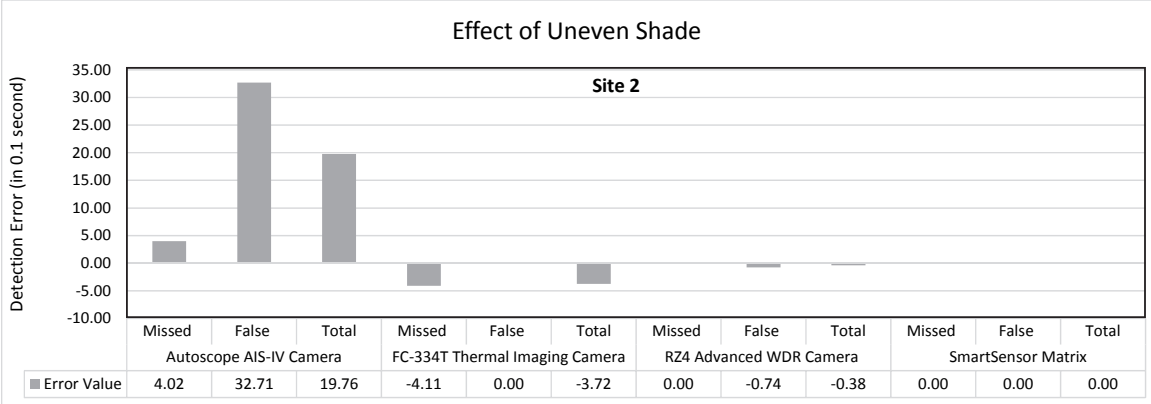

Figure 9.1 Effect of uneven shade at site 2.

As shown, uneven shade has a much larger effect on the Autoscope AIS IV camera than the other three devices. Specifically, uneven shade increases the false call error of the Autoscope AIS IV camera by about 3.3 seconds. Surprisingly, the uneven shade slightly reduces the missed call of the FC-334T Thermal Imaging camera, which might be due to the increased difference in temperature between vehicles and pavement because of the cooler pavement under shade.

Effect of site

The effects of site are only applicable to four devices (Autoscope AIS IV camera, FC-334T Thermal Imaging camera, RZ4 Advance WDR camera, and SmartSensor Matrix) installed at both site 1 and site 2. For visual comparison, the effects of site for the four devices in Table 9.1 are plotted in Figure 9.2. Note the effect is of site 1 with respect to site 2.

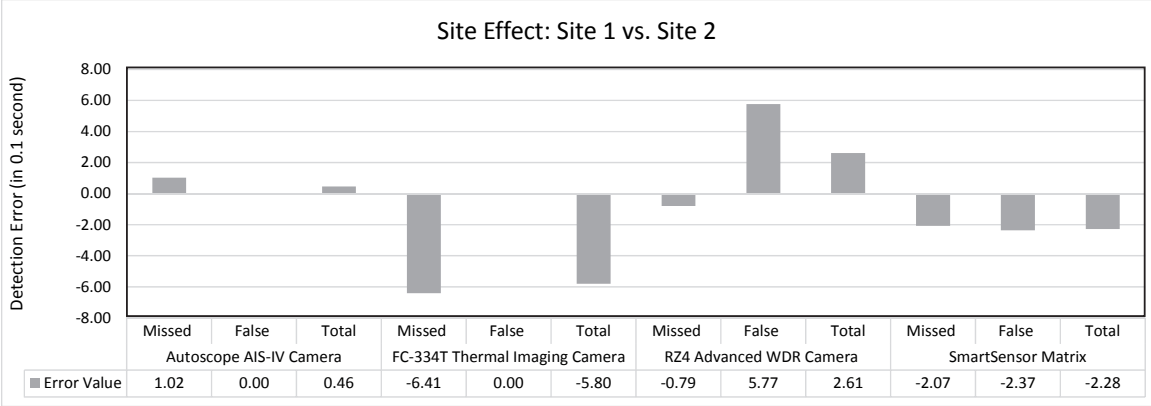

Figure 9.2 Effect due to the site.

The Autoscope AIS IV camera has slightly larger missed call errors (increased by about 0.1 seconds) at site 1 with respect to site 2. The RZ4 Advance WDR camera has slightly larger false call errors (increased by about 0.6 seconds) at site 1 as compared to site 2. This is mainly due to the larger aspect ratio of the camera mount at site 1 as compared to those at site 2. The offset of the cameras at site 1 was also larger than those at site 2.

In contrast, the FC-334T thermal imaging camera has smaller missed call errors at site 1 compared to site 2 (reduced by about 0.6 seconds) and the SmartSensor Matrix has smaller missed and false calls at site 1 compared to site 2 (reduced by about 0.2 seconds). This is likely due to the fact that the SmartSensor Matrix was mounted to detect the near side approach at site 1 while it was mounted to detect the far side approach at site 2.

Effect of repeater

Note that the repeater is only applicable to wireless magnetometers installed at site 3. As shown in Table 9.1, the addition of the repeater tends to reduce both missed and false call errors.

Effects of the factors common to all six stop bar devices

The factors common to all six stop bar devices were used for a multicriteria evaluation and are discussed below. To visually compare the effects of those common factors, they were plotted based on the error data in Table 9.1 and are shown in Figures 9.3-9.5.

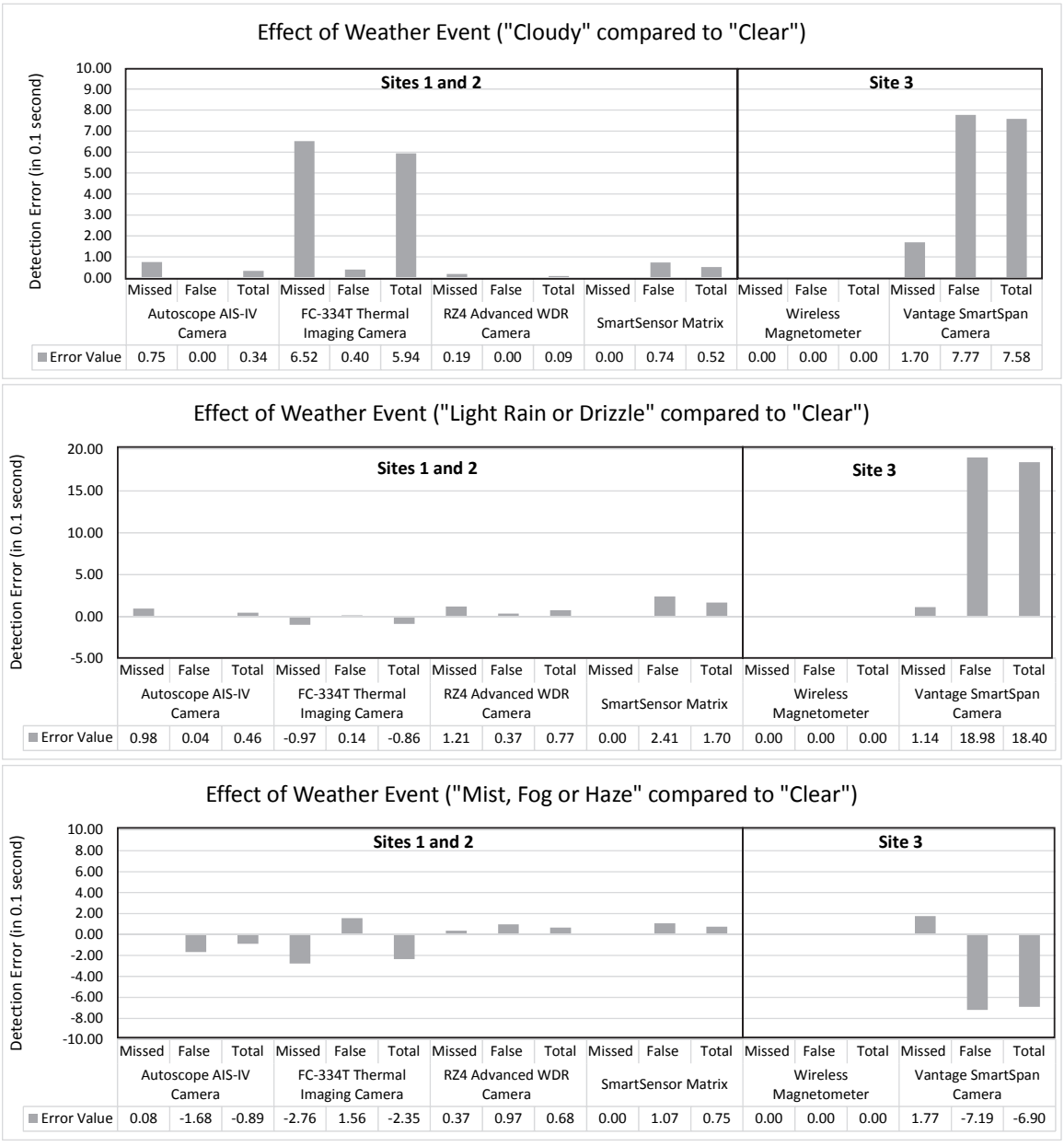

	Autoscope AIS-IV Camera			FC-334T Thermal Imaging Camera			RZ4 Advanced WDR Camera			SmartSensor Matrix			Wireless Magnetometer			Vantage SmartSpan Camera		
	Missed	False	Total	Missed	False	Total	Missed	False	Total	Missed	False	Total	Missed	False	Total	Missed	False	Total
Error Value	0.75	0.00	0.34	6.52	0.40	5.94	0.19	0.00	0.09	0.00	0.74	0.52	0.00	0.00	0.00	1.70	7.77	7.58
Error Value	0.98	0.04	0.46	-0.97	0.14	-0.86	1.21	0.37	0.77	0.00	2.41	1.70	0.00	0.00	0.00	1.14	18.98	18.40
Error Value	0.08	-1.68	-0.89	-2.76	1.56	-2.35	0.37	0.97	0.68	0.00	1.07	0.75	0.00	0.00	0.00	1.77	-7.19	-6.90

Figure 9.3 Marginal effect of weather events.

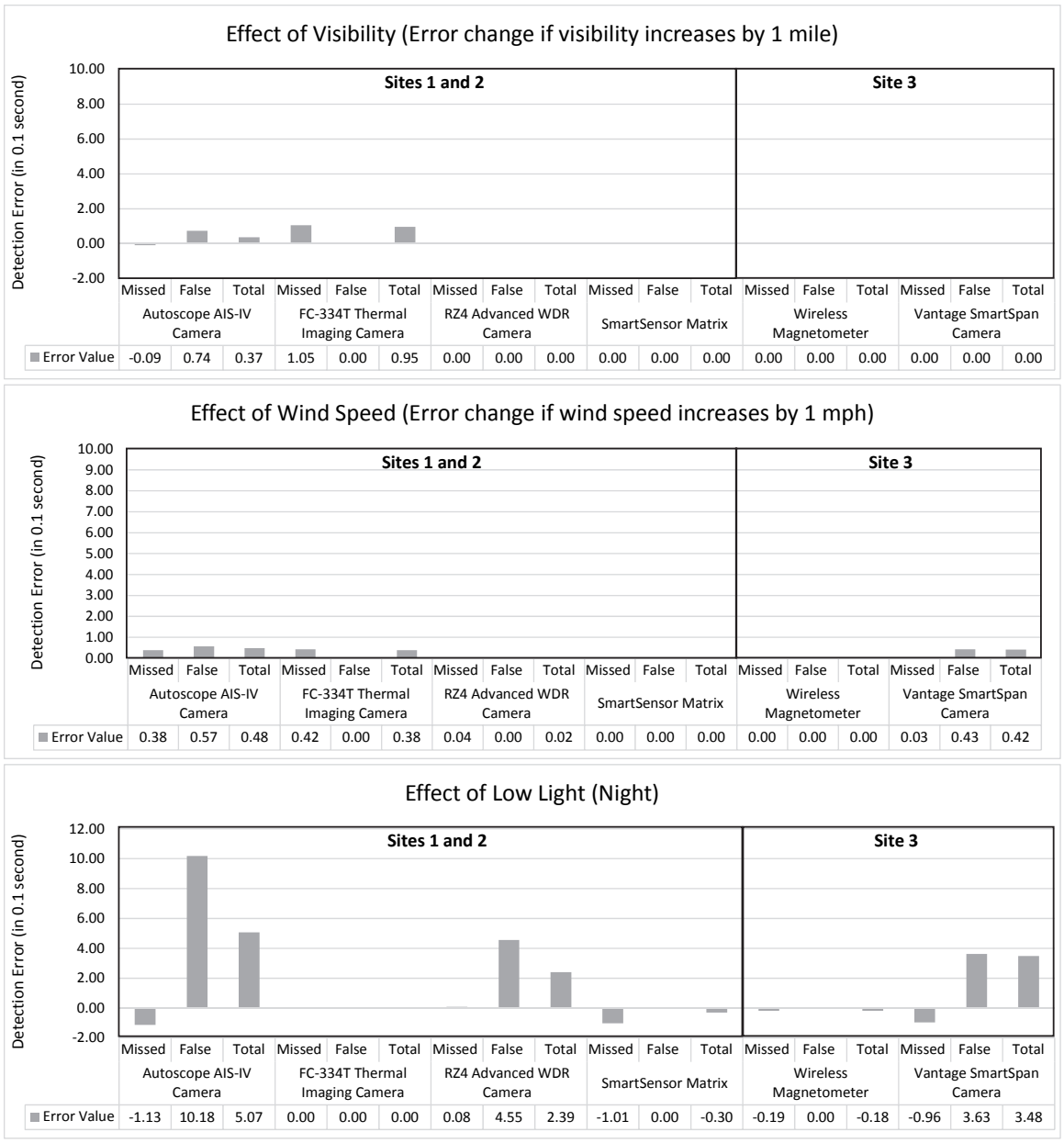

Figure 9.4 Marginal effect of environmental factors (wind speed, visibility, and lighting).

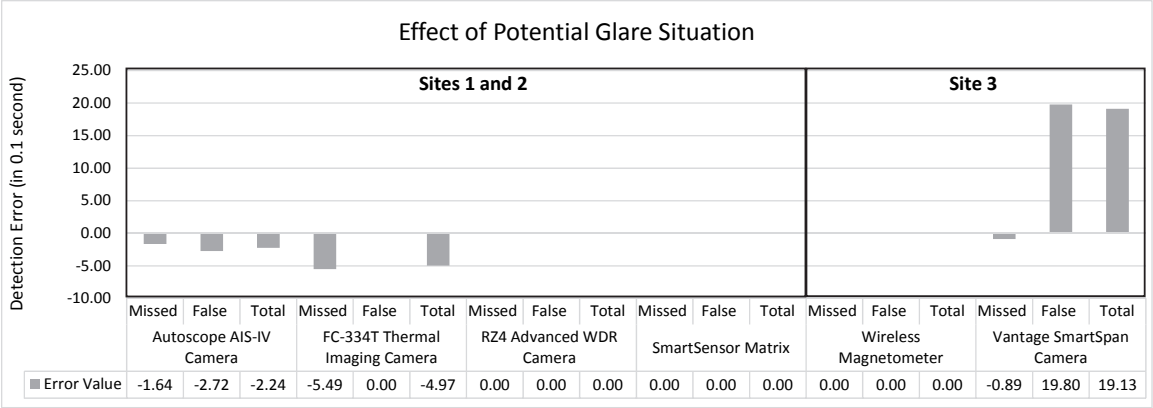

Figure 9.5 Marginal effect of environmental factors (glare).

As shown in Figure 9.3, the cloudy weather (C1) results in a larger missed call error (increased by about 0.7 seconds) for the FC-334T Thermal Imaging camera. This is likely due to the reduced difference in temperature between vehicles and pavement because of the cloudy weather. Note this is different than the effect of uneven shade discussed previously. The cloudy weather results in a larger false call error (increased by about 0.8 seconds) for the Vantage SmartSpan camera. However, those changes in error are relatively small to not practically effect any operational difference. Light rain or drizzle (C2) has negligible effects on most test devices, but increases the false call error of the Vantage SmartSpan camera by about 2 seconds. Similarly, mist, fog or haze has negligible effects on most test devices, but reduces the false call error of the Vantage SmartSpan camera by about 0.7 seconds. This appears to be intuitive as obscure conditions caused by mist, fog or haze tend to mask possible erroneous (false) events from being detected by the camera.

As shown in Figure 9.4, no practically large effects were found by wind speed and visibility. Except for the FC-334T thermal camera and wireless magnetometers, night condition consistently results in larger false call errors for all three video imaging cameras (increasing by about 1.0 second for the Autoscope AIS IV camera, about 0.5 seconds for the RZ4 Advance WDR camera, and about 0.4 seconds for the Vantage SmartSpan camera).

As indicated in Figure 9.5, potential glare results in a much larger false call (increased by about 2.0 seconds) for the Vantage SmartSpan camera. This might be due to the sway of the camera, which makes it susceptible to the glare issue. For other devices, the glare situation results in reduced errors or no practical effects.

Finally, the accuracy and reliability measures for all six devices in Table 9.1 are presented in Figure 9.6

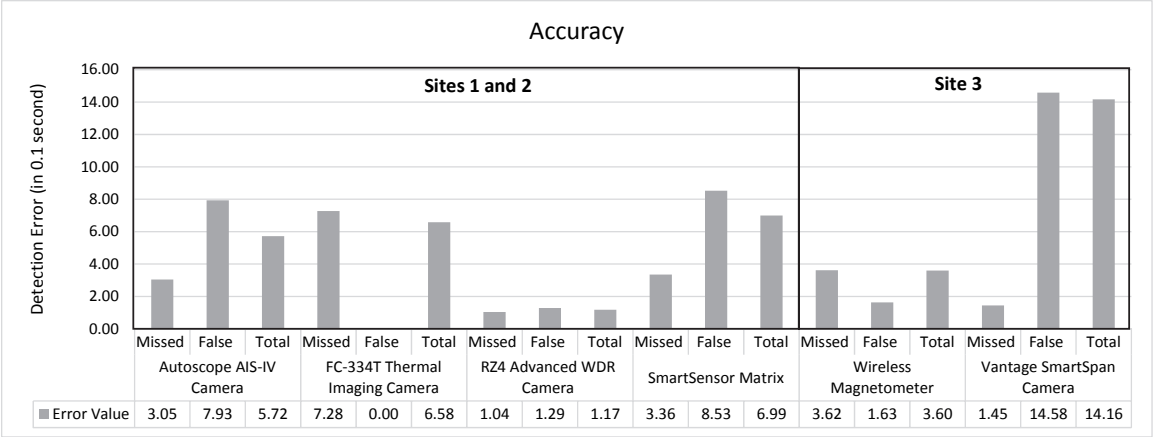

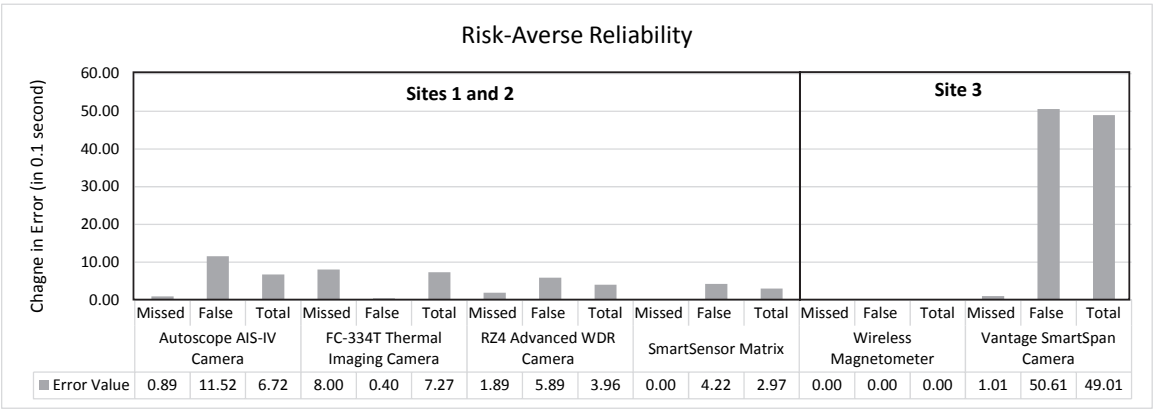

Figure 9.6 Measure of Accuracy and Reliability.

As shown in Figure 9.6, the RZ4 Advanced WDR camera has the highest level of accuracy (i.e., the smallest error under the ideal-mean condition). On the other hand, the FC-334T camera and the Autoscope AIS-IV camera have lower but similar levels of accuracy. This difference is likely due to the higher mount of the RZ4 Advanced WDR camera, approximately 26 feet from the pavement, compared to the FC-334T and Autoscope AIS-IV cameras, which were mounted at approximately 22 feet from the pavement (Figure 5.6). The wireless magnetometers ranked the second by accuracy (note that the ideal-mean condition for the wireless magnetometers did not include the new repeater). Overall, the Vantage SmartSpan camera is least accurate of the six devices.

In terms of reliability, the wireless magnetometers ranked highest and is generally robust to adverse weather and environmental conditions. The SmartSensor Matrix ranked the second. The RZ4 Advance WDR ranked the third, followed by the Autoscope AIS-IV camera and the FC-334 thermal imaging camera. The Vantage SmartSpan camera is least reliable and generally sensitive to adverse weather events and environmental conditions.

9.2 Nontechnical Criteria

Besides accuracy and reliability defined previously, other nontechnical criteria that are of importance to agencies are considered as well. Those include ease of installation and maintenance, and life cycle cost.

9.2.1 Ease of Installation and Maintenance

To quantify the ease of installation and maintenance of different technologies, the survey ratings presented in Section 4 were used.

9.2.2 Life Cycle Cost

The life cycle cost of each vehicle detection technology was estimated based on the equipment quotes received from manufacturers or distributors. Those actual costs are subjected to market conditions and expected to decrease as detection technologies continue to evolve and mature. Knowing the cost for vehicle detection depends largely on the design of detection systems, two commonly used detection design schemes were considered for estimating life cycle costs.

- Scheme 1: stop bar detection for Minor Street plus Major Street left turns; setback detection for Major Street through lanes. This type of detection design is commonly used in practice and represents economical detection solutions.
- Scheme 2: stop bar detection for both Minor Street and Major Street; setback detection for Major Street through lanes. In this scheme, the stop bar detection for Major Street through lanes is used for right turn screening and queue clearance.

The two schemes are illustrated in Figure 9.7

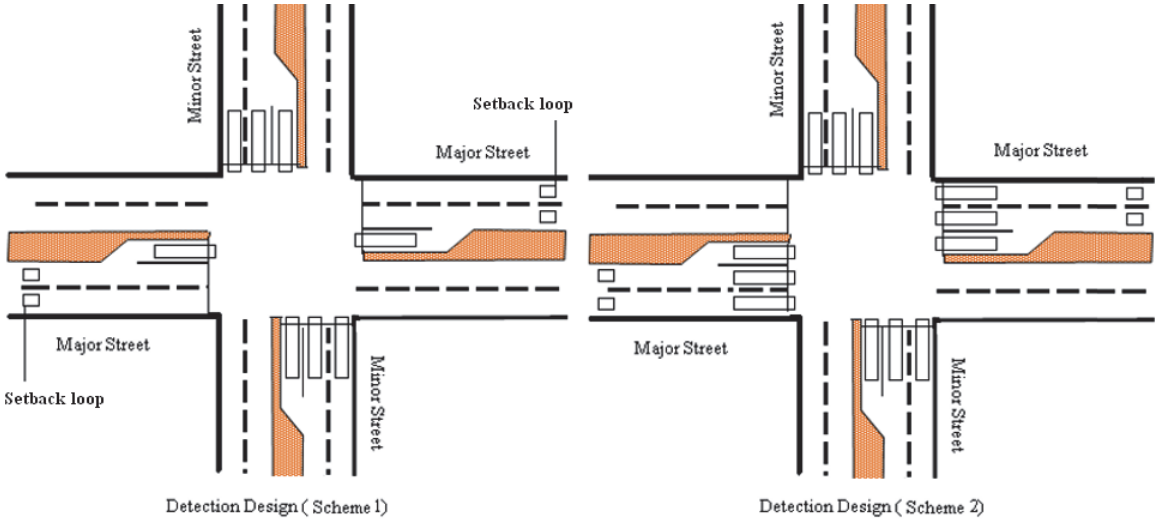

Figure 9.7 Illustration of vehicle detection design schemes by inductive loops

In addition, different technologies may have different scales of economy depending on the size of intersection, which determines the required intensity of detection. Eight typical intersection geometries (in terms of the number of left-turn, through, and right-turn lanes per approach) were identified in Figure 9.8 and used for the life cycle cost analysis. As indicated in Figure 9.8, the solid arrows indicate the lanes where detection is needed for stop bar detection in scheme 1. The hashed arrows indicate additional lanes for stop bar detection in scheme 2. Life cycle cost in terms of equivalent uniform annual cost (EUAC) was estimated for each test device with respect to each combination of detection design schemes (Figure 9.7) and intersection geometries (Figure 9.8).

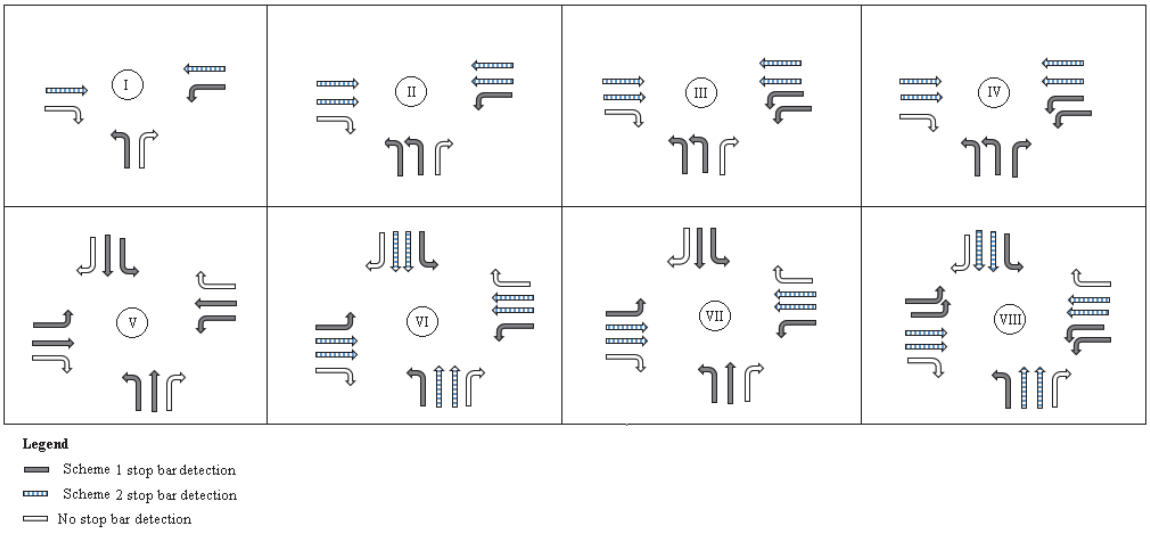

Figure 9.8 Stop bar detection for typical intersection geometries

The following assumptions were made for deriving the life cycle cost estimates.

- Installation cost: $50/man-hour
- Service life = 10 years for all devices
- Interest rate = 5%
- Camera annual maintenance cost: $500/year/camera
- Mast arm camera cabling: 2 man-hours/camera
- Span wire camera cabling: 1 man-hour/camera
- Time for installation of wireless magnetometers: 20 minutes/unit
- Time for configuring wireless magnetometers: 10 minutes/unit
- For stop bar detection: 3 magnetometers per lane

9.3 Multicriteria Evaluation of Detection Devices

Multicriteria evaluation was conducted using the ranking and rating method. The weight for each evaluation criterion was derived from the survey results presented in Section 4. A weight of 1-5 was assigned to each criterion. As indicated by the survey, the most important criterion is reliability with a weight of 5, followed by accuracy with a weight of 4.5. The ease of installation and maintenance was assigned a weight of 4.1. The price is the least important criterion of the three based on the survey and was assigned a weight of 3.1. The same weight was used for the life cycle cost. Given the different scales of measurement for different criteria, linear scaling was applied to convert all scales to a uniform scale of 0-100 points. The final score of each device is calculated based on a weighted average by Equation 9. The devices with higher scores are generally preferred based on the criteria considered.

$$Score_{\ i} = \frac{\sum_{j=1}^{n} W_j O_{ij}}{\sum_{j=1}^{n} W_j} \tag{9}$$

where,
$Score_{\ i}$ = the weighted average score for device i
W_j = the weight of criterion j,
O_{ij} = the scaled measure on the degree to which criterion j is achieved by device i

Since the life cycle cost varies depending on the detection design scheme and the size of intersections, the multicriteria evaluation was conducted with respect to all combinations of the detection design scheme and the intersection geometry. The results are presented in Table 9.2.

As seen in Table 9.2, the life cycle costs for different detection technologies are quite comparable. Wireless magnetometers can be costly for larger intersections because more magnetometers are generally required for detecting more lanes. It should be pointed out that the life cycle costs in Table 9.2 were estimated based on quotes received from manufacturers or distributors. Those quotes are time sensitive, and subjected to changes in market conditions.

It should be pointed out that the accuracy measure largely depends on how well the detection zone is configured in the field, which is sensitive to the mounting height of cameras. For a detection camera, higher accuracy can usually be achieved with a higher mount. As such, the accuracy measure is not a good performance indicator especially when comparing cameras mounted at different heights. For this reason, the accuracy criterion was excluded from the multicriteria evaluation.

Table 9.2 Multicriteria Evaluation

Criterion			Unit	Detection Technology for Stopbar Detection						Weight
				Test Sites 1 and 2				Test Site 3		
				A	F	R	SM	WM	VS	
Accuracy*			100 ms	5.72	6.58	1.17	6.99	3.09	14.16	4.5
			Scaled (0-100)	**85.69**	**83.54**	**97.07**	**82.51**	**92.28**	**64.60**	
Reliability			100 milliseconds	6.72	7.27	3.96	2.97	0.00	49.01	5
			Scaled (0-100)	**86.56**	**85.45**	**92.08**	**94.07**	**100.00**	**1.98**	
Ease of Install/Maintenance			Rating (1-5)	3.44	3.44	3.44	4.00	3.43	3.44	4.1
			Scaled (0-100)	**61.00**	**61.00**	**61.00**	**75.00**	**60.75**	**61.00**	
Life-Cycle Cost (EUAC) Detection Scenario 1	Intersection Type	I	US Dollar	$2,049	$1,919	$2,216	$2,235	$1,765	$2,558	3.1
		II		$2,049	$1,919	$2,216	$2,235	$2,327	$2,558	
		III		$2,049	$1,919	$2,216	$2,235	$2,889	$2,558	
		IV		$2,049	$1,919	$2,216	$2,235	$3,451	$2,558	
		V		$4,058	$3,810	$4,104	$4,394	$5,309	$4,788	
		VI		$4,058	$3,810	$4,104	$4,394	$3,062	$4,788	
		VII		$4,058	$3,810	$4,104	$4,394	$4,185	$4,788	
		VIII		$4,058	$3,810	$4,104	$4,394	$4,185	$4,788	
	Intersection Type	I	Scaled (0-100)	**88.34**	**89.79**	**86.49**	**86.28**	**91.50**	**82.69**	
		II		**88.34**	**89.79**	**86.49**	**86.28**	**85.26**	**82.69**	
		III		**88.34**	**89.79**	**86.49**	**86.28**	**79.02**	**82.69**	
		IV		**88.34**	**89.79**	**86.49**	**86.28**	**72.77**	**82.69**	
		V		**66.02**	**68.77**	**65.51**	**62.29**	**52.12**	**57.91**	
		VI		**66.02**	**68.77**	**65.51**	**62.29**	**77.09**	**57.91**	
		VII		**66.02**	**68.77**	**65.51**	**62.29**	**64.61**	**57.91**	
		VIII		**66.02**	**68.77**	**65.51**	**62.29**	**64.61**	**57.91**	
Weighted Score Detection Scenario 1	Intersection Type	I	Scaled (0-100)	**78.42**	**78.34**	**80.22**	**85.68**	**84.65**	**42.32**	
		II		**78.42**	**78.34**	**80.22**	**85.68**	**83.06**	**42.32**	
		III		**78.42**	**78.34**	**80.22**	**85.68**	**81.48**	**42.32**	
		IV		**78.42**	**78.34**	**80.22**	**85.68**	**79.89**	**42.32**	
		V		**72.75**	**73.00**	**74.88**	**79.58**	**74.64**	**36.03**	
		VI		**72.75**	**73.00**	**74.88**	**79.58**	**80.99**	**36.03**	
		VII		**72.75**	**73.00**	**74.88**	**79.58**	**77.82**	**36.03**	
		VIII		**72.75**	**73.00**	**74.88**	**79.58**	**77.82**	**36.03**	
Life-Cycle Cost (EUAC) Detection Scenario 2	Intersection Type	I	US Dollar	$3,034	$2,845	$3,140	$3,295	$2,889	$3,660	3.1
		II		$3,034	$2,845	$3,140	$3,295	$4,574	$3,660	
		III		$3,034	$2,845	$3,140	$3,295	$5,136	$3,660	
		IV		$3,034	$2,845	$3,140	$3,295	$5,698	$3,660	
		V		$4,058	$3,810	$4,104	$4,394	$5,309	$4,788	
		VI		$4,058	$3,810	$4,104	$4,394	$7,557	$4,788	
		VII		$4,058	$3,810	$4,104	$4,394	$6,433	$4,788	
		VIII		$4,058	$3,810	$4,104	$4,394	$8,681	$4,788	
	Intersection Type	I	Scaled (0-100)	**77.40**	**79.50**	**76.22**	**74.50**	**79.02**	**70.45**	
		II		**77.40**	**79.50**	**76.22**	**74.50**	**60.28**	**70.45**	
		III		**77.40**	**79.50**	**76.22**	**74.50**	**54.04**	**70.45**	
		IV		**77.40**	**79.50**	**76.22**	**74.50**	**47.80**	**70.45**	
		V		**66.02**	**68.77**	**65.51**	**62.29**	**52.12**	**57.91**	
		VI		**66.02**	**68.77**	**65.51**	**62.29**	**27.15**	**57.91**	
		VII		**66.02**	**68.77**	**65.51**	**62.29**	**39.63**	**57.91**	
		VIII		**66.02**	**68.77**	**65.51**	**62.29**	**14.66**	**57.91**	
Weighted Score Detection Scenario 2	Intersection Type	I	Scaled (0-100)	**75.64**	**75.72**	**77.60**	**82.69**	**81.48**	**39.21**	
		II		**75.64**	**75.72**	**77.60**	**82.69**	**76.72**	**39.21**	
		III		**75.64**	**75.72**	**77.60**	**82.69**	**75.13**	**39.21**	
		IV		**75.64**	**75.72**	**77.60**	**82.69**	**73.54**	**39.21**	
		V		**72.75**	**73.00**	**74.88**	**79.58**	**74.64**	**36.03**	
		VI		**72.75**	**73.00**	**74.88**	**79.58**	**68.30**	**36.03**	
		VII		**72.75**	**73.00**	**74.88**	**79.58**	**71.47**	**36.03**	
		VIII		**72.75**	**73.00**	**74.88**	**79.58**	**65.12**	**36.03**	

Notes:

Letter code for test device

A – Autoscope AIS-IV Camera
F – FC-334T Thermal Imaging Camera
R – RZ4 Advanced WDR Camera
SM – SmartSensor Matrix
WM – Wireless Magnetometer
VS–Vantage SmartSpan Camera

Scaling

Accuracy: minimum = 0 ms; maximum = 40 ms
Reliability: minimum = 0 ms; maximum = 50 ms
East of installation and maintenance: minimum = 1; maximum = 5
Life cycle cost (EUAC): minimum = $1,000; maximum = $10,000

*Accuracy criterion was not used for multicriteria evaluation.

As shown in Table 9.2, based on the three criteria (i.e., reliability, ease of installation and maintenance, and life cycle cost) similar overall scores were computed for the three mast arm mounted cameras. By referencing the detection scheme 1, the RZ4 Advance WDR camera has the highest score (in the range of 74.88-80.22), followed by the FC-334T thermal imaging camera (73.00-78.34), and the Autoscope AIS-IV camera (72.75-78.42). In most cases, the SmartSensor Matrix scored the highest (79.58-85.68) of all six stop bar detection devices. The wireless magnetometers has the second highest score (74.64-84.65) in most cases. However, the score drops (65.12-81.48) as more intensive detection (detection scheme 2) is required. Among the six devices, the Vantage SmartSpan camera has the lowest score (36.03-42.32), which is mainly due to its much lower reliability rating compared to other devices.

Comparing to detection scheme 1, the scores of all devices are generally lower or remain the same under detection scheme 2. The score for the wireless magnetometers decreases to a much larger degree because more magnetometers are required for stop bar detection under detection scheme 2.

10. APPLICATION CONTEXTS AND GENERAL GUIDELINES

The multicriteria evaluation is insightful. However, it does not consider site specific features and practical constraints. For successful use of detection technologies or devices at particular sites, site specific features and constraints must be considered. More often, those specific features and practical constraints govern whether a particular technology is chosen or not. To assist with context-sensitive decisions on selecting proper detection technologies or devices, general guidelines have been developed and are discussed below.

Regular Video Imaging Cameras

- Overall, the video imaging cameras offer comparable performance. Selection of a particular type of cameras largely depends on users' experience, such as user-friendliness (e.g., firmware), and ease of operations and maintenance.
- One camera can possibly detect up to four (4) or five (5) lanes per approach depending on the mounting location. This translates to a cost saving. However, accuracy and reliability decrease in general as more travel lanes are assigned a single camera. For typical site conditions, one camera can effectively handle up to three (3) lanes side by side (assuming no separation area between left turn lane(s) and through lane(s) on the same approach). If there are dual left turn lanes, a single camera is recommended for the dual left turn lanes only.
- Mast arms are generally required for mounting cameras to ensure stability and proper vertical and lateral viewing angles.
- For the same mounting height, far-side mount (i.e., a larger aspect ratio) is generally preferred over near-side mount if the approach is relatively straight because it can tolerate a larger lateral offset and minimize potential lateral occlusion. Too far away from the detection approach could render cameras more sensitive to windy and adverse weather conditions and thus likely reduce reliability. For curved approaches, near-side mount is preferred so to minimize potential false calls triggered by adjacent movements.
- Beside mast arms, detection cameras could be mounted on existing luminaires. This often achieves desirable mounting heights and alleviates the truck occlusion issue. However, the much higher mount make cameras more susceptible to wind and adverse weather conditions. Those competing factors should be carefully evaluated during site inspection.
- The uneven shade is common at intersections in Georgia. This condition typically occurs on a sunny and clear day, and may cause false calls depending on the type of cameras. This particular factor should be considered when choosing a camera.
- Regular video cameras might not be appropriate at locations with no street light. This is generally the case for intersections in a rural or suburban area. The head

light or tail light likely trigger a false call when the intersection is on a sharp horizontal curve.

- They may not be appropriate at locations subject to frequent foggy or mist conditions, such as in the vicinity of a large body of water (lake or river).
- Glare appears not to be an issue if the camera is set up properly.
- Preferred contexts
    - Signal structure support: mast arms
    - Practical mounting locations are available to satisfy the requirements of height, offset, and distance to the stop bar of detection.
    - Locations less susceptible to wind especially when cameras are mounted on the far side.
    - Low spots or elevation of intersections (downgrade approaches)
    - Minor street approaches (low speed and less truck traffic)
    - Existence of street lighting
    - Presence of bridge decks or bad pavements

Thermal Imaging Cameras

- Thermal imaging cameras are robust to night, low visibility, glare and uneven shade conditions.
- The thermal imaging cameras are generally more suitable to locations with the following characteristics:
    - Signal structure support: mast arms
    - Practical mount locations are available to satisfy the requirements of height, offset, and distance to the stop bar of detection.
    - Absence of street lighting
    - Presence of bridge decks or bad pavements
    - Presence of uneven shade conditions
    - Frequent foggy or mist conditions (such as locations near a large water body, e.g., a lake or river)
    - Glare and/or reflection concerns

Span Wire Video Imaging Cameras

- Require span wire for installation.
- Require good pavement and clear lane marking.
- Glare could be a concern for span wire cameras installed on a single wire due to the sway of the camera during windy conditions.
- They might be considered for locations with following characteristics:
    - Signal structure support: span wire

- Locations less susceptible to wind (e.g., urban areas, lower spots or elevations comparing to the surroundings)
- New pavements with clear lane marking
- Approaches that are not oriented east-west

Radar-Based Detectors

- Even though the mounting locations for radar-based devices are more flexible than those of detection cameras, near-side mounting is generally preferred.
- Possible blocking or interruption of signal transmission due to heavy trucks should be evaluated for choosing specific mounting locations.
- More suitable for locations with following characteristics:
  - Signal structure support: mast arms preferred
  - Practical mount locations are available to satisfy the requirements of height, offset, and distance to the stop bar of detection.
  - Absence of street lighting
  - Presence of bridge decks or bad pavements
  - Presence of uneven shade conditions
  - Susceptible to adverse weather and environmental conditions
  - Glare and/or reflection concerns

Wireless Magnetometers

- Generally more accurate and reliable than cameras and other nonintrusive devices because of its ground-level detection.
- Easier to install and maintain as compared to inductive loops
- Independent of signal support structure (mast arm or span wire)
- Reliable communication between in-pavement sensors and the access points and/or repeater(s) is required. The slow passing of frequent heavy trucks (e.g. heavy truck corridor during the peak hours) might affect wireless signal transmission. This communication issue can usually be resolved by additional radio(s) and/or repeater(s).
- Wireless magnetometers might not be cost-effective for larger intersections. Based on the quotes received from the distributor, the life cycle cost for wireless magnetometers is similar to those of other detection devices if three or less lanes are to be detected per approach. When the number of lanes for detection exceeds three lanes per approach, wireless magnetometers appear to be less economical.
- More suitable contexts:
  - Signal support structure: span wire or mast arm. In practice, intersections with span wire are generally "preferred locations" for wireless magnetometers. However, intersections with span wire are usually larger

(i.e., greater span) and may not be cost-effective for wireless magnetometers. Cost-effectiveness may be retained if the stop bar detection is only required for left turn movements with single or dual left turn lanes for each approach.

- Locations where a high level of detection reliability is required.

For advance detection applications, wireless magnetometers appear to be an alternative to inductive loops. Many agencies have used wireless magnetometers for both volume-density and indecision zone applications.

Besides the stop bar presence detection, two radar-based vehicle detection devices (i.e., Vantage Vector Hybrid and SmartSensor Advance) were evaluated and compared with each other by referencing the volume-density loop located at the entry point of the indecision zone as defined at site 2. Based on frequency analysis, there is approximately 87 percent consistency between the two devices. But, duration analysis indicates a significant difference in capturing the detection duration of vehicles within the defined indecision zone. This could be due to many factors, such as technological difference, detection algorithms, and/or field setup and configuration requirements. Further studies with more rigorous test design and appropriate benchmark are required to evaluate those types of detection devices for indecision zone protection.

11. REFERENCES

1. A Policy on Geometric Design of Highways and Streets, 6th Edition, American Association of State Highway and Transportation Officials (AASHTO), 2011

2. Achim Zeileis, Christian Kleiber, Simon Jackman (2008). Regression Models for Count Data in R. Journal of Statistical Software 27(8).

3. Ahmed Abdel-Rahim, Brian k. Johnson. An Intersection Traffic Data Collection Device Utilizing Logging Capabilities of Traffic Controllers and Current Traffic Sensors. Report No. N08-13, US Department of Transportation, November 2008.

4. Avery Rhodes, Darcy M. Bullock, James Sturdevant, Zachary Clark, and David G. Candey, Jr. Evaluation of The Accuracy of Stop Bar Video Vehicle Detection at Signalized Intersections. Journal of the Transportation Research Board, No. 1925, Transportation Research Board of the National Academies, Washington, D.C., 2005, pp. 134–145.

5. Cameron AC, Trivedi PK (1998).Regression Analysis of Count Data. Cambridge University Press, Cambridge.

6. Cameron AC, Trivedi PK (2005). Microeconometrics: Methods and Applications. Cambridge University Press, Cambridge.

7. Christopher M. Day, Hiromal Premachandra, Thomas M. Brennan, Jr., James R. Sturdevant, and Darcy M. Bullock. Operational Evaluation of Wireless Magnetometer Vehicle Detectors at Signalized Intersection. Journal of the Transportation Research Board, No. 2192, Transportation Research Board of the National Academies, Washington, D.C., 2010, pp. 11–23.

8. Dan Middleton, Eun Sug Park, Hassan Charara, and Ryan Longmire. Evidence of Unacceptable Video Detector Performance for Dilemma Zone Protection. Journal of the Transportation Research Board, No. 2080, Transportation Research Board of the National Academies, Washington, D.C., 2008, pp. 100–110.

9. Dan Middleton, Hassan Charara, and Ryan Longmire. Alternative Vehicle Detection Technologies for Traffic Signal Systems: Technical Report. Report No. FHWA/TX-09/0-5845-1, Texas Department of Transportation, February 2009.

10. Dan Middleton, Mark Shafer, Debbie Jasek. Initial Evaluation of the Existing Technologies for Vehicle Detection. Publication FHWA/TX/99/1715-1, Texas Department of Transportation, October 1997.

11. Dan Middleton, Ryan Longmire, Hassan Charara, and Darcy Bullock. Proposed Test Protocol for Video Imaging Detection at Intersection Stop Lines. Research Report 0-6030-P1, Texas Transportation Institute, Texas A&M University System, College Station, Texas, April 2010

12. Dan Middleton, Ryan Longmire, Hassan Charara, and Darcy Bullock. Proposed Test Protocol for Video Imaging Detection at Intersection Stop Lines. Research Report 0-6030-P2, Texas Transportation Institute, Texas A&M University System, College Station, Texas, August 2010

13. Dan Middleton, Ryan Longmire, Darcy M. Bullock, and James R. Sturdevant. Proposed Concept for Specifying Vehicle Detection Performance. Journal of the Transportation Research Board, No. 2128, Transportation Research Board of the National Academies, Washington, D.C., 2009, pp. 161–172.

14. Dan Middleton, Ricky Parker, and Ryan Longmire. Investigation of Vehicle Detector Performance and ATMS Interface. Publication FHWA/TX-07/0-4750-2, Texas Department of Transportation, March 2007.

15. Dan Middleton, Ricky Parker. Vehicle Detector Evaluation. Report number FHWA/TX-03/2119-1, Texas Department of Transportation, October 2002.

16. Edward J. Smaglik, Zachary Davis, R. Christopher Steele,William Nau, and Craig A. Roberts. Supplementing Signalized Intersection Infrastructure To Provide Automated Performance Measures With Existing Video Detection Equipment. Journal of the Transportation Research Board, No. 2192, Transportation Research Board of the National Academies, Washington, D.C., 2010, pp. 77–88.

17. Erik Minge, Jerry Kotzenmacher, Scott Peterson. Evaluation of Non-Intrusive Technologies for Traffic Detection. Report No. MN/RC 2010-36, Minnesota Department of Transportation, September 2010.

18. Georgia Department of Transportation (GDOT) Signal Design Guideline, 2014

19. Hartmann, D., D. Middleton, and D. Morris. Assessing Vehicle Detection Utilizing Video Image Processing Technology, FHWA/TX-97/1467-4. Texas Transportation Institute, College Station, TX, 1996.

20. Hothorn T, Hornik K, Zeileis A (2006). Unbiased Recursive Partitioning: A Conditional Inference Framework. Journal of Computational and Graphical Statistics, 15 (3), 651–674.

21. James Bonneson and Montasir Abbas. Intersection Video Detection Manual, Report No. FHWA/TX-03/4285-2, Texas Department of Transportation, September 2002

22. JD Margulici, Samuel Yang, Chin-Woo Tan, Pulkit Grover, and Andre Markarian. Evaluation of Wireless Traffic Sensors by Sensys Networks, Inc. California Center for Innovative Transportation, Final Report, October 2006.

23. Jialin Tian, Mark R. Virkler, and Carlos Sun. Field Testing for Automated Identification of Turning Movements at Signalized Intersections. Journal of the Transportation Research Board, No. 1867, TRB, National Research Council, Washington, D.C., 2004, pp. 210–216.

24. Jonathan Corey, Yunteng Lao, Yao-Jan Wu, and Yinhai Wang. Detection and Correction of Inductive Loop Detector Sensitivity Errors by Using Gaussian Mixture Models. Journal of the Transportation Research Board, No. 2256, Transportation Research Board of the National Academies, Washington, D.C., 2011, pp. 120–129.

25. Juan C. Medina, Rahim F. Benekohal, and Ali Hajbabaie. Evaluation of Sensys Wireless Vehicle Detection System: Results from Adverse Weather Conditions. Research Report ICT-11-81, Illinois Center for Transportation, March 2011.

26. Juan C. Medina, Rahim F. Benekohal, and Hani Ramezani. Field Evaluation of Smart Sensor Vehicle Detectors at Intersections— Volume 1: Normal Weather Conditions. Research Report FHWA-ICT-12-016, Illinois Center for Transportation, October 2012

27. Juan C. Medina, Madhav Chitturi, Rahim F. Benekohal. Illumination and Wind Effects on Video Detection Performance at Signalized Intersections. University of Illinois at Urbana-Champaign, 2008 TRB Annual Meeting CD-ROM.

28. J. Grossman, A. Hainen, S. Remias, D. M. Bullock (2012). Evaluation of Thermal Image Video Sensors for Stop Bar Detection at Signalized Intersections. Transportation Research Record: Journal of the Transportation Research Board, No. 2308, pp. 184-198.

29. Iwasaki Y., Misumi M., and Nakamiya T. (2013). Robust Vehicle Detection under Various Environmental Conditions Using an Infrared Thermal Camera and Its Application to Road Traffic Flow Monitoring. Sensors 2013, 13, 7756-7773; doi:10.3390/s130607756.

30. Karl Zimmerman, Devendra Tolani, Roger Xu, Tao Qian, and Peter Huang. Detection, Control, and Warning System for Mitigating Dilemma Zone Problem. Journal of the Transportation Research Board, No. 2298, Transportation Research Board of the National Academies, Washington, D.C., 2012, pp. 30–37.

31. Karl Zimmerman, James A. Bonneson, Dan Middleton, and Montasir M. Abbas. Improved Detection and Control System for Isolated High-Speed Signalized Intersections. Publication 03-3732, Texas Department of Transportation, 2003.

32. Lambert D (1992). "Zero-inflated Poisson Regression, With an Application to Defects in Manufacturing." Technometrics 34, 1–14.

33. Lawrence A. Klein, Milton K. Mills, and David R.P. Gibson 2006). Traffic Detector Handbook, Publication No. FHWA-HRT-06-108.

34. MacCarley, C.A., S. Hockaday, D. Need, and S. Taff. "Evaluation of Video Image Processing Systems for Traffic Detection," Transportation Research Record No. 1360. Transportation Research Board, National Research Council, Washington, DC, 1992.

35. Peter Koonce, Lee Rodegerdts, Kevin Lee, Shaun Quayle, Scott Beaird, Cade Braud, Jim Bonneson, Phil Tarnoff, and Tom Urbanik. Traffic Signal Timing Manual, Federal Highway Administration, Report No. FHWA-HOP-08-024, June 2008, Washington D.C.

36. Peter T. Martin, Gayathri Dharmavaram, and Aleksandar Stevanovic . Evaluation of UDOT'S Video Detection Systems - System's Performance in Various Test Conditions. Salt Lake City, Utah, December 2004.

37. Peter T. Martin, Yuqi Feng, Xiaodong Wang. Detector Technology Evaluation. Report number MPC03-154, U.S. Department of Transportation and Utah Department of Transportation, November 2003.

38. R Core Team (2014). R: A language and environment for statistical computing. R Foundation for Statistical Computing, Vienna, Austria.

39. Raghuram Dharmaraju, David A. Noyce, Joshua D. Lehman. An Evaluation of Technologies for Automated Detection and Classification of Pedestrians and Bicycles. Publication 2001-0049, U.S. Massachusetts Highway Department, 2001.

40. Special Provision Section 937 of the GDOT Standard Specifications – Construction of Transportation Systems

41. Strasser H and Weber C (1999). “On the Asymptotic Theory of Permutation Statistics.” Mathematical Methods of Statistics, 8, 220-250.

42. Traffic Surveillance and Detection Technology Development: Phase II and III Test Results, Troy, MI, JPL Pub. D-15779. California Institute of Technology, Jet Propulsion Laboratory, Pasadena, CA, May 1998.

43. White Paper: The Iteris Vantage Vector® Solution Eliminates the Dilemma Zone, November 2013

44. Woeber W., Kefer M., Kubinger W., and Szuegyi D. Evaluation of Daylight and Thermal Infra-red Based Detection for Platooning Vehicles. Annals of DAAAM for 2012 and Proceedings of the 23rd International DAAAM Symposium, Volume 23, No.1, ISSN 2304-1382, ISBN 978-3-901509-91-9, CDROM version, Ed. B. Katalinic, Published by DAAAM International, Vienna, Austria, EU, 2012

45. Zong Tian, Thomas Urbanik. Green Extension and Traffic Detection Schemes at Signalized Intersections. Journal of the Transportation Research Board, No. 1978, Transportation Research Board of the National Academies, Washington, D.C., 2006, pp. 16–24.

Appendix A - Plots of Detection Errors by Time (Site 1)

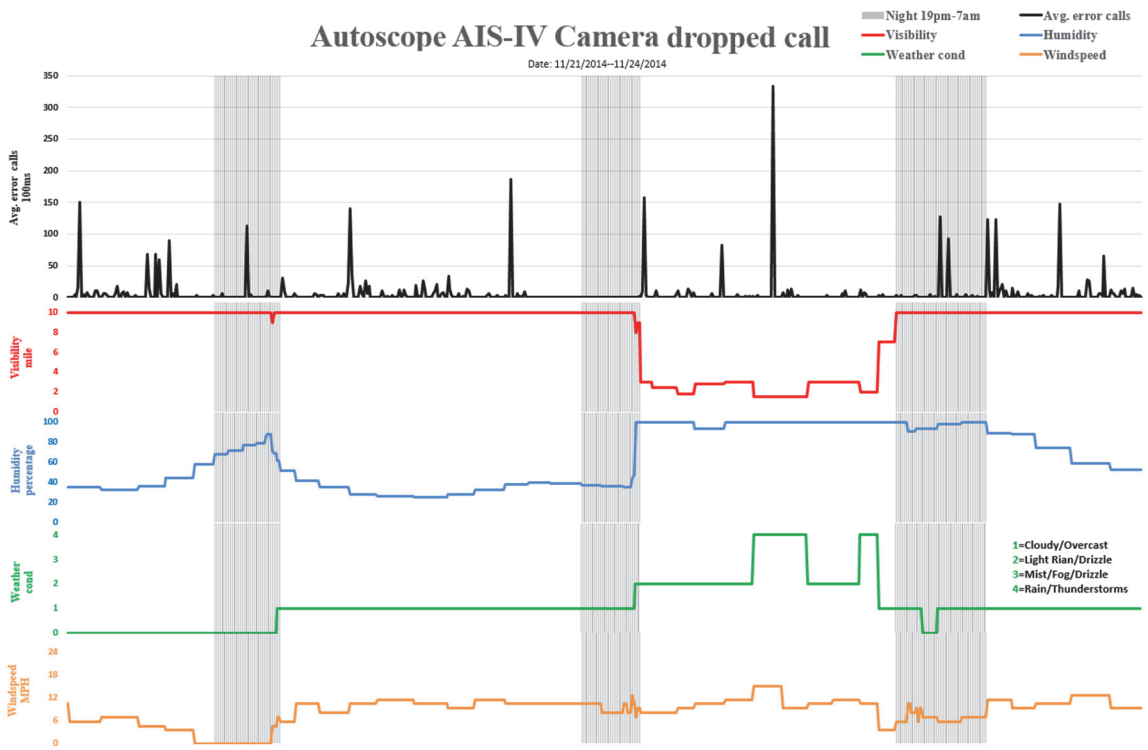
Autoscope AIS-IV Camera dropped call
Date: 11/21/2014--11/24/2014
Night 19pm-7am
Avg. error calls
Visibility
Humidity
Weather cond
Windspeed
Avg. error calls 100ms
Visibility mile
Humidity percentage
Weather cond
Windspeed MPH
1=Cloudy/Overcast
2=Light Rian/Drizzle
3=Mist/Fog/Drizzle
4=Rain/Thunderstorms

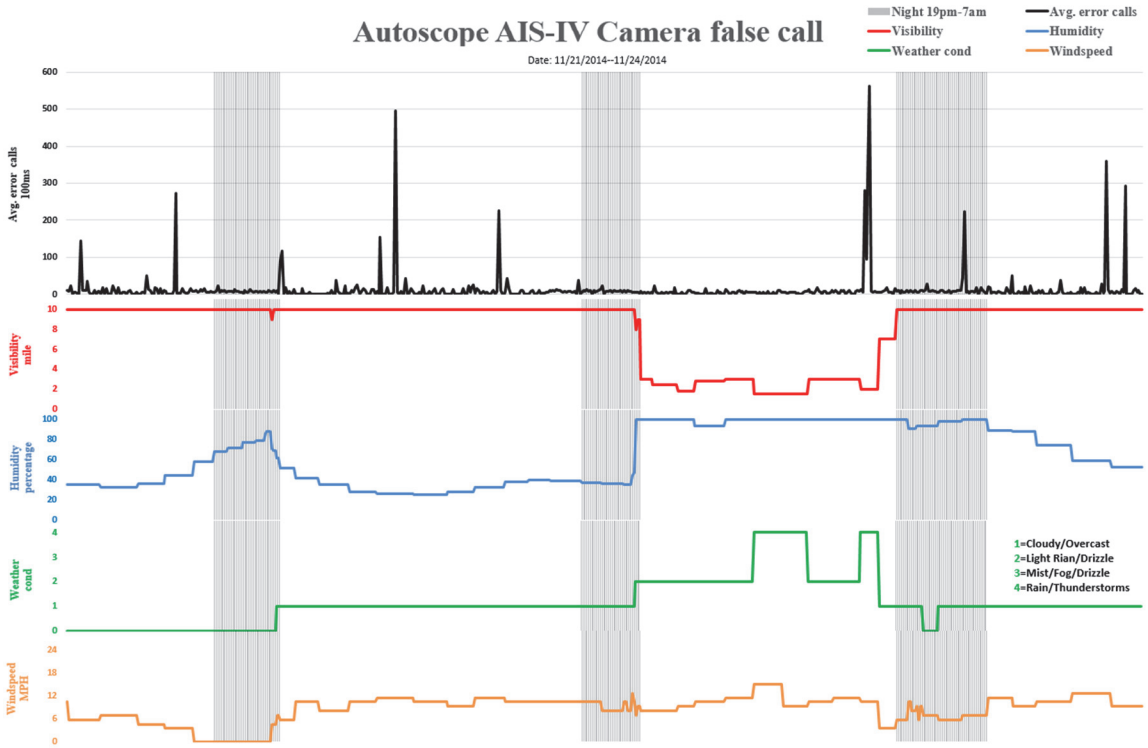
Autoscope AIS-IV Camera false call
Date: 11/21/2014--11/24/2014
Night 19pm-7am
Avg. error calls
Visibility
Humidity
Weather cond
Windspeed
Avg. error calls 100ms
Visibility mile
Humidity percentage
Weather cond
Windspeed MPH
1=Cloudy/Overcast
2=Light Rian/Drizzle
3=Mist/Fog/Drizzle
4=Rain/Thunderstorms

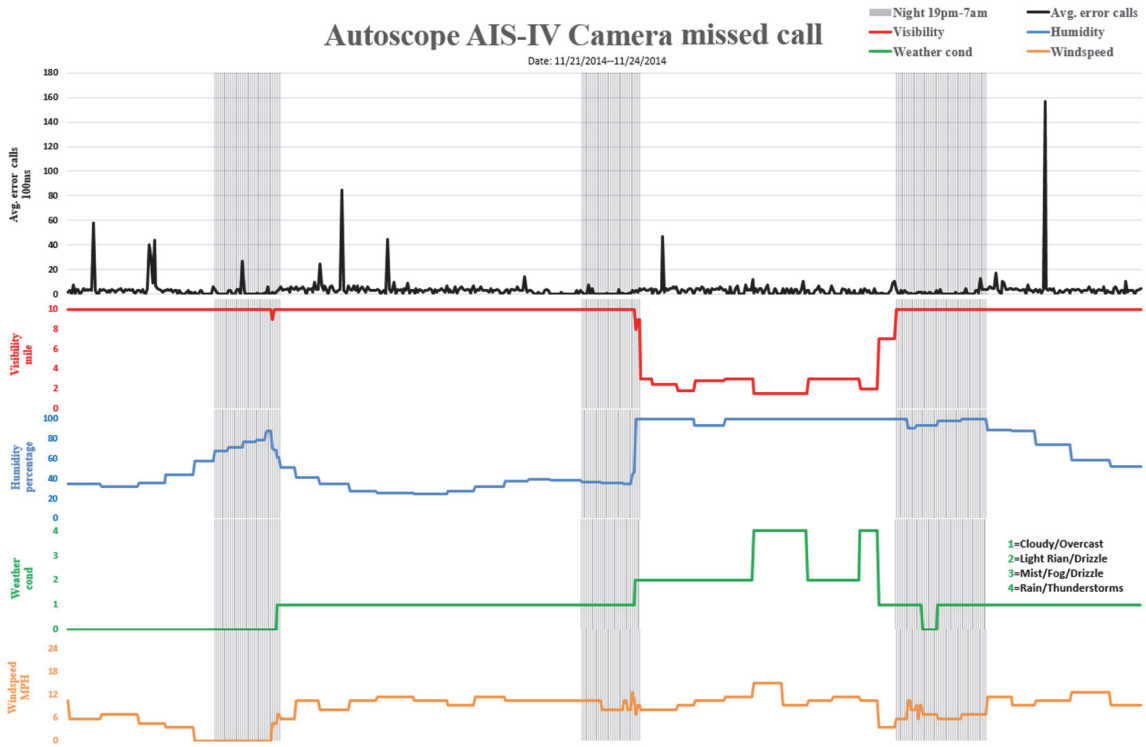
Autoscope AIS-IV Camera missed call
Date: 11/21/2014--11/24/2014
Night 19pm-7am
Visibility
Weather cond
Avg. error calls
Humidity
Windspeed
Avg. error calls 100ms
Visibility mile
Humidity percentage
Weather cond
Windspeed MPH
1=Cloudy/Overcast
2=Light Rian/Drizzle
3=Mist/Fog/Drizzle
4=Rain/Thunderstorms

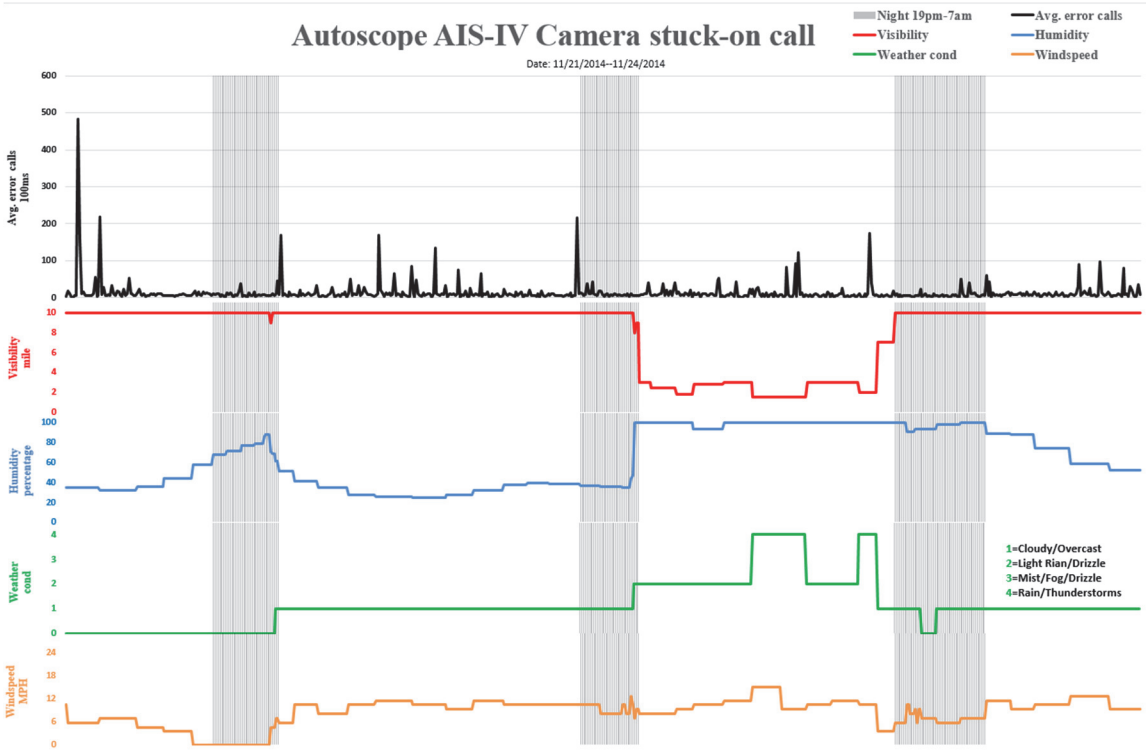
Autoscope AIS-IV Camera stuck-on call
Date: 11/21/2014--11/24/2014
Night 19pm-7am
Visibility
Weather cond
Avg. error calls
Humidity
Windspeed
Avg. error calls 100ms
Visibility mile
Humidity percentage
Weather cond
Windspeed MPH
1=Cloudy/Overcast
2=Light Rian/Drizzle
3=Mist/Fog/Drizzle
4=Rain/Thunderstorms

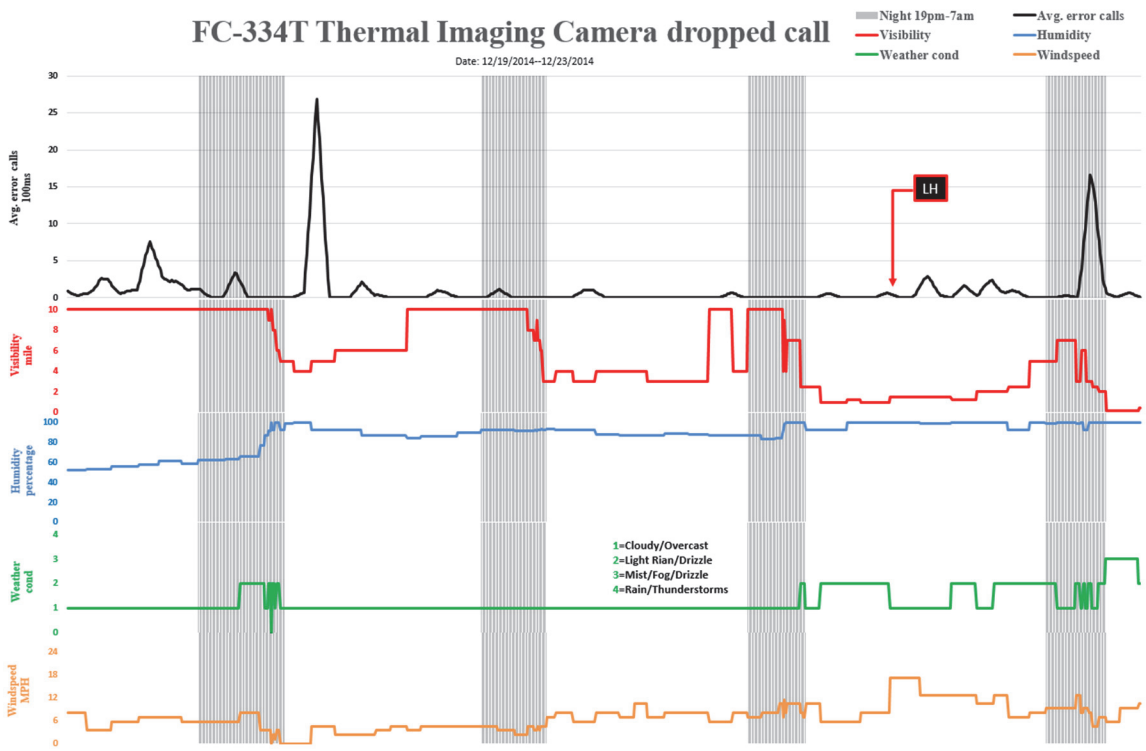
FC-334T Thermal Imaging Camera dropped call
Date: 12/19/2014--12/23/2014
Night 19pm-7am
Visibility
Weather cond
Avg. error calls
Humidity
Windspeed
Avg. error calls 100ms
LH
Visibility mile
Humidity percentage
Weather cond
1=Cloudy/Overcast
2=Light Rian/Drizzle
3=Mist/Fog/Drizzle
4=Rain/Thunderstorms
Windspeed MPH

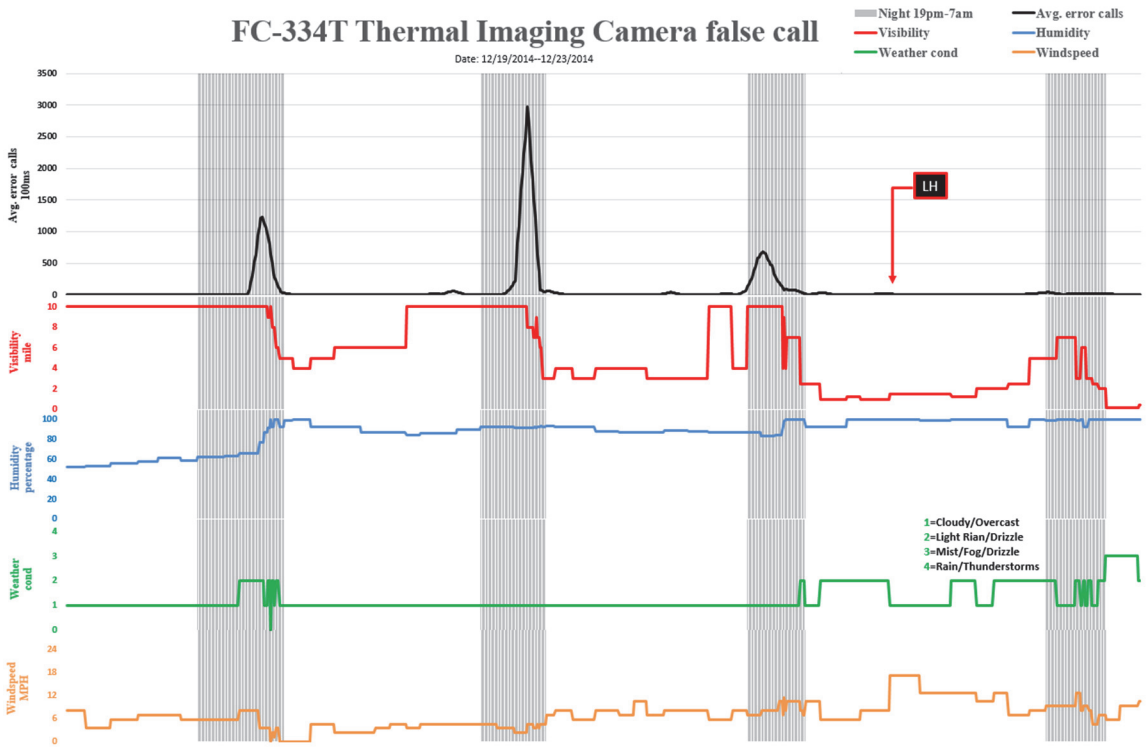
FC-334T Thermal Imaging Camera false call
Date: 12/19/2014--12/23/2014
Night 19pm-7am
Visibility
Weather cond
Avg. error calls
Humidity
Windspeed
Avg. error calls 100ms
LH
Visibility mile
Humidity percentage
Weather cond
1=Cloudy/Overcast
2=Light Rian/Drizzle
3=Mist/Fog/Drizzle
4=Rain/Thunderstorms
Windspeed MPH

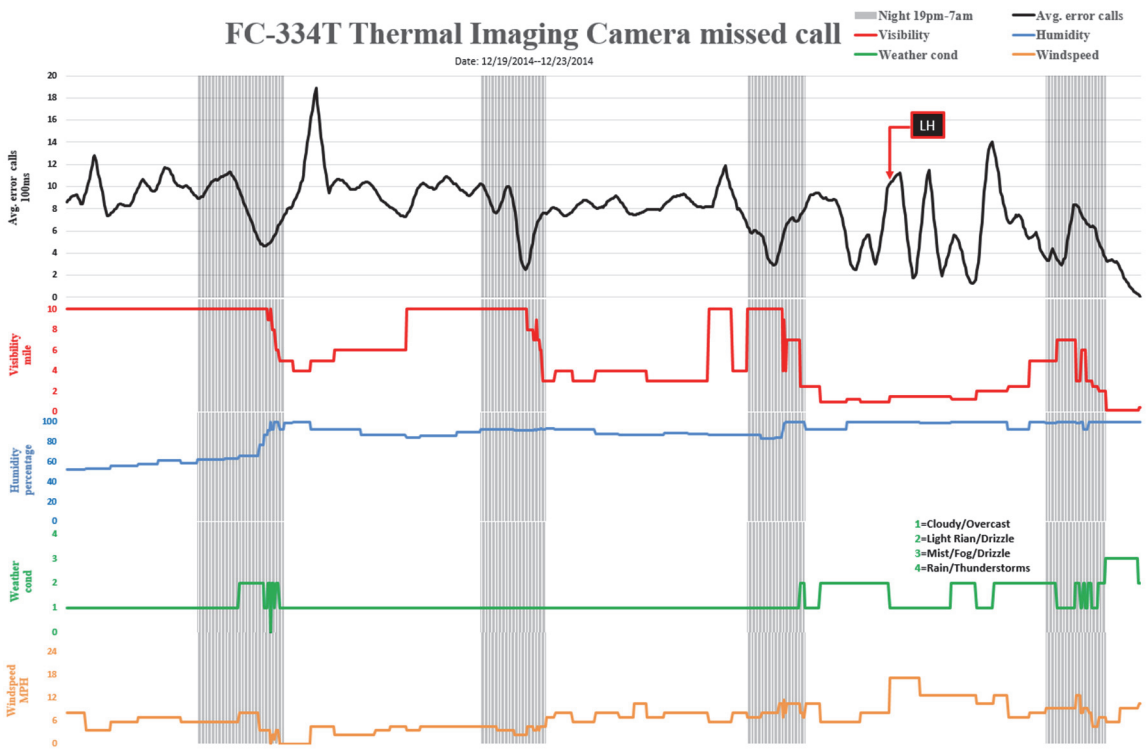
FC-334T Thermal Imaging Camera missed call
Date: 12/19/2014--12/23/2014
Night 19pm-7am
Visibility
Weather cond
Avg. error calls
Humidity
Windspeed
Avg. error calls 100ms
LH
Visibility mile
Humidity percentage
Weather cond
1=Cloudy/Overcast
2=Light Rian/Drizzle
3=Mist/Fog/Drizzle
4=Rain/Thunderstorms
Windspeed MPH

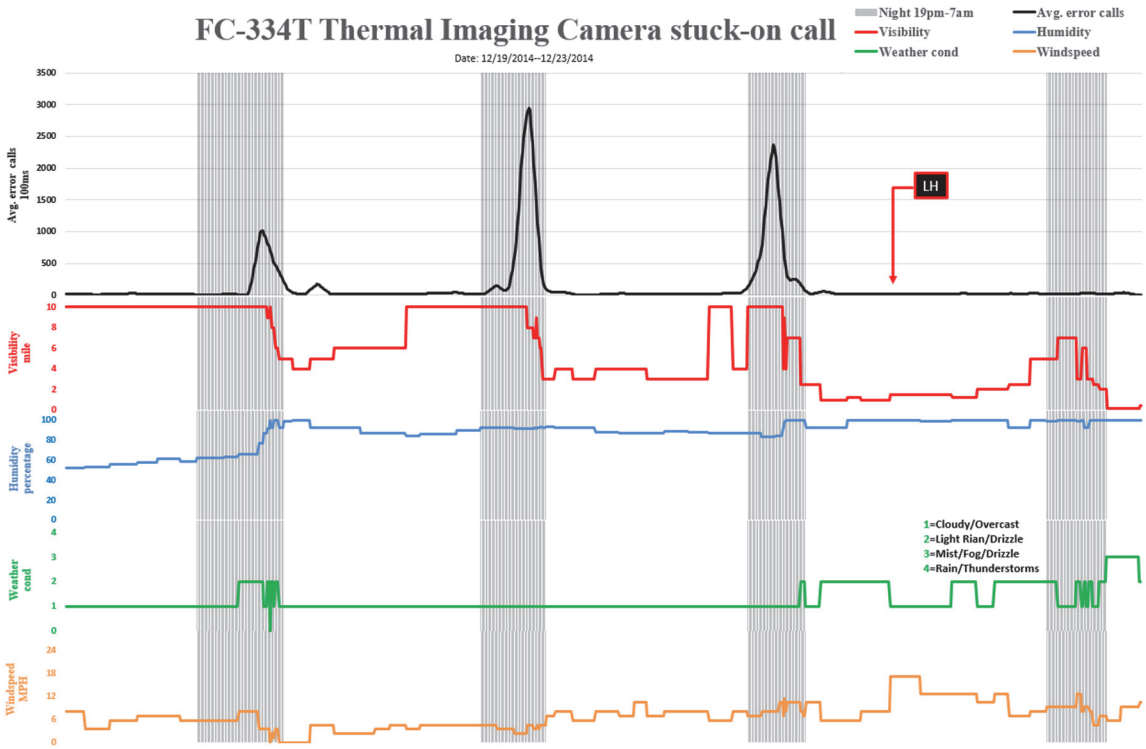
FC-334T Thermal Imaging Camera stuck-on call
Date: 12/19/2014--12/23/2014
Night 19pm-7am
Visibility
Weather cond
Avg. error calls
Humidity
Windspeed
Avg. error calls 100ms
LH
Visibility mile
Humidity percentage
Weather cond
1=Cloudy/Overcast
2=Light Rian/Drizzle
3=Mist/Fog/Drizzle
4=Rain/Thunderstorms
Windspeed MPH

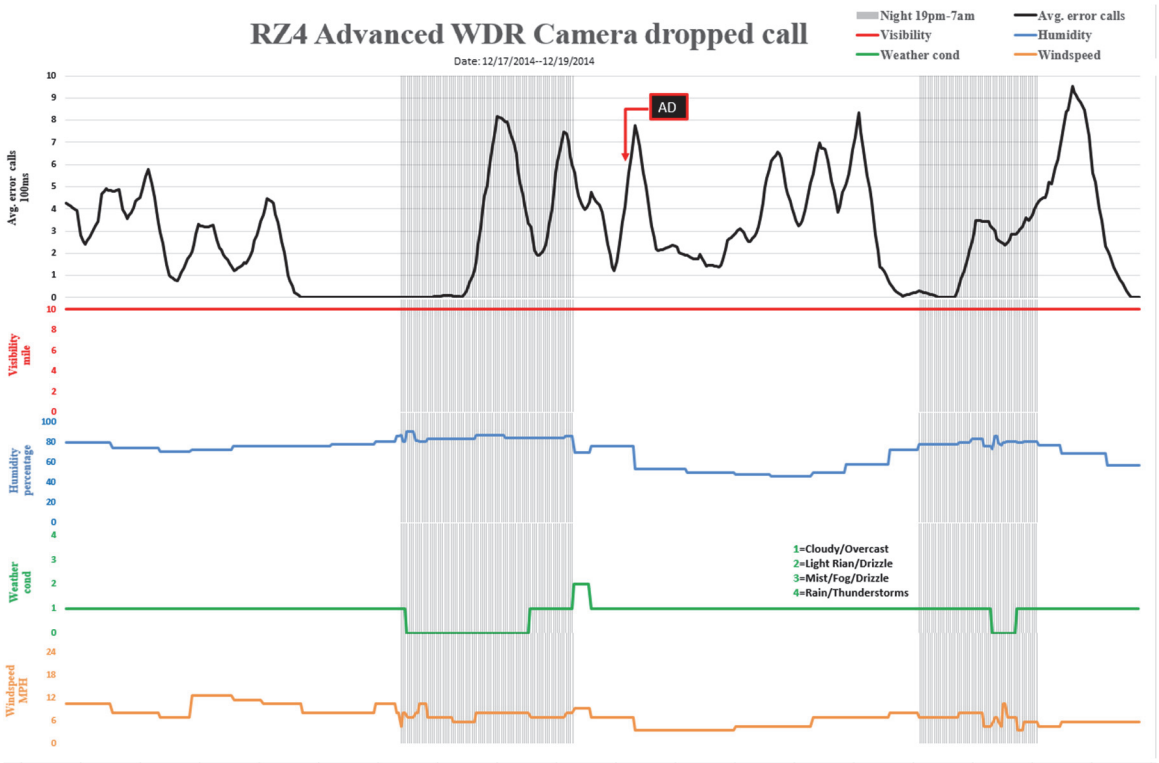
RZ4 Advanced WDR Camera dropped call
Date: 12/17/2014--12/19/2014
Night 19pm-7am
Avg. error calls
Visibility
Humidity
Weather cond
Windspeed
AD
Avg. error calls 100ms
Visibility mile
Humidity percentage
Weather cond
Windspeed MPH
1=Cloudy/Overcast
2=Light Rian/Drizzle
3=Mist/Fog/Drizzle
4=Rain/Thunderstorms

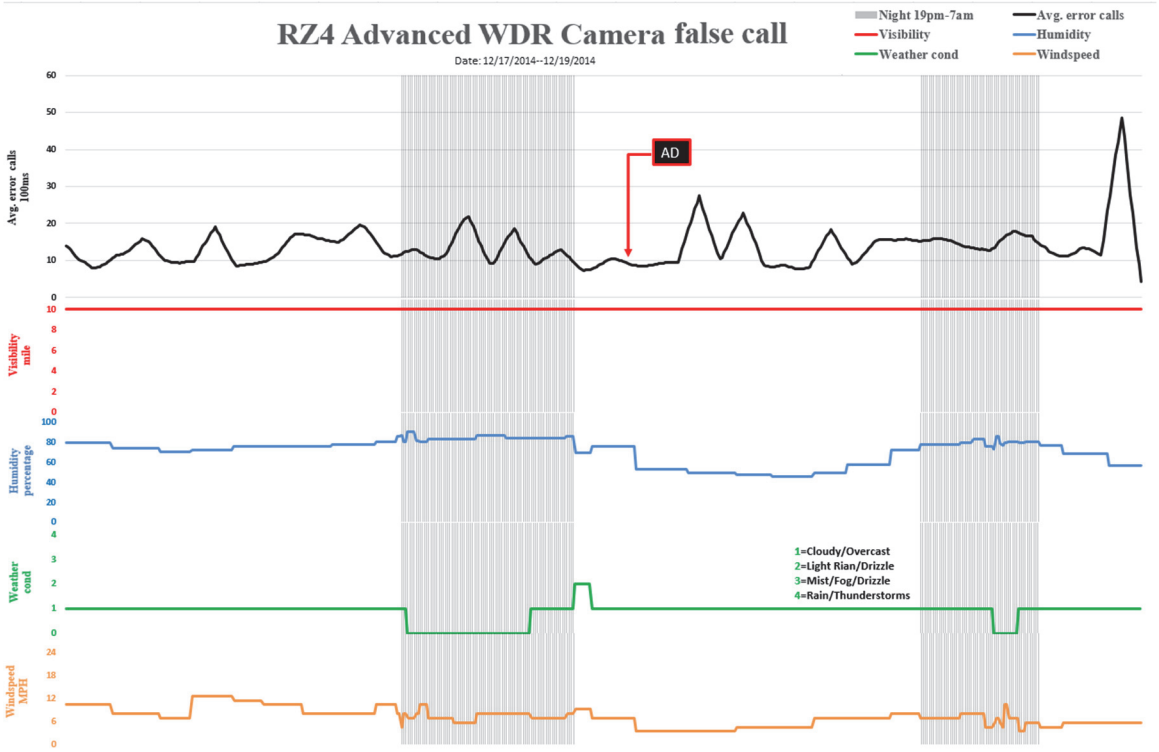
RZ4 Advanced WDR Camera false call
Date: 12/17/2014--12/19/2014
Night 19pm-7am
Avg. error calls
Visibility
Humidity
Weather cond
Windspeed
AD
Avg. error calls 100ms
Visibility mile
Humidity percentage
Weather cond
Windspeed MPH
1=Cloudy/Overcast
2=Light Rian/Drizzle
3=Mist/Fog/Drizzle
4=Rain/Thunderstorms

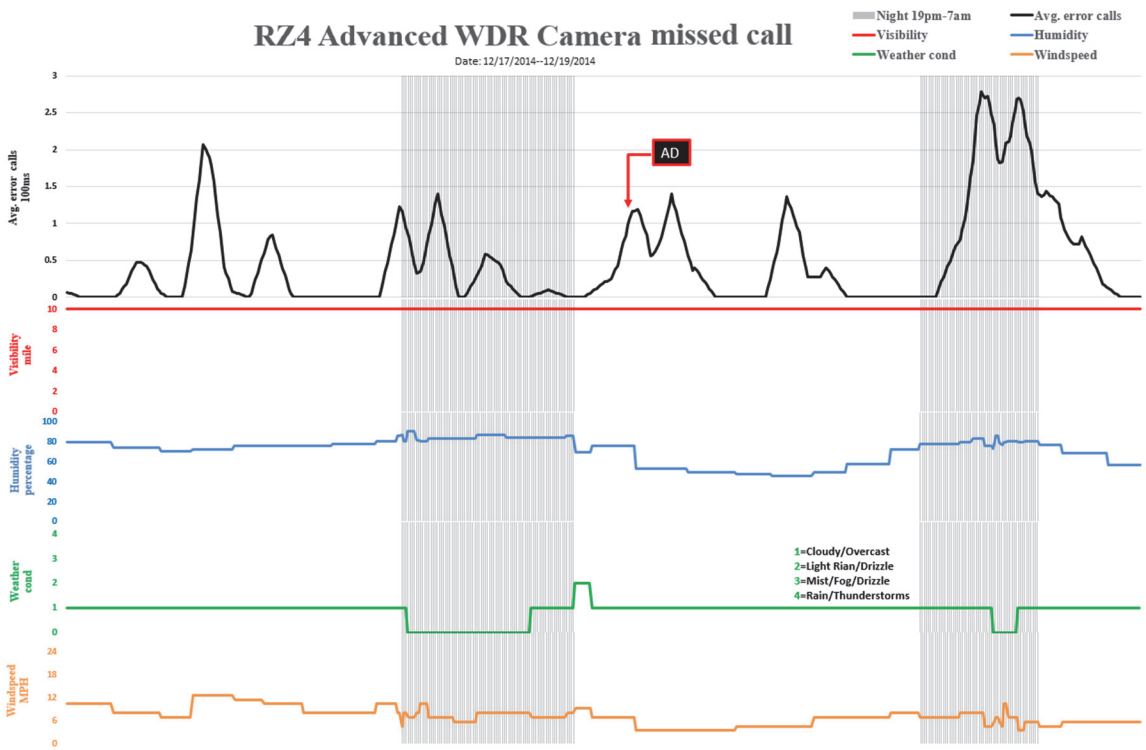
RZ4 Advanced WDR Camera missed call
Date: 12/17/2014--12/19/2014
Night 19pm-7am
Avg. error calls
Visibility
Humidity
Weather cond
Windspeed
AD
Avg. error calls 100ms
Visibility mile
Humidity percentage
Weather cond
Windspeed MPH
1=Cloudy/Overcast
2=Light Rian/Drizzle
3=Mist/Fog/Drizzle
4=Rain/Thunderstorms

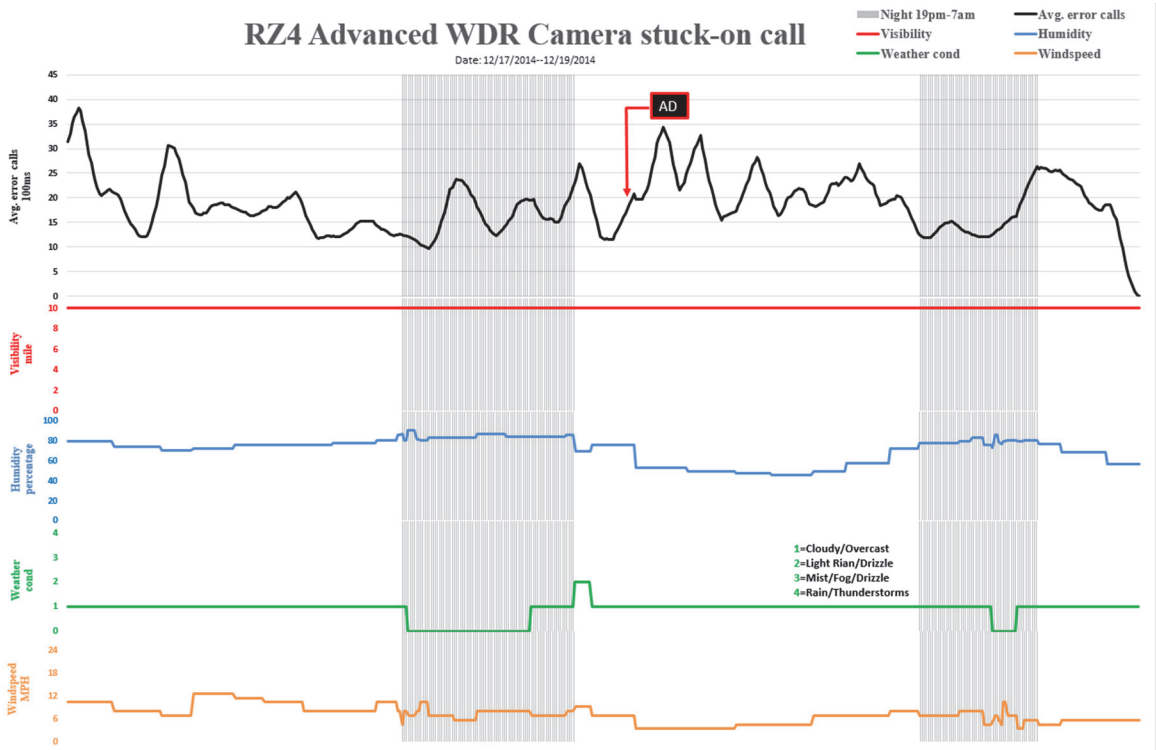
RZ4 Advanced WDR Camera stuck-on call
Date: 12/17/2014--12/19/2014
Night 19pm-7am
Avg. error calls
Visibility
Humidity
Weather cond
Windspeed
AD
Avg. error calls 100ms
Visibility mile
Humidity percentage
Weather cond
Windspeed MPH
1=Cloudy/Overcast
2=Light Rian/Drizzle
3=Mist/Fog/Drizzle
4=Rain/Thunderstorms

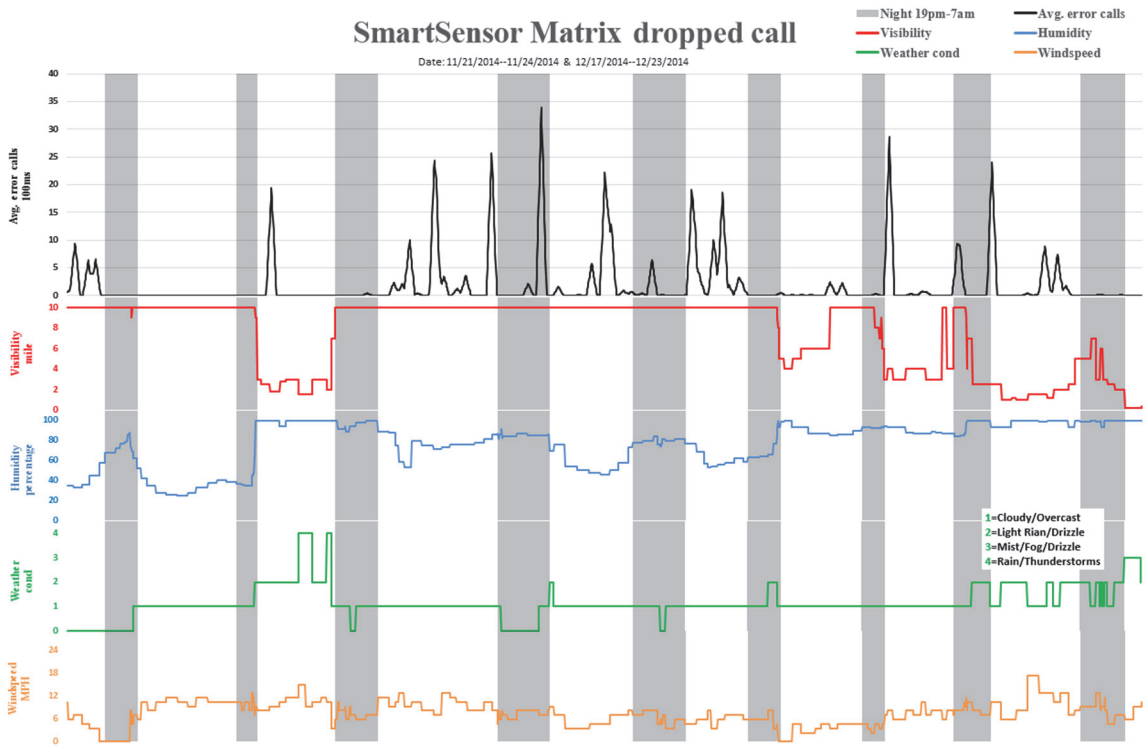
SmartSensor Matrix dropped call
Date: 11/21/2014--11/24/2014 & 12/17/2014--12/23/2014
Night 19pm-7am
Avg. error calls
Visibility
Humidity
Weather cond
Windspeed
Avg. error calls 100ms
Visibility mile
Humidity percentage
Weather cond
Windspeed MPH
1=Cloudy/Overcast
2=Light Rian/Drizzle
3=Mist/Fog/Drizzle
4=Rain/Thunderstorms

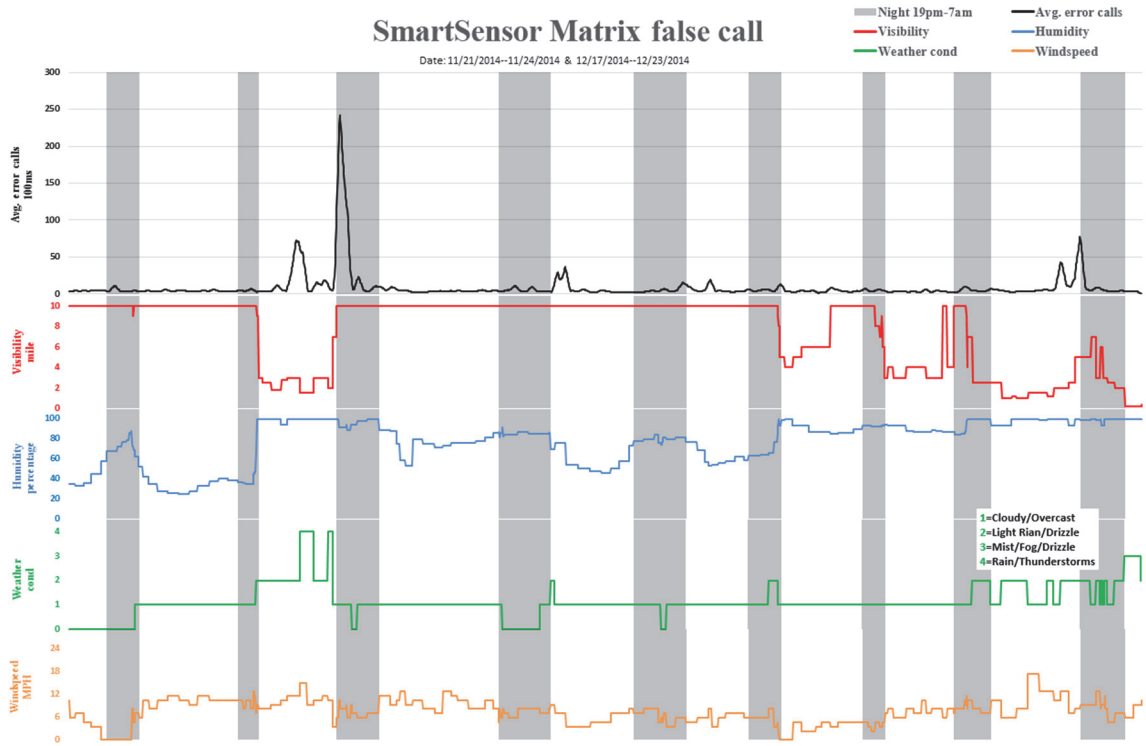
SmartSensor Matrix false call
Date: 11/21/2014--11/24/2014 & 12/17/2014--12/23/2014
Night 19pm-7am
Avg. error calls
Visibility
Humidity
Weather cond
Windspeed
Avg. error calls 100ms
Visibility mile
Humidity percentage
Weather cond
Windspeed MPH
1=Cloudy/Overcast
2=Light Rian/Drizzle
3=Mist/Fog/Drizzle
4=Rain/Thunderstorms

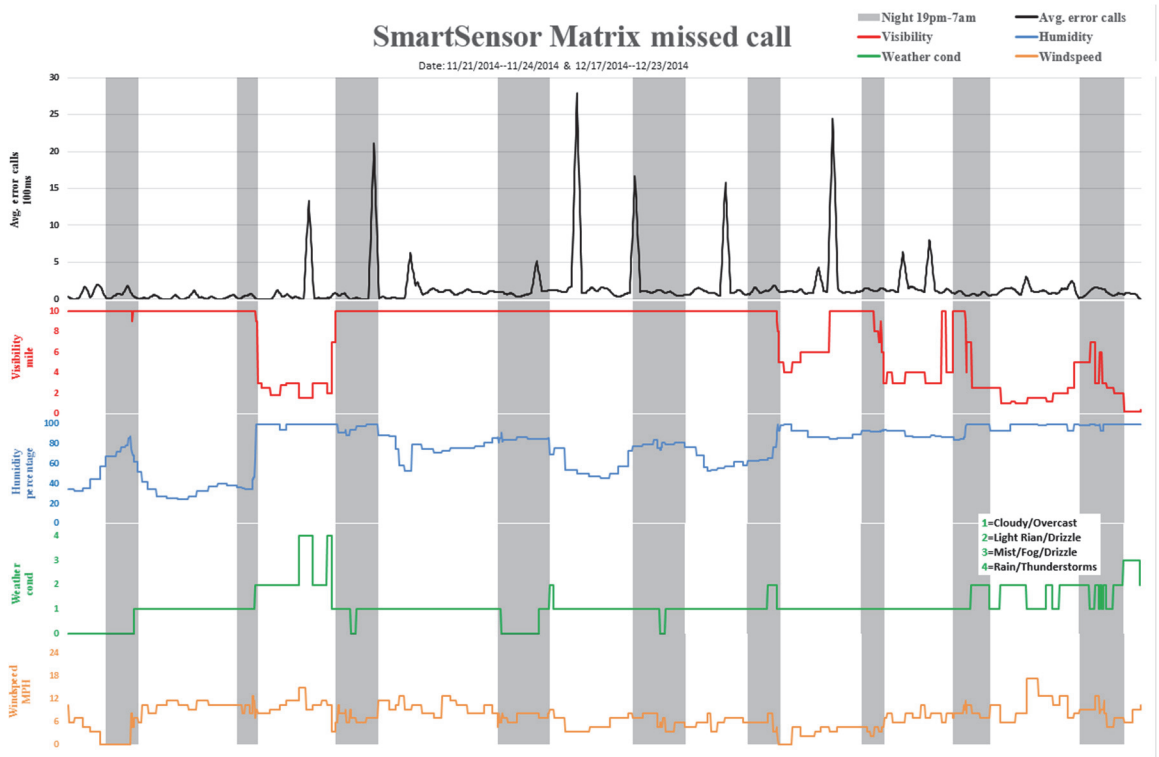
SmartSensor Matrix missed call
Date: 11/21/2014--11/24/2014 & 12/17/2014--12/23/2014
Night 19pm-7am
Avg. error calls
Visibility
Humidity
Weather cond
Windspeed
Avg. error calls 100ms
Visibility mile
Humidity percentage
Weather cond
Windspeed MPH
1=Cloudy/Overcast
2=Light Rian/Drizzle
3=Mist/Fog/Drizzle
4=Rain/Thunderstorms

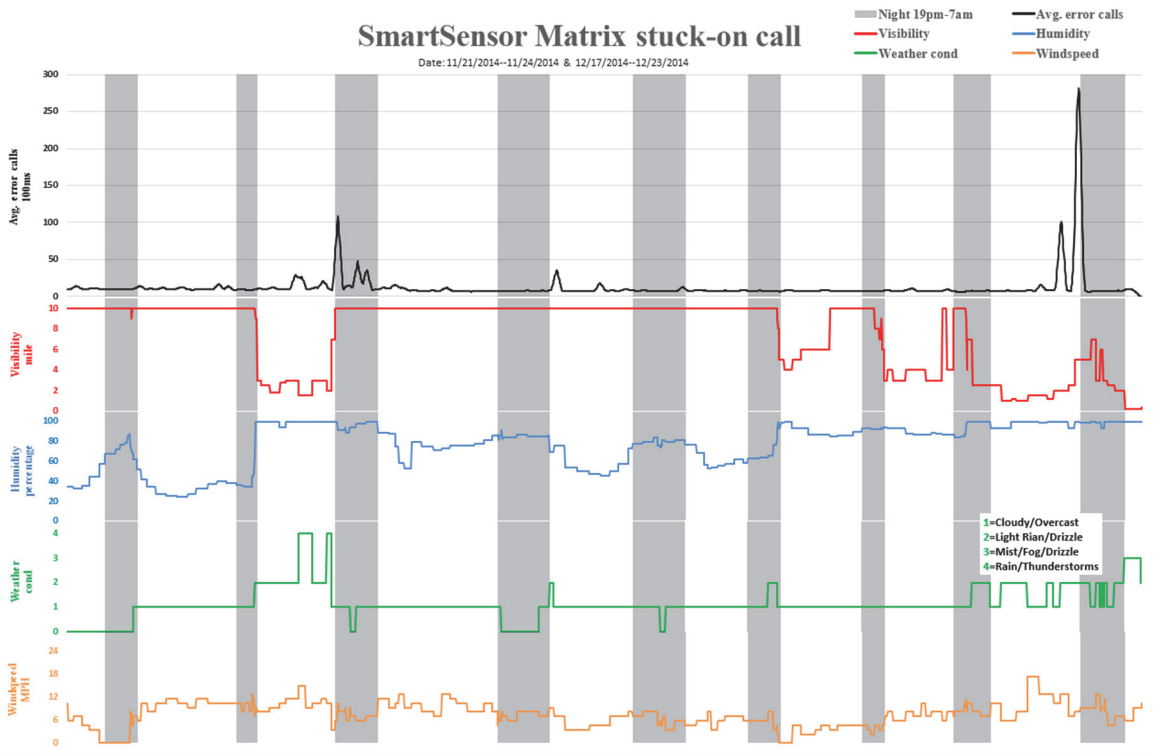
SmartSensor Matrix stuck-on call
Date: 11/21/2014--11/24/2014 & 12/17/2014--12/23/2014
Night 19pm-7am
Avg. error calls
Visibility
Humidity
Weather cond
Windspeed
Avg. error calls 100ms
Visibility mile
Humidity percentage
Weather cond
Windspeed MPH
1=Cloudy/Overcast
2=Light Rian/Drizzle
3=Mist/Fog/Drizzle
4=Rain/Thunderstorms

Appendix B - Plots of Detection Errors by Time (Site 2)

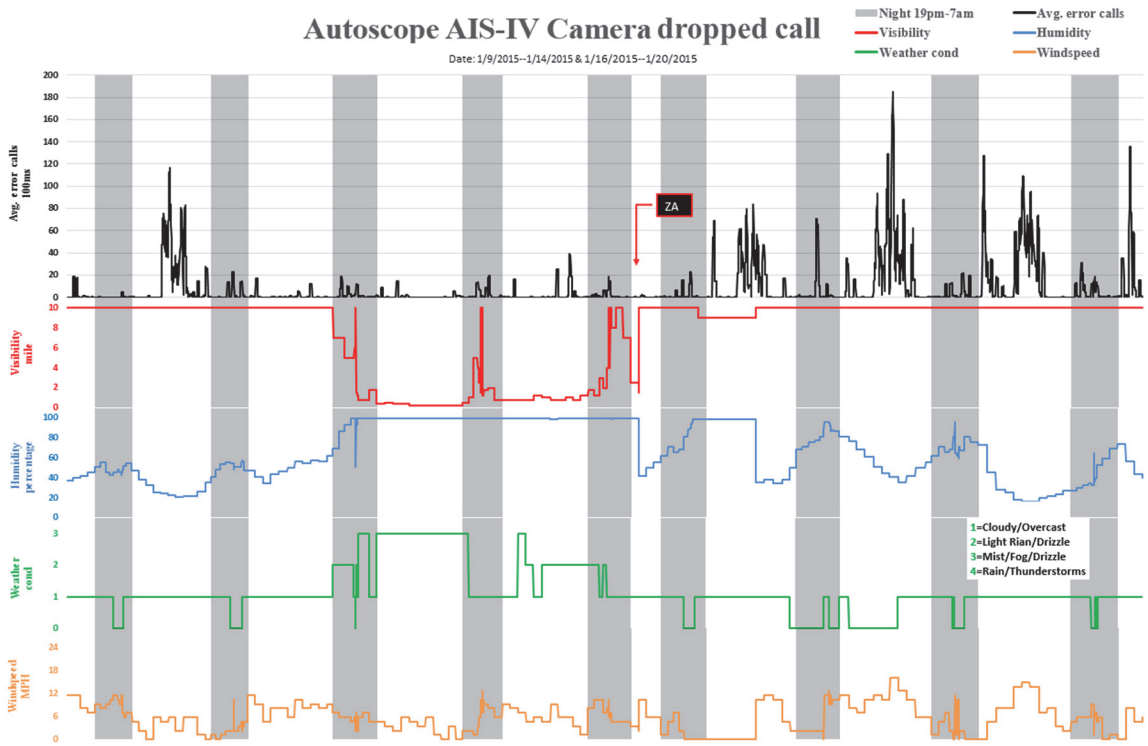
Autoscope AIS-IV Camera dropped call
Date: 1/9/2015--1/14/2015 & 1/16/2015--1/20/2015
Night 19pm-7am
Visibility
Weather cond
Avg. error calls
Humidity
Windspeed
Avg. error calls 100ms
ZA
Visibility mile
Humidity percentage
Weather cond
1=Cloudy/Overcast
2=Light Rian/Drizzle
3=Mist/Fog/Drizzle
4=Rain/Thunderstorms
Windspeed MPH

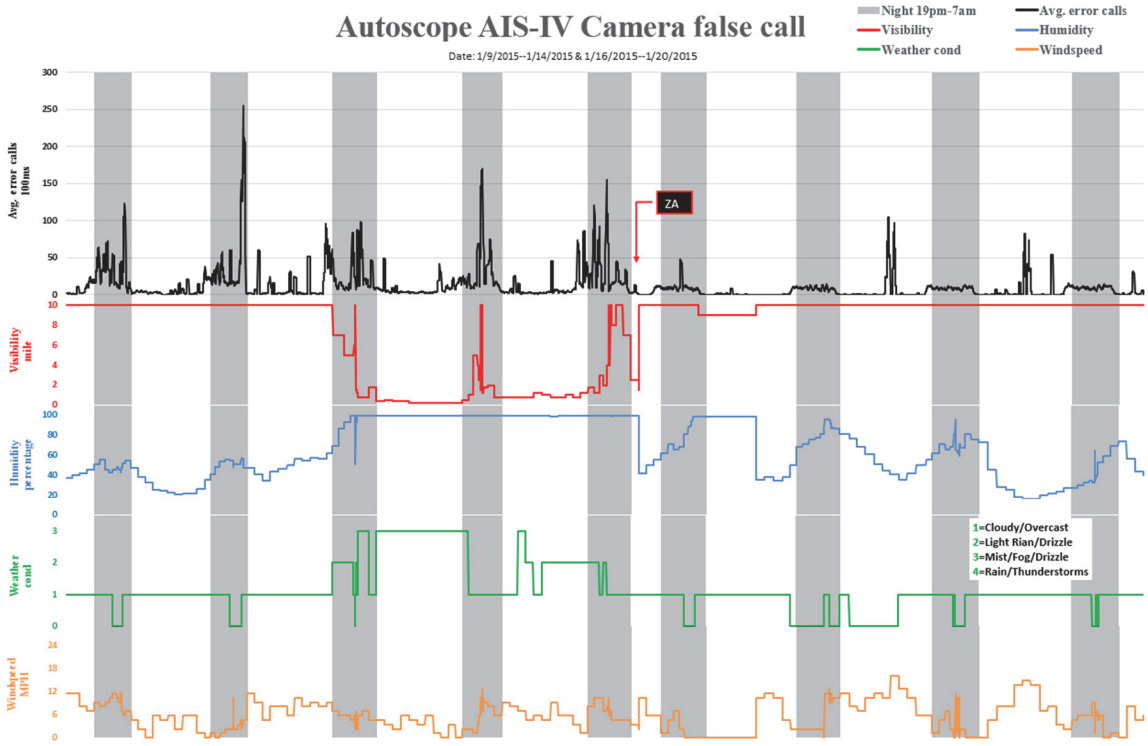
Autoscope AIS-IV Camera false call
Date: 1/9/2015--1/14/2015 & 1/16/2015--1/20/2015
Night 19pm-7am
Visibility
Weather cond
Avg. error calls
Humidity
Windspeed
Avg. error calls 100ms
ZA
Visibility mile
Humidity percentage
Weather cond
1=Cloudy/Overcast
2=Light Rian/Drizzle
3=Mist/Fog/Drizzle
4=Rain/Thunderstorms
Windspeed MPH

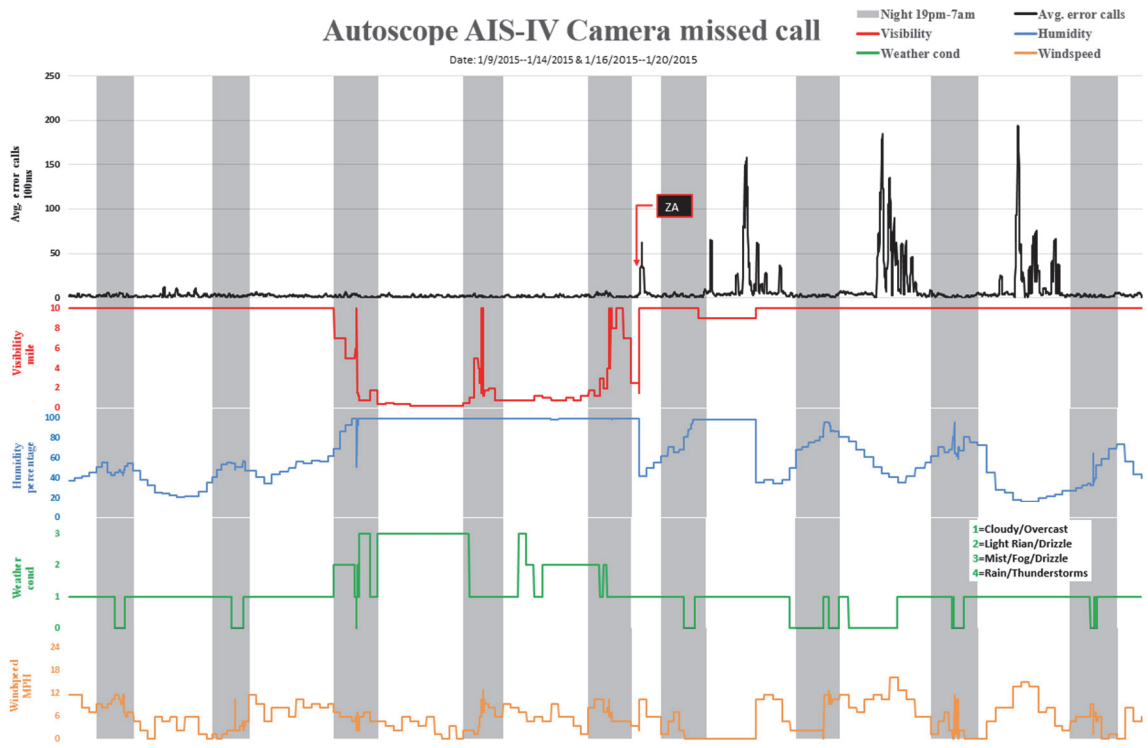
Autoscope AIS-IV Camera missed call
Date: 1/9/2015--1/14/2015 & 1/16/2015--1/20/2015
Night 19pm-7am
Visibility
Weather cond
Avg. error calls
Humidity
Windspeed
Avg. error calls 100ms
ZA
Visibility mile
Humidity percentage
Weather cond
1=Cloudy/Overcast
2=Light Rian/Drizzle
3=Mist/Fog/Drizzle
4=Rain/Thunderstorms
Windspeed MPH

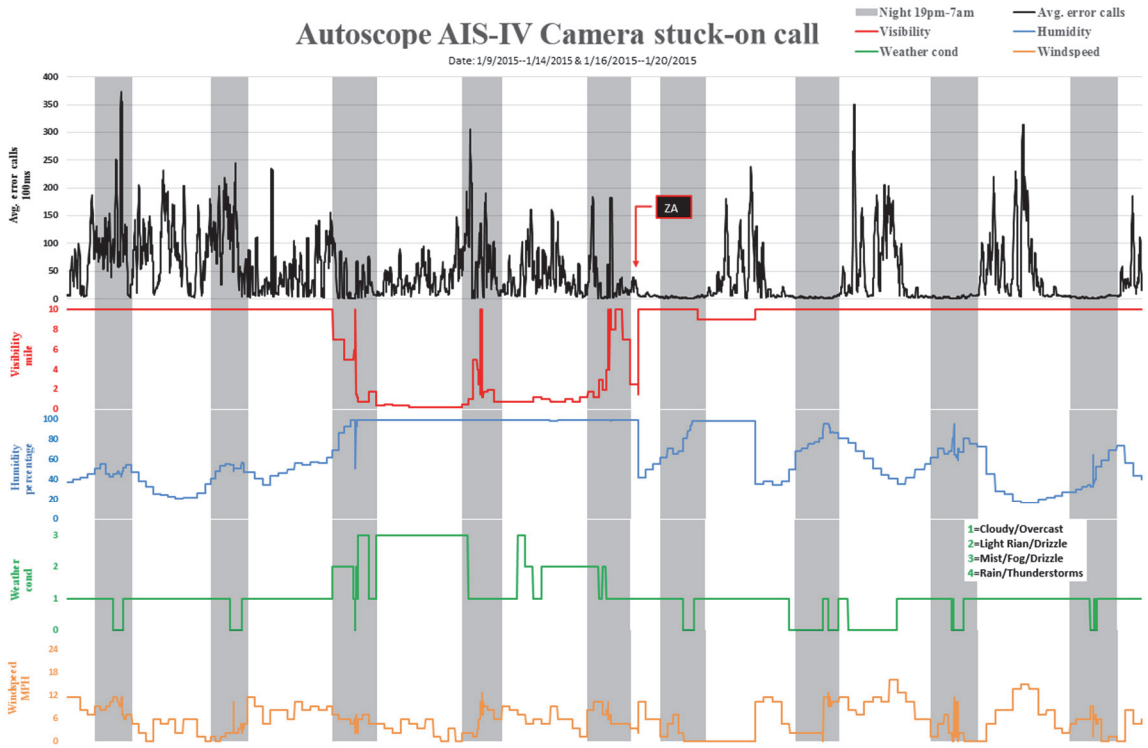
Autoscope AIS-IV Camera stuck-on call
Date: 1/9/2015--1/14/2015 & 1/16/2015--1/20/2015
Night 19pm-7am
Visibility
Weather cond
Avg. error calls
Humidity
Windspeed
Avg. error calls 100ms
ZA
Visibility mile
Humidity percentage
Weather cond
1=Cloudy/Overcast
2=Light Rian/Drizzle
3=Mist/Fog/Drizzle
4=Rain/Thunderstorms
Windspeed MPH

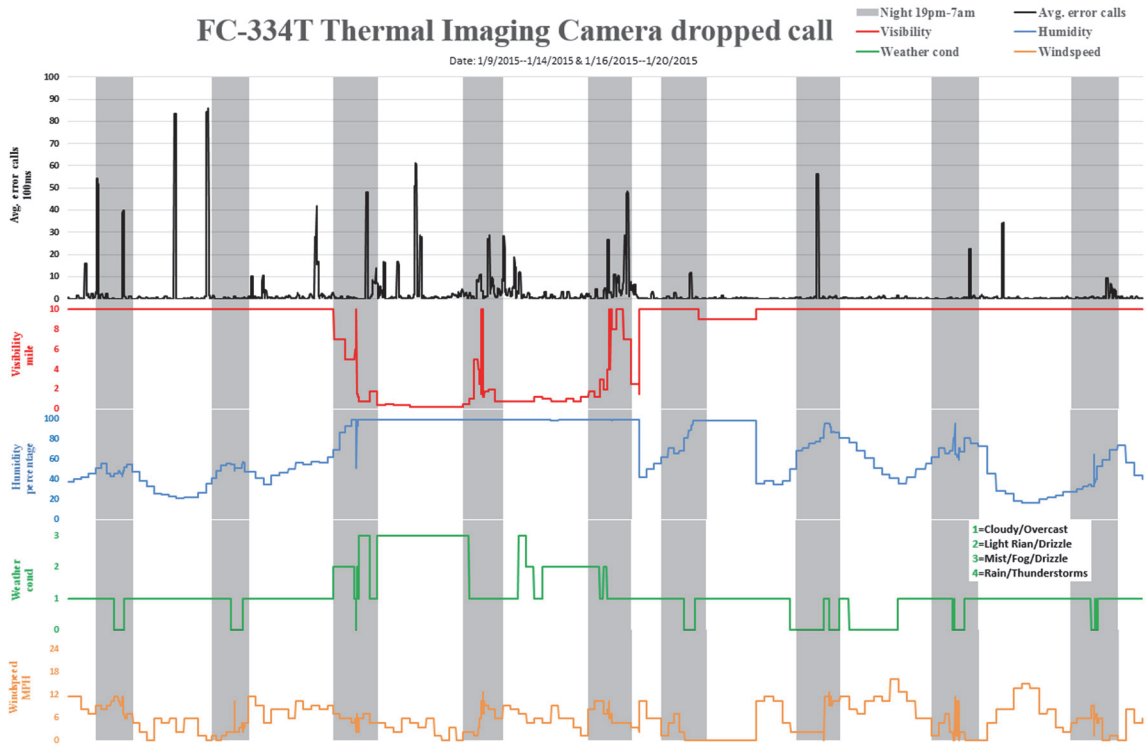
FC-334T Thermal Imaging Camera dropped call
Date: 1/9/2015--1/14/2015 & 1/16/2015--1/20/2015
Night 19pm-7am
Avg. error calls
Visibility
Humidity
Weather cond
Windspeed
Avg. error calls 100ms
Visibility mile
Humidity percentage
Weather cond
Windspeed MPH
1=Cloudy/Overcast
2=Light Rian/Drizzle
3=Mist/Fog/Drizzle
4=Rain/Thunderstorms

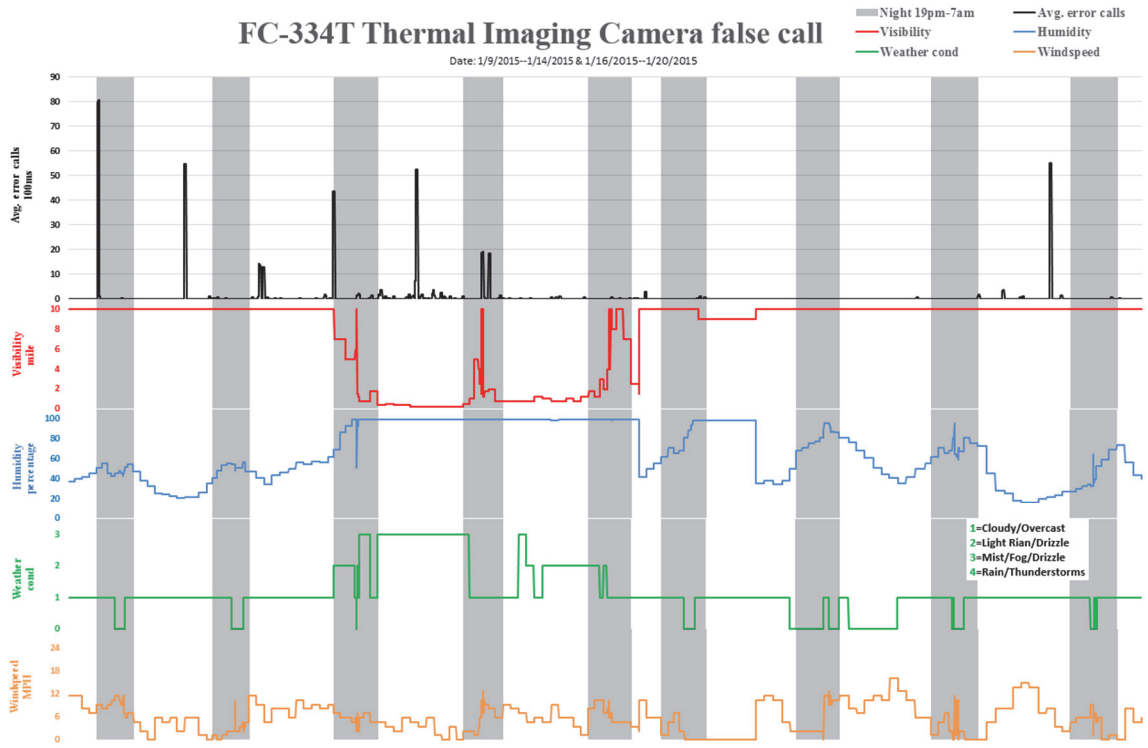
FC-334T Thermal Imaging Camera false call
Date: 1/9/2015--1/14/2015 & 1/16/2015--1/20/2015
Night 19pm-7am
Avg. error calls
Visibility
Humidity
Weather cond
Windspeed
Avg. error calls 100ms
Visibility mile
Humidity percentage
Weather cond
Windspeed MPH
1=Cloudy/Overcast
2=Light Rian/Drizzle
3=Mist/Fog/Drizzle
4=Rain/Thunderstorms

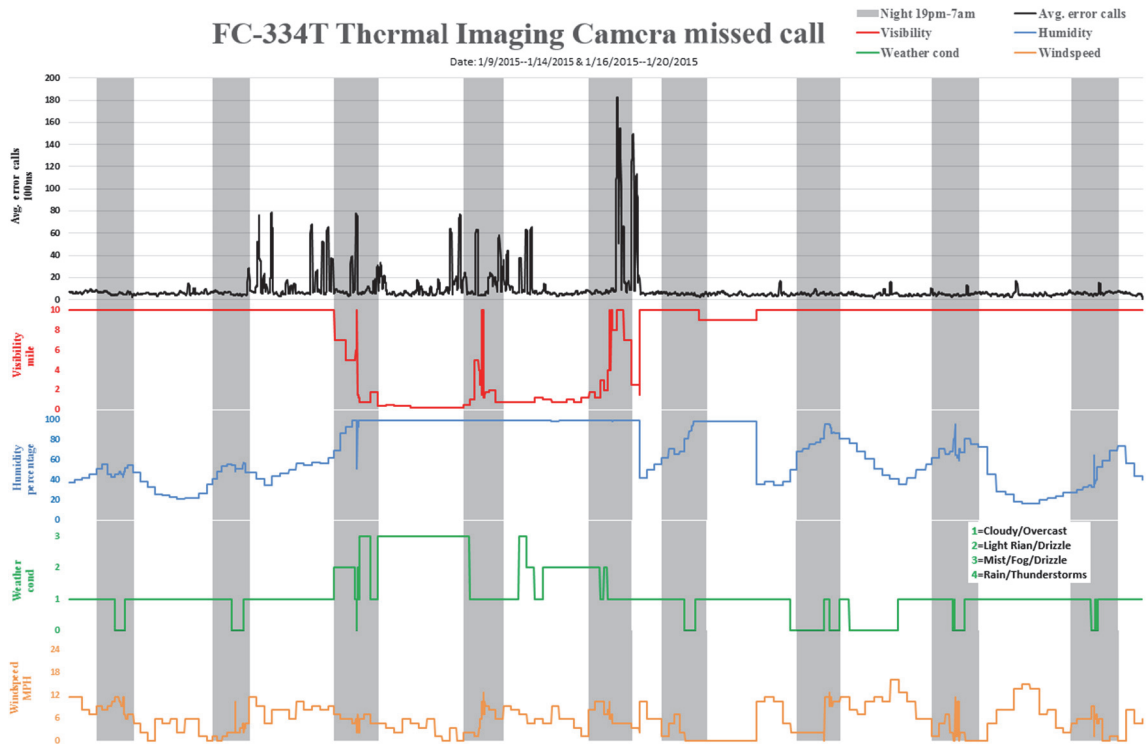
FC-334T Thermal Imaging Camera missed call
Date: 1/9/2015--1/14/2015 & 1/16/2015--1/20/2015
Night 19pm-7am
Avg. error calls
Visibility
Humidity
Weather cond
Windspeed
Avg. error calls 100ms
Visibility mile
Humidity percentage
Weather cond
Windspeed MPH
1=Cloudy/Overcast
2=Light Rian/Drizzle
3=Mist/Fog/Drizzle
4=Rain/Thunderstorms

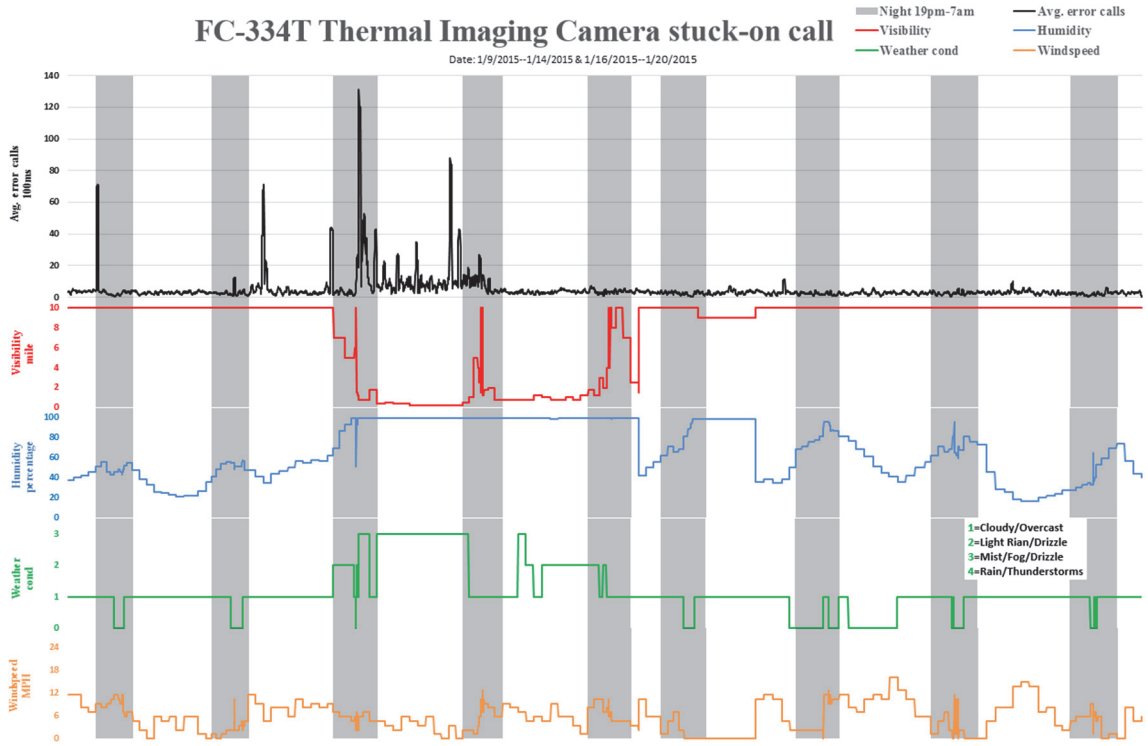
FC-334T Thermal Imaging Camera stuck-on call
Date: 1/9/2015--1/14/2015 & 1/16/2015--1/20/2015
Night 19pm-7am
Avg. error calls
Visibility
Humidity
Weather cond
Windspeed
Avg. error calls 100ms
Visibility mile
Humidity percentage
Weather cond
Windspeed MPH
1=Cloudy/Overcast
2=Light Rian/Drizzle
3=Mist/Fog/Drizzle
4=Rain/Thunderstorms

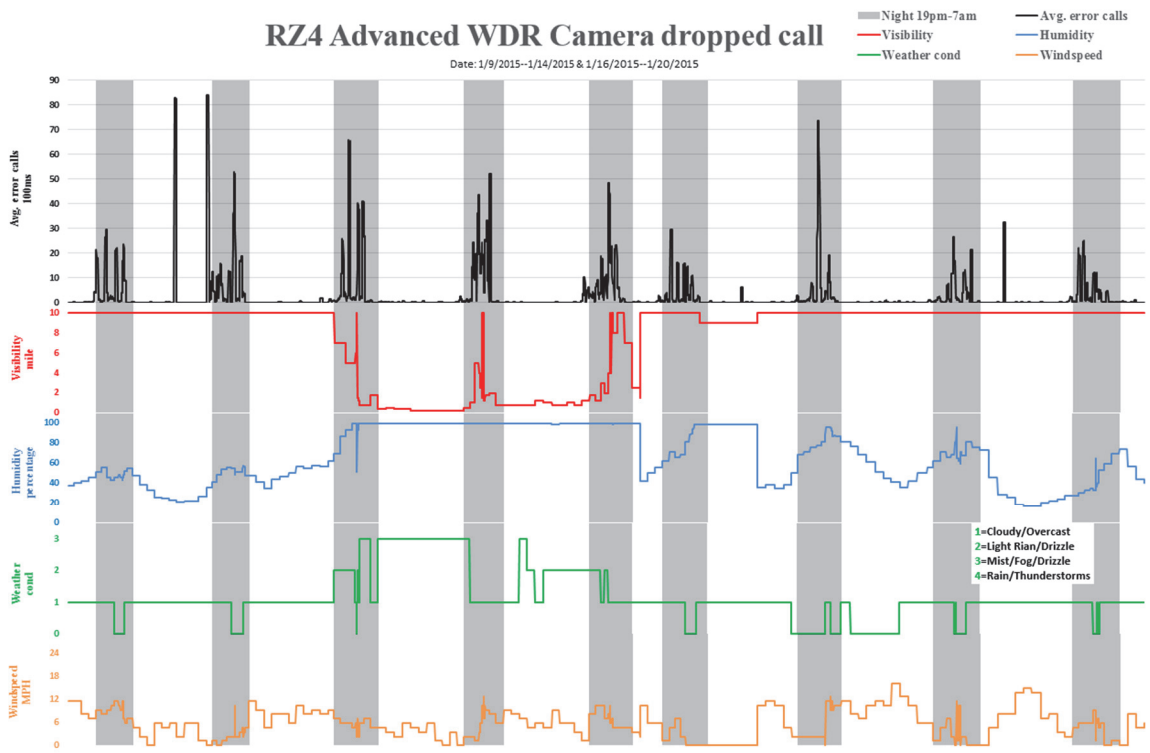
RZ4 Advanced WDR Camera dropped call
Date: 1/9/2015--1/14/2015 & 1/16/2015--1/20/2015
Night 19pm-7am
Avg. error calls
Visibility
Humidity
Weather cond
Windspeed
Avg. error calls 100ms
Visibility mile
Humidity percentage
Weather cond
Windspeed MPH
1=Cloudy/Overcast
2=Light Rian/Drizzle
3=Mist/Fog/Drizzle
4=Rain/Thunderstorms

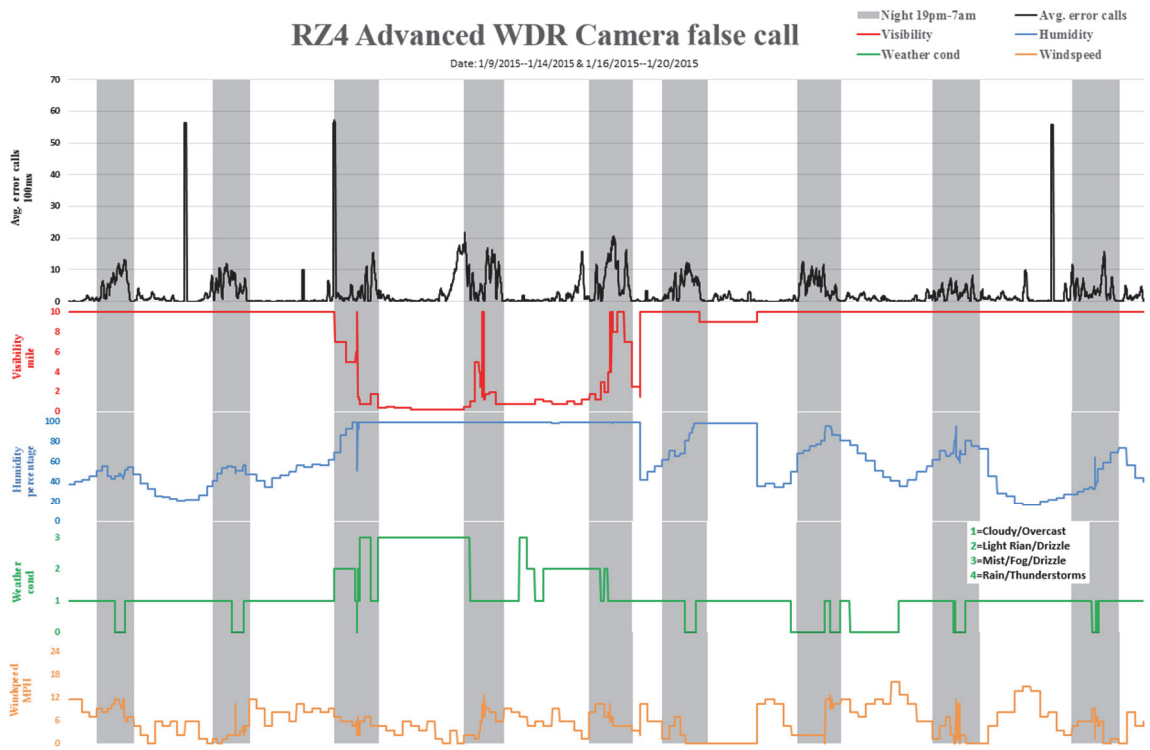
RZ4 Advanced WDR Camera false call
Date: 1/9/2015--1/14/2015 & 1/16/2015--1/20/2015
Night 19pm-7am
Avg. error calls
Visibility
Humidity
Weather cond
Windspeed
Avg. error calls 100ms
Visibility mile
Humidity percentage
Weather cond
Windspeed MPH
1=Cloudy/Overcast
2=Light Rian/Drizzle
3=Mist/Fog/Drizzle
4=Rain/Thunderstorms

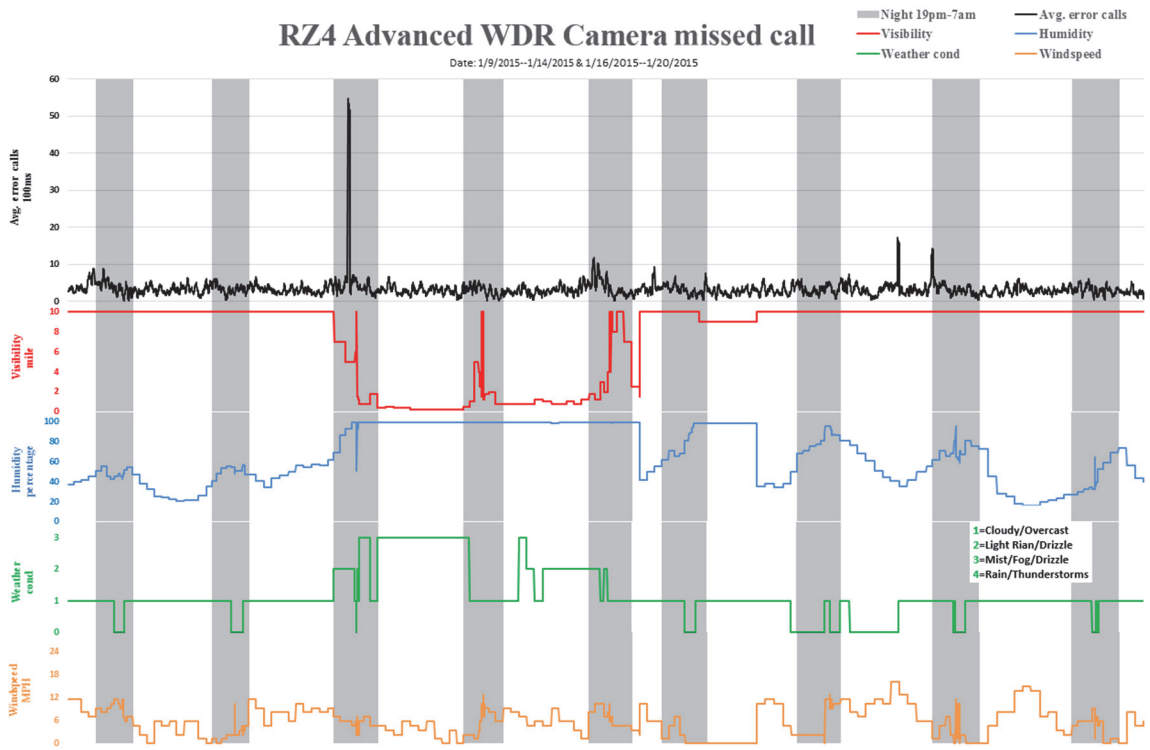
RZ4 Advanced WDR Camera missed call
Date: 1/9/2015--1/14/2015 & 1/16/2015--1/20/2015
Night 19pm-7am
Avg. error calls
Visibility
Humidity
Weather cond
Windspeed
Avg. error calls 100ms
Visibility mile
Humidity percentage
Weather cond
Windspeed MPH
1=Cloudy/Overcast
2=Light Rian/Drizzle
3=Mist/Fog/Drizzle
4=Rain/Thunderstorms

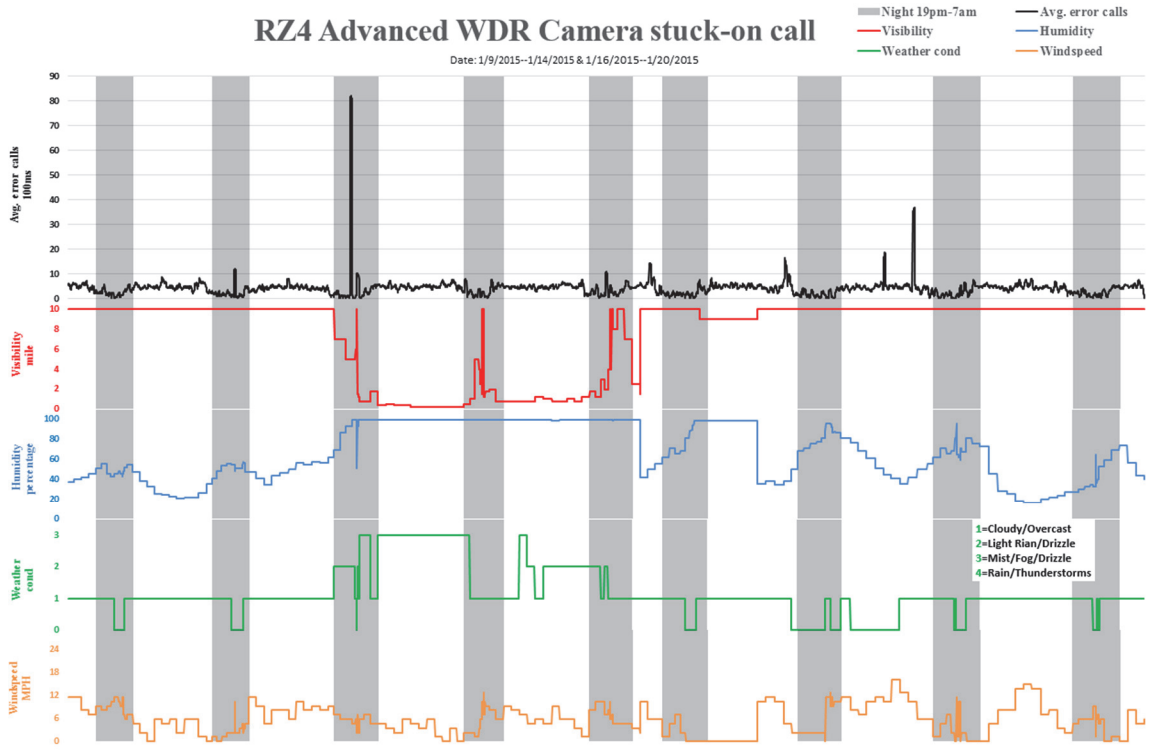
RZ4 Advanced WDR Camera stuck-on call
Date: 1/9/2015--1/14/2015 & 1/16/2015--1/20/2015
Night 19pm-7am
Avg. error calls
Visibility
Humidity
Weather cond
Windspeed
Avg. error calls 100ms
Visibility mile
Humidity percentage
Weather cond
Windspeed MPH
1=Cloudy/Overcast
2=Light Rian/Drizzle
3=Mist/Fog/Drizzle
4=Rain/Thunderstorms

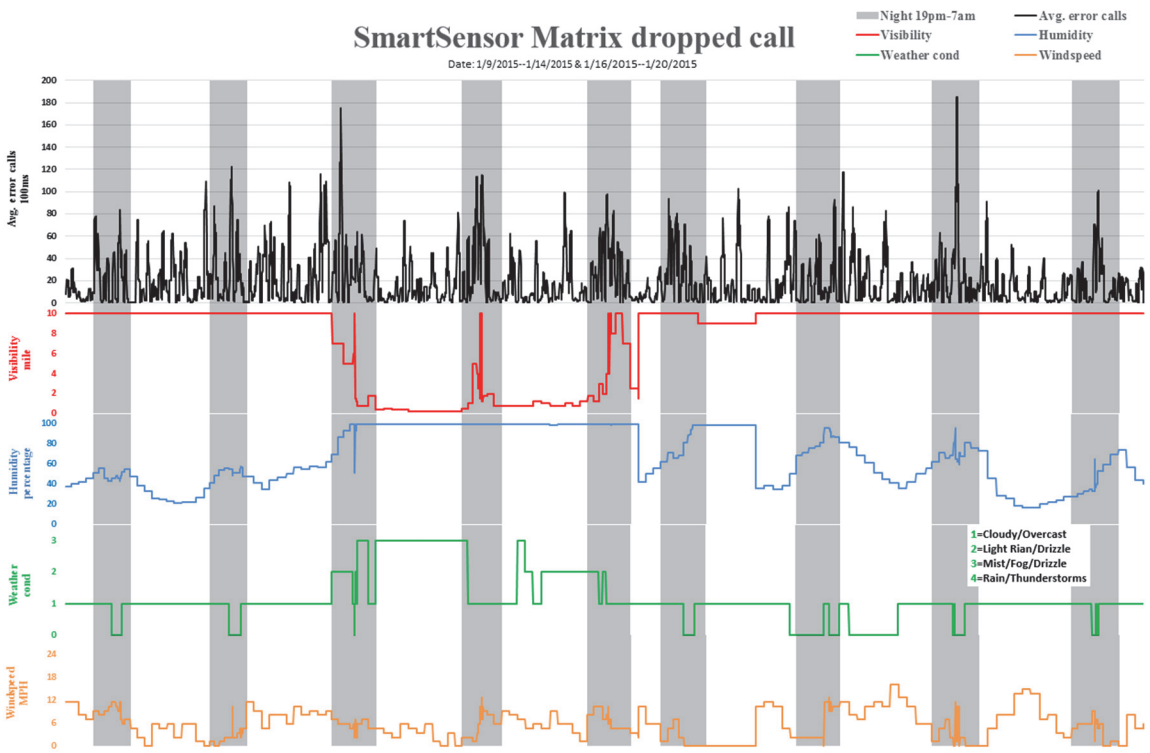
SmartSensor Matrix dropped call
Date: 1/9/2015--1/14/2015 & 1/16/2015--1/20/2015
Night 19pm-7am
Avg. error calls
Visibility
Humidity
Weather cond
Windspeed
Avg. error calls 100ms
Visibility mile
Humidity percentage
Weather cond
Windspeed MPH
1=Cloudy/Overcast
2=Light Rian/Drizzle
3=Mist/Fog/Drizzle
4=Rain/Thunderstorms

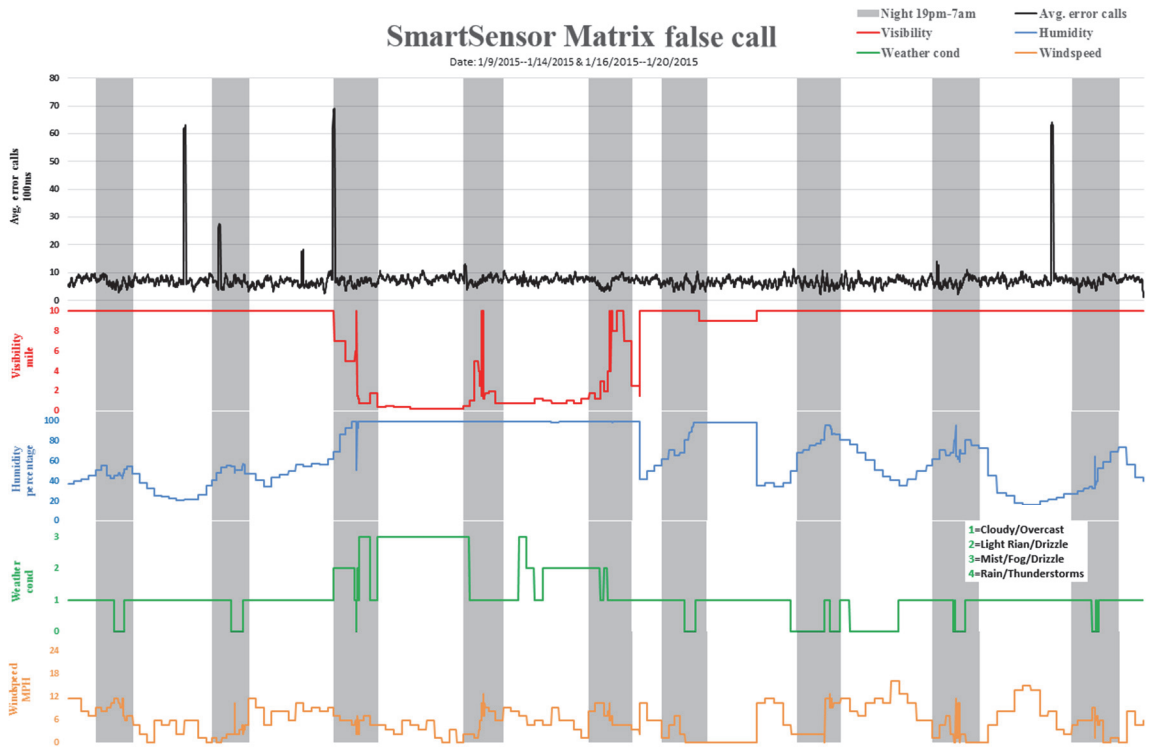
SmartSensor Matrix false call
Date: 1/9/2015--1/14/2015 & 1/16/2015--1/20/2015
Night 19pm-7am
Avg. error calls
Visibility
Humidity
Weather cond
Windspeed
Avg. error calls 100ms
Visibility mile
Humidity percentage
Weather cond
Windspeed MPH
1=Cloudy/Overcast
2=Light Rian/Drizzle
3=Mist/Fog/Drizzle
4=Rain/Thunderstorms

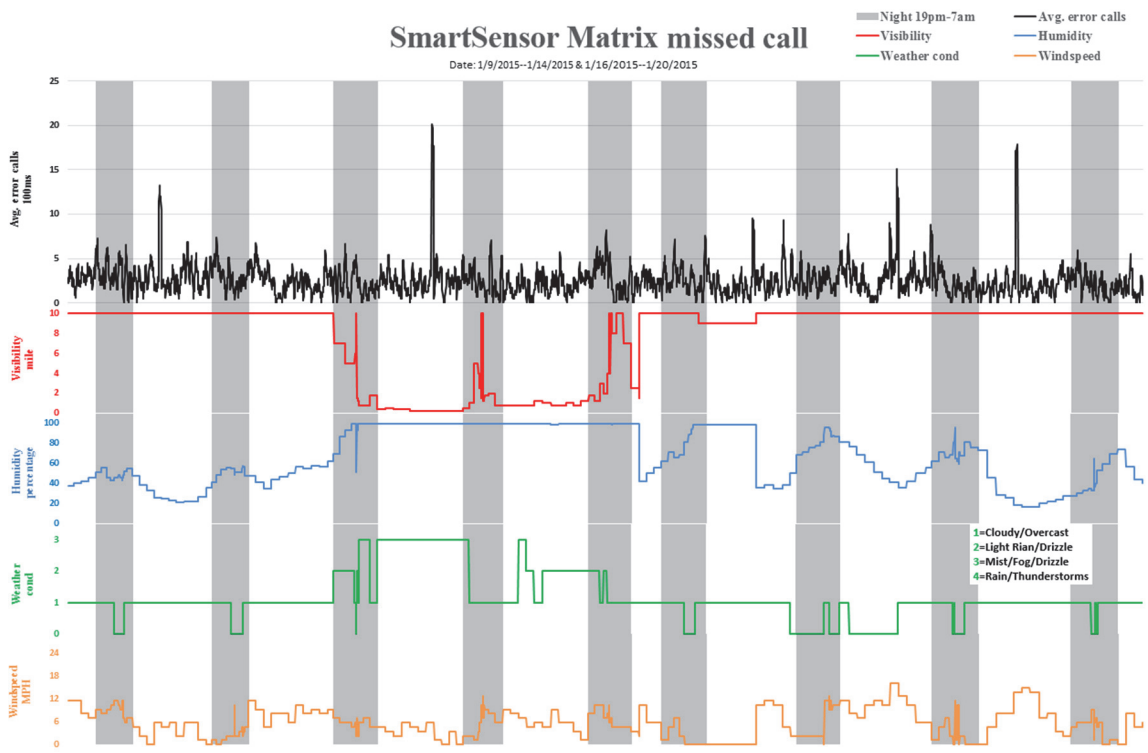
SmartSensor Matrix missed call
Date: 1/9/2015--1/14/2015 & 1/16/2015--1/20/2015
Night 19pm-7am
Avg. error calls
Visibility
Humidity
Weather cond
Windspeed
Avg. error calls 100ms
Visibility mile
Humidity percentage
Weather cond
Windspeed MPH
1=Cloudy/Overcast
2=Light Rian/Drizzle
3=Mist/Fog/Drizzle
4=Rain/Thunderstorms

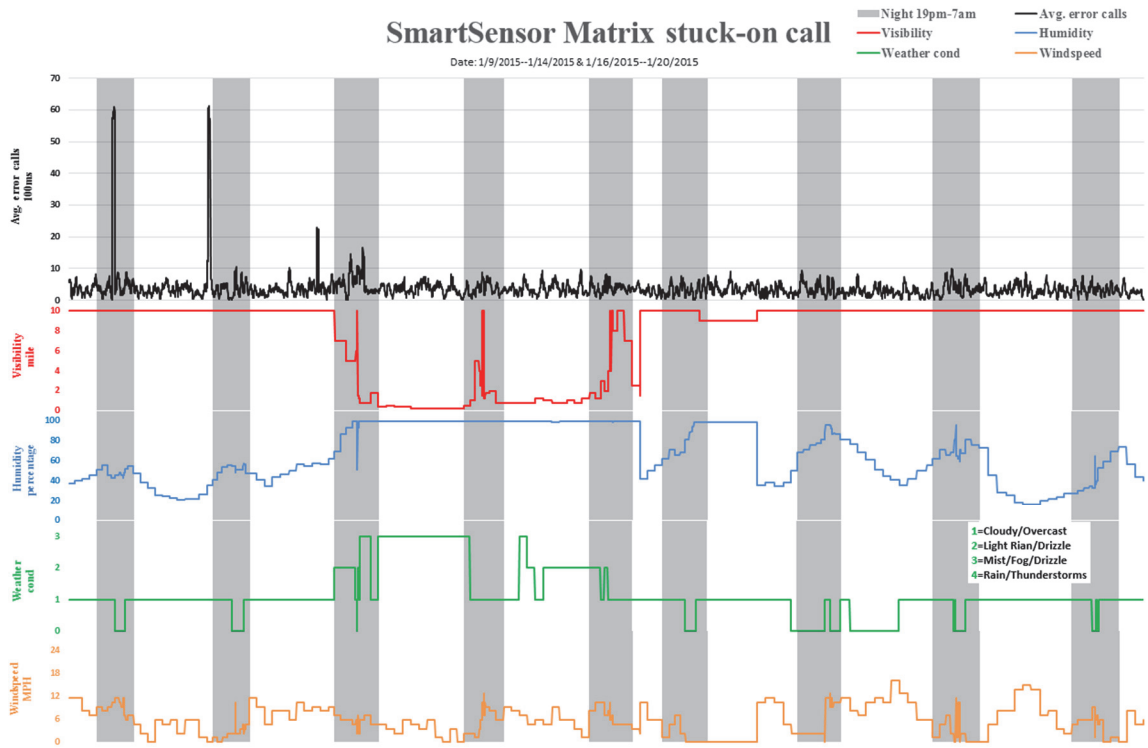
SmartSensor Matrix stuck-on call
Date: 1/9/2015--1/14/2015 & 1/16/2015--1/20/2015
Night 19pm-7am
Avg. error calls
Visibility
Humidity
Weather cond
Windspeed
Avg. error calls 100ms
Visibility mile
Humidity percentage
Weather cond
Windspeed MPH
1=Cloudy/Overcast
2=Light Rian/Drizzle
3=Mist/Fog/Drizzle
4=Rain/Thunderstorms

Appendix C: Plots of Detection Errors by Time (Site 3)

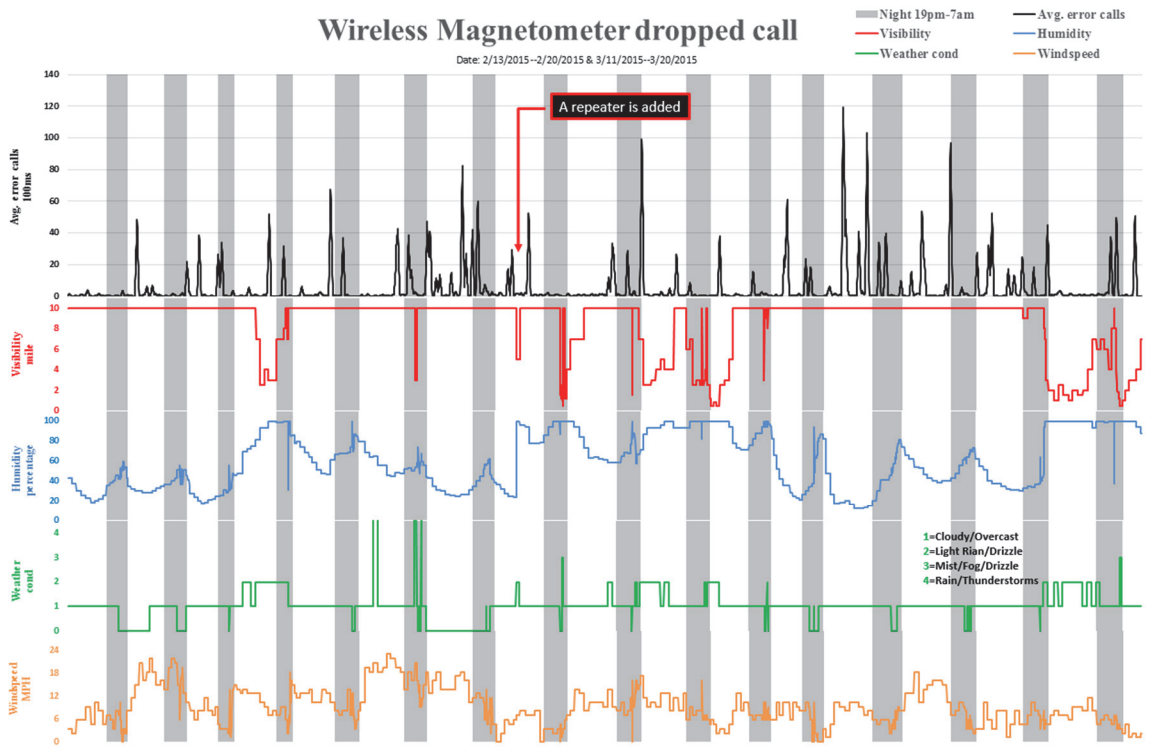
Wireless Magnetometer dropped call
Date: 2/13/2015--2/20/2015 & 3/11/2015--3/20/2015
Night 19pm-7am
Avg. error calls
Visibility
Humidity
Weather cond
Windspeed
A repeater is added
Avg. error calls 100ms
Visibility mile
Humidity percentage
Weather cond
Windspeed MPH
1=Cloudy/Overcast
2=Light Rian/Drizzle
3=Mist/Fog/Drizzle
4=Rain/Thunderstorms

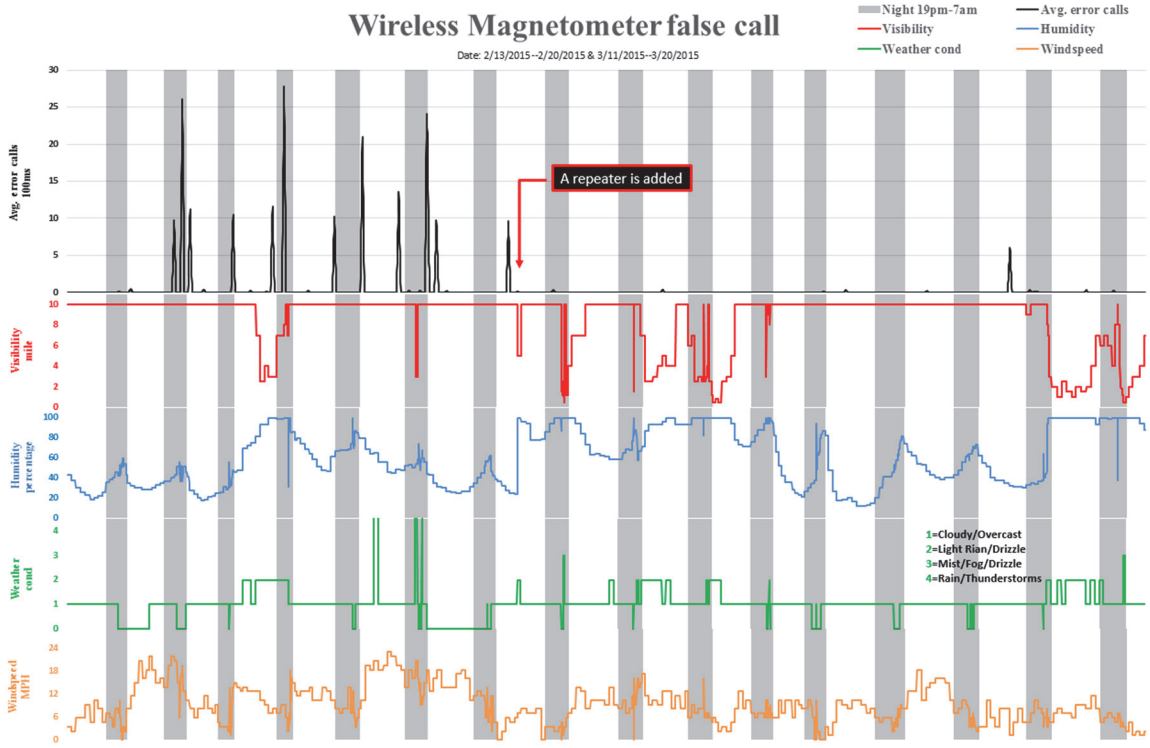
Wireless Magnetometer false call
Date: 2/13/2015--2/20/2015 & 3/11/2015--3/20/2015
Night 19pm-7am
Avg. error calls
Visibility
Humidity
Weather cond
Windspeed
A repeater is added
Avg. error calls 100ms
Visibility mile
Humidity percentage
Weather cond
Windspeed MPH
1=Cloudy/Overcast
2=Light Rian/Drizzle
3=Mist/Fog/Drizzle
4=Rain/Thunderstorms

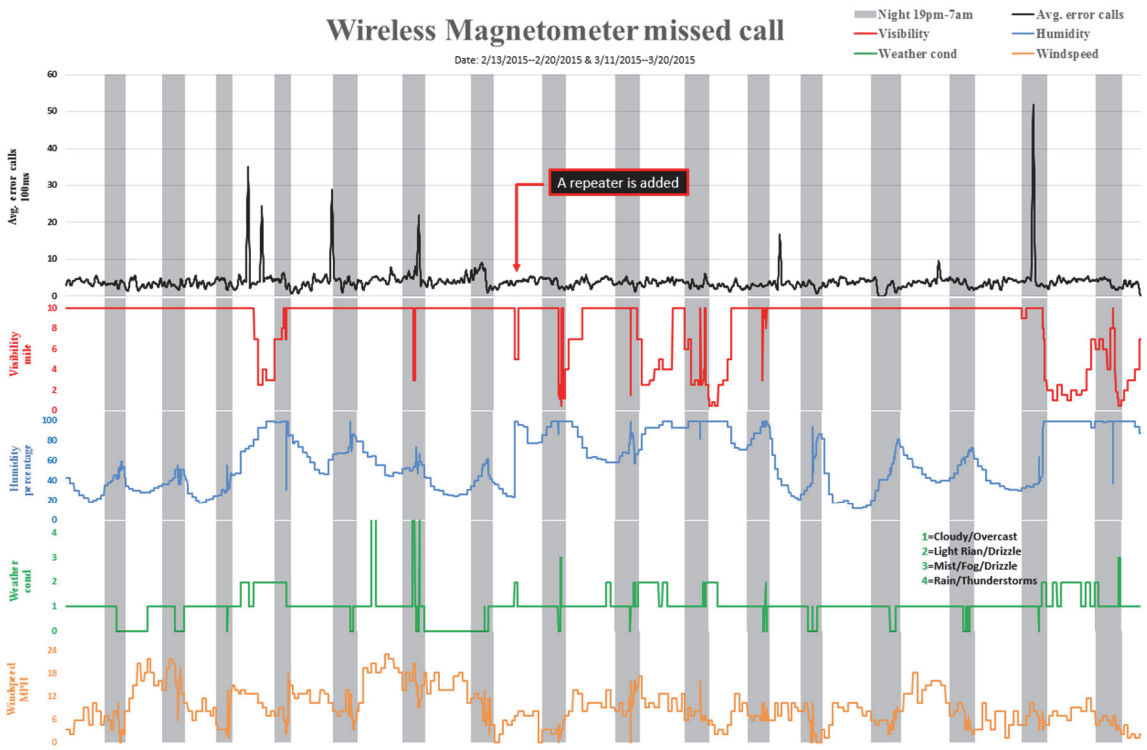
Wireless Magnetometer missed call
Date: 2/13/2015--2/20/2015 & 3/11/2015--3/20/2015
Night 19pm-7am
Avg. error calls
Visibility
Humidity
Weather cond
Windspeed
Avg. error calls 100ms
A repeater is added
Visibility mile
Humidity percentage
Weather cond
1=Cloudy/Overcast
2=Light Rian/Drizzle
3=Mist/Fog/Drizzle
4=Rain/Thunderstorms
Windspeed MPH

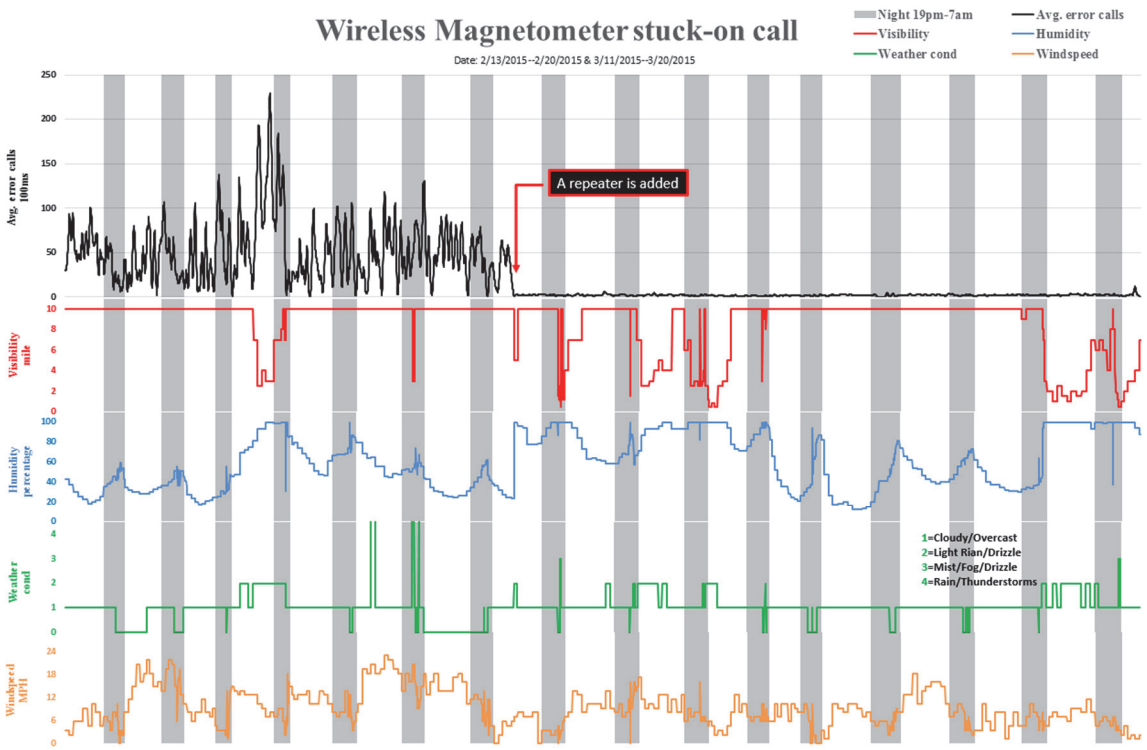
Wireless Magnetometer stuck-on call
Date: 2/13/2015--2/20/2015 & 3/11/2015--3/20/2015
Night 19pm-7am
Avg. error calls
Visibility
Humidity
Weather cond
Windspeed
Avg. error calls 100ms
A repeater is added
Visibility mile
Humidity percentage
Weather cond
1=Cloudy/Overcast
2=Light Rian/Drizzle
3=Mist/Fog/Drizzle
4=Rain/Thunderstorms
Windspeed MPH

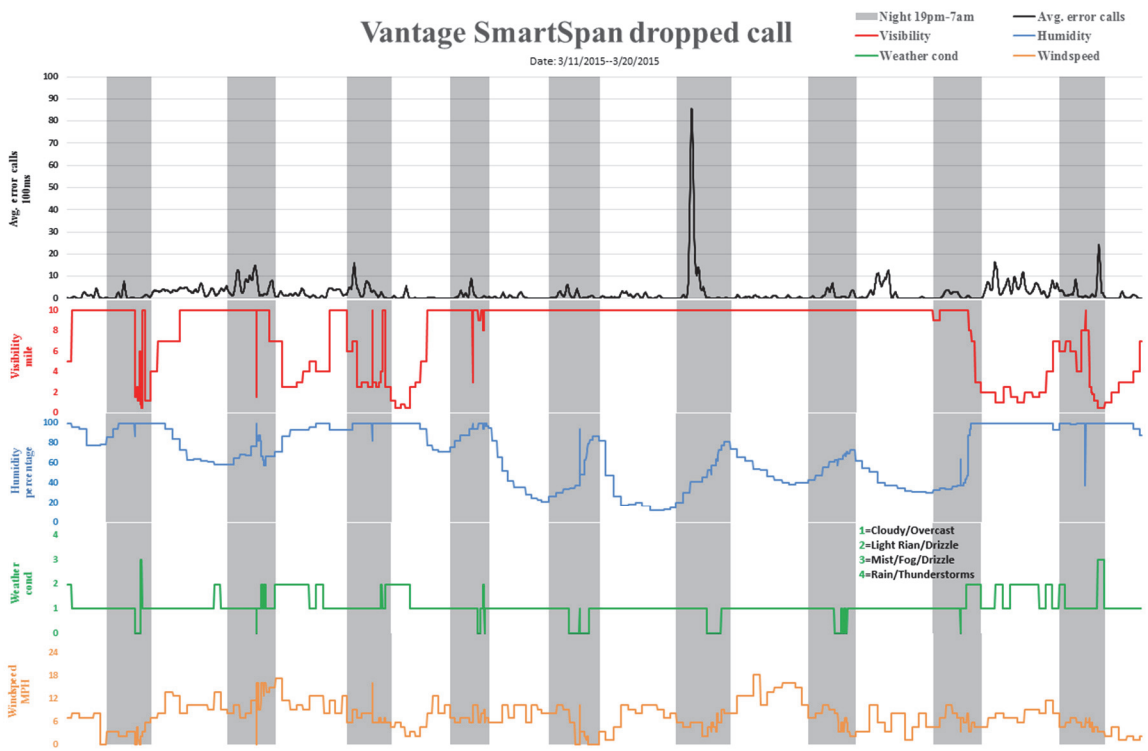
Vantage SmartSpan dropped call
Date: 3/11/2015--3/20/2015
Night 19pm-7am
Avg. error calls
Visibility
Humidity
Weather cond
Windspeed
Avg. error calls 100ms
Visibility mile
Humidity percentage
Weather cond
Windspeed MPH
1=Cloudy/Overcast
2=Light Rian/Drizzle
3=Mist/Fog/Drizzle
4=Rain/Thunderstorms

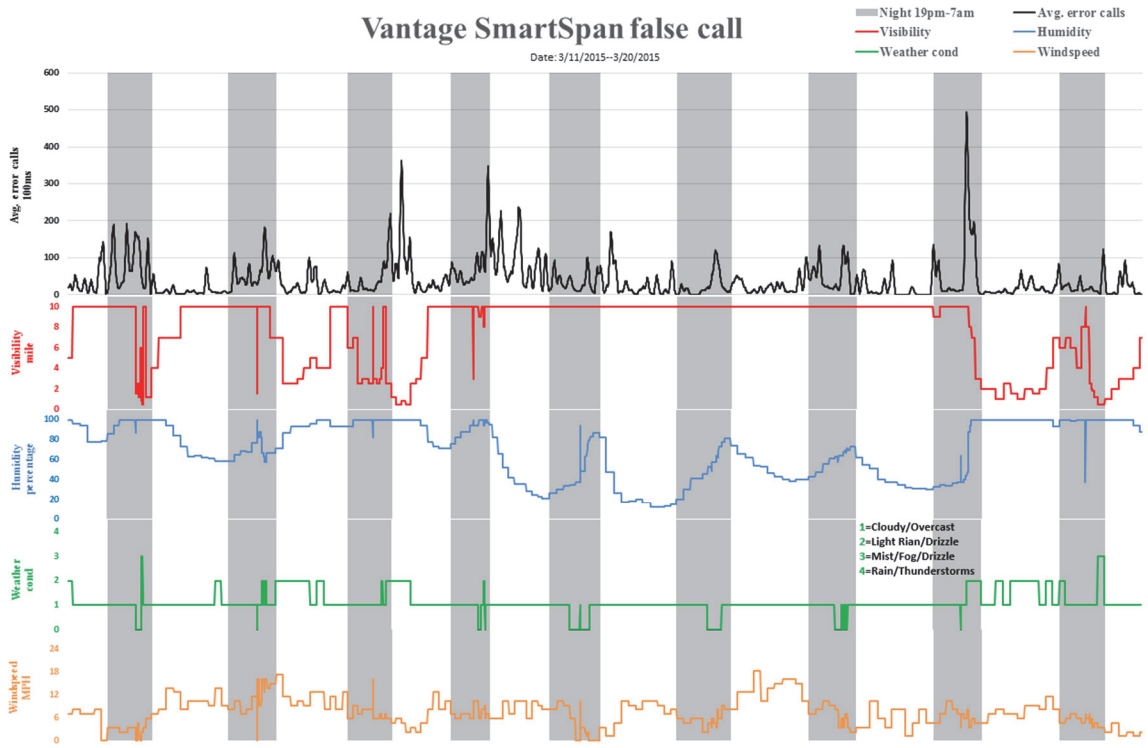
Vantage SmartSpan false call
Date: 3/11/2015--3/20/2015
Night 19pm-7am
Avg. error calls
Visibility
Humidity
Weather cond
Windspeed
Avg. error calls 100ms
Visibility mile
Humidity percentage
Weather cond
Windspeed MPH
1=Cloudy/Overcast
2=Light Rian/Drizzle
3=Mist/Fog/Drizzle
4=Rain/Thunderstorms

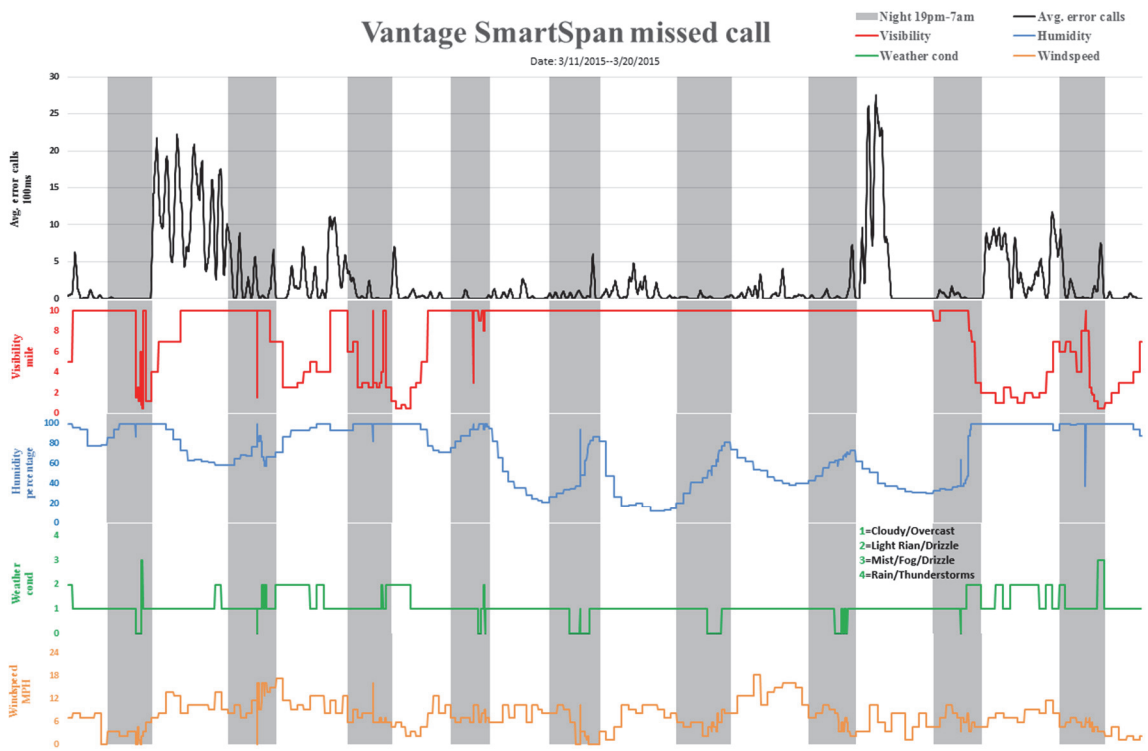
Vantage SmartSpan missed call
Date: 3/11/2015--3/20/2015
Night 19pm-7am
Avg. error calls
Visibility
Humidity
Weather cond
Windspeed
Avg. error calls 100ms
Visibility mile
Humidity percentage
Weather cond
Windspeed MPH
1=Cloudy/Overcast
2=Light Rian/Drizzle
3=Mist/Fog/Drizzle
4=Rain/Thunderstorms

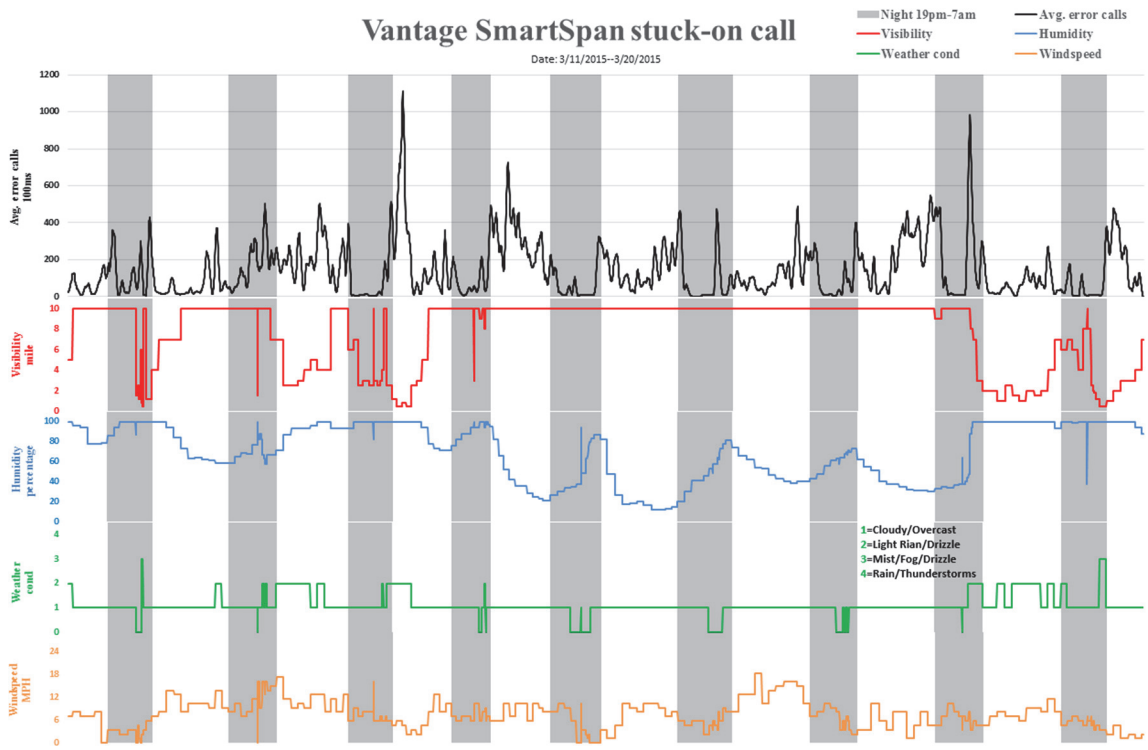
Vantage SmartSpan stuck-on call
Date: 3/11/2015--3/20/2015
Night 19pm-7am
Avg. error calls
Visibility
Humidity
Weather cond
Windspeed
Avg. error calls 100ms
Visibility mile
Humidity percentage
Weather cond
Windspeed MPH
1=Cloudy/Overcast
2=Light Rian/Drizzle
3=Mist/Fog/Drizzle
4=Rain/Thunderstorms

Appendix D: Survey Form

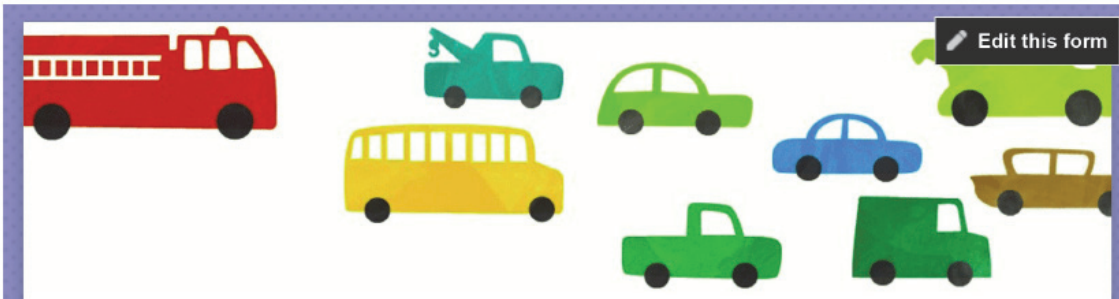

Survey on the use of vehicle detection devices for traffic signal operations

This survey seeks your opinions and experience with different types of vehicle detection devices currently used for traffic signal operations in your jurisdiction.

* Required

Agency *

Your Name

1. Which of the following detection devices are currently used by your agency for STOP Bar Detection? *

Please select one or more as applicable.

- ☐ Inductive loop
- ☐ Iteris RZ-4 Advanced WDR
- ☐ Iteris VerisCam
- ☐ Iteris Vantage Vector Hybrid
- ☐ Iteris SmartSpan
- ☐ Econolite Autoscope AIS IV
- ☐ Econolite Autoscope AIS V
- ☐ Econolite Autoscope AIS Color
- ☐ Econolite Autoscope Duo
- ☐ GridSmart fisheye camera
- ☐ Flir thermal imaging camera
- ☐ Wavetronix SmartSensor Matrix
- ☐ Sensys Magnetometer

☐ Other:

2. Which of the following detection devices are currently used by your agency for Advance Detection (Dilemma zone or Volume-Density)? *

Please select one or more as applicable.

☐ Inductive loop

☐ Iteris Vantage Vector Hybrid

☐ Autoscope Duo

☐ SmartMicro Radar

☐ Wavetronix SmartSensor Advance

☐ Sensys Magnetometer

☐ Other:

Evaluate factors related to your purchasing decisions

3. How would you rate the importance of "Detection Accuracy" when purchasing any vehicle detection devices? *

Please use a 5-point scale (5 - most important; 4 - very important; 3 - important; 2 - moderately important; 1 - somewhat important).

1	2	3	4	5
○	○	○	○	○

4. How would you rate the importance of "Reliability" when purchasing any vehicle detection devices? *

Please use a 5-point scale (5 - most important; 4 - very important; 3 - important; 2 - moderately important; 1 - somewhat important).

1	2	3	4	5
○	○	○	○	○

5. How would you rate the importance of "Durability" when purchasing any vehicle detection devices? *

Please use a 5-point scale (5 - most important; 4 - very important; 3 - important; 2 - moderately important; 1 - somewhat important).

1	2	3	4	5
○	○	○	○	○

6. How would you rate the importance of "Ease of Installation and Maintenance" when purchasing any vehicle detection devices? *

Please use a 5-point scale (5 - most important; 4 - very important; 3 - important; 2 - moderately important; 1 - somewhat important).

1	2	3	4	5
○	○	○	○	○

7. How would you rate the importance of "Price" when purchasing any vehicle detection devices? *

Please use a 5-point scale (5 - most important; 4 - very important; 3 - important; 2 - moderately important; 1 - somewhat important).

1	2	3	4	5
○	○	○	○	○

Evaluate "Ease of Installation and Maintenance" comparing to inductive loops

8. If your agency is currently using any vehicle detection cameras (regular or thermal), how would you rate their level of "Ease of Installation and Maintenance" comparing to inductive loops?

If your agency doesn't use any cameras for vehicle detection, you can skip this question.

- ○ Much easier than loops
- ○ Somewhat easier than loops
- ○ Almost same as loops
- ○ Somewhat difficult than loops
- ○ Much difficult than loops

9. If your agency is currenlty using Sensys Magnetometer, how would you rate its level of "Ease of Installation and Maintenance" comparing to inductive loops?

If your agency doesn't use Sensys Magnetometer, you can skip this question.

- ○ Much easier than loops
- ○ Somewhat easier than loops
- ○ Almost same as loops
- ○ Somewhat difficult than loops
- ○ Much difficult than loops

10. If your agency is currenlty using Wavetronix SmartSensor (Matrix or Advance), how would you rate their level of "Ease of Installation and Maintenance" comparing to inductive loops?

If your agency doesn't use Wavetronix SmartSensor, you can skip this question.

- ○ Much easier than loops

- ○ Somewhat easier than loops
- ○ Almost same as loops
- ○ Somewhat difficult than loops
- ○ Much difficult than loops

Additional comments that you may have on the vehicle detection devices currently used by your agency.

You can describe any good or bad experience with the devices currently used by your agency.

Submit

Never submit passwords through Google Forms.

100%: You made it.

Powered by Google Forms

This content is neither created nor endorsed by Google.

Report Abuse - Terms of Service - Additional Terms